INVESTIGATING THE MACHINING CHARACTERISTICS OF TITANIUM USING ULTRASONIC MACHINING

A thesis submitted
in fulfillment of the requirements
for the award of the degree
of

DOCTOR OF PHILOSOPHY

By

JATINDER KUMAR
Reg. No. 9030554

DEPARTMENT OF MECHANICAL ENGINEERING
THAPAR UNIVERSITY
PATIALA-147004 (INDIA)
2009

PREFACE

This research work was carried out by the author under the guidance of Dr. J.S. Khamba, Professor & Head, Department of Mechanical Engineering at University College of Engineering, Punjabi University, Patiala and Dr. S.K. Mohapatra, Professor & Head, Department of Mechanical Engineering, Thapar University, Patiala 147004 (India).

Ultrasonic Drilling machine, Surface roughness measuring instruments (Perthometer), Weighing machine apparatus and other facilities available at the Department of Mechanical Engineering at Thapar University, Patiala were used for this research work. Also, some instruments like Diamond polishing apparatus and Image analyzer available at Thapar Center for Industrial Research and Development (TCIRD), Patiala were used for the investigation of ultrasonically machined samples. For analyzing the microstructure of the machined samples, Scanning Electron Microscope (SEM) apparatus available at CIL, Punjab University, Chandigarh was used.

Several research papers were published out of this research work. **The list of Journals/Conferences in which the papers find place is given below:**

1. Kumar Jatinder, Khamba J.S., Mohapatra S.K. (2008), "An investigation into the machining characteristics of pure titanium using ultrasonic machining", *International Journal of Machining and Machinability of Materials* (Inderscience publishers, UK), **Vol. 3, no. 1-2,** pp. 143-161.
2. Kumar Jatinder, Khamba J.S., Mohapatra S.K. (2008), "Investigating and modeling tool-wear rate in the ultrasonic machining of titanium", *International Journal of Advanced Manufacturing Technology (Springer-Verlang London Ltd.),* **DOI 10.1007/s00170-008-1556-8** (online version).
3. Kumar Jatinder, Khamba J.S., (2008), "An experimental study on ultrasonic machining of pure titanium using designed experiments", *Journal of Brazilian Society of Mechanical Sciences and Engineering,* **Vol. 30, No. 2**, pp. 231-238.

4. Kumar Jatinder, Khamba J.S., Mohapatra S.K. (2008), "Surface quality evaluation in ultrasonic machining of titanium using Taguchi method", *Journal of Manufacturing Technology & Research* (Int. Journal)*,* **Vol. 4, No. 1-2**, pp. 133-145.
5. Kumar Jatinder, Khamba J.S. and Mohapatra S.K. (2007), "Ultrasonic machining of titanium-a state of the art review", *Journal of Manufacturing Technology Today*, **Vol. 6, No. 9**, pp. 3-9.
6. Kumar Jatinder, Khamba J.S., Mohapatra S.K. (2008), "An experimental investigation of the influence of work material properties on performance indices of ultrasonic machining", *Journal of Manufacturing Technology Today*, **Vol. 7, No. 3**, pp. 23-27.
7. Kumar Jatinder, Khamba J.S., Mohapatra S.K. (2007), "An experimental investigation on ultrasonic machining of pure titanium using Taguchi method", *Proceedings of International Conference on Theoretical, Applied, Computational and Experimental Mechanics*, IIT Kharagpur, India, Dec 27-29, 2007.
8. Kumar Jatinder, Khamba J.S., Mohapatra S.K. (2007) "Investigating tool wear rate and surface quality in ultrasonic machining of titanium", *Proceedings of International Conference on Advanced Manufacturing Technologies*, CMERI, Durgapur, India, 29-30 Nov., 2007, pp. 181-190.
9. Kumar Jatinder, Khamba J.S., Mohapatra S.K. (2007), "An experimental investigation into the ultrasonic machining of pure titanium", *Proceedings of National Conference on Advances in Materials and Manufacturing Technologies,* Punjab Engineering College, Chandigarh, India, Sep. 21-22, 2007, pp. 316-320.
10. Kumar Jatinder and Khamba J.S. (2006), "Ultrasonic machining and its capabilities in machining of titanium-a state of the art review", *Proceedings of International Conference on Advanced Design and Manufacture*, Harbin Engineering University, Harbin, China in association with Nottingham Trent University, UK, Jan 8-10, 2006, pp. 276-281.

11. Kumar Jatinder, Khamba J.S., Mohapatra S.K. (2005), "Ultrasonic machining (USM) and its application to the machining of tough materials-A review"; *Proceedings of International Conference on Materials, Product design and manufacturing (ICMPM*), BIT Coimbtore, India in association with North Carolina State A & T University, Greensboro, USA, Dec 12-15, 2005, pp. 313-318.

The list of Journals in which the papers are communicated is given below:

1. Kumar Jatinder, Khamba J.S., Mohapatra S.K., "Multiple response optimization in ultrasonic machining of titanium using Taguchi's approach and utility concept", communicated to *International Journal of Manufacturing Research (*Inderscience publications, UK*)*.
2. Kumar Jatinder, Khamba J.S., Mohapatra S.K., "Micro-Model for material removal rate in ultrasonic machining of titanium: designed experiments", communicated to *International Journal of Advanced Manufacturing Technology (*Springerlink publications*)*.
3. Kumar Jatinder, Khamba J.S., Mohapatra S.K., "An investigation into the influence of abrasive slurry properties on machining efficiency in ultrasonic machining of titanium", communicated to *Journal of Manufacturing Technology Today* (National Journal).

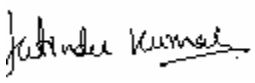

(Jatinder Kumar)

ACKNOWLEDGEMENT

The author wishes to express his deep sense of gratitude to Dr. J.S. Khamba, Professor and Head, Department of Mechanical Engineering, University College of Engineering, Punjabi University, Patiala and Dr. S.K. Mohapatra, Professor and Head, Department of Mechanical Engineering, Thapar University, Patiala, for having given me an opportunity to do research in the area of ultrasonic machining and for inspiring guidance given throughout this research work.

Heartfelt thanks are due to Dr. Abhijeet Mukharjee (Director, Thapar University Patiala) and Dr. K.K. Raina (Dean, Research and Sponsored Projects, T.U. Patiala), Dr. Rajneesh Prakash (Director, A.K.G.E.C. Ghaziabad), Dr. M.K. Muju (Professor, Department of Mechanical Engineering, A.K.G.E.C. Ghaziabad) and Dr. K.S. Kasana (Chairman, Department of Mechanical Engineering, N.I.T. Kurukshetra) for their encouragement and support during this research work.

The author wishes to place on record his profound gratitude to Dr. Rupinder Singh (Assistant Professor, Department of Production Engineering, G.N.E. College, Ludhiana), Dr. O.P. Pandey (Head, Department of Physics & Material Science, T.U. Patiala), Dr. S.K. Das (Lecturer, Department of Physics & Material Science, T.U. Patiala), Dr. Hari Singh (Assistant Professor, Department of Mechanical Engineering, N.I.T. Kurukshetra), Mr. Charlie White (SONIC-MILL, Albuquerque, NM) and Dr. Simon Barnard (Sr. Consultant, BSI International, UK) for their technical advice and support throughout this research work.

The author is grateful to Mr. K. Ramesh (General Manager, Mishra Dhatu Nigam Ltd., Hyderabad) and Mr. S.S. Arora (Manager, Punjab Abrasives Ltd., Mohalli) for providing titanium and powdered slurry for this research work. The author is grateful to Dr. M.L. Sharma (Lab Incharge, CIL, Panjab University, Chandigarh) for granting permission to use scanning electron microscope (SEM) facility for analyzing the microstructure of the machined samples.

The author wishes to thank Mr. Trilok Singh and Mr. Sukhdev Chand (Lab superintendents, Machine Tool Lab, Department of Mechanical Engineering, T.U. Patiala) for providing all the possible assistance and co-operation during the course of experimentation.

Grateful thanks are due to faculty and staff of Department of Mechanical Engineering at T.U. Patiala and A.K.G. Engineering College, Ghaziabad for providing encouragement and moral support from time to time.

My firm faith in the Almighty God has led me to face all the problems with smile and helped me to cross all the bridges which came my way during this journey of success.

Last, but not the least, my family deserves special mention for the love, affection and blessings showered on me to undertake and successfully complete this research work leading to Ph.D. degree. Special ones deserve special acknowledgement.

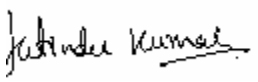

Jatinder Kumar

CERTIFICATE

Certified that the thesis entitled "**INVESTIGATING THE MACHINING CHARACTERISTICS OF TITANIUM USING ULTRASONIC MACHINING**" which is being submitted by Mr. Jatinder Kumar, to the Department of Mechanical Engineering, Thapar University, Patiala, in the fulfillment of the requirements for the award of the degree of **DOCTOR OF PHILOSPHY,** is a record of bonafide research work carried out by him under our guidance and supervision. The matter presented in this thesis has not been submitted either in part or full to any other University or Institute for the award of any degree.

15/2/09

(Dr. J. S. Khamba)
Professor & Head,
Department of Mechanical Engineering,
University College of Engineering,
Punjabi University, Patiala-147004.
Supervisor

15/2/09

(Dr. S.K. Mohapatra)
Professor & Head,
Department of Mechanical Engineering,
Thapar University, Patiala.
Co-Supervisor

ABSTRACT

Titanium has been known as the 'metal of the future' for last few decades owing to its ever increasing applications in aerospace; marine; defense; nuclear energy; missiles; chemical production; hydrocarbon processing; power generation; desalination; nuclear waste storage and processing; metal recovery; offshore; marine deep sea applications; anodes; automotive components, food and pharmaceutical processing, medical implants and surgical devices and many other emerging fields of science and technology. Titanium is branded as difficult-to-machine metal as the conventional machining processes are unable to provide cost-effective solution for its commercial machining. Titanium is machined commercially by non-traditional methods such as Electric Discharge Machining (EDM) and Laser Beam Machining (LBM), but the surface quality obtained is not satisfactory from the prospect of surface integrity as well as surface finish. Ultrasonic Machining (USM) is another non-traditional machining process that is widely used in commercial machining of hard and brittle materials such as ceramics, refractory materials and precision stones. USM is a process known for its capabilities in providing excellent surface finish without any significant alterations is surface integrity or structure of the work material. Moreover, the compressive stress induced in the sub-surface as a result of repeated impacts of abrasive grains contributes in improving the fatigue strength of the machined components; which is a very important aspect especially for a material like titanium. Hence, the study was aimed to investigate the machining characteristics of titanium using different tool materials in ultrasonic machining and to model these characteristics for their application in the concerned manufacturing industry. The machining characteristics investigated are material removal rate (MRR); tool wear rate (TWR) and surface roughness. In the present investigation, the work has been limited to commercially pure titanium (ASTM Grade-I) as work material, in combination with five different tool materials (High carbon steel; High speed steel; titanium; titanium alloy and cemented carbide) for experimentation. The results showed that the response variables were strongly influenced by control factors (input parameters).

LIST OF TABLES

LIST OF FIGURES

LIST OF APPENDICES

CONTENTS

CHAPTER 1
INTRODUCTION

With the development of technology, the scientists and technologists in the field of manufacturing are facing more and more challenges. Technologically advanced industries such as aeronautics, nuclear reactors and automobiles have been demanding high strength temperature resistant (HSTR) materials having high strength to weight ratio. Researchers in the area of materials science are developing materials having higher strength, hardness, toughness and other diverse properties. This also needs the development of improved cutting tool materials so that productivity is not hampered.

It is a well established fact that during conventional machining processes an increase in the hardness of work material results in a decrease in the economic cutting speed. It is no longer possible to find tool materials which are sufficiently hard and strong to cut (at economic cutting speeds) materials such as titanium, stainless steel, nimonics, fiber-reinforced composites, ceramics and stellites. Production of complex shapes in such materials is still more difficult using conventional methods [37, 101]. Other higher level requirements such as better surface quality, low value of tolerances, higher production rates and miniaturization pose greater problems in machining of such materials. Making of holes (shallow entry angles, non-circular, micro holes, large aspect ratio, contoured holes and holes without burr) in difficult to machine materials is another area where extensive research is the need of the hour [65].

To meet such demands, a different class of machining processes known as non-traditional machining processes has been developed. These newer methods are also called unconventional in the sense that conventional tools are not employed for metal cutting. Instead, the energy in its direct form is utilized to remove the material from the workpiece. The range of application of the newly developed machining processes is determined by the work material properties such as electrical and thermal conductivity, melting temperature, electrochemical equivalent etc. The use of these processes is becoming increasingly unavoidable and popular at the shop floor.

Non-traditional machining processes can be classified into four basic categories on the basis of type of energy involved for machining purpose. Table 1.1 shows the various advanced machining processes and some basic aspects of these processes.

Table 1.1 Classification of Non-Traditional Manufacturing Processes

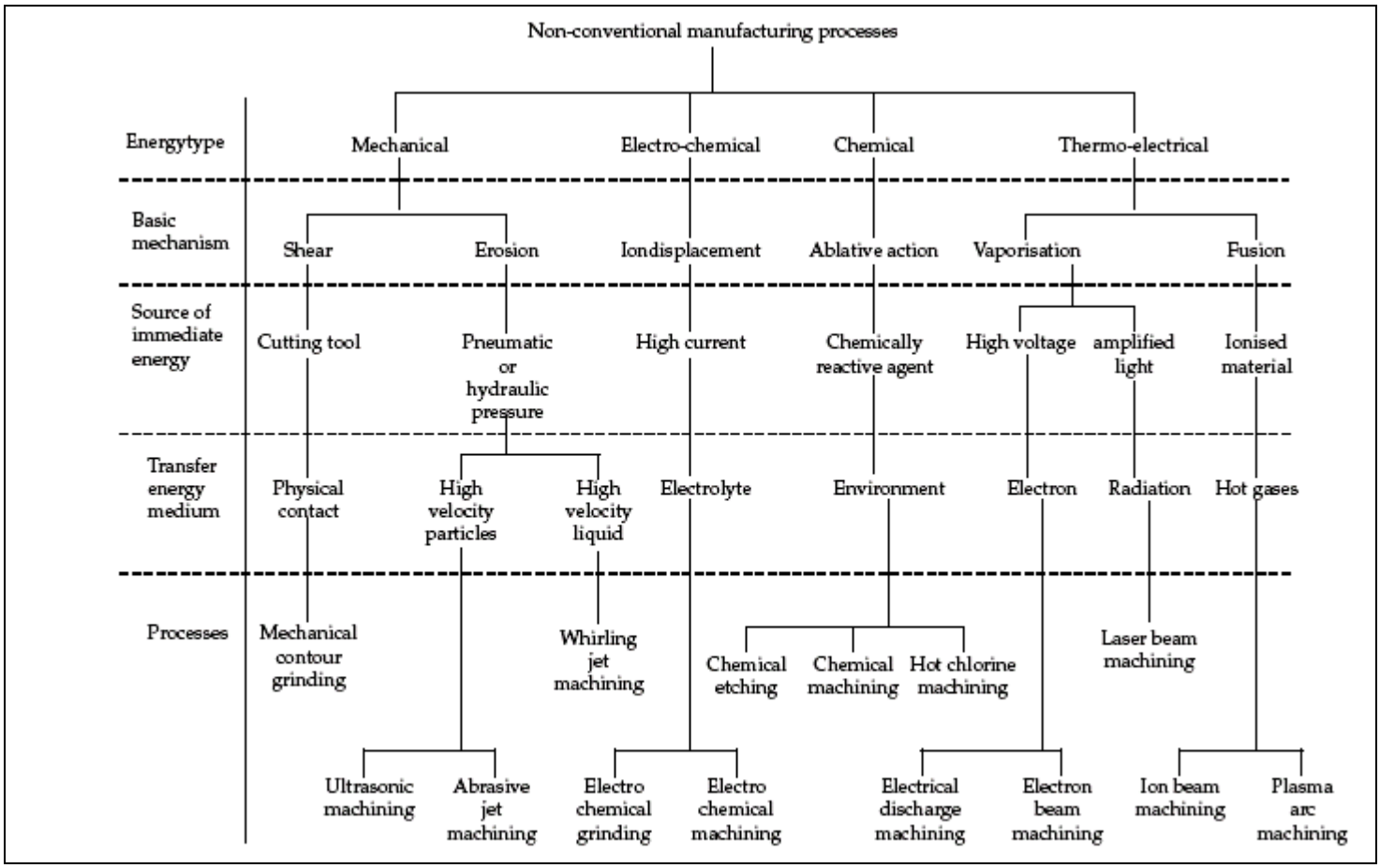

Quite often, non-traditional machining processes are able to provide a capability that simply cannot be met with conventional techniques. These processes are applied to increase productivity either by reducing the number of overall manufacturing operations required to produce a product or by performing operations faster than the previously used method. In other cases, these processes are used to reduce the number of rejects experienced by conventional machining method by increasing repeatability, reducing in-

process-breakage of fragile materials or by minimizing adverse effect on work material properties.

A comparative analysis of the various non-traditional manufacturing processes should be made before selecting a particular process for a given situation [168]. The analysis can be made from the point of view of:

- Physical parameters involved in the process.
- Capability of machining different types of shapes
- Applicability of different processes to various types of materials i.e. metals
- Operational characteristics of manufacturing
- Economics involved in the various operations.

The physical parameters have a direct impact on the metal removal and energy consumed in various manufacturing processes. From a comparative study of the effect of metal removal rate on power consumption (Figure 1.1) in various manufacturing processes, it has been found that some of the processes such as EBM and ECM consume a great amount of energy than the other processes [20]. These processes involve a higher capital cost than those processes that lie below the mean power consumption line.

The capability of different manufacturing processes has been analyzed on the basis of various machining operation point of view such as drilling, contouring, cavity sinking, through cutting (shallow and deep). A summary of the shape applications of various non-traditional manufacturing methods has been given in table 1.2.

For micro-drilling operation, laser beam machining (LBM) can be adjudged as most suitable processes, whereas for drilling holes with higher slenderness ratio ($l/d>20$), processes such as USM, EDM and ECM would be best applicable. For surface contouring operation, only EDM process is a feasible alternative to ECM [115].

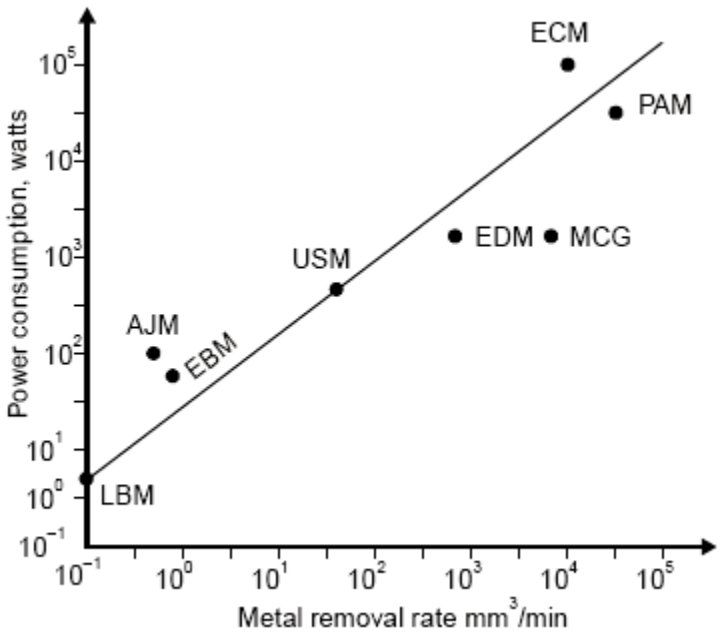

Figure 1.1 Comparative energy consumption for various processes

Table 1.2 Shape applications of various processes

Process	Holes				Through Cavities		Surfacing	Through Cutting	
	Precision small holes		Standard		Precision	Standard	Double Contouring	Shallow	Deep
	Dia < .025 mm	Dia > .025 mm	Length < 20 mm	Length < 20 mm					
USM	___	___	good	poor	good	good	poor	poor	___
AJM	___	___	fair	poor	poor	fair	____	good	___
ECM	___	___	good	good	fair	good	good	good	good
CHM	fair	fair	____	____	poor	fair	____	good	___
EDM	___	___	good	Fair	good	good	fair	poor	___
LBM	good	good	fair	poor	poor	poor	____	good	fair
PAM	___	___	good	___	poor	poor	____	good	good

Material applications of various non-traditional machining processes have been summarized in table 1.3. For machining of electrically non-conductive materials, EDM and ECM are unsuitable whereas mechanical processes such as USM and AJM can be used easily, particularly in the case of refractory materials or hard and brittle metals [130].

The machining characteristics of various processes can be analyzed with respect to the material removal rate (MRR), tolerance maintained, surface finish obtained, depth of surface damage and power required for machining. A summary of the machining characteristics of various non-traditional machining methods has been given in table 1.4.

Table 1.3 Material applicability of various processes

Metals/Alloys					
Process	**Aluminium**	**Steel**	**Super alloy**	**Titanium**	**Refractories**
USM	Poor	Fair	Poor	Fair	Good
AJM	Fair	Fair	Good	Fair	Good
ECM	Fair	Good	Good	Fair	Fair
CHM	Good	Good	Fair	Fair	Poor
EDM	Fair	Good	Good	Good	Good
EBM	Fair	Fair	Fair	Fair	Good
LBM	Fair	Fair	Fair	Fair	Poor
PAM	Good	Good	Good	Fair	Poor

The material removal rates by ECM and PAM are about one fourth and 1.25 times that of conventional whereas others are only small fractions of it. The surface finish and tolerance obtained by USM process is best among the various non-traditional processes [104].

The economy of various non-traditional processes can be adjudged on the basis of the capital cost, tooling cost, material removal efficiency and tool wear. The capital cost of ECM is very high when compared with traditional contour machining and other non-

traditional processes, whereas capital costs for USM and AJM are comparatively lower. EDM has got higher tooling cost than other processes, whereas material removal efficiency is higher for EBM and LBM processes.

Table 1.4 Machining characteristics of various processes

Process	MRR (mm^3/min)	Tolerance (µm)	Surface (µm) CLA	Depth of Surface damage (µm)	Power (watts)
USM	300	7.5	0.2-0.5	25	2400
AJM	0.8	50	0.5-1.2	2.5	250
ECM	15000	50	0.1-2.5	5.0	100000
CHM	15	50	0.5-2.5	50	-
EDM	800	15	0.2-1.2	125	2700
EBM	1.6	25	0.5-2.5	250	150 (avg.)
LBM	0.1	25	0.5-1.2	125	2000 (peak)
PAM	75000	125	Rough	500	50000
Machining	50000	50	0.5-5.0	25	3000

In conclusion, the suitability of application of any of the processes is dependant on various factors and choice of a particular process for a given situation must be based on the consideration of some or all of these factors.

1.1 ULTRASONIC MACHINING

Ultrasonic Machining (USM) is a non-conventional mechanical material removal process used for machining both electrically conductive and non-metallic materials; preferably those with low ductility and a hardness above 40 HRC [130, 134, 149, 162, 168] such as inorganic glasses, ceramics, quartz etc. The process came into existence in 1945 when L. Balamuth was granted the fist patent for the process. USM has been variously termed ultrasonic drilling; ultrasonic cutting; ultrasonic abrasive machining and slurry drilling.

In USM, high frequency electrical energy is converted into mechanical vibrations via a transducer/booster combination, which are then transmitted to an energy focusing as well as amplifying device known as horn or sonotrode. This causes the tool to vibrate

along its longitudinal axis at high frequency; usually greater than 20 kHz with an amplitude of 12–50 μm [20, 37-39, 73, 84, 112-115]. The power ratings range from 50 to 3000 W and a controlled static load is applied to the tool to provide feed in the longitudinal direction. Abrasive slurry, which is a mixture of abrasive material such as silicon carbide, boron carbide or alumina suspended in water or some suitable carrier medium is continuously pumped across the gap between the tool and work (25–60 μm). The vibration of the tool causes the abrasive particles held in the slurry to impact the work surface leading to material removal by micro-chipping [103, 138]. Figure 1.2 shows the basic elements of an USM set up using a magnetostrictive or piezoelectric transducer with brazed or screwed tooling.

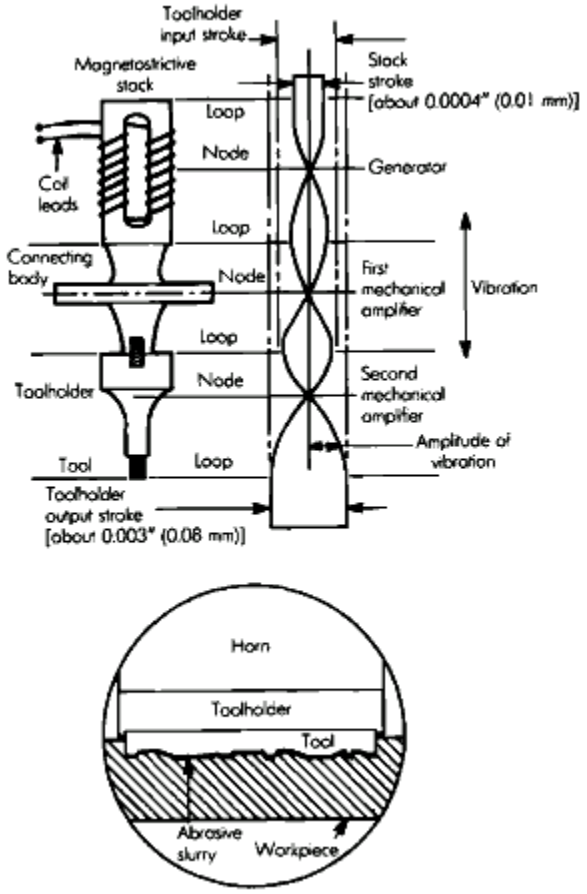

Figure 1.2 Ultrasonic machining

Variations of this basic configuration include:

1. Rotary Ultrasonic Machining (RUM). In this process, tool vibrates and rotates simultaneously thereby improving the material removal rate (MRR) and reducing the geometric inaccuracies; for example, oversize and out of roundness, etc. [60, 96, 116-118, 123, 161, 173, 175]. The construction of RUM machines is similar to USM except for the addition of a 0.37-0.56 kW rotary spindle motor capable of rotating up to 5000 rpm [120].
2. USM combined with electric discharge machining [158,167,174,177-178].
3. Ultrasonic assisted cutting or grinding. Ultrasonic aided turning is the most common process in this category and is claimed to reduce machining time, work residual stresses and improve surface quality and tool life compared to conventional turning [14, 17, 25, 62, 67, 72, 99, 105].
4. Other non-machining applications such as cleaning, welding and coating.

USM is generally associated with low material removal rates; however its application is not limited by the electrical or thermal characteristics of the work material. Because the process is non-thermal and non-chemical, the materials processed are not altered either chemically or metallurgically [168]. Holes as small as 76 μm in diameter can be drilled, however the depth to diameter ratio is limited to 3:1 [73, 159]. For efficient machining to take place, the tool and horn must be designed with consideration given to mass and shape so that resonance can be achieved within frequency range capability of the ultrasonic machine.

1.1.1 Basic elements of an ultrasonic machine tool

Ultrasonic machines range from small tabletop-sized units to large capacity machine tools. In addition to the part-size capacity of a USM machine, suitability for a particular application is also determined by power rating [20]. All ultrasonic machines share common subsystems regardless of the physical size or power [20]. The most important of

these subsystems are the power supply, transducer element, tool holder or horn and abrasive supply system. A detailed description of these components is given as following:

1.1.1.1 The ultrasonic power supply and transducer

The power supply for an ultrasonic machine tool is more accurately characterized as a high power sine wave generator that offers the user control over both the frequency and power of the generated signal [20]. It converts low frequency (50 Hz) electrical power to high frequency (approx. 20 kHz). This electrical signal is applied to the transducer for further conversion into the mechanical motion in form of vibrations. The power supplied depends upon the size of transducer [16]. Some generators are designed with safety features such as an auto cut-off in cases of horn fracture, tool failure or overloading [39].

Transducers convert electrical energy into mechanical motion. With a conventional generator system, the tool and horn are set up and mechanically tuned by adjusting their dimensions to achieve resonance [43]. They can accommodate very small errors in set up or tool wear, giving minimum acoustic energy loss and very small heat generation [81]. Two types of transducers used for USM are based on two different principles of operation, piezoelectric and magnetostrictive [20, 84]. Because of its lower Q value (Q is a measure of the sharpness of the peak value of energy); the magnetostrictive transducer allows vibration to be transmitted over a wide frequency band [70]. It also allows greater horn design flexibility and can accommodate tool wear. The major drawback of magnetostrictive transducer is high electrical losses and low energy efficiency (about 55-60%). On the other hand, piezoelectric transducers are more energy efficient (90-96%). Also this type of transducers can generate high vibration intensities as compared to magnetostrictive transducers [20, 37, 39, 130, 139, 172]. Magnetostrictive transducers are usually constructed from a laminated stack of nickel sheets.

1.1.1.2 The ultrasonic horn and tool assembly

The function of tool holder (horn) is to attach and hold the tool to the transducer. Tool holders are attached to the transducer by means of a large, loose-fitting screw [102]. The oscillation amplitude at the face of the transducer is too small (0.001-0.1 μm) to achieve

any reasonable cutting rate [9], therefore, the horn is used as an amplification device. Half hard copper washers are used between the transducer and tool holder to dampen and cushion the interface, which reduces the chances of any unwanted ultrasonic welding [130]. Figure 1.3 shows the amplifying tool holders and mechanically attached tools for USM [151].

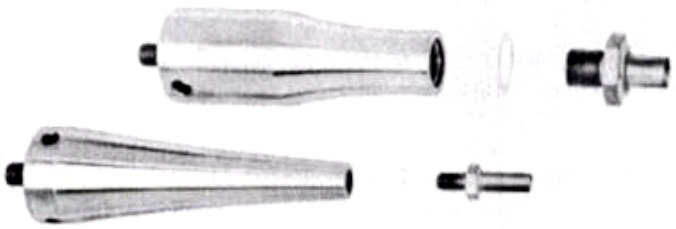

Figure 1.3 Amplifying tool holders

The material used for fabrication of horn must possess high wear resistance, good elastic and fatigue strength properties; and corrosion resistance [135]. Monel, titanium, stainless steel and aluminium bronze materials are used for making tool holder for ultrasonic machines. Figure 1.4 shows different horn designs with and without additional tool heads [159].

The tool should be so designed to provide the maximum amplitude of vibration at the free end at a given frequency [135, 137]. The material used should have high wear resistance, good fatigue strength and optimum values of hardness and toughness [102]. Tungsten carbide, silver steel, monel are the commonly used tool materials. Polycrystalline diamond (PCD) has recently been detailed for the machining of very hard work materials such as hot isostatically pressed silicon nitride [160].

Tools can be joined to the horn either by soldering or brazing, screw fitting. Alternatively, the actual tool configuration can be machined to the end of the horn [151]. Threaded joints have also been used conventionally to achieve the ease of tool changing,

however problems such as self-loosening, loss of acoustic power and fatigue failure have been reported for such tools [89].

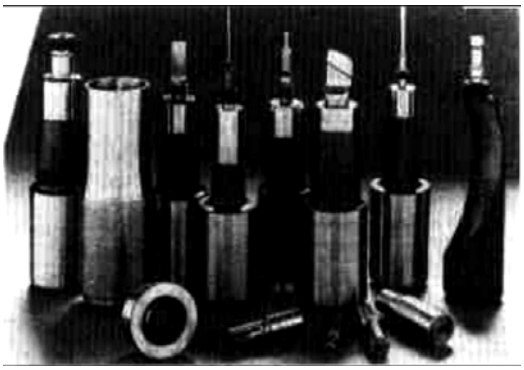

Figure 1.4 Different horn designs for USM [159]

Depending upon the abrasive used, the work/tool wear ratio can range from 1:1 to 1:100. [104]. Tool is usually held against the workpiece by a static load exerted via a counter weight, spring, pneumatic/hydraulic or solenoid feed system [84, 115, 149]. For optimum results, the system must maintain a uniform working force while machining and be sufficiently sensitive to overcome the resistance due to cutting action [130-131]. Static load values of about 0.1-30 N are commonly used. This force is particularly critical when drilling small holes less than 0.5 mm diameter as bending of tool can occur under too high load.

1.1.1.3 Abrasives

In ultrasonic machining, abrasive slurry (mixture of abrasive and fluid such as water) is used to achieve the cutting action. Different types of abrasive materials can be used for making the slurry. Aluminium oxide, silicon carbide and boron carbide are the most commonly used abrasive materials. For precision machining and very hard workpiece materials, cubic boron nitride or diamond powder is also used as abrasive. Table 1.5 details some commonly used abrasive materials and their relative hardness and cutting abilities.

The transport medium for the abrasive should possess low viscosity with a density approaching to that of the abrasive, good wetting properties and preferably, high thermal conductivity and specific heat for efficient cooling [18, 79, 159]. The most commonly used concentration is 50% by weight [70]. Thinner mixtures are used to promote efficient flow when drilling deep holes or forming complex cavities [71, 119].

Table 1.5 Abrasives used in USM

Abrasive	**Knoop Hardness**	**Relative cutting power**
Diamond	6500-7000	1.0
Cubic Boron Nitride	4700	0.95
Boron carbide (B_4C)	2800	0.50-0.60
Silicon carbide (SiC)	2480-2500	0.25-0.45
Alumina (Al_2O_3)	1850-1920	0.14-0.18

Once the abrasive is selected and mixed with water, it is stored in a reservoir at the USM machine and is pumped to the tool-work interface by the re-circulating pumps at rate up to 36.5 L/min.

1.1.2 Tooling considerations and applications

The tool is shaped conversely to the desired hole or cavity and positioned near, but not touching, the work surface [20], generally manufactured by silver brazing [146]. In many cases, a tool of either simple or complex cross-section is penetrated axially to the work piece to produce either a through or blind hole of the required dimensions [20, 159]. For three dimensional cavities, a process analogous to die sinking is generally employed [54, 106, 111, 131]. Figure 1.5 shows an example of three dimensional cavity forming.

Use of special tools to simultaneously produce a multitude of holes in precise patterns has also been reported [105]. The gang drilling technique has significantly improved the productivity of USM without compromising on quality.

Although the volumetric material removal rate in USM is quite low, the process remains competitive because of its ability with a single pass of the tool, to generate complex cavities or multiple holes in work materials that are too hard or fragile to be machined by alternate processes [168]. Application of USM for simultaneous drilling of multiple holes has been illustrated in figure 1.6.

Figure 1.5 Silicon nitride turbine blade counter-sunk using USM

In a similar application, 2176 square holes measuring 0.79 mm on a side were simultaneously machined in a 1.01 mm thick carbon plate in 10 minutes [159]. Because such a large number of holes were drilled simultaneously, an alternative process that drills one hole at a time would have to generate holes at rate of 3.6 per second to be able to match the rate of USM [20]. Figure 1.7 shows drilling of multiple holes in ceramic metal composite matrix panel of 0.96 mm thickness using USM [96].

USM has been applied for machining of plastics and engraving of coins. Because of its ability to machine the exact shape of the tool into the work surface, the accuracy obtained in engraving operations is exceptional [44]. Figure 1.8 shows a plastic sample that has inner groves machined by USM.

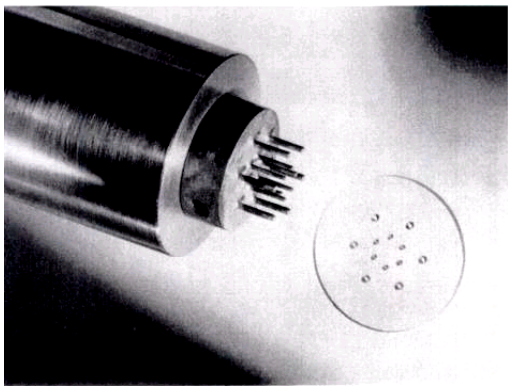

Figure 1.6 USM gang drilling tool for drilling 12 holes simultaneously

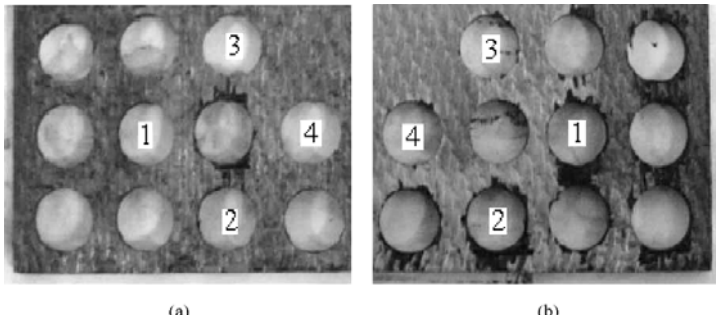

Figure 1.7 Drilling of multiple holes in CMC panel [96]

Using ultrasonic machining, graphite electrode for EDM was shaped in 30 minutes instead of the 20 hours required by copy milling [45, 83, 105]. The problem of using tools of complex form, however, was that they were not subjected to same machining rate over the whole of working surface and experienced differential wear rate, both of which affect the product shape [41].

An alternative approach has been to use a simple pencil tool and contour machine the complex shape with a CNC programme. Figure 1.9 shows hypodermic needle that was used to ultrasonically drill small holes through a silicon nitride workpiece. Recently, this technique has been investigated in a number of countries including the UK, France, Switzerland, Japan etc [107, 159]. Most successful USM applications involve drilling

holes or machining cavities in non-conductive ceramic materials. Figure 1.10 shows a cylindrical specimen of quartz machined with USM [51].

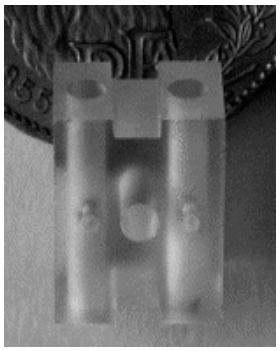

Figure 1.8 Plastic sample machined with USM

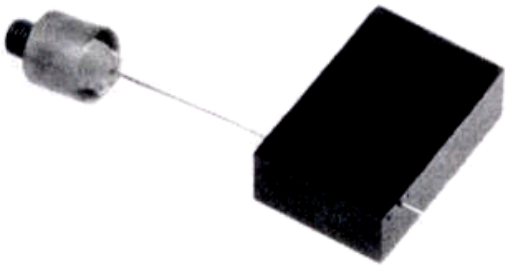

Figure 1.9 Silicon nitride machined by hypodermic needle using USM [127]

Recently, the use of USM for machining of $Al_2O_3/LaPO_4$ composites was explored by Majeed et al. [98]. No appreciable surface damage or defects were reported while machining these composites with USM. In another investigation [59], a preliminary study on ultrasonic drilling of fiber-reinforced plastics was conducted. The machining efficiency for drilling of multiple holes in FRP has been found to be superior to other conventional processes, without any structural alterations.

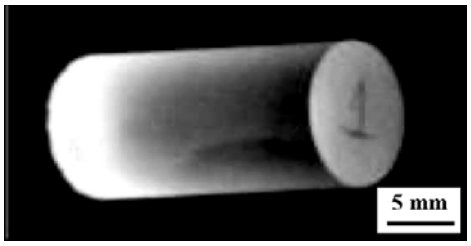

Figure 1.10 Cylindrical specimen of quartz machined by USM [51]

A novel use for USM has been the multi-step process for fabricating ceramic turbine blades (Figure 1.11). The technique removes a large volume of material that would otherwise have been removed by much slower technique of pantograph profile grinding [127]. The selection of USM as a manufacturing process has occurred because no other process was capable of performing the task. The alternative processes would have required substantially longer processing times [20].

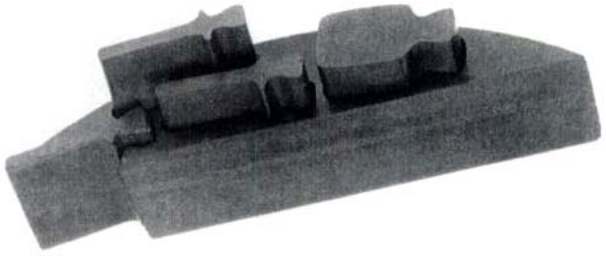

Figure 1.11 Ceramics turbine blade blank machined by USM

1.1.3 MRR models and mechanism of material removal

Various analytical MRR models suggested thus far by various investigators [28, 68, 95, 103, 110, 124, 131, 138, 169] have been presented in table 1.6. Shaw [138] was the first researcher to propose a static and simple analytical model giving the relationship between MRR and vibration amplitude, frequency, abrasive grit size and concentration and feed force. However, its predictions do not agree well with the experimental observations. Miller [103] proposed a MRR model based on the plastic deformation restricting its application to ductile materials only, while Rosenberg and Kazantsev [131] included the statistical distribution of abrasive particle size in their

computational model. Cook [28] developed a simplest model to predict the linear machining rate. Kainth et al. [68] proposed another static and complicated model using the abrasive particle size distribution. Nair and Ghosh [110] also proposed a computationally intensive model simulating the principles of elastic wave propagation. Wang and Rajurkar [124] suggested a more realistic model taking into account the stochastic and dynamic nature of the process. But this is applicable to perfectly brittle materials only. Lee and Chan [95] developed an analytical model to predict the effects of vibration amplitude, grit size and feed force on MRR and surface roughness for ceramic composites. Wiercigroch et al. [169] have proposed another model to predict the MRR in ultrasonic drilling using an impact oscillator approach. The inherent non-linearity of the discontinuous impact process has been modelled to generate the pattern of impact forces. This model explains the experimentally observed fall in MRR at higher static forces.

From all these models, four different mechanisms can be identified, which are responsible for removal of material from the work surface (figure 1.12). These are described as:

- Material abrasion by direct hammering of the abrasive particles against the work piece surface [28, 68, 95, 103, 110, 131, 138, 169].
- Micro chipping by impact of free moving particles [43, 103, 110, 131, 153].
- Cavitation effect from the abrasive slurry [43, 128, 138, 152].
- Chemical action associated with the fluid employed [138, 168].

The individual or combined effect of the above listed mechanisms results in material removal by shear [138] or by fracture [28, 68, 95, 110, 131] and by displacement of the material at surface, without removal, by plastic deformation [103], which occurred simultaneously at the transient surface. With porous materials such as graphite, cavitation erosion has been found to be a significant contributor of material removal as opposed to hardened steels and ceramics [128]. Riddie [128], Bulat [22] and Willard [170] reported that the cavitational bubbles formed during the ultrasonic oscillations produce a pressure

more than 1000 kgf/cm^2 on the work surface when they collapse. This pressure rise also causes material removal.

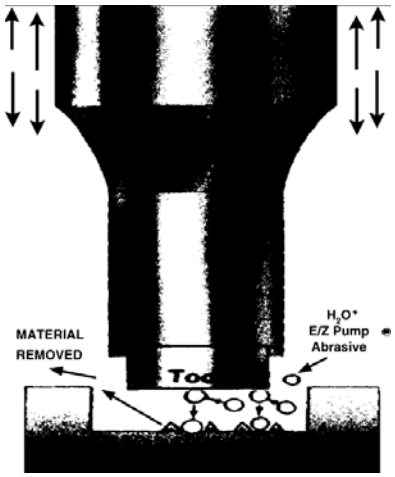

Figure 1.12 USM material removal mechanisms [142]

The initiation and propagation of median as well as lateral cracks has been considered to contribute greatly to the material removal process in ultrasonic machining [42, 52, 66, 95] of ceramic composites. The sharp point of indenter (abrasive grain) produces an inelastic deformation zone and at some threshold, a deformation-induced flow suddenly develops into a small crack, termed as a median crack. An increase in the load causes further growth of the median crack. During unloading, the median crack begins to close; inducing the formation of lateral vents [95, 118, 124]. Upon complete unloading, the lateral vents continue their extension towards the work surface and lead to chipping.

It has been reported that as long as the working gap between the tool and work piece surface is more than the mean size of the abrasive grains used, no significant machining can take place [152, 166]. The free impact mechanism has been found to be more effective and significant with larger grain sizes of abrasive used. With fine grit sizes of abrasive grains, direct hammering mode has been found to be predominant for material removal.

Table 1.6 MRR models for USM

Name of Investigator	Mechanism of material removal	Assumptions	Limitations
M.C. Shaw [138]	Direct hammering of abrasive particle (Primary) Impacting by free moving particles (secondary)	All abrasive particles are identical, rigid, spherical in shape. All impacts are identical. Material removal is proportional to volume of material removed per impact, number of particles impacting per cycle and frequency of impacting. Penetration depth is inversely proportional to flow stress of work material. For a given area of tool face, number of active grains is inversely proportional to square of the mean diameter of grains.	Analysis does not agree with experimental results qualitatively. Does not predict the effect of variation in amplitude, feed force or frequency correctly. Predicts infinite increase in machining rate with static force while an optimum value exists due to grain crushing. No allowance for grain size variation and for crushed grains.
G.E. Miller [103]	By chipping plastically deformed and work hardened material. In ductile material, MRR depends upon work hardening while in brittle material on size and rate of chip formation.	Abrasive particles are of cubical size. Plastic deformation is directly proportional to the stress. Plastic flow stress equals Burger vector times shear modulus. Cross –sectional area of the cut does not change during machining. Viscosity effects in water slurry are almost negligible.	Applicable to ductile materials only as MRR is assumed to depend on plastic deformation. Some non-realistic assumptions such as cubical shape of grains and participation of all grains in cutting action (under the tool tip) have been made. No allowances for grain size variation. Number of active grains is derived assuming slurry is drawn when tool recedes.
Rozenberg Kazantsev [131]	Brittle fracture	Abrasive particles are incompressible and are of irregular shape but can be considered as spheres having projections whose radii of curvature are proportional to the mean dimensions of particle. Based on the experimental evidence, the statistical distribution of abrasive particle size d is given by: $\varphi(d) = 1.095 \frac{N}{d_m}\left[1-\left(\frac{d}{d_m}-1\right)^2\right]^3$ where N is number of active abrasive grains, d_m is the mean diameter of grains.	Involves tedious computation and its solution requires numerous integration.

N.H. Cook [28]	Hemispherical indentation fracture	Abrasive grains are spheres of uniform radius. Tool and abrasives are rigid. Viscosity effects are negligible. A linear relationship between fraction of active grits and ratio of indentation depth to grit-radius has been assumed.	Model predicts linear relationship between static stress and MRR, while MRR drops after a certain value of feed force. It predicts that MRR is proportional to square root of the grain radius, while practically an optimum value exists.
G.S. Kainth et al. [68]	Indentation fracture due to direct hammering action	Abrasive grains are spherical in shape and follow Rozenberg's size distribution functions to take into account particle size inhomogeneity. Motion of tool remains sinusoidal under loaded conditions.	Computationally intensive. Predicts linear relationship between MRR and static force F that is practically not true. Predicts linear increase in MRR with grain size, while and optimum value exists. Theoretical machining rate is higher than practical values.
Nair and Ghosh [110]	Brittle fracture	Abrasive particles are rigid spheres No consideration for MRR due to particle impacting, cavitation or chemical action of slurry Tool tip motion is SHM and abrasive particle rests on a brittle half-space and receives only a single impact in this position.	Derivation of the model is computationally intensive. The volume fractured by a single abrasive grain is to be calculated using fracture profile.
Wang and Rajurkar [124]	Combined effect of impact indentation and fracture phenomenon	Work-piece is assumed to be semi-infinite solid. Axis of moving grit is perpendicular to the free surface during machining. Speed of abrasive is same as that of vibrating tool.	Can be used for perfectly brittle materials only like amorphous glass. Results are not true for materials which exhibit some plastic behavior like carbides.
Lee and Chang [95]	Brittle fracture	Pre-existing flaws are assumed in the material for the initiation of median or lateral cracks. Size of median or lateral crack is related to pseudo pressure between tool and work-piece. Cutting tool is assumed to be a slender column	Applicable to brittle materials only.
Wiercigroch et al. [169]	Micro-cracking due to impacts of grains	MRR is a function of the magnitude of impact force and its frequency. Diamond is uniformly distributed over the working part of tool with a uniform grit size. Ultrasonic vibration amplitude, frequency and tool geometry remain unchanged.	Applicable to hard and brittle materials only. Tool geometry changes with progress in machining as the wear on the surface of tool is not uniform.

From the dynamic impact tests, material removal in USM process appears to be a function of the impact velocity, which is determined by the frequency and amplitude of the vibrating tool [166]. Material in the impact zone is removed by fragmentation and due to high compressive stresses developed in the region. At low impact velocities, structural disintegrations and particle dislocations occur, which are responsible for material removal. At higher velocities, material is removed by a network of intergranular micro-cracks and from the intersection of lateral and median cracks [166].

1.1.4 Process Capabilities of conventional work and tool materials

USM is valuable process for precision machining of hard, brittle materials. Although USM is not limited by high-hardness materials, best machining rates are obtained for materials having hardness more than HRC 60 [130, 134, 149, 162, 168]. Materials such as carbides, ferrites, germanium, ceramics, glass and tungsten are representative of those that are difficult to process conventionally and can benefit the most from the USM process [16-17, 48, 52, 54, 58, 74, 82, 99, 150]. When performing drilling operation, USM can produce holes as small as 76 μm in diameter [159]. The best tolerance that can be obtained practically in ultrasonic drilling is of the order of ± 25 μm; however with special considerations given to slurry circulation and abrasive selection, tolerances of the order of ± 10 μm can be achieved [73]. Holes of up to 64 mm thickness can be drilled successfully without applying special efforts. When optimum flushing techniques are used, hole-depth capabilities can be extended to 150 mm with aspect ratio up to 40:1 [40-41, 79-81]. However, effective machining rate is reduced for machining of work piece thickness more than 12.7 mm, due to inefficient slurry flow through the cutting gap [18, 45, 47, 69, 93]. Penetration rates, ranging from 0.025-25 mm/min can be obtained depending upon the shape being machined, input parameter settings and work material properties [100, 106-107, 119]. Surface finish is generally governed by abrasive particle size [4, 30, 34, 37, 44, 51, 58, 71, 78, 86]. From the literature available on USM, best surface finish has been reported while using 800 grit abrasives and is of the order of 0.25 μm [21]. Because USM is a non-thermal and non-electrical process, the work material properties remain unaltered [106-107, 111-115]. Table 1.7 shows the machining

performance of USM for different work materials while using a cold rolled steel tool and boron carbide abrasive (particle size 32 μm) [104].

Currently, the principle fields of application of ultrasonic machining are:

1. Manufacture of hard alloy wire drawing, punching and blanking dies, also making small complicated dies of steel.
2. Machining semi-conducting materials such as germanium and silicon.
3. Machining ferrite and other special metal-ceramic materials used in electrical installations.
4. Making instruments and optical parts of glass, quartz, fluoride and barium titanate.
5. Making components of porcelain and special ceramics.
6. Cutting accurate shallow holes of rectangular or other section in cemented or nitrided steel.
7. Cutting of industrial diamonds.
8. Grinding of glass, quartz and ceramics.
9. Cutting holes with curved or spiral center line and cutting threads in glass and mineral ceramics.
10. Machining the graphite electrodes used in EDM process.
11. Counter-sinking of silicon nitride or ceramic turbine blades.
12. Drilling multiple holes simultaneously in ceramic metal composite matrix (CMC) panels.

Table 1.8 shows various materials that have been reported to be successfully machined by using USM A comprehensive review has been carried out on the machining characteristics of USM, by comparing and analyzing the investigations of many researchers. Table 1.9 presents detailed review on machining characteristics and process capabilities of USM. Table 1.10 gives operational summary of the process.

Table 1.7 Machining performance of USM [104]

Material	**Ratio of MRR to TWR**	**Max. machining area (sq. mm)**	**Avg. machining rate (mm/min)**
Glass	100:1	25.8	3.81
Ceramics	75:1	19.4	1.51
Germanium	100:1	22.6	2.16
Tungsten carbide	15:1	7.7	0.25
Tool steel	1:1	5.6	0.13
Mother of pearl	100:1	25.8	3.81
Synthetic Ruby	2:1	5.6	0.51
Carbon-graphite	100:1	19.4	2.00
Ferrite	100:1	22.6	3.18
Quartz	50:1	19.4	1.65
Boron Carbide	2:1	5.6	0.20
Glass bonded mica	100:1	22.6	3.18

Table 1.8 Materials successfully machined by USM

Aluminium	Cold rolled steel	Micarata	Ti-alloys
Aluminium Oxide	Febony	Molybdenum	Tungsten
Barium Titanate	Ferrite	Mother of Pearl	Tungsten carbide
Beryllium Oxide	Garnet	Plaster of Paris	Thorium Oxide
Boron carbide	Germanium	Quartz	Uranium Carbide
Boron composites	Glass	Ruby	Zirconium Oxide
Brass	Glass bonded Mica	Sapphire	Diamond
Calcium	Graphite	Silicon Carbide	Fiber-reinforced
Carbides	Hardened Steel	Silicon Nitride	Plastic
Carbon	High Pressure Laminates	Stainless Steel	
Ceramics	Limestone	Stellite	
Composites	Lithium-fluoride	Tool Steel	

Table 1.9 Review on Machining characteristics of USM

Investigator	Work materials	Process Conditions	Characteristics investigated	Results
Dam H. et al. [30]	Glass, SiC Al_2O_3, TiB_2 Hot pressed silicon nitride (HPSN) Zirconium Oxide (TZ3YB)	Fixed: Tool: Steel Slurry: B_4C Grit: 280 Variables: work material	MRR TWR Deviation in hole size (Dev.) Surface roughness (SR)	MRR/TWR Dev. (μm) SR (μm) Glass: 108 10 13.5 Al_2O_3: 30.8 25 9.0 TiB_2 : 23.5 100 3.2 SiC: 4.5 75 6.0 HPSN: 1.2 75 4.0 TZ3YB 0.75 150 2.0
Adithan and Krishnamurthy [2]	Glass	Fixed: Tool: MS Slurry: B_4C Grit: 280 Variable: Static load	Surface roughness (SR) Conicity, Out-of-Roundness (at entry, exit)	Load (kg) SR (μm) Conicity (μm) Roundness (μm) 0.15 10.5 75 55,55 0.35 12.5 65 53, 68 0.50 17.0 85 40,43 0.85 18.2 70 45,75 1.00 18.6 40 43,117
Hocheng and Hsu [59]	Fiber reinforced Plastics	Fixed: Tool: MS Slurry: SiC Variable: Grit: 150-600 Conc: 13-26%	Surface Roughness Deviation in hole size (Dev.)	Surface roughness: 1.2 -2.0 μm Hole clearance: 0.12-0.27 mm
Majeed et al. [98]	$Al_2O_3/LaP0_4$ Composites	Fixed: Slurry: B_4C Grit: 280 Tool: L.C.S. Variable: Work Hardness Tool geometry	MRR	Hardness (kg/mm^2) MRR (mm^3/s) Tool 1 Tool 2 400 0.65 0.25 800 0.60 0.20 1200 0.45 0.12 1600 0.10 0.05 (tool 1: hollow, 2: solid)
Guzzo et al. [51]	Quartz crystal	Fixed: Slurry: SiC Tool: S.S. Variable: Grain size 6-50 μm	TWR Surface roughness (SR)	TWR: 3.4-16.5 μm/s SR: 1.0-1.9 μm
Dvivedi and Kumar [34]	Titanium alloy (6Al-4V)	Fixed: Slurry (B_4C) Variable: Tool material Grain size: 18-64 μm Slurry Conc.	Surface Roughness (SR)	SR: 0.96-3.40 μm Optimized value of SR: 0.97 μm

Komaraiah et al. [78]	Glass (G) Ferrite (F) Porcelain (P) Alumina (A)	Fixed: Static load Amplitude Slurry: SiC Variable: Grit size 220, 280, 320	Surface Roughness (SR) MRR Out-of-roundness	Grit Size A P F G SR (μm) 220 1.2 3.9 1.8 2.6 280 0.7 2.1 0.9 1.6 320 0.4 1.4 0.4 1.3 MRR (mm^3/min) 220 1.8 20.5 2.2 4.5 Out-of- roundness (μm) 180 45 120 56 82
Jadoun et al. [63]	Ceramic Composites	Fixed: Slurry: SiC Static load Variable: Tool materials: HCS, WC, HSS Grit: 18-64 μm Power: 40-60%	Tool wear rate (TWR)	TWR : 0.072-0.34 mm^3/min Optimized value: 0.075 mm^3/min
Komaraiah and Reddy [77]	Glass	Fixed: Slurry and grit size (SiC/220) Variable: Tool MS, Ti, S.S., Niamonic-80, Silver steel	MRR (mm^3/min) Tool wear (mm) Tool hardness (H) after machining (VPN)	Tool MRR Tool wear H MS 3.0 0.77 250 Ti 3.4 0.56 255 S.S. 4.2 0.22 375 Ni-80 5.8 0.11 590 Si Steel 5.5 0.20 535 (Depth of machining: 24 mm)
Jianxin and Taichiu [66]	Ceramic Composites (alumina based)	Fixed: Slurry: B_4C/80 Static load: 10 N Variable: Fracture toughness (work)	MRR Surface Roughness (SR)	Fracture Toughness MRR (mm^3/min) SR (μm) 5.0 0.95 1.75 6.0 0.75 1.20 7.8 0.44 0.82 8.6 0.38 0.60
Komaraiah and Reddy [76]	Glass, ferrite Alumina, WC Porcelain	Variable: Work hardness Fracture toughness	MRR	$MRR \propto \frac{P^2}{K^{1.5}H^{0.5}} \cdot \frac{f}{N}$ P is the static load, f is frequency K is fracture toughness, H is hardness N is effective no. of grains in the gap
Zhang et al. [176]	Alumina ceramics	Tool: L.C.S. B_4C/120 Variable: Static load Amplitude Grain size	MRR (mm^3/min)	Load (N): 10 15 20 25 30 MRR: 3.5 4.5 5.5 5.0 3.0 Grit (μm) 50 100 150 200 MRR: 4.0 5.3 5.5 5.3 Amp (μm) 03 06 09 12 MRR: 2.8 4.5 5.6 5.8

Table 1.10 Operational Summary for USM Process

Power	200-4000 W
Frequency	15-30 kHz (most commonly ~20kHz)
Abrasives	
Type	Cubic Boron nitride (very few cases) Boron Carbide (specific applications) Silicon Carbide (most commonly used) Alumina (frequently)
Size	Mesh 120-1200 Size: 06-142 µm
Concentration	20-60% by volume with water as medium Oil is used for finishing operations.
Flow	Max. 36.5 L/min.
Amplitude	05-70 µm (for optimum results, amplitude should be equal to mean abrasive particle diameter)
Static Force	0.45 to 5 kg, generally 4.5 kg
Tool Material	Stainless Steel, Silver Steel, Monel, Molybdenum
Cutting gap	20-150 µm
Over-cut	Twice the grit size (approx.)
Depth of Cut (max.)	Up to 90 mm, normally 64 mm
Accuracy	± 25 µm
Taper	05 µm per mm
Surface Roughness	0.25 to 1.5 µm
Minimum size of the hole drilled	76 µm.

1.2 TITANIUM AND ITS MACHINING

Titanium has been recognized as an element (symbol Ti; atomic number 22 and atomic weight 47.9) for at least 200 years. Titanium products can be grouped into three categories according to the predominant phase or phases in their microstructure namely; alpha, alpha-beta and beta. Although each of these three types of the titanium requires a specific and unique mill processing methodology, each offers a unique combination of properties which may be suitable for a particular application. Titanium alloys are common, readily available engineering metals that compete directly with specialty steels, copper alloys, nickel based alloys and composites [12]. In addition to its attractive strength-to-density characteristics, titanium's exceptional corrosion resistance derived from its protective oxide film has motivated extensive application in aerospace, marine, defense, nuclear energy and biomedical applications apart from aggressive industrial service. Titanium is increasingly being used in the following applications: missiles; spacecraft, chemical production; hydrocarbon processing; power generation; desalination; nuclear waste storage and processing; metal recovery; offshore; marine deep sea applications; anodes; automotive components, medical implants and surgical devices and many other applications [12, 36, 61, 133, 171].

Titanium is branded as difficult-to-machine material owing to its distinct properties as discussed above. The machining characteristics of titanium and its alloys have been summarized as following [61]:

–Titanium and its alloys are poor thermal conductors. As a result, the heat generated when machining titanium cannot dissipate quickly; rather, most of the heat is concentrated on the cutting edge and tool face. About 50% of the heat generated is absorbed by into the tool while machining titanium alloy (Ti-6Al-4V) [7, 36, 155].

–During machining, titanium alloys exhibit thermal plastic instability that leads to unique characteristics of chip formation. The shear strains in the chip are not uniform; rather, they are localized in a narrow band that forms serrated chips [8, 46, 61].

–The contact length between the chip and the tool is extremely short (less than one-third the contact length of steel with the same feed rate and depth of cut). This implies that the high cutting temperature and the high stress are simultaneously concentrated near the cutting edge [164].

–Serrated chips create fluctuations in the cutting force; this situation is further promoted when alpha-beta alloys are machined. The vibrational force, together with the high temperature, exerts a micro-fatigue loading on the cutting tool, which is believed to be partially responsible for severe flank wear [53, 171].

– The surface finish achieved by a single machining process is poor. Hence, use of some finishing process is a must for obtaining acceptable surface quality while machining titanium or its alloys [143, 155]

Therefore, there is a crucial need for reliable and cost-effective machining processes for titanium and its alloys. Over the last few decades, there have been great advancements in the development of cutting tools, including coated carbides, ceramics, cubic boron nitride and polycrystalline diamond. These have found applications in the machining of cast iron, steels and high temperature alloys such as nickel based alloys and super alloys. However, none of these newer developments in cutting tool materials have had successful application in improving the machinability of titanium alloys [36, 133]. Most cryogenic machining studies on titanium and its alloys have documented improved machinability when freezing the workpiece or cooling the tool using a cryogenic coolant. However, inherent weaknesses exist in these approaches [61].

Although the basic machining properties of titanium metal cannot be altered significantly, their effects can be greatly minimized by decreasing temperatures generated at the tool face and cutting edge. Economical production techniques have been developed through use of low cutting speeds, maintaining high feed rates, using generous amounts of cutting fluid and using sharp tools and replacing them at the first sign of wear [8, 36, 46, 53, 61, 97, 109]. However, these machining recommendations may require modification to fit particular circumstances in a given shop. For example; cost, storage or other requirements may make it impractical to accommodate a very large number of

different cutting fluids. Savings achieved by making a change in cutting fluid may be offset by the cost of changing fluids. Likewise, it may be uneconomical to inventory cutting tools which may have only infrequent use. Also, the design of parts may limit the rate of metal removal in order to minimize distortion without excessive inertia effects [171].

Nontraditional machining processes such as electric discharge machining and laser beam machining have been applied to the machining of titanium and its alloys in recent times, but even these processes have their own limitations; the most prominent are the surface finish and dimensional inaccuracies besides their undesirable effects on the machined surface such as heat affected zone, recast layer and thermal stresses [84]. These adverse effects can lower the working life of the components critically. Loss of fatigue strength and hence surface integrity is another problematic area in machining of titanium. The basic fatigue properties of many titanium alloys rely on a favorable compressive surface stress induced by tool action during machining [8, 26]. Ultrasonic Machining (USM) could be another alternative machining process for commercial machining of titanium due to the following characteristics:

1. Titanium and its alloys have low thermal conductivity and in USM there is a thinner zone affected by machining, generous quantity of cutting fluid is used resulting in better heat dissipation, efficient slurry flow can be maintained, depth of cut can be maintained due to rigidity of the tool fixed in the horn and chemically active medium can be used to transfer the heat efficiently and there are no cutting forces between the tool and workpiece [37, 39, 107, 109, 131].
2. Titanium has a tendency to react with the cutting tools which contributes to seizing, galling, abrasion and pick up on the cutting edges and faces and in USM there is no tool work contact preventing all the above-mentioned side effects.
3. USM is known to be free from all the possible adverse effects on the machined component. Moreover, the repeated impacts of abrasive grains on the work surface lead to induction of a favorable compressive surface stress in

the micro layers thereby improving the fatigue life of titanium components and hence the surface integrity [26, 34, 109].

4. USM is better than other non-traditional processes in terms of simplicity, cost of tooling and provides better stability and control [103-104, 111-115].

In the present investigation, an attempt has been made to explore the use of ultrasonic machining for machining titanium (ASTM Grade-I) and to establish cost effective methods while machining titanium with USM.

1.3 OBJECTIVES AND ISSUES

The study was aimed to investigate the machining characteristics of titanium using different tool materials in ultrasonic machining and to model these characteristics for their application in the concerned manufacturing industry. The following issues have been taken up during this research work:

1. The process capability of ultrasonic machining has been discussed for conventional work and tool materials.
2. Material removal rate (MRR) of titanium (ASTM Grade-I**)** as work material has been explored in ultrasonic machining with the following tool materials; high carbon steel, high speed steel, cemented carbide, titanium (ASTM Gr.-I), and titanium alloy (ASTM Grade-V).
3. Tool wear rate (TWR) of aforesaid tool materials has also been explored with Titanium as work material.
4. Relationships between different machining parameters (grain size of the abrasive slurry, slurry type, tool material, work material, and power rating of the machine) and machining characteristics (material removal rate, tool wear rate, and surface roughness) have been established in this regard.
5. Material characteristics like microstructure and hardness have also been determined for the given work samples.
6. The results obtained have been modeled for their application in the concerned manufacturing industry.

1.4 SCOPE OF WORK

The work has been limited to commercially pure titanium (ASTM Grade-I) as work material in combination with five different tool materials; high carbon steel, high speed steel, titanium (ASTM Grade-I), titanium alloy (ASTM Grade-V) and cemented carbide for experimentation. Machining characteristics of titanium has been explored using USM for their application in concerned manufacturing industry. The typical composition and important mechanical properties of titanium have been detailed in table 1.11. Table 1.12 details the composition and important properties of the tool materials used in this work.

Table 1.11 Chemical Composition of Titanium

Chemical composition (by weight %) of Titanium (ASTM Grade-I)						
O	**N**	**C**	**H**	**Fe**	**Ti**	**balance**
0.18	0.03	0.08	0.01	0.2	99.1	0.4
Yield Strength 220 MPa Ultimate strength 340 MPa Hardness 115 HV Density 4.51 g/cm^3 Mod. of elasticity 103 GPa						

Table 1.12 Chemical composition and properties of tool materials

Material	**Chemical Composition**	**Density (g/cm^3)**	**Elastic Modulus (GPa)**	**Micro-Hardness (GPa)**	**Fracture Toughness (MPam$^{1/2}$)**
High Carbon Steel	Fe+ C (1.01%) + Cr (0.5%)	7.5	195	1.90	37.5
High Speed Steel	Fe+ C (0.97%) + Cr (3.5%) + W (17%) + V (0.6%)	8.0	214	1.68	48.0
Titanium	Ti (pure)	4.5	103	1.15	60.5
Titanium alloy	Ti + Al (5.8%) + V (4.1%)	4.4	114	1.36	68.0
Cemented Carbide	WC	15.0	650	18.5	12.0

Three different abrasive materials were used in this work; aluminium oxide, silicon carbide and boron carbide. The power rating of ultrasonic machine was included as another factor and the levels were fixed by conducting a preliminary experimentation.

1.5 OVERALL METHODOLOGY OF THE STUDY

The overall research work has been divided into four phases:

i) Detailed literature survey

ii) Design of Experiments (D.O.E.)

iii) Experimentation

iv) Modeling the results

Literature on ultrasonic machining and its aspects has been reviewed extensively to design a methodology for carrying out analysis on machining characteristics of titanium. The literature survey has been focused on various aspects of USM covering economic and technical viability. In the beginning of D.O.E. phase, pilot experiments have been performed for preliminary study of the capability of USM for machining of titanium. The various machining conditions, their ranges and levels have been selected based upon the results of pilot study.

Using D.O.E. methodology, statistical planning and designing of experiments has been performed to determine MRR of titanium (ASTM Grade-I) with different tool materials (H.C.S., H.S.S., WC, Ti and Ti alloy) under controlled experimental conditions. Accordingly tool wear rate (TWR) of the aforesaid tool materials in combination with titanium as work material has been established. Taguchi technique for robust design, using L18 orthogonal array has been used to design the experiments.

The experimentation has been done on 500 W ultrasonic drilling machine (Sonic Mill, USA). The impact of input parameters on MRR, TWR and surface roughness (SR) has been established for machining of titanium with aforesaid tool materials. The input parameters considered are given as following:

- Type of slurry used
- Grain size of the slurry
- Power rating of the ultrasonic drilling machine

The results showed that the response variables were strongly influenced by the control factors (input parameters). So, the results obtained after experimentation have been modeled using both "MACRO" and "MICRO" modeling approaches. This has been done using Taguchi's offline quality control approach for robust design (for macro modeling) and Buckingham-π theorem (for micro modeling).

1.6 ORGANIZATION OF THE THESIS

The thesis has been divided into six chapters. Brief description of the contents of each chapter has been given as following:

Chapter 1 contains introduction to non-traditional machining methods, their comparative features, applications and relative merits and demerits. Various aspects of Ultrasonic machining (USM) have been detailed; including the basic principle, USM equipment, tooling considerations and applications. Extensive review has been undertaken on the mechanism of material removal in USM. Process capability of ultrasonic machining has been explored for conventional tool and work materials. A brief introduction to titanium and its alloys has also been included in this chapter. The problems faced while machining titanium with conventional machining processes have been reviewed.

Chapter 2 contains a detailed literature review on machining characteristics of USM such as material removal rate (MRR), tool wear rate (TWR) and surface roughness and the factors affecting these machining characteristics in ultrasonic machining. The effect of work material properties, tool material properties on the machining characteristics in USM has been reviewed. The literature reported on USM of titanium and its alloys has also been reviewed. Extensive review has also been done on application of Taguchi's Robust design methodology for designing and analyzing the experiments.

Chapter 3 details the selection of input factors and factor levels for the experimentation (pilot experimentation), statistical planning of experiments and execution of the experiments, followed by data collection and recording (for results of MRR, TWR and SR). The microstructure of the machined surface for titanium work pieces has been obtained using Scanning Electron Microscopy (SEM). Important

observations from the microstructure study have been discussed. The hardness of machined surface has been evaluated using a micro-hardness tester and the results obtained have also been discussed.

Chapter 4 highlights the analysis of the results obtained from designed experiments, followed by further discussion. The discussion is also based on the analysis of the experimental data.

Chapter 5 outlines modeling of the results. Both macro modeling and micro modeling approaches have been adopted. The output of micro-model has been used to obtain regression equations for MRR and TWR in terms of input parameters.

Chapter 6 is all about the conclusions of this research work. This chapter also highlights the limitations of the study and scope for future work in this area. This chapter is followed by references.

CHAPTER 2
LITERATURE REVIEW

2.1 INTRODUCTION

A comprehensive review of literature on diverse aspects of ultrasonic machining and machining of titanium (using USM) has been presented here. A detailed review has also been performed for Taguchi's concept of Robust design for designing the experiments. It had helped to formulate the problem by a systematic identification of the areas to be explored in this investigation.

2.2 HISTORY OF USM

The history of USM began with a paper by R.W. Wood and A. L. Loonis in 1927 [114, 159] and the first patent was granted to an American Engineer Lewis Balamuth in 1945 [130,159,168]. USM has been variously termed ultrasonic drilling; ultrasonic abrasive machining; ultrasonic cutting; ultrasonic dimension machining and slurry drilling [111,136,168]. However from early 1950's it was commonly known either as ultrasonic impact grinding or USM [72]. Since its invention, USM has been relied upon to solve some of the manufacturing community's toughest problems [20].

The literature available on USM has been reviewed for different machining characteristics such as material removal rate (MRR), tool wear rate (TWR) and Surface roughness. Machining of titanium using USM has also been reviewed thereafter.

2.2.1 Material removal rate (MRR) in USM

To identify the potential factors affecting material removal rate in USM, a cause and effect diagram was constructed (figure 2.1). As the diagram indicates, the material removal rate in USM is dependant on four primary factors workpiece; tool; slurry and machine related factors. The literature corresponding to these factors has been reviewed and presented here.

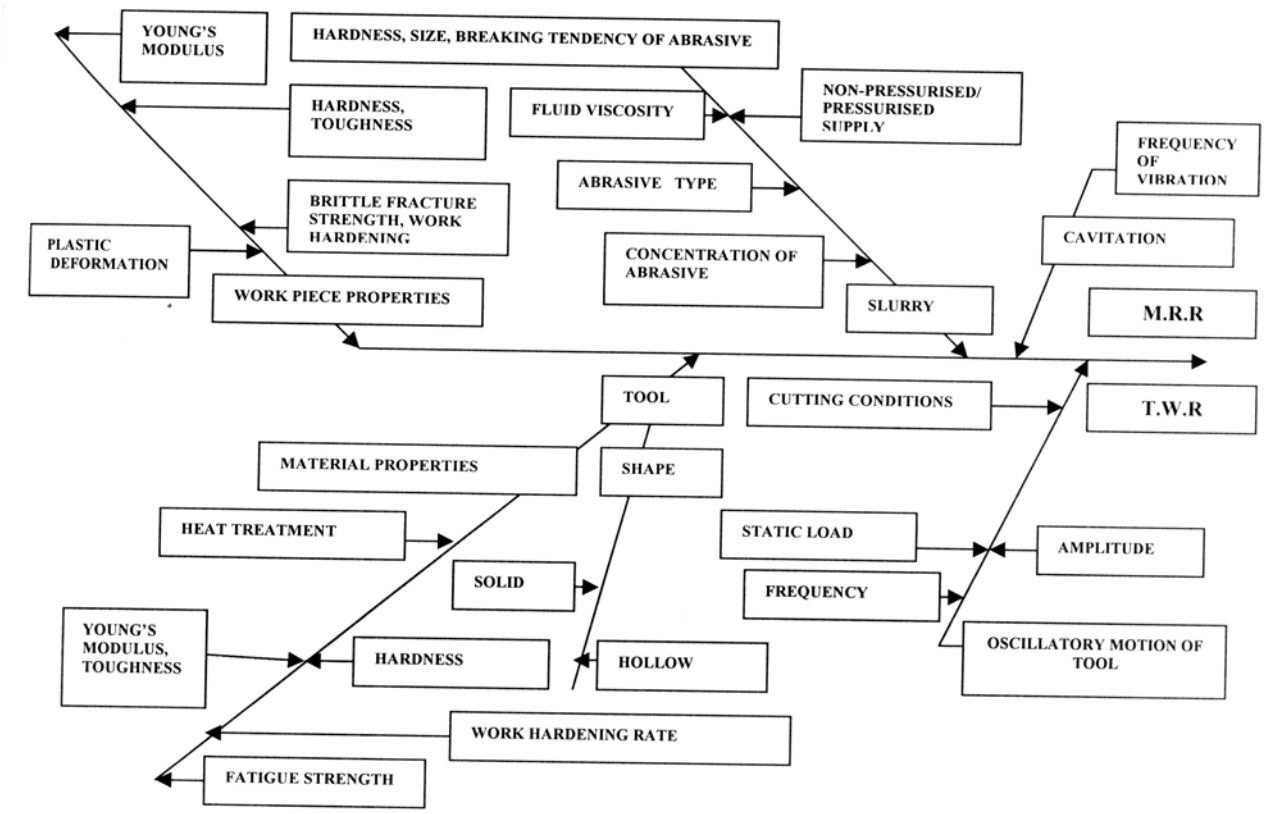

Figure 2.1 Cause and effect diagram for MRR, TWR

2.2.1.1 Work-piece properties

Komaraiah and Reddy [76] investigated the influence of work material properties such as fracture toughness and hardness on material removal rate in ultrasonic machining of hard and brittle materials. The work-piece materials machined in this investigation were glass, ferrite, porcelain, alumina and tungsten carbide. MRR was reported to decrease with an increase in work material hardness and fracture toughness in almost linear fashion under controlled experimental conditions. In another investigation by Komaraiah et al. [78], the MRR was reported to depend upon the brittleness ratio (ratio of work hardness to elastic modulus) of the work material. Materials with higher brittleness ratio were found to result in better machining rates.

Jianxin and Taichiu [66] investigated the effect of properties and microstructure of work materials on the MRR in USM of alumina-based ceramic composites. MRR was

reported to be low while machining composites of higher fracture toughness such as whisker-reinforced composites. The particle reinforced composites yielded higher values of MRR on account of their low fracture toughness. The composites of higher flexural strength demonstrated better surface integrity while machining with USM.

Guzzo et al. [50] outlined the ultrasonic abrasion of different hard and brittle materials using stationary USM. Results show that machining rate decreased with increase in hardness of the work material. For partially stabilized zirconia, an increase in the fracture toughness was reported because of the martensitic transformations induced by the mechanical stresses acting on the work surface due to repeated impacts of grains.

Majeed et al. [98] outlined the machining of $Al_2O_3/LaPO_4$ composites using static USM. Results show that an increase in the hardness of the composite (due to addition of $LaPO_4$) improves the machining rate up to a critical limit after which it tends to stabilize. The use of hollow tools was also reported to improve the MRR obtained.

Khairy [75] presented an assessment of the influence of work material properties on mechanism of material removal in USM. Results showed that hard and brittle materials such as glass were machined by brittle fracture at selective cleavage planes, whereas the tough materials face considerable plastic deformation before failure. The contribution of free impact mechanism in material removal was also found to be more in case of brittle materials.

Dam, Quist and Schreiber [30] investigated the material removal rate in ultrasonic drilling of several different ceramic materials. Results showed that for tougher work materials, the MRR observed was quite low as compared to the hard and brittle materials. However, the surface quality obtained (in terms of finish) was found to be superior for tough materials.

It has been concluded that productivity by USM (in terms of machining rate) is primary determined by the brittleness of the work material [70, 100, 112]. The plasticity of work material is associated with low productivity. The impact hardness has been found to have an adverse effect on machining rate [78]. However, while machining annealed steel, the machining rates observed have been found to be significantly better than

normalized or quenched ones [85]. Kennedy and Grieve [73] concluded that such a behavior contradicted the generally accepted criterion. However, this unusual behavior was explained better by Kremer et al. [84], considering the increase in tensile strength of steel upon normalizing or quenching, which is unfavorable from the point of view of USM.

2.2.1.2 Tool Characteristics

Komaraiah and Reddy [77] investigated the influence of tool material properties i.e. hardness on the material removal rate in USM of glass. Results showed that the MRR increased with an increase in the hardness of the tool material. The different tool materials were arranged in the increasing order of superiority as mild steel<titanium < stainless steel < silver steel < niamonic-80 A < thoriated tungsten. The tool materials used were found to undergo a significantly different amount of work-hardening, which contributed to the variation in their machining performance. Neppiras [113] using other tool materials gave the following ranking: copper < stainless steel < silver steel < mild steel < brass < tungsten carbide. Kumar and Khamba [86] reported achievement of higher material removal rates using a high carbon steel tool, which had higher hardness in comparison to other tools used for the experimentation. Tools with diamond tips have been shown to have good material removal characteristics [70].

It has been reported that the machining rate is directly proportional to the tool form [37, 73, 113] and shape factor (ratio of tool perimeter to tool area). The tool form defines the resistance to slurry circulation: a tool of narrow rectangular cross-section yielding a better machining rate than one with a square cross- section of the same area [73, 101, 149]. Use of hollow tools has been reported to result in higher rates of material removal than ones with solid geometry for same area of cross-section [115]. Goetze [47] presented a study on effect of tool geometry on the penetration rate obtained in the USM of ketos tool steel. For tools with equal contact areas, an increase in the pentration rate was reported for tools with larger parimeters. This was explained on the basis of difficulty of adequately distributing the abrasive slurry over the machining zone [73, 84, 113, 153].

Several authors have reviewed the theory and art of designing the tool/horns, but it is not yet fully understood [9, 16, 29, 39, 43, 69, 89, 102, 135]. Detailed guidelines for tool design for optimum MRR have been described by Rozenberg et al. [131]. Traditional methods of acoustic horn design are based upon differential equation which considers the equilibrium of an infinitesimal element under the action of elastic and inertia factors, which is then integrated over the horn length to achieve resonance [43, 115]. Typical design includes cylindrical, stepped, conical and exponential types. Recently, finite element modeling (FEM) has been used [20, 137] to design symmetric horn shapes. The analysis can take into the consideration the weight of the tool [20]. Dam et al. [30] has claimed that a horn can be designed which converts the longitudinal ultrasonic action into a mixed lateral and longitudinal vibration mode. This lateral motion obviously aids contouring work [81].

2.2.1.3 Slurry properties

Various investigators [10, 18, 75, 79-80, 119, 136, 170] have reported results indicating that the rate of material removal for a certain abrasive is a function of its concentration, grain size and hardness besides the feed system. On increasing the abrasive girt size or slurry concentration, an optimum value of MRR is reached. Any further increase in either aspect results in difficulty in the larger grains reaching the cutting zone [47, 79-80] or a subsequent fall in MRR. Guzzo et al. [51] reported a substantial increase in MRR obtained while using abrasive of larger grain size on account of the increase in the stress caused by the impact of abrasive particle over the workpiece surface. Neppiras [112] and Markov [100] reported that when grain size is comparable to the amplitude of vibration, the optimum level of MRR can be reached. Experimentally the ratio of the double amplitude to the mean size of the principal fraction of abrasive is 0.6 to 0.8. Goetze [47] has reported the optimum value of slurry concentration to be close to 12% for all the abrasive grit sizes used in the investigation. The optimum concentration is thought to be one providing a single layer of abrasive over the entire work surface [84]. The values given for the optimum concentration are inconsistent, with a range of 30% to 60% [100], 25% to 40% [111] and 15% to 40 % [114].

The disagreement in the quoted values for the optimum range of concentration can be attributed to the variation of concentration within the working zone under the tool. Obviously such effective local concentration under the tool can not be the same as that of the feed suspension especially when the static load is too high for the particular acoustic setting [84]. Kennedy et al. [74] pointed out the difficulty of machining a flat at the bottom of a hole because of uneven slurry distribution across the machining face, resulting in fewer active grits at the tool centre. Kazantsev [70-71] claimed that the forced delivery of the slurry increased the output of USM five fold without the need to increase grit size or machine power. When compared with suction pumping system, it yielded a 2-3 times higher MRR. Pentland [119] and others [79-80, 136] found that by improving slurry circulation, the adverse effects such as contamination and blockage can be reduced or overcome. Barash and Watanapongse [18] reported a four to five fold increase in MRR while increasing the fluid pressure from 10 to 90 psi, attributed to suppression of cavitation at higher pressure of the slurry fluid.

The hardness of the abrasive has been found to affect the machining rate. For machining of soda glass, the removal rate with boron carbide has been reported to be 15-20% higher than that with silicon carbide [73]. Ramulu [125] reported that use of boron carbide abrasive resulted in material removal rates which were approximately 75% higher than the silicon carbide abrasive for the 400 grit size and 320% higher for 220 grit size while machining silicon carbide ceramics. The effect of slurry hardness on MRR has been found to be dependant on the other experimental conditions such as work material properties, tool properties, amplitude of vibration and static load; which could be regarded as the reason for a wide inconsistency of the results reported in the literature available on USM.

2.2.1.4 Operating parameters affecting MRR

Power primarily determines the mass of the tool-horn assembly that can be utilized for an application and the frontal cutting area of the tool. The more is power available in an ultrasonic machine, the larger the frontal cutting area of the tool can be supported [20]. The amplitude of vibration (ξ) has been found to affect the machining performance of

USM by a number of investigators [10, 47, 68, 71, 103, 113, 130, 148, 165, 166, 168, 176]. Higher amplitude is obtained by using a tool with a larger transformation ratio i.e. the ratio of transducer/tool diameter [73, 81, 84, 159]. Shaw [138] showed that MRR is proportional to $\xi^{3/4}$ while other researchers [47, 68, 71, 103, 176] have advocated that MRR is linearly proportional to ξ and yet others [111-113, 119, 131, 166, 168] have suggested that MRR depends upon ξ^2 for constant frequency and static load conditions. Goetze [47] reported a linear increase in MRR while increasing the amplitude of vibration, provided all other factors such as frequency of vibration and abrasive grit size are kept constant. The linear trend of MRR while increasing the amplitude has been found to be more prevalent when high impact strength materials are machined or fine abrasive powders are used for machining. Lee and chan [95] reported an optimum value of amplitude beyond which the MRR obtained tends to stabilize. When a larger grit size of the abrasive is coupled with a low value of amplitude, the MRR obtained is reported to be substantially poor due to ineffective circulation of slurry under the tool.

Experiments conducted by Neppiras [113] have shown that in the range of 20 to 50 kHz, the removal rate is proportional to square root of the vibration frequency. However, Kazantsev [70] stated that the abrasion rate is proportional to the frequency while the non linear frequency dependence of machining rate is due to the variation in abrasive concentration in the working zone. Some other researchers have also reported the linear dependence of machining rate on frequency of vibration [45, 47, 176]. Above an upper threshold value, the MRR falls off rapidly where MRR is proportional to square root of frequency [71, 114].

Kainth et al. [68] carried out an analysis considering the non uniformity of abrasive grains to assess the relation between the removal rate and static load/amplitude. Their calculations yielded approximately a linear relation between material removal rate and static load. Rozenberg [131] has also reported similar results while all other factors are kept unchanged. Koops [79] indicated that use of a smaller than optimum value for static load is better for reducing the abrasive wear and increasing the tool life. Above the optimum value, the MRR decreases owing to a reduction in the size of abrasive grains

reaching the cutting interface (due to crushing effect) and inefficient slurry circulation [48, 73, 112, 114, 130, 149, 176]. The optimum static load for the maximum machining rate has been found to be dependant on the tool configuration, amplitude of vibration and mean grit size [44, 73, 84, 111]. A previous analysis carried out by Markov [100] on the experimental results of ENIMS yielded a wide range for the power exponent relating MRR with amplitude for different static loads. The values ranged from 0.5 to 1.7 depending upon the value of static load used.

2.2.2 Tool wear in USM

Tool wear is an important variable influencing both MRR and accuracy in USM [1, 47, 91, 148, 163, 168]. Tool wear in USM has been classified into two types: longitudinal wear, W_L [99, 137, 148] and lateral/diametral wear, W_D [3] as depicted in figure 2.2. Besides these, some of the tool wears occur as a result of cavitation or suction wear [128, 137, 163]. Tool wear in USM is a complex phenomenon and is affected by a number of factors such as static load; work material; tool material; tool size; type of abrasive and its grain size; machining time; depth of hole drilled etc. As a result of the tool wear, both tool length and weight decrease, which affects the resonance frequency of the machine and reduces the amplitude of vibration [1-4], thereby, lowering the MRR.

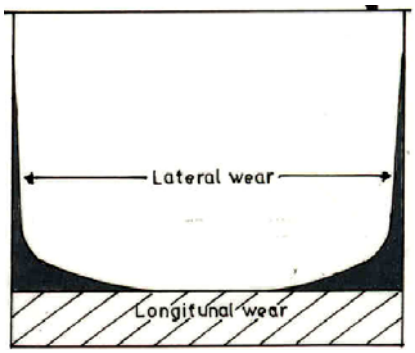

Figure 2.2 Tool wear in USM [4]

Adithan and Venkatesh [6] reported that the tool wear is maximum at a particular static load, which may be considered optimum for the point of view of MRR. The tool

wear increases linearly with the total depth of holes drilled. As the depth of hole drilled increases, there is a reduction in the MRR and an increase in the associated tool wear [4]. The tool wear is proportional to the cutting time and the rate of tool wear has been found to increase with time [77, 152]. Adithan [1, 3, 6] found that for all tool and work combinations, the tool wear rate is proportional to the wear that has already taken place.

The tool wear tends to increase when harder and coarser abrasives are used. As a consequence, harder abrasives like boron carbide, cause higher tool wear as compared to softer abrasives like, silicon carbide for a tool of the same cross-sectional area [6, 163]. Ramu and Krishnamurthy [10] reported an optimum slurry concentration range (1: 5.7) from tool wear aspect in USM of transformation toughened ceramics. Zheng et al. [175] investigated tool wear in rotary ultrasonic machining of advanced ceramics. Tool wear was concluded to follow two stages; attritious wear and bond fracture. Longitudinal tool wear was found to be prevalent, while the lateral wear observed was not of significant order.

Dam et al [30] has reported that work material properties such as hardness and toughness affect the tool wear in ultrasonic machining. Their results showed that work materials with higher fracture toughness and hardness cause more tool wear. Ramu and Krishnamurthy [10] have reported that transformation toughened ceramics show poorer USM behavior giving relatively high tool wear. This has been attributed to their higher fracture toughness which is unfavorable from the point of view of tool wear in USM. They also tend to wear the abrasive at higher rate than the conventional ceramics [79]. Adithan [1] reported absence of lateral wear in machining of softer materials such as porcelain, while it was found to be more prevalent in case of hard work materials such as tungsten carbide.

Adithan [1] has reported that stainless steel tools exhibit low tool wear as compared to tungsten carbide or mild steel tools. This is due to high resistance to cavitation erosion of stainless steel. In USM, hardness of the tool increases by work hardening, therefore the penetration of the abrasive grains into the tool decreases resulting in higher MRR [77]. In addition, material removal from the periphery of the

work zone becomes greater so that a convex surface is formed in the work piece. This causes plastic deformation of the centre of the tool face, forming a dish. It has also been found that the degree of hardening is higher at the periphery and lowest at the centre for all tool materials [77]. As a result, soft materials such as copper and brass are unsuitable as tools as they develop burrs at large oscillatory amplitudes [113]. They are also acoustically poor and attenuate the stress wave in large tools. The use of hard metals such as tungsten carbide reduces plastic deformation of the tool surfaces [52].

To decrease longitudinal wear (W_L), use of a tool material with a high value of product of hardness and impact strength (e.g. Niamonic-80 A) has been recommended by Komaraiah and Reddy [77]. However, the lateral wear (W_D) has been found to be independent of the impact strength [1, 77]. Komaraiah and Reddy [77] ranked the various tool materials in the order of superiority (decreasing tool wear) as mild steel > titanium > stainless steel > silver steel > thoriated tungsten > niamonic-80 A. Kumar and Khamba [86] compared the machining performance of high carbon steel and titanium alloy tools in USM of titanium. High carbon steel tool was found to experience more tool wear as compared to titanium alloy tool because of its higher hardness and poor toughness and impact strength as compared to titanium alloy tool. Jadoun et al. [63] reported that use of a tool with higher abrasion resistance such as tungsten carbide results is lesser tool wear rate as compared to high carbon steel or high speed steel tools. Similar results have been reported by Markov [99-100] and smith [148].

2.2.3 Surface quality/finish in USM

USM does not generate significant heating which might otherwise lead to the development of a thermally damaged layer/zone or residual stress. Abrasive grain size has been found to be the main factor governing the work-piece accuracy and surface finish [20, 34, 44, 47, 51, 73, 78, 86, 159]. Neppiras [112] concluded that surface roughness is closely controlled by abrasive grain size alone. Kumar and Khamba [86] and others [51] have also reported similar results. A decrease in abrasive grain size while machining with USM leads to lower values of surface roughness, in addition, the accuracy of the hole drilled is improved [20, 34, 78, 168]. A better surface finish is also

obtained on the bottom walls of the cavity [104, 105-106, 136, 148]. Dam et al [29] reported that better surface finish is obtained when feed rates and depth of cut are increased. Kennedy et al. [74] and Koval'Chenko et al. [80] pointed out the difficulty of machining a flat at the bottom of a hole because of uneven slurry distribution across the machining face, resulting in fewer active grits at the center of the tool. Komaraiah and Reddy [77] compared the performance of stainless steel, titanium and niamonic-80 tools for surface finish of the glass work-piece while machining with USM. Results showed that tool materials with higher wear resistance (niamonic-80) gave better surface finish as they retain their shape and finish even under the repeated impact of abrasive particles.

The production inaccuracies in USM consist of both dimensional inaccuracy (oversize) and form inaccuracy (conicity) [4, 20, 78, 100, 130]. Conicity can be reduced by using tungsten carbide and stainless steel tools [4], an internal slurry delivery system [4, 84] and tools with negative tapering walls or fine abrasives [73, 84, 101, 113]. Adithan [4] reported that oversize is greatest at entry and increase in diameter-length ratio increases lateral vibrations which cause greater oversize. Shaw [138] and Komaraiah et al. [78] has shown that surface roughness improves with increase in static load which reduces the abrasive size and suppresses the lateral vibrations of the tool, so minimizing the production inaccuracies in the hole drilled. Komaraiah et al. [78] reported that the out-of-roundness of the drilled holes increases with a corresponding increase in the ratio of work material hardness to Young's modulus of elasticity. Adithan [ ] found that the oversize with rectangular tools was greater than that obtained with circular tools.

It was established by Komaraiah et al. [78] that work-piece materials with higher ratio of hardness to elastic modulus involve inferior surface quality. The materials which observed higher MRR were also reported to have higher surface roughness values. Gilmore [45] reported that slightly better surface finish is obtained while machining a hard material such as ceramics as compared to that obtained in machining of the material with lower hardness. Markov [100] suggested that the relative roughness for two different materials can be related to their respective volumetric machining ratio in a square relation. Dam et al [30] concluded that the work materials can be graduated according to

their respective machining rates, so that the most productive materials give the greatest surface roughness and vice-versa. Therefore, higher productivity is not obtained without cost as the surface roughness increases. Kremer et al. [82] reported that USM of graphite resulted in poor surface finish due to cavitation, contamination and debris blockage. Adithan [4] found that for the same abrasive size and static load, the surface roughness for glass work-piece was almost double that for graphite. Ramu and Krishnamurthy [10] compared the surface quality obtained while machining alumina-based and zirconia-based ceramics with USM. Results show that better surface finish was obtained for alumina-based ceramics and the oversize for the drilled hole was also lesser.

Ramulu [125] investigated the surface finish and accuracy while machining silicon carbide and Titanium diboride ceramics with static USM. Results show that the values of oversize were approximately equal to 1.4 to 12.8 times the mean abrasive particle size. A linear increase in the oversize was reported while decreasing the abrasive grit size, which was found to be in contradiction to the findings of other investigators. It was also found that both work materials behaved differently regarding the variation in hole taper as an effect of change in grit size.

2.2.4 Hybridization of USM with other processes

Babitsky et al. [14] highlighted ultrasonic assisted turning of aviation materials through simulation and experimental study. The suggested finite element model provides numerical comparison between conventional and ultrasonic turning of inconel 718 alloy in terms of stress/strain rate, cutting forces and contact conditions at the work-tool interface. Xu and Han [172] outlined piezoelectric actuator based active error compensation of precision machining. Experimental results have shown that the cutting tool developed is satisfactory in terms of improved roundness and surface roughness of the machined work-piece. Sharma et al. [139] outlined a new longitudinal mode ultrasonic transducer with an eccentric horn for micro machining. This device can produce an angular vibration of the order of 40 kHz at the cutting tip attached at the end of the horn. The vibrating tip can be used for precision machining of straight micro groves, which are difficult to cut using existing precision machine tools. The appearance

of machined surface has been found to be excellent when compared with that obtained in conventional grove machining. Kai and Takahira [67] highlighted micro machining by the application of work-piece vibration. Using this set up, successful machining of micro holes in quartz, glass and silicon substrates has been achieved.

Ishikawa et al. [62] contrived a new drilling method that combines ultrasonic vibrations of a diamond core drill and low-frequency vibrations of the work-piece and produced a combined vibration drilling apparatus for experimentation. The drilling force was observed to decrease by 70% as compared to conventional drilling using this newly developed method. Roughness of the drilled hole was found to be higher than non-vibration drilling, but chipping at the edge of the hole was reduced significantly. Chang and Bone [25] outlined the application of ultrasonic vibration for burr size reduction in drilling process. High-frequency and low-amplitude vibration were added in the feed direction during drilling of the work-piece which was composed of aluminium. The results demonstrated that under suitable ultrasonic vibration conditions, the burr height and width could be reduced in comparison to conventional drilling.

Choi et al. [27] explored the use of chemical-assisted ultrasonic machining for machining of glass. To obtain the chemical effects, a low concentration hydrofluoric acid solution was added to the slurry. The hybrid method was found to be superior in terms of material removal rate and integrity of the machined surface. The surface roughness was also found to improve and the machining load was decreased significantly as compared to the conventional USM method. Lau et al. [92] investigated the ultrasonic-aided laser drilling of alumina-based metal matrix composites. The conventional pulsed Nd: YAG laser drilling involved problems of limited depth of drill, non-cylindrical hole profile and the presence of excessive recast layer. The hybrid ultrasonic-laser drilling technique was found to improve the capabilities in deep hole drilling with more precision. The thickness of heat affected zone (HAZ) was reduced by 30% under the action of ultrasonic vibration which aided in effective utilization of the laser energy in vaporizing the material. A mathematical model was also proposed to describe the shape of the machined hole. Tsutsumi et al. [162] investigated the machining performance of ultrasonic-aided core

drilling method for machining of ceramics. The thrust force was reported to decrease by 70% without affecting the surface quality of the machined hole. This was contributed to the more effective penetration of diamond grits into the surface of work material, reducing the required drilling thrust force. The width of the chip produced was increased and the chipping of the edges was found to be lowered.

Many investigators have explored hybrid EDM-USM process for machining of tough materials and advanced ceramics [97,167,174,177]. The results from these investigations reveal a superior performance of the hybrid method in terms of improved machining rate, reduced heat affected zone and recast layer along with better stability and control when compared to the conventional EDM process. This has been attributed to effective flushing of the debris and wear particles from the machining zone due to the action of ultrasonic vibration, which improves process stability and promotes more efficient heat transfer from the work surface.

2.2.5 USM applied to machining of titanium

The application of USM for titanium and its alloys has been reported by few researchers. Sharman et al. [180] outlined the application of ultrasonic assisted turning to γ-titanium aluminide. As compared to conventional turning, the cutting forces were reported to be of very small magnitude (approx. 12%) in this process, thereby, improving both the tool life and surface finish. Aspinwall and Kasuga [11] have reported the use of USM for production of 3 mm holes in titanium aluminide. While machining with conventional methods, titanium aluminide; an alloy of titanium, encounters problems of surface integrity and micro-cracking. When machined with USM, satisfactory results have been achieved with polycrystalline diamond tooling. Grit size has been identified as the greatest factor affecting MRR followed by static load; tool type: solid/hollow and power level. In contrast to brittle materials, the combination of fine grit size, low power level and solid tool type gives maximum TWR. The surface finish obtained has been found to be superior to ceramics.

Wansheng et al. [167] investigated the effect of ultrasonic vibration introduction in EDM process to machine micro-holes in titanium alloy Ti-6Al-4V; concluding an

increase in MRR as well as the process stability along with reduction in arcing phenomenon. When applied to machining of titanium alloy, the combined EDM-USM process has been found to demonstrate better performance in terms of improved MRR, discharging efficiency and reduced thickness of the recast layer [167]. Lin et al. [97] have also shown a similar result; the introduction of ultrasonic vibration in EDM for deep hole drilling in titanium alloy (Ti-6Al-4V) can improve the machining quality and efficiency distinctly. This is due to the fact that the debris and small particles generated by erosion of the work surface are efficiently disposed by the ultrasonic vibration induced, which gives a better stability to the process. Zhinxin et al. [177] studied a combined EDM-USM machining of titanium alloy. Results show that the machining efficiency obtained was 2-3 times higher than conventional EDM process. The surface integrity of the machined samples were also found to be better when compared to conventional EDM.

Singh and Khamba [140-146] investigated the machining characteristics of titanium alloy (Ti-6Al-4V) using stationary USM. Results show that optimum MRR and TWR was achieved with boron carbide as abrasive material with grit size 220 and stainless steel as tool material. Optimum surface quality was generated while using a stainless steel tool; slurry concentration of 25% and slurry temperature equal to 27 C. The surface finish has been reported to be better (50 microns) than that obtained while machining brittle materials such as ceramics. Kumar and Khamba [86-88] reported use of a hard tool material such as high carbon steel or tungsten carbide for optimal results in terms of material removal rate of pure titanium. Dvivedi and Kumar [34] investigated surface quality in USM of titanium alloy (Ti-6Al-4V). Results show that the best results for surface quality were obtained with H.C.S. tool; medium grit size (320) and low power rating of USM machine (40%). The other factors such as slurry concentration were found to be relatively insignificant from the point of view of surface quality. The literature review reflected that:

1. There is a considerable gap between the effective application of USM for machining of a tough material (such as titanium) and the research activity going on in this regard. Moreover, most of the work reported has been

concentrated on machining of titanium alloy (Ti-6Al-4V). Thus, there is an opportunity for exploring the use of USM for machining of pure titanium grades.

2. The work material properties, such as fracture toughness, hardness and impact strength significantly affect the machining characteristics like material removal rate, tool wear rate and surface roughness in ultrasonic machining process. In this regard, some practical work has been evidenced for machining hard and relatively brittle materials using USM. But there appears to be no great effort put in to explore the machining performance of tough materials (such as titanium) using ultrasonic machining process.

In the light of these facts, it was decided to explore the application of USM for commercial machining of pure titanium (ASTM Grade-I) and to investigate the machining characteristics of this material (titanium) using USM for their application in concerned manufacturing industry.

2.3 TAGUCHI'S APPROACH TO DESIGN OF EXPERIMENTS

Dr. Genichi Taguchi is regarded as the foremost proponent of robust parameter design, which is an engineering method for product or process design that focuses on minimizing variation and sensitivity to noise. When used properly, Taguchi's approach provides a powerful and efficient method for designing products that operate consistently and optimally over a variety of conditions [19, 24]. This approach allows quality considerations to be included at an early stage of any new venture; in the design phase for a product, during routine maintenance or during installation of a manufacturing process. Taguchi's approach emphasizes on changing the definition of quality from 'achieving conformance to specification' to 'achieving the target and minimizing the variability'. The traditional "one factor at a time" approach is changed to varying many factors at a time through statistical experimental design techniques. This is done in conjunction with a change of attitude for dealing with the uncontrollable factors; removing the effect and not the cause, by appropriately tuning the controllable factors.

There are two main aspects to the Taguchi technique. First the behavior of a product or process is characterized in terms of factors (parameters) which are classified in two types:

1. Controllable or design factors – those whose values may be set or adjusted by designer or process engineer.
2. Uncontrollable factors or noise factors – which are sources of variation often associated with the production or operational environment; overall performance should ideally be insensitive to their variation.

The noise factors causing variation are either impossible or difficult to control. The noise is invariably defined as outer noise; which is either due to operating conditions or environmental factors and inner noise which is concerned with the deterioration of the product and manufacturing imperfections. The purpose of applying Taguchi's approach is to make the product or process insensitive to the both inner and outer noise [32].

The controllable factors can be classified in three different types, as shown in figure 2.3. Those factors which affect the average levels of the response of interest are referred to as target control factors (TCF), also known as signal factors. The factors that affect the variability in the response are variability control factors (VCF); and those factors which neither the mean response nor the variability, and can thus are adjusted to fit the economic requirements, called the cost factors. The focus is on the reduction of variability by changing the variability control factors (VCF), while maintaining the required average performance through adjustment to target control factors [129].

2.3.1 Parameter Design

Taguchi's approach involves a systematic identification of those particular settings of controllable factors that reduce the process variation; which is caused by the uncontrollable or noise factors while keeping the quality characteristic of interest on target. The focus is on reducing the effect of the noise rather than the noise factors themselves [121-122]. The variation is simulated during the experimentation, by

systematically varying the noise factors at each of the various settings of the controllable factors.

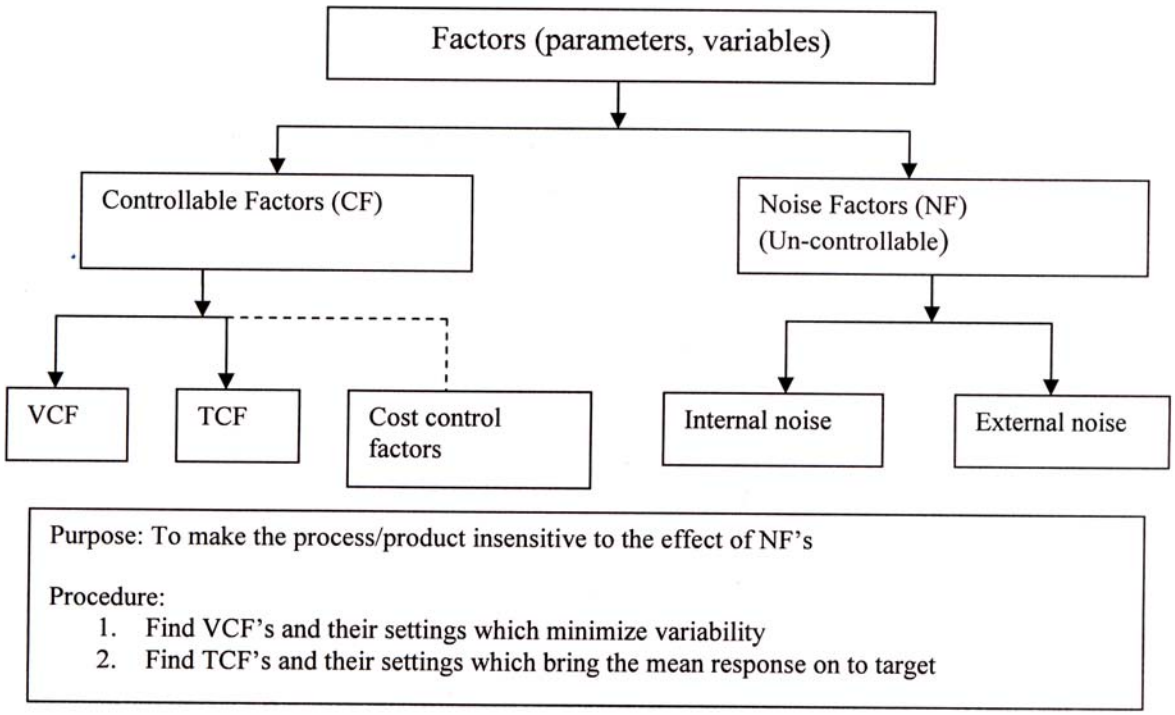

Figure 2.3 Controllable and Noise factors

The controllable or design factors settings are decided by the rows of an experimental design known as inner array; which is usually a fractional orthogonal array. In such a design, every level of one factor is coupled with every level of all other factors the same number of times. At every combination of the levels of controllable factors, the observations for the response under interest are taken while changing the settings of the noise factors. A fractional orthogonal array is used to determine the level combinations for the noise factors (known as outer array). In such a case, the experimenter can simulate the effect of variation in the noise factors on each controllable factor levels setting and thus reach at the setting that minimizes this variability [132].

2.3.2 Steps in conducting experimental study

There are certain steps that Taguchi has suggested to be taken in conducting the experimental study using robust design approach, which are discussed as following [132]:

1. **Define the problem:** This is concerned with establishment of the aim of the experimental investigation. A clear and accurate statement of the problem to be solved is a must before going ahead with the investigation.
2. **Determine the objective:** At this stage, identification of the output characteristics or response of interest that is to be optimized is done. The response must be measurable and preferably, with good additivity. To establish measurement reliability, additional experiment may be required.
3. **Conduct a brainstorming session:** This is undertaken by the people who are closely related to the product or process under investigation to collectively decide the controllable and uncontrollable factors, to define the experimental range and appropriate factor levels. Taguchi believes that it is generally preferable to include as many factors as possible for the initial screening. The information required can also be obtained from the already available literature or research data.
4. **Design the experiment:** In this phase, the selection of appropriate experimental design is done by assigning the levels of the design factors and their interactions to the columns of the inner array. Taguchi has also recommended some rules for appropriate allocation of columns to the interactions and these must be followed while designing the experiment. The noise factors levels are allocated to outer array columns.
5. **Conduct the experiment:** Perform the experimental trails, preferably replicating each trial (with randomization) to minimize the effect of experimental error. The experimental results are collected and recorded.
6. **Analyze the data:** The performance measures are evaluated for each trial of the inner array and analysis is made using appropriate statistical techniques such as analysis of variance, regression etc.

7. **Interpret the results:** The optimal levels for variability control factors (VCF) and target control factors (TCF) are identified from the information obtained by conducting analysis phase. For the variability control factors, the optimal levels are considered to be those which reduce the variation in the response under interest. For target control factors, optimal levels are defined as those which bring the mean response nearest to the target value. The performance of product or process is then predicted at the optimal levels settings.
8. **Run a confirmatory experiment:** It is necessary to verify, by some follow up trails that the new parameter settings; which are claimed to be optimal**,** improve the response or performance measures over their value at initial settings. Hence, experiments are conducted at the optimal process settings to conform the optimality of the solution. A successful confirmation experiment alleviates the concerns regarding the possibilities of wrong selection of factor levels or assumptions of no interactions or any other improper assumptions underlying the response model. If the predicted results are not conformed, additional experiment may be required or reiteration of steps 3-8 may be necessary.

2.3.3 Selection of orthogonal array

Orthogonal arrays are special experimental designs that require comparatively a small number of experimental trails to measure the effects of the parameters included in the study. Orthogonal arrays could be considered as 'fractional factorial designs' and are composed of symmetrical subsets of all the combinations of the levels of input parameters corresponding to full factorial designs [55]. Before selection of an appropriate orthogonal array for a particular experimental investigation, it is mandatory to determine the number of factors to be included, their levels and the possible interactions that have to be accommodated and included in the design. The selection of two factor interactions is based on the previous experience of the experimenter or some already available experimental data. Otherwise, a hit and trail approach can be used to decide the potential interactions between the factors. The levels of the parameters included in the study can

also be decided from conducting a preliminary study, which is based on 'one factor at a time approach'. Here, a number of levels can be tried for each factor (by deciding a range) and then those levels which lead to a change in the trend of performance or response magnitude can be short listed for further investigation.

The next step in selecting the correct array (OA) is to quantify the total degrees of freedom (DF) present in the study. The degrees of freedom are first calculated for the individual factors and then summed up to get the total DF. The degrees of freedom for a 2 factor interaction are determined by taking the product of the DF of the two factors involved. Estimation of total DF involved fixes the minimum number of experiments that must be conducted to study the factors involved in the investigation. It may be possible that a number of alternate arrays qualify this condition. Then, the experimenter tries to find out which array could be more suitable from the point of view of economy and the possible error in the results obtained through experimentation [129].

2.4 MULTIPLE RESPONSE OPTIMIZATION

Taguchi's method of off-line quality control has been successfully used in the design and selection of optimal process parameters in many areas of manufacturing processes for single response optimization. A single setting of process parameters may be optimal for one quality characteristic but the same setting may yield sub-optimal results for other quality characteristics. Hence, it is necessary to go for multiple response optimization so that a single setting of parameters that is optimal for all the quality characteristics could be realized.

A number of techniques have been developed by researchers for optimizing multiple characteristics [24, 35, 122, 126, 156, 157, 179]. Taraman [156] has investigated multi machining output – multi independent variable turning research by response surface methodology. The objective of this research was to develop a methodology which would help determination of cutting conditions (cutting speed, feed rate and depth of cut) such that each of the several machining characteristics (surface finish, tool force and tool life) could be optimized collectively. A central composite design was used to develop mathematical models correlating the dependant and independent parameters of the

process. Byrne and Taguchi [24] illustrated a case of the optimization of two quality characteristics- the force required to insert the tube into connector and pull off force using Taguchi's approach. The selected characteristics were independently optimized using Taguchi's approach and then the results were compared subjectively to select the best levels of the parameters in terms of the both quality characteristics.

Phadke [122] presented multiple characteristics optimization for polysilicon deposition process. Two quality characteristics- surface defects and thickness of deposition were optimized simultaneously by assigning a weight to each of them. Elsayed and Chen [35] presented a model using loss function approach to determine the optimal settings of the process parameters of production processes for products with multiple characteristics. Reddy et al. [126] illustrated an approach to optimization of multiple responses in injection moulding process using goal programming in conjunction with Taguchi's robust design methodology. The optimization study revealed that the optimum conditions obtained for a single response are not compatible with those of other responses. So trade offs were made in the selection of levels for factors using engineering judgment. The further study revealed that the optimum conditions obtained using goal programming as compared to robust design. Tarang et al. [157] reported the use of fuzzy logic in association with Taguchi method to optimize the submerged arc welding process with multiple performance characteristics. A multiple response performance index was employed to optimize the performance characteristics. The process parameters namely arc current, arc voltage, welding speed and preheat temperature were optimized for deposition rate and dilution as the performance characteristics. Singh and Kumar [179] presented a research on optimization of multi machining characteristics using Taguchi's approach and utility concept. In this paper, a simplified methodology based on utility concept was developed for determining the settings of the process parameters for simultaneous optimization of surface roughness, cutting force, tool life and power consumption in turning of EN 24 steel.

Based on the review of literature on multi-response optimization, it was decided to use utility concept as a technique in conjunction with Taguchi's robust design

approach for arriving at a single optimal solution for various machining characteristics undertaken in the study. The methodology adopted for application of the technique is discussed as following.

2.4.1 Utility concept

A customer evaluates a product based on a number of different quality characteristics. The evaluations of different characteristics should then be combined to obtain a composite index. Such a composite index represents the utility of the product. The utility of a product on a particular characteristic measures the usefulness of that particular characteristic of the product. It is assumed that the overall utility is the sum of utilities of individual quality characteristics.

Thus if X_i is the measure of effectiveness of an attribute *i* and there are n attributes evaluating the outcome space, then the joint utility function can be expressed as [32]:

$$U(X_1, X_2 \ldots\ldots\ldots X_n) = f[U_1(X_1), U_2(X_2) \ldots\ldots\ldots U_n(X_n)] \qquad (2.1)$$

Where $U_i(X_i)$ is the utility of the *ith* attribute. As the overall utility function is a linear sum of individual utilities, the function becomes:

$$U(X_1, X_2 \ldots\ldots\ldots X_n) = \sum_{1}^{n} U_i X_i$$

The attributes may be given priorities as per customer requirements and corresponding weights for the individual utility index. The overall utility function then can be written as,

$$U(X_1, X_2 \ldots\ldots\ldots X_n) = \sum_{1}^{n} W_i \, U_i X_i \qquad (2.2)$$

Where W_i is the weight assigned to the attribute *i* and the sum of the weight attributes is equal to 1. The utility function is of "Larger-the-better" type composite measure. When Utility function is maximized, the quality characteristics being considered are optimized collectively.

2.4.2 Determination of utility value

To determine the utility value for a number of quality characteristics, a preference scale for each quality characteristic is constructed. Later these scales are allotted weights to obtain a composite number (overall utility). The preference scale chosen [49] is given as,

$$P_i = A \log [X_j/X'] \qquad (2.3)$$

Where X_j is the value of quality characteristic *j, X'* is the non-acceptable value of characteristic *j* and *A* is a constant whose value can be determined as given under:

$$A = 9/ [\log X^*/X'] \qquad (2.4)$$

A is chosen such that $P_i = 9$ at $X_j = X^*$, where X^* is the most desirable (optimum) value of X_j assuming that such a number exists.

Various quality characteristics are then assigned weightings to represent the relative importance of each one of them. The weightage assigned to each quality characteristic may be identical or different, depending upon the requirements of the investigator. They can be assigned any value between 0 and 1 depending upon the customer priorities and subjected to the condition that the sum of individual weights should not exceed 1.

The value of the composite measure is then calculated using the following equation (overall utility function);

$$U(n, R) = P_1(n, R) X W_1 + P_2(n, R) X W_2 + \ldots\ldots P_x(n, R) X W_x \qquad (2.5)$$

Where, *n* = trial number; *R* = replication number, x = no. of quality characteristics.

The data thus obtained by transforming the experimental results for various quality characteristics is known as utility data. This data is subsequently analyzed by the appropriate statistical techniques for further analysis for arriving at the optimal setting or optimal solution. This composite optimal setting provides a simultaneous optimization of multi-machining characteristics investigated in the study and therefore is better than the individual optimal settings (for different characteristics) obtained through single response optimization, as the achievement of optimality for one quality characteristic may lead to a sub-optimal situation for all other quality characteristics.

CHAPTER 3
EXPERIMENTATION

3.1 INTRODUCTION

Ultrasonic drilling machine AP-500 (Sonic Mill, USA) was used for this experimentation. The size and shape of the workpiece was selected based on its availability from the supplier (figure 3.1). The tool design for this experimentation was finalized keeping in view the limitations of tool weight and horn shape to ensure optimum performance in machining the workpiece.

An electronic balance (Metler, least count: 0.1 mg); and stop watch (least count: 0.01 min) was used to determine material removal rate (MRR) and tool wear rate (TWR). For measuring surface roughness Perth meter (Mahr, least count 0.01 microns) was used. In order to minimize the effect of slurry temperature variation on the machining characteristics of titanium, the entire experimentation was carried out in controlled temperature conditions with maximum permissible variation of $2^{\circ}C$. Each experimental run was replicated twice during the entire experimentation to minimize the effect of noise in the machining parameters. The corresponding material removal rate (MRR) and tool wear rate (TWR) for each experimental run were recorded.

The microstructure testing of the machined samples was performed on a scanning electron microscope (SEM) at a magnification of 1500 X, after preparing and treating the samples with Kroll's reagent (2% HF, 10% HNO_3, 88% distilled water). The hardness testing of the machined samples was performed on micro hardness tester under a static load of 500 gm. The samples for micro-hardness testing were prepared by polishing the machined cavities with boron carbide abrasive powder with a very fine slurry grit size (600, mean particle size 10 μm) to obtain the required surface finish for the testing.

3.2 DESCRIPTION OF THE MACHINING SET UP

The ultrasonic drilling Machine used for the experimentation consisted of an ultrasonic spindle kit; a constant pressure feed system and slurry flow system. The maximum power

input to the machine was 500 W. Figure 3.2 shows the static USM set up used for the experimentation.

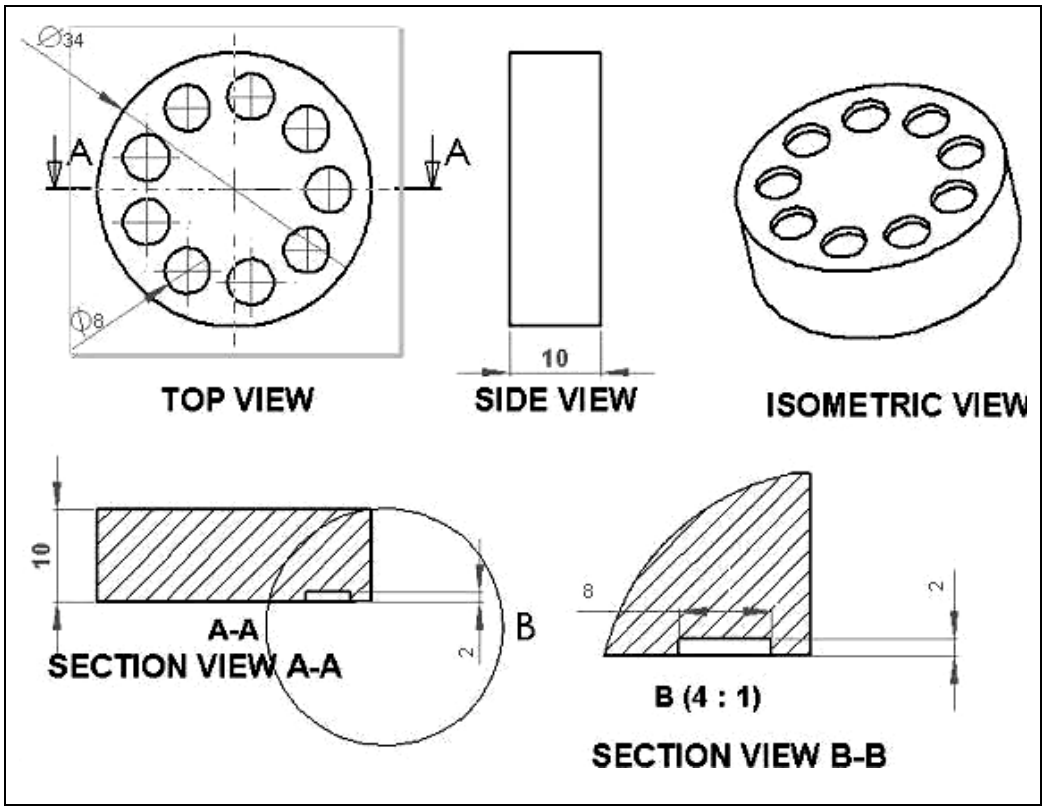

Figure 3.1 Workpiece geometry

The ultrasonic spindle kit comprises an ultrasonic spindle mounted with cylindrical horn, a power supply unit that converts 50 Hz electrical supply to high frequency 20 kHz output. This high frequency electric signal is applied to a piezoelectric transducer positioned in the spindle. The function of this transducer is to convert the applied electrical signal into mechanical vibrations. The amplitude of vibration was in range of 25.3-25.8 μm with a frequency of 20 kHz +/- 200 Hz. The static load for feed rate was fixed at 1.636 Kg and slurry flow was maintained at 36.4 X 10^3 mm^3/min. Various components of the USM set-up have been shown in figures 3.3 and 3.4.

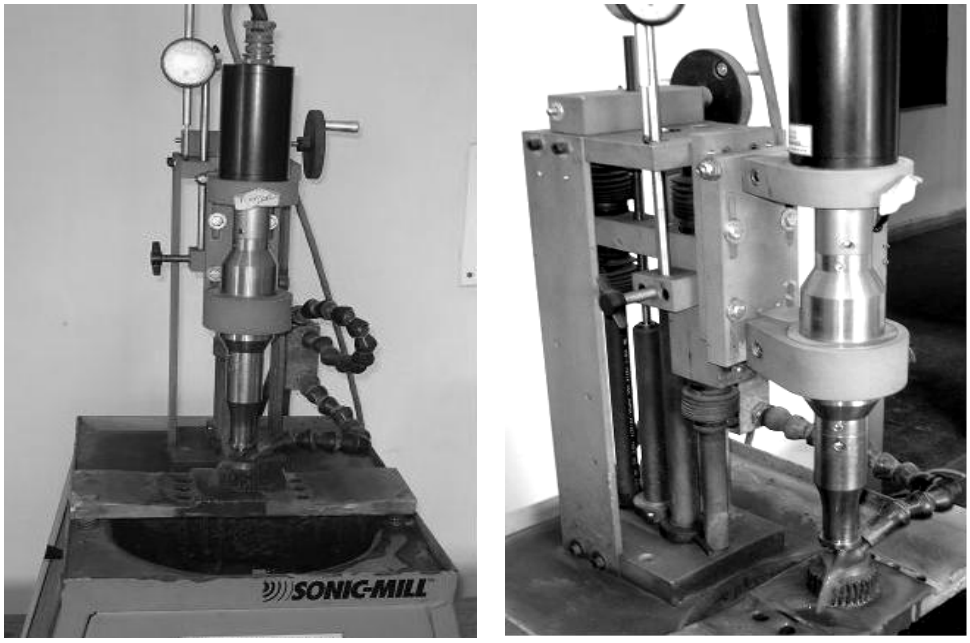

a) Front view **b) Side view**

Figure 3.2 Ultrasonic machining set-up

a) Machining zone (horn-tool-slurry jet-work) **b) Slurry Pump and tank**

Figure 3.3 Components of USM Set-up

a) Dial gauge

b) Amplitude coupling

C) High frequency power supply for USM

Figure 3.4 Components of USM Set-up

All the tools except cemented carbide were made as solid, single piece unit by machining on a center lathe. Tools for cemented carbide material were made in two parts; with the tip brazed to the shank of the tool by silver brazing process at 1200° F. All the tools were made as having same area of cross-section (8 mm Ø).

3.3 PRELIMINARY STUDY TO SELECT THE PARAMETERS

To identify the parameters those affect the machining performance (in terms of MRR, TWR) and quality of the components machined by USM (in terms of surface roughness), a cause and effect diagram [79] was prepared as shown in figure 2.1. The parameters for USM process can be classified as follows:

1. Machine based parameters: ultrasonic power, amplitude of vibration, frequency of vibration, slurry flow rate, temperature of the slurry, tool material, tool geometry (circular, rectangular or any other shape) and shape of the horn.
2. Abrasive Media based parameters: viscosity of the media, type of abrasive material, grain size (type and shape), slurry concentration (by volume or mass).
3. Work-piece based parameters: work-piece geometry (circular, rectangular, irregular shape etc), work-piece thickness, chemical composition of the work material.

The following four independent parameters were selected for this study:

1. Tool material
2. Abrasive material
3. Ultrasonic machine power rating
4. Slurry grit size

The ranges of these parameters were selected on the basis of 'pilot experimentation' conducted to assess the influence of a specific parameter on the machining characteristics of interest (MRR, TWR) by using "one factor at a time approach". The work material for this experimentation was selected as pure titanium (ASTM Grade-I). Three abrasive materials were chosen for the slurry preparation: aluminium oxide (Al_2O_3), silicon carbide (SiC) and boron carbide (B_4C). The slurry was prepared with a volumetric concentration of 25% for all the abrasive materials with water as slurry media.

3.3.1 Pilot Experimentation

The response variables for this investigation have been selected as material removal rate (MRR), tool wear rate (TWR) and surface roughness (SR). MRR is defined as the loss of weight (for work material) per unit time after processing with USM. Similarly, TWR is defined as loss of weight (tool material) per unit time after machining with USM.

Mathematically,

$$MRR = (W_1 - W_2)/t$$

Where**:**

'W_1' is initial weight of the work-piece in gm (before machining)

'W_2' is final weight of the work-piece in gm (after machining)

't' is the time in min for '02 mm' fixed depth of cut in the work-piece.

$$TWR = (V_1 - V_2)/t$$

Where:

'V_1' is initial weight of the tool in gm (before machining)

'V_2' is final weight of the tool in gm (after machining)

't' is the machining time in min for '02 mm' fixed depth of cut in work.

As the tool materials used for the experimentation possess different values of densities, the tool wear rate in terms of 'change in volume' per unit time could be a better measure of the rate at which the different tool materials are eroded while machining takes place. Hence, the tool wear rate as well as material removal rate was calculated as reduction in volume per unit time (mm^3/min) so as to facilitate more accurate comparison of the TWR for different tool materials under varying process conditions.

Mathematically,

$$\boldsymbol{MRR = (W_1 - W_2)/t.\ \rho}$$

Where,

ρ = density of the work material in gm/mm^3

Similarly,

$$\boldsymbol{TWR = (V_1 - V_2)/t.\ \rho}$$

Where,

ρ = density of the corresponding tool material in gm/mm^3

SR is measured using a surface roughness measuring instrument (Perthometer). The experiments were conducted using "one factor at a time" approach. The pilot experimentation has been performed in seven steps.

Case 1: Aluminium oxide slurry, Grit size 220, Slurry Concentration 25%

The experimentation at first stage was conducted with two different tool materials-high carbon steel (HCS) and titanium alloy (ASTM Grade-V). The power rating factor was made to assume four levels (range 100 W-400 W) with equal intervals of 100 W. Power levels less than 100 W were not used as the machining efficiency was very low. Power levels beyond 400 W could not be used as machining status was highly unstable at very high values of power rating. In USM process, the volume of slurry circulating in the working gap undergoes some inevitable variations; hence to minimize the effect of fluctuations in the slurry flow rate a large volume of slurry was prepared. The depth of cut was closely monitored from the dial indicator provided in the set up. Each experiment was repeated twice. Material removal rate (MRR) and tool wear rate (TWR) were calculated for each trial and recorded. The output variables (MRR, TWR) have been plotted for different work-tool combinations (refer figures 3.5-3.8).

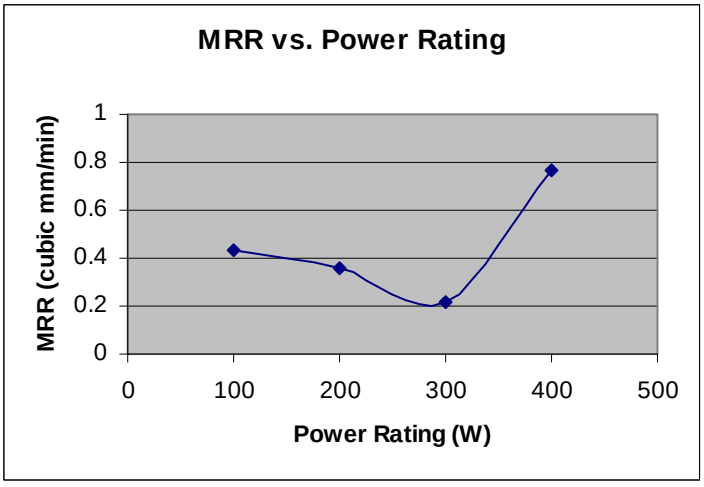

Figure 3.5 MRR Vs. Power Rating for Titanium work-piece using HCS tool

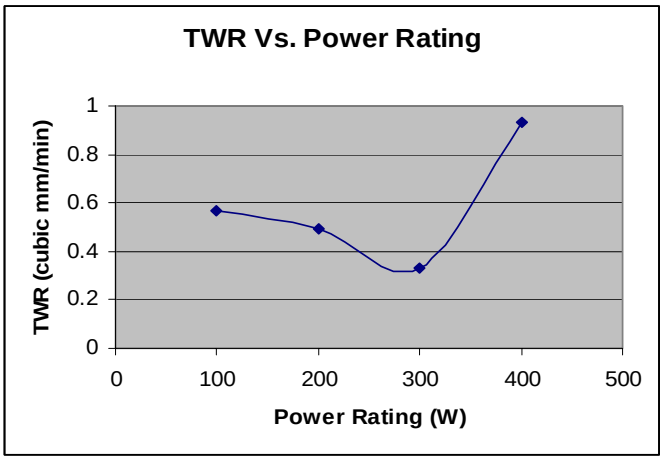

Figure 3.6 TWR Vs. Power Rating for HCS tool while machining Titanium

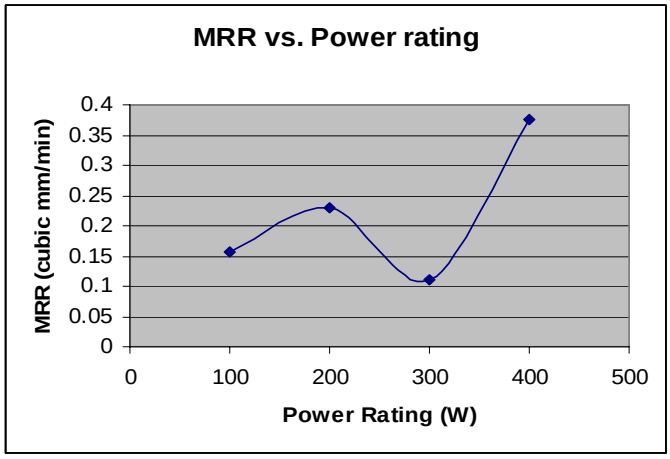

Figure 3.7 MRR Vs. Power Rating for Titanium using Ti alloy tool

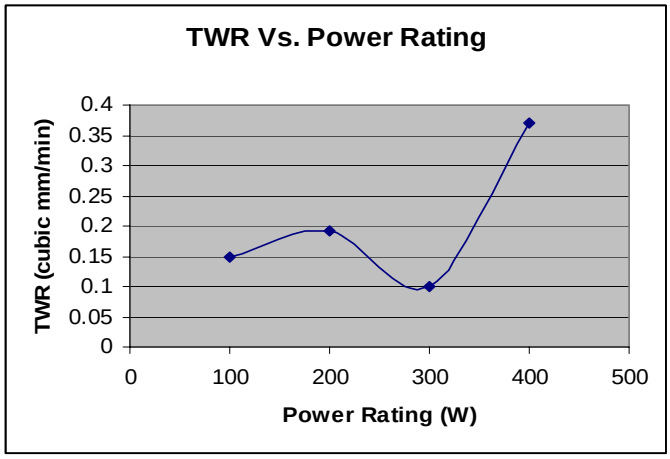

Figure 3.8 TWR Vs. Power Rating for Ti alloy tool while machining Ti

Case 2: Aluminium oxide Slurry, Grit size 320, Slurry concentration 25%

For second stage of pilot experimentation, all other factors were kept unchanged while the slurry grit size was changed to 320. The values of MRR and TWR were recorded for both the tool materials used- high carbon steel and titanium alloy. The entire experimentation was conducted in similar manner as in previous stage. The output variables have been plotted for different work-tool combinations (figure 3.9-3.12).

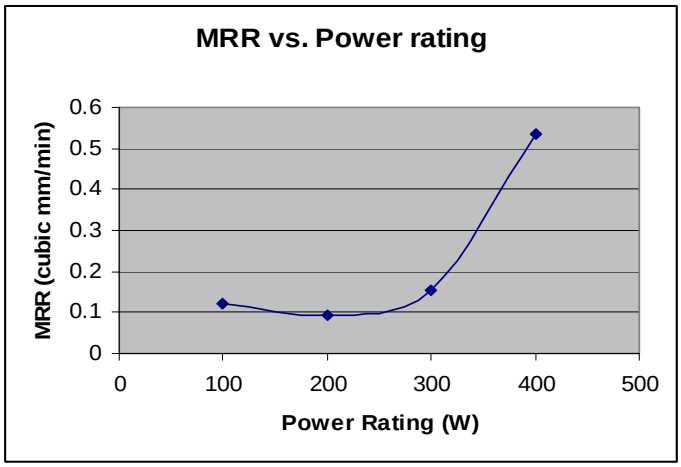

Figure 3.9 MRR vs. Power Rating for Titanium using HCS tool

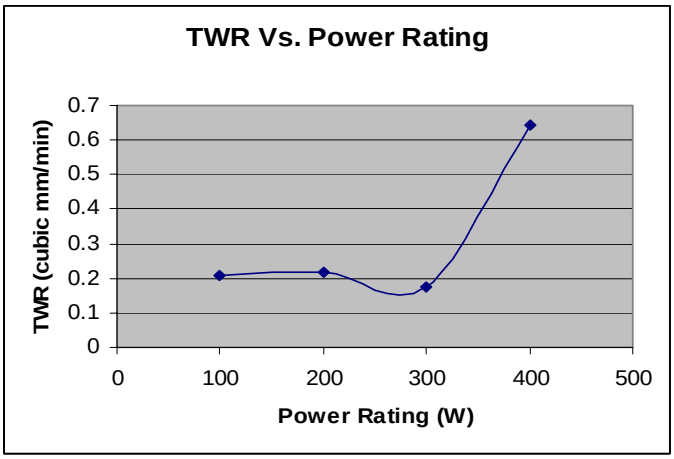

Figure 3.10 TWR vs. Power Rating for HCS tool while machining titanium

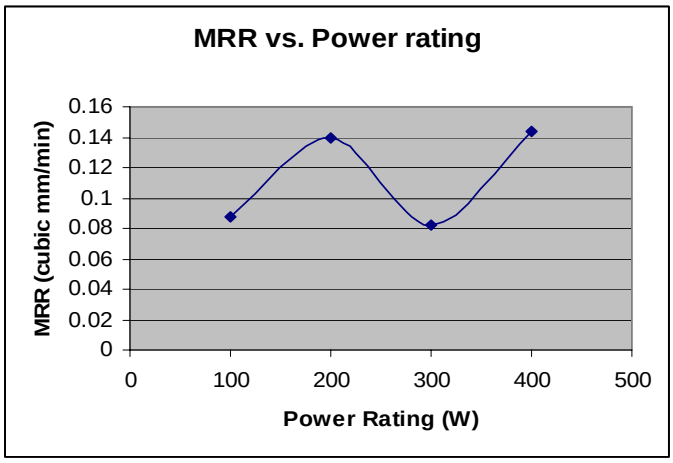

Figure 3.11 MRR Vs. power Rating for Titanium using Titanium alloy tool

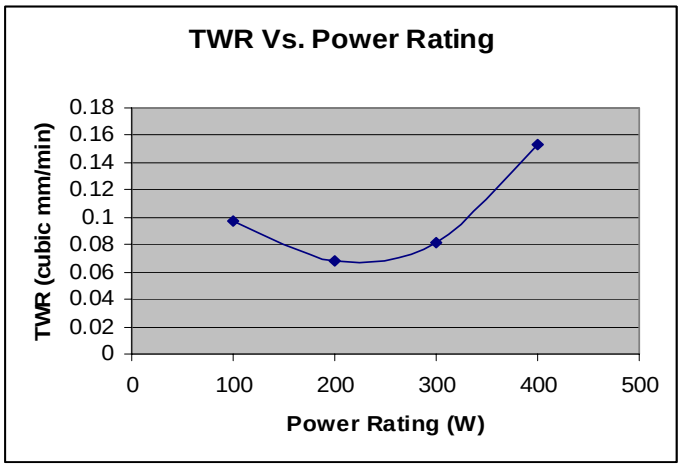

Figure 3.12 TWR vs. Power Rating for Ti alloy tool while machining titanium

Case 3: Aluminium oxide Slurry, Grit size 500, Slurry concentration 25%

In third stage, the experimentation was carried out with slurry grit size 500 for alumina. The output variables (MRR, TWR) have been plotted for various work-tool combinations as shown in figure 3.13-3.16.

The machining characteristics for these three stages have been summarized in figures 3.17-3.18. The values of the response variables (MRR, TWR) for three different slurry grit sizes (220, 320 and 500) and two different tool materials (HCS, Titanium alloy) have been plotted to compare and contrast the machining performance under different process conditions.

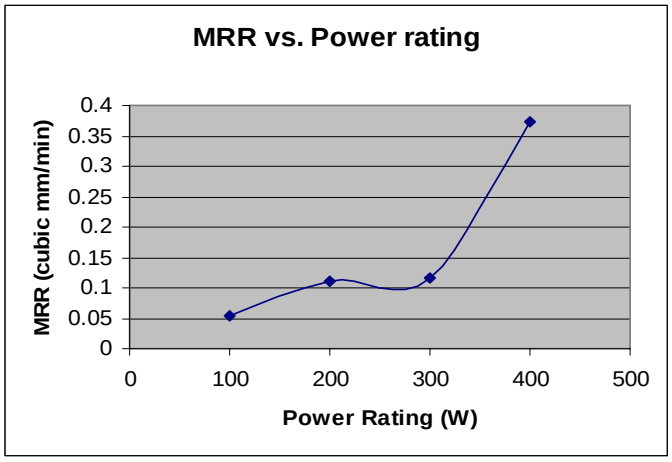

Figure 3.13 MRR Vs. Power Rating for Titanium with HCS tool

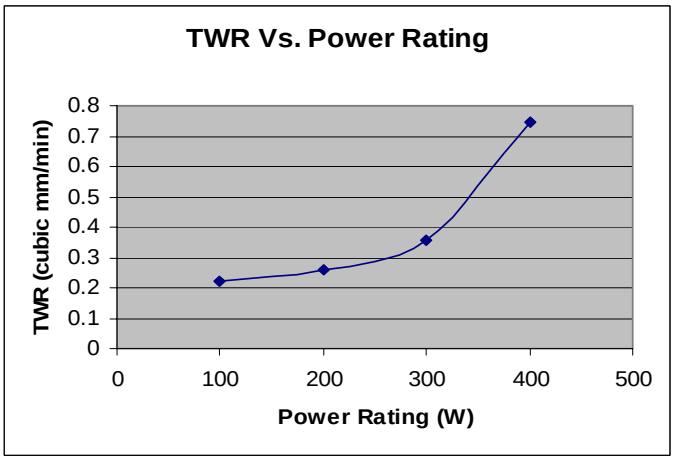

Figure 3.14 TWR Vs. Power Rating for HCS tool while machining titanium

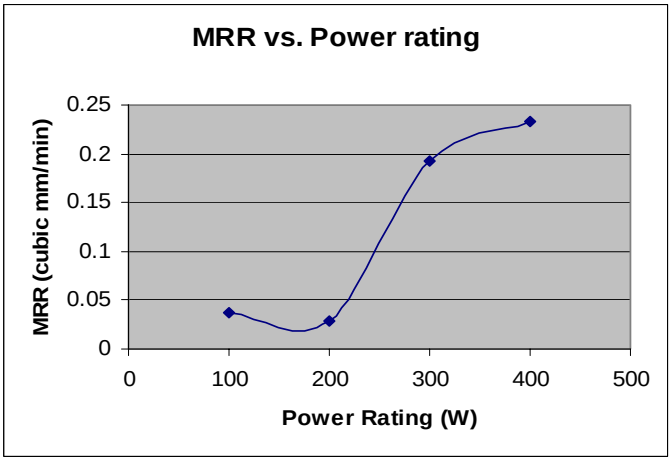

Figure 3.15 MRR Vs. Power Rating for Titanium using Titanium alloy tool

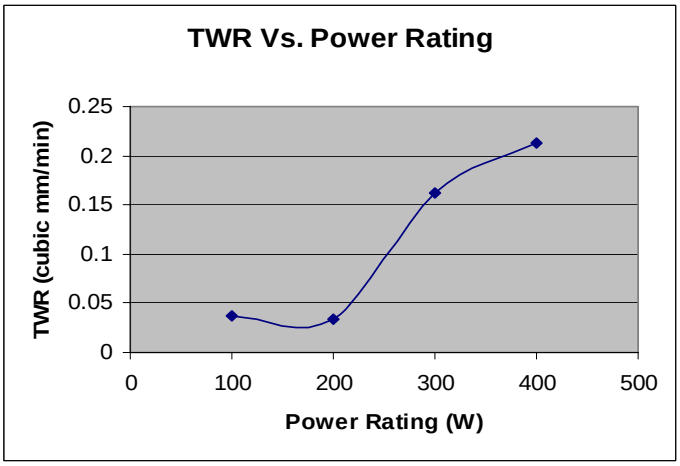

Figure 3.16 TWR Vs. Power Rating for Ti alloy tool while machining titanium

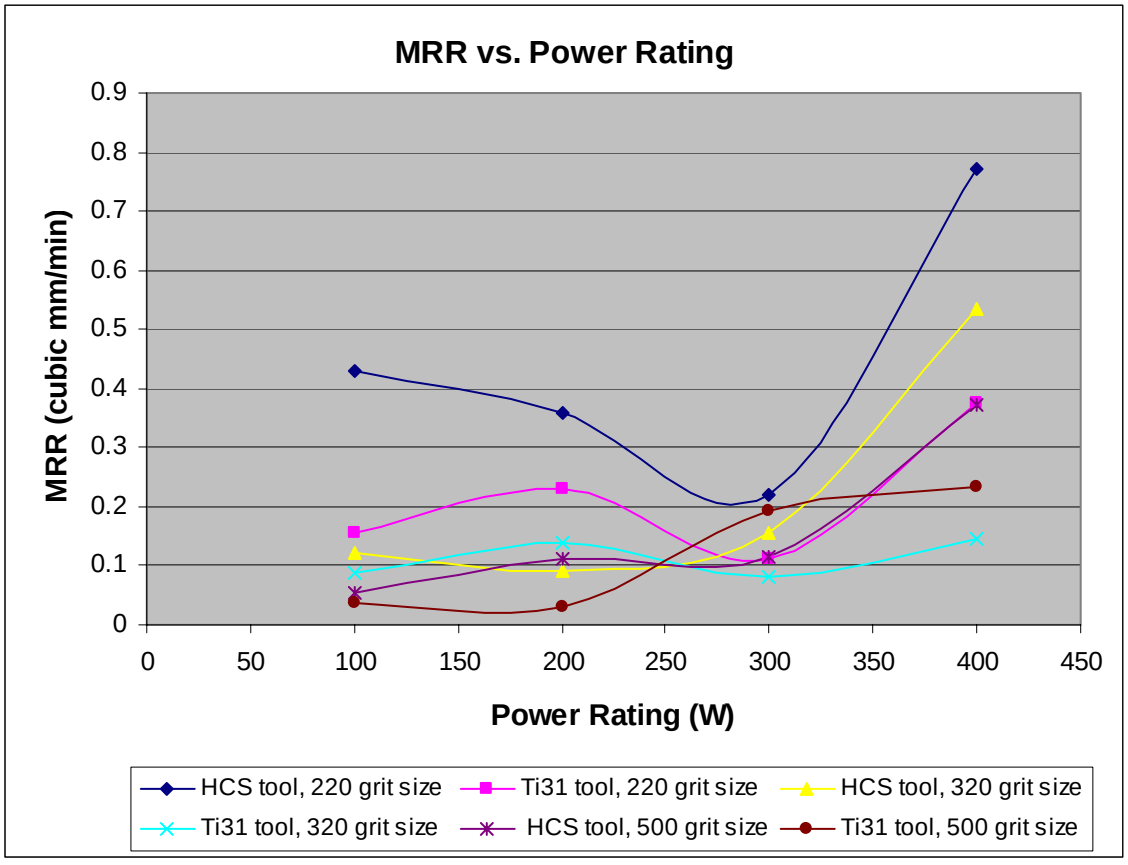

Figure 3.17 MRR vs. Slurry grit size, Power rating and Tool material (alumina slurry)

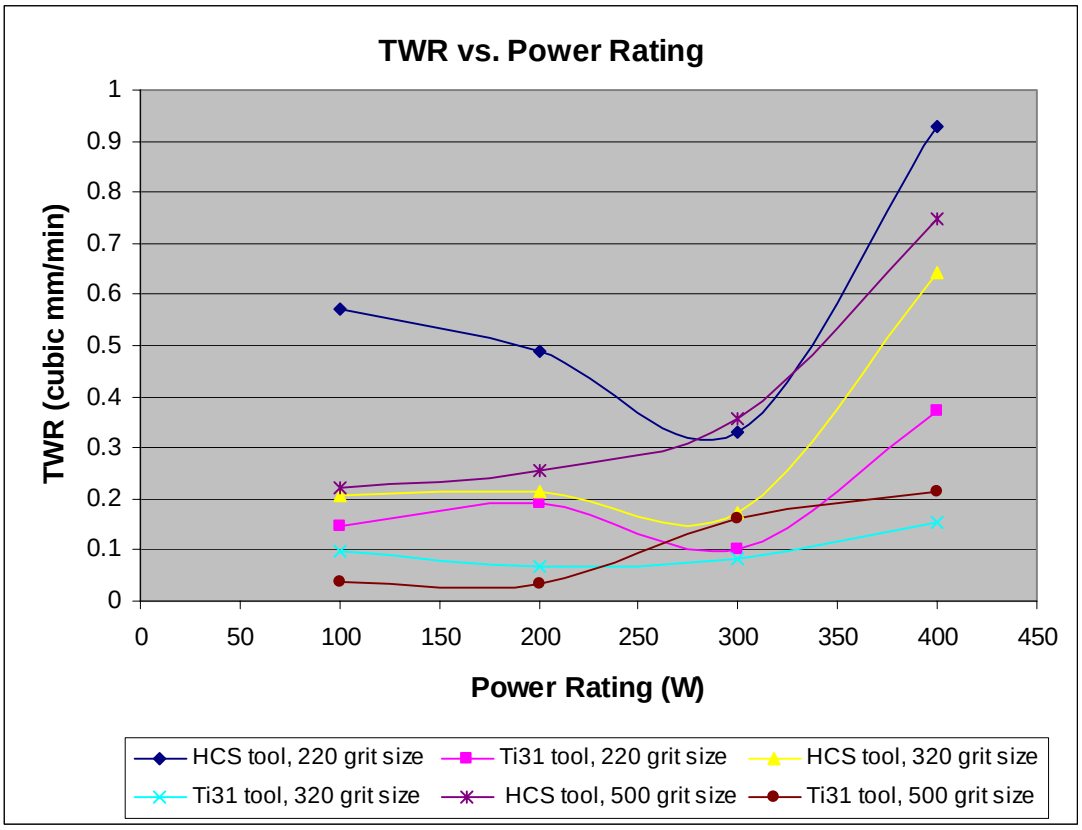

Figure 3.18 TWR vs. Slurry grit size, Power rating and Tool material (alumina slurry)

It can be observed from the figures 3.17-3.18 that use of HCS tool leads to higher MRR and TWR than that obtained while using titanium alloy tool irrespective of the slurry grit size used. Any increase in the coarseness of the slurry grit size leads to realization of higher MRR as well as TWR while other factors such as tool material and power rating are kept constant. Also, the trend of variation of MRR/TWR with respect to power rating is not same or uniform for different process conditions i.e. tool materials and slurry grit sizes.

Case 4: Silicon carbide slurry, 220 Grit size, Slurry concentration 25%

The experimentation in fourth stage was conducted with silicon carbide slurry with a coarse grit size of 220. Three different tool materials were used; high speed steel, titanium (ASTM Grade-I) and cemented carbide. The values of output variables (MRR, TWR) were recorded and plotted as shown in figures 3.19-3.24.

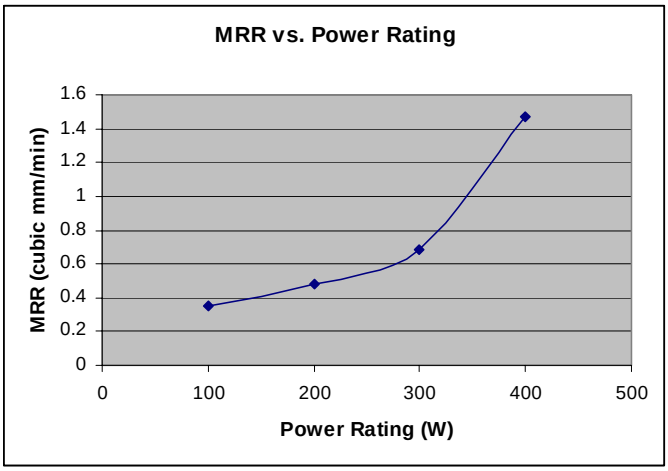

Figure 3.19 MRR vs. Power Rating for Titanium using HSS tool

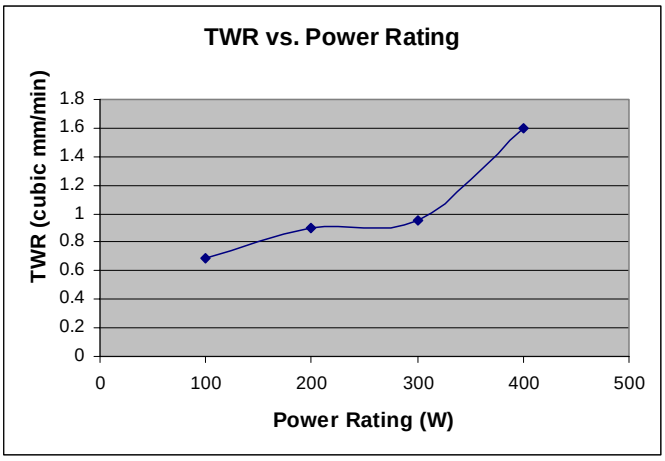

Figure 3.20 TWR vs. Power Rating for HSS tool while machining Titanium

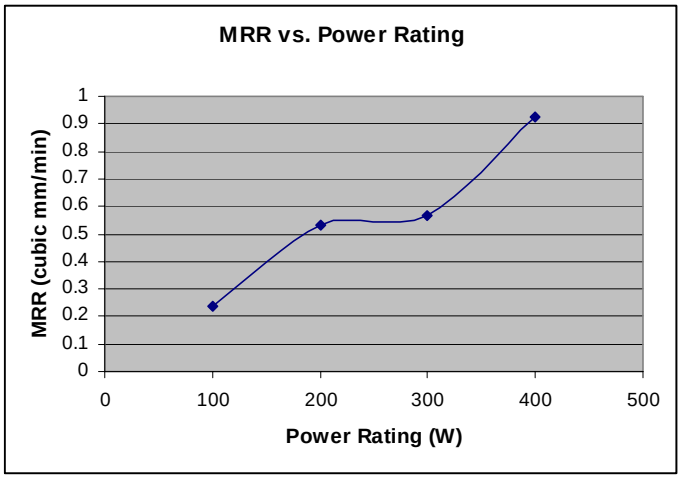

Figure 3.21 MRR vs. Power Rating for Titanium using Titanium tool

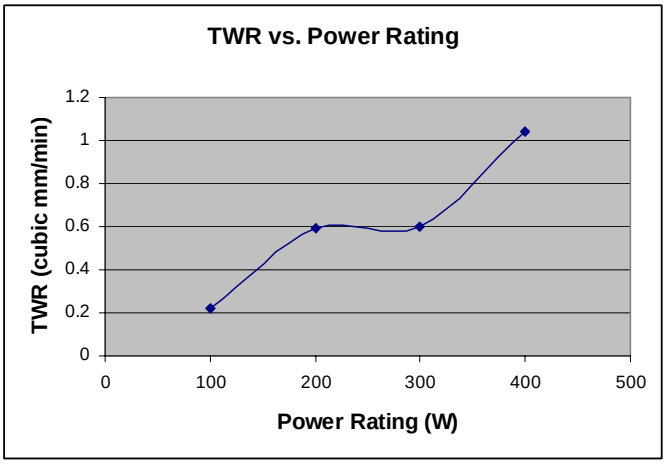

Figure 3.22 TWR vs. Power Rating for Titanium tool while machining Titanium

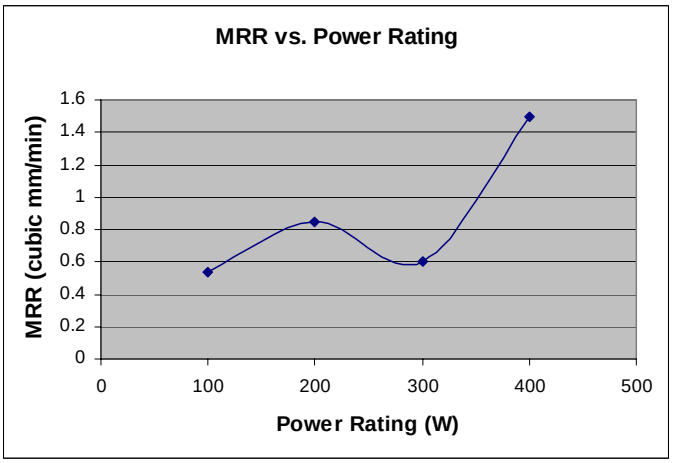

Figure 3.23 MRR vs. Power Rating for Titanium Workpiece using Carbide tool

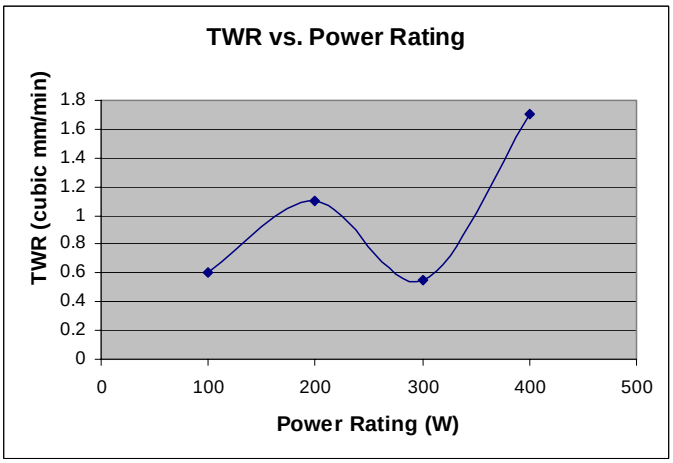

Figure 3.24 TWR vs. Power Rating for Carbide tool while machining Titanium

Case 5: Silicon carbide slurry, 320 Grit size, Slurry concentration 25%

The experimentation at this stage was carried out by using tools made of high speed steel and titanium (ASTM Grade-I). The slurry was prepared with a concentration of 25% (by volume) and the temperature of the slurry was controlled. The output variables have been presented in figures 3.25-3.28.

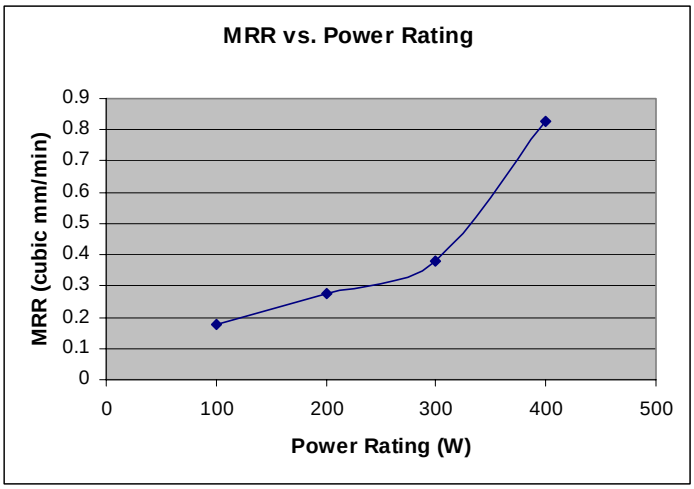

Figure 3.25 MRR vs. Power Rating for Titanium Workpiece using HSS tool

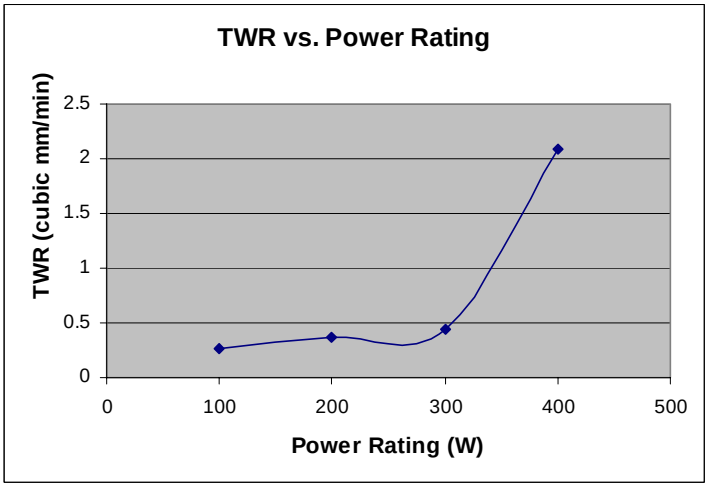

Figure 3.26 TWR vs. Power Rating for HSS tool while machining Titanium

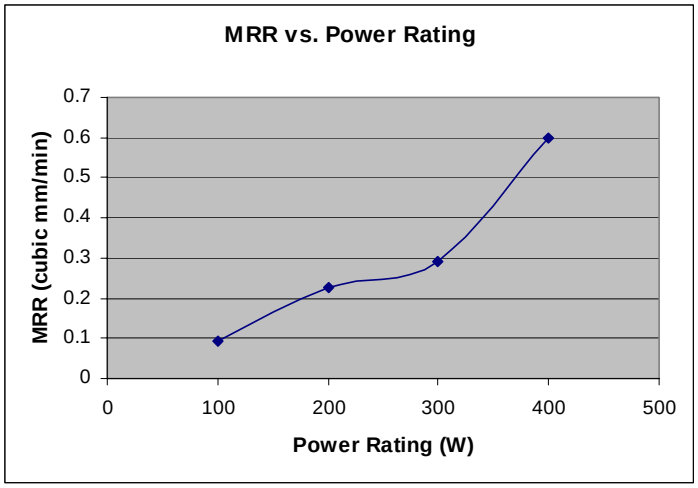

Figure 3.27 MRR vs. Power Rating for Titanium using Titanium tool

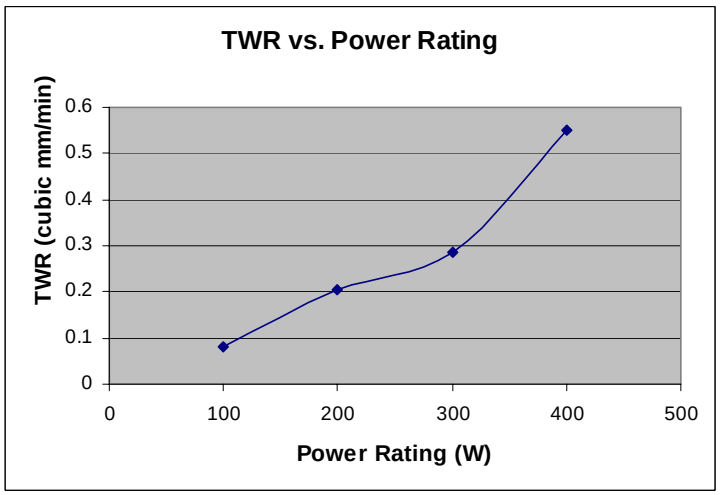

Figure 3.28 TWR vs. Power Rating for Titanium tool while machining Titanium

Case 6: Silicon carbide slurry, 500 Grit size, 25% Slurry concentration

The experimentation at sixth stage was performed to know the influence of power rating and tool material on the response variables (MRR, TWR). A very fine grit size (mesh 500, mean grain size: 18 μm) of silicon carbide abrasive was used for preparation of slurry with 25% concentration. Power rating of the ultrasonic machine was varied from 100 W to 400 W keeping all other factors constant (figures 3.29-3.32).

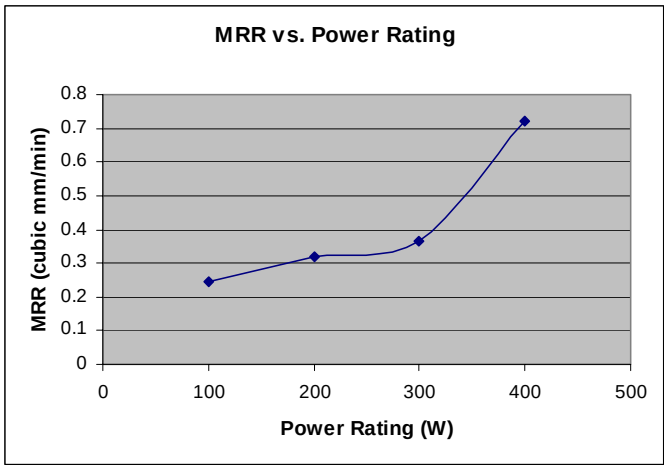

Figure 3.29 MRR vs. Power Rating for Titanium work-piece using HSS tool

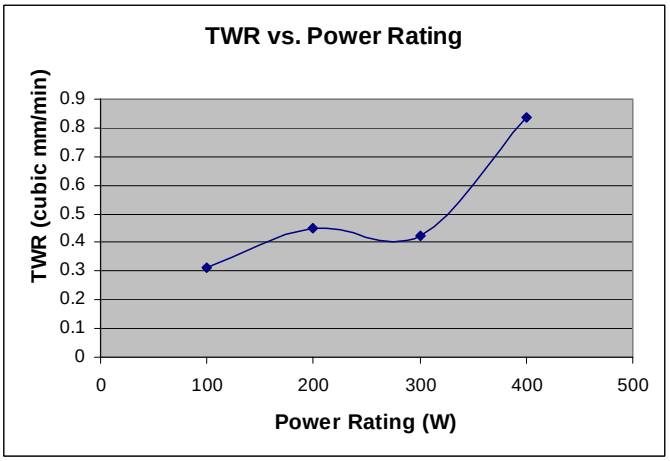

Figure 3.30 TWR vs. Power Rating for HSS tool while machining Titanium

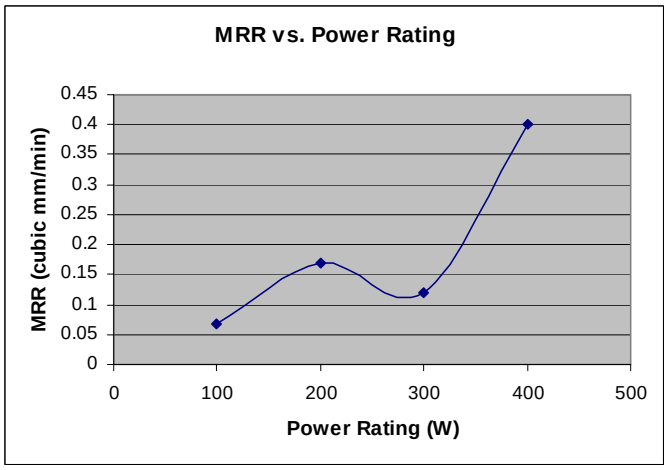

Figure 3.31 MRR vs. Power Rating for Titanium work-piece using Titanium tool

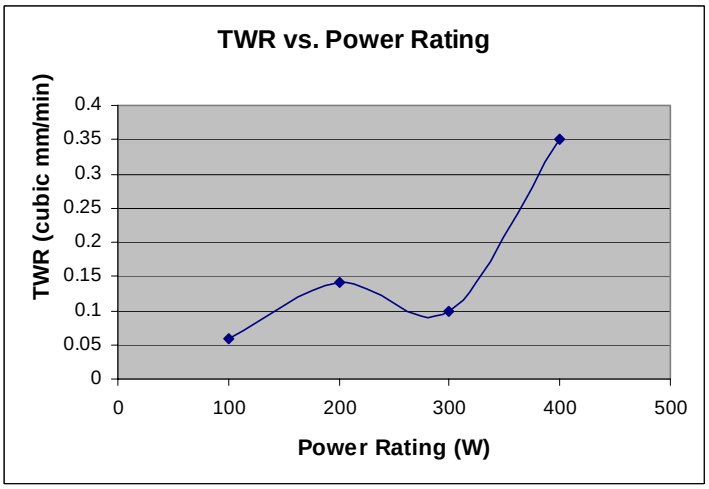

Figure 3.32 TWR vs. Power Rating for Titanium tool while machining Titanium

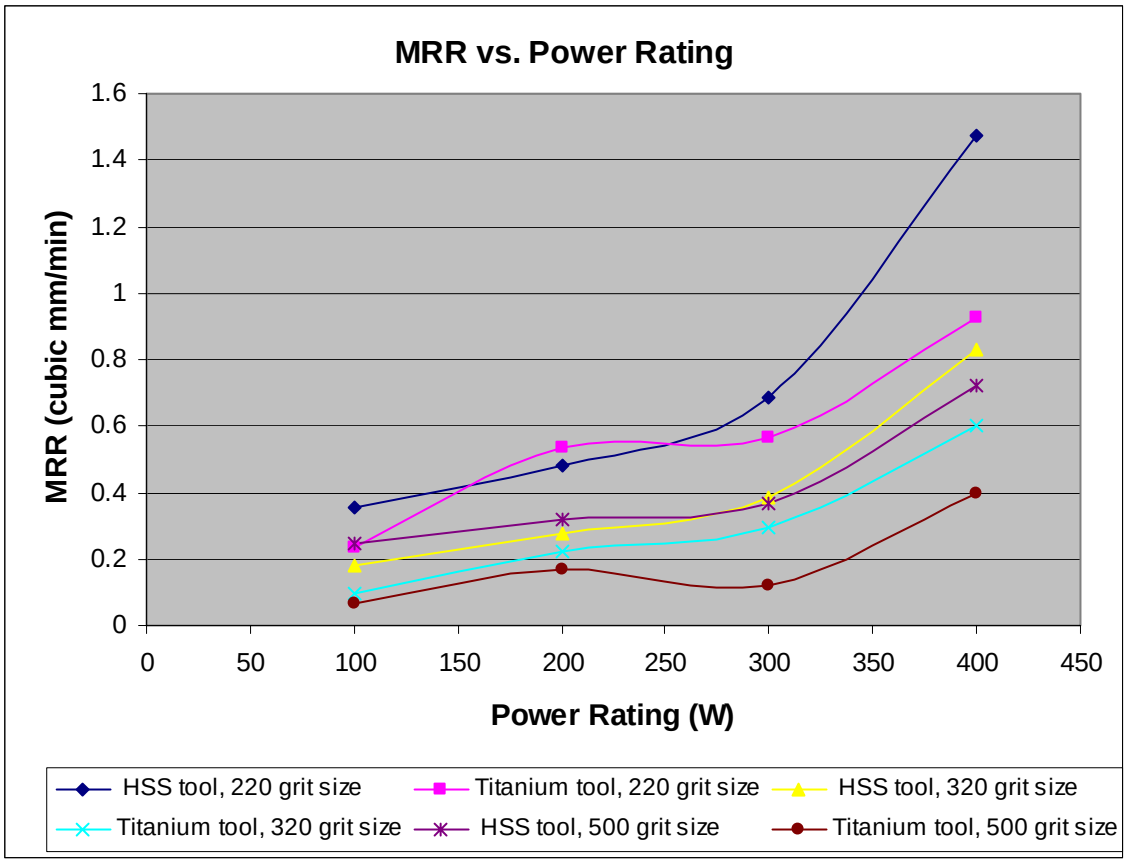

Figure 3.33 MRR vs. Slurry grit size, Power Rating and Tool material (slurry: SiC)

The values of the response variables (MRR, TWR) under the influence of different power rating levels; three different slurry grit sizes (220, 320 and 500) of silicon carbide slurry and two different tool materials (HSS, Titanium) have been summarized and plotted to compare and contrast the machining performance under different process conditions (refer figures 3.33-3.34).

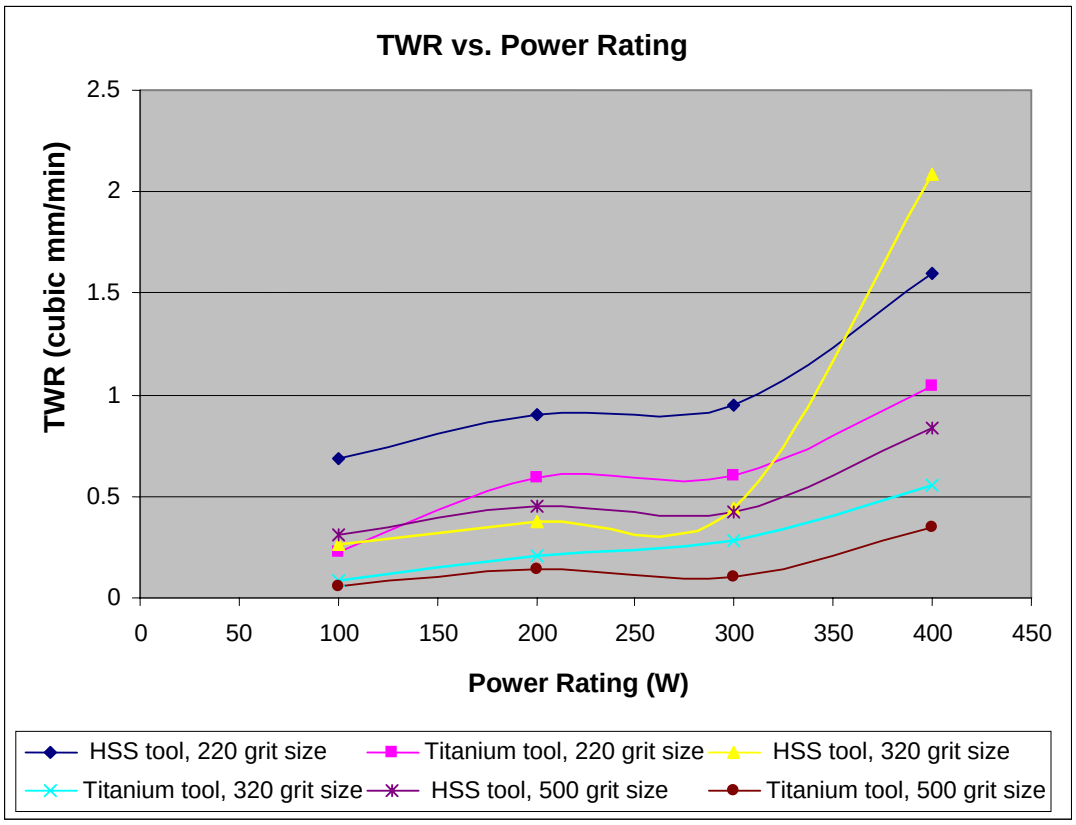

Figure 3.34 TWR vs. Slurry grit size, Power Rating and Tool material (slurry: SiC)

Case 7: Boron carbide slurry, Grit size 320, Slurry concentration 25%

Boron carbide abrasive with grit size 320 was used for experimentation at this stage. Tools made of cemented carbide and high carbon steel were used and the power rating was varied in four equal intervals of 100 W. The slurry was prepared with a concentration level of 25% (by volume). The values of output variables (MRR, TWR) were recorded for each trial and thereafter, have been plotted (figures 3.35-3.38) to present the variation of machining performance of USM with respect to the different process conditions.

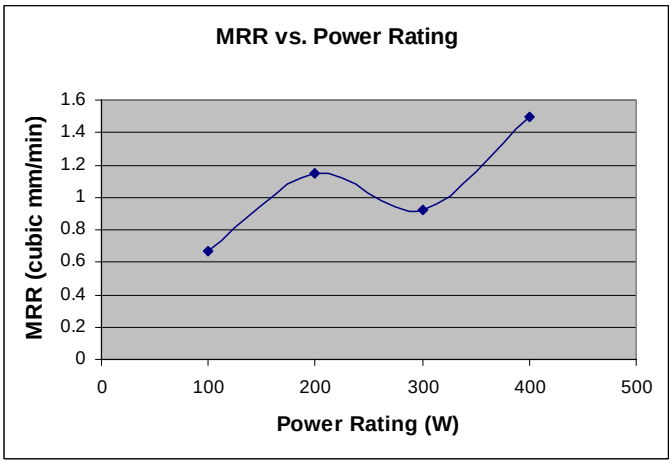

Figure 3.35 MRR vs. Power Rating for Titanium using Cemented Carbide tool

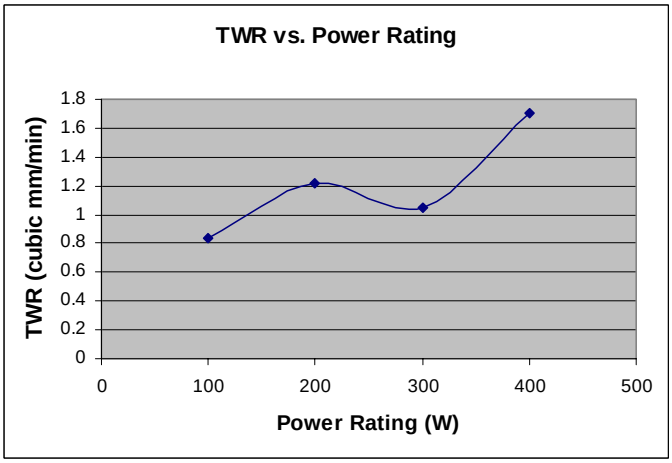

Figure 3.36 TWR vs. Power Rating for Carbide tool while machining titanium

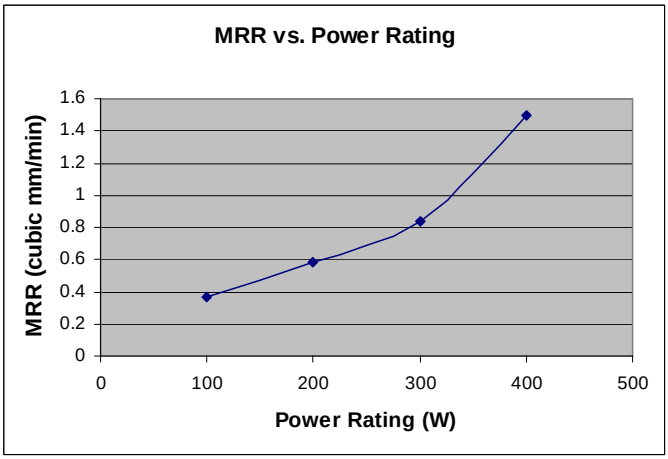

Figure 3.37 MRR vs. Power Rating for Titanium workpiece using HCS tool

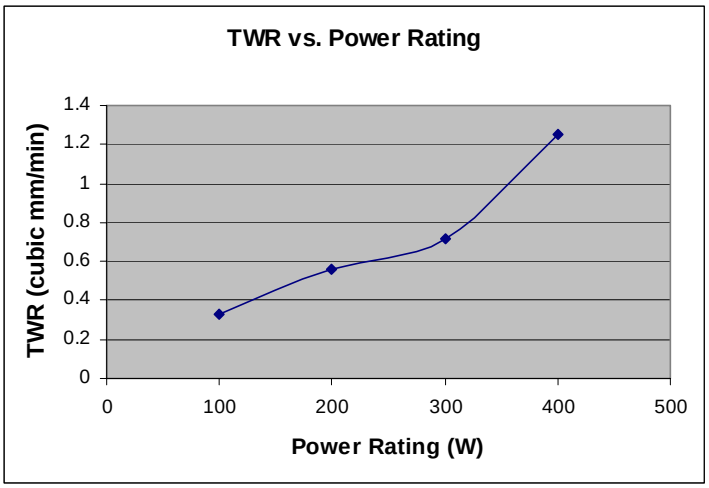

Figure 3.38 TWR vs. Power Rating for HCS tool while machining Titanium

From the pilot experimentation, the following conclusions could be drawn:

1. The machining characteristics (MRR, TWR) in ultrasonic machining of titanium (ASTM Grade-I) have been found to be correlated and dependent upon the input parameters such as power rating of the ultrasonic machine, slurry grit size and type of tool material used. It can be observed (figures 3.17-3.18, 3.33-3.34) that both MRR as well as TWR tend to increase with a corresponding increase in the coarseness of the slurry used irrespective of the abrasive used for preparation of the slurry. Also, the MRR and TWR obtained with different tool materials (HSS, HCS, titanium, titanium alloy and cemented carbide) are significantly different when all other input parameters are controlled and remain fixed. Thus, the tool material properties such as hardness and toughness have been found to control the machining characteristics in USM of titanium.
2. The variation of MRR and TWR with ultrasonic power rating is not uniform or linear; in some cases the MRR/TWR increases with increase in power rating but after crossing certain level of power rating, MRR/TWR drops. This might be attributed to the relative strain hardening of the work/tool material. This has also been found to be dependent on the type of tool material being used. Different tool materials behave differently with respect to power rating of the

ultrasonic machine; thereby giving different trends of variation of MRR/TWR with ultrasonic power rating.

3. As the MRR/TWR obtained with different work-tool combinations has been found to differ significantly, there is a critical need for optimizing the process conditions in terms of input parameters such as power rating, slurry grit size and abrasive material proprieties for a specific work-tool combination.
4. The type of abrasive used also affects the MRR as well as TWR. It could be concluded (figures 3.17-3.18, 3.33-3.34) that use of silicon carbide slurry results in better MRR for titanium work-piece for same process conditions than that obtained with alumina as slurry material. This can be attributed to the higher hardness and cutting ability of silicon carbide abrasive over alumina.
5. The tool wear rate (TWR) for all the tool materials has been found to be higher for those process settings that contribute to higher material removal rate (MRR). In other words, in USM of titanium the tool wear rate is directly correlated with material removal rate of the work-piece. Hence, TWR has been found to be maximum at points of maximum MRR. Therefore, both the machining characteristics need to be optimized in combination for USM of titanium.
6. It is possible to drill holes in commercially pure titanium (ASTM Grade-I) by ultrasonic machining, without causing any surface damage to the work material in form of micro-cracking, heat affected zones or residual stresses.
7. Tool design is a very important characteristic for obtaining optimum MRR and cost effectiveness in USM of titanium. The mass, length of the tool should be decided with immense practical consideration as the effective amplitude of vibration is reduced; thereby reducing the ultrasonic energy available for machining of the work-piece, if the mass of the tool is increased beyond certain limit. Large tool also causes over stressing and deformation.

From the above stated points, it can be concluded that there is a large scope for exploring the machining characteristics of titanium in ultrasonic machining; using different slurry, tool and work material combinations together with different ultrasonic

power rating levels for optimum utilization in manufacturing industry. In the present investigation, cylindrical horn of 25.4 mm was used with tool weight constraint of 55 g maximum. As observed practically, the use of tool weight above 55 g leads to overloading of the machine and auto cut-off (experimental setup limitation).

3.3.2 Selection of factor levels

As the objective of this study is to investigate the machining characteristics of titanium using different tool materials in ultrasonic machining and to model these characteristics for their application in the concerned manufacturing industry**,** the following issues have been taken up during this research work:

1. Material removal rate (MRR) of titanium (ASTM Grade-I) as work material has been explored in ultrasonic machining with the following tool materials; high carbon steel, high speed Steel, cemented carbide, titanium and titanium alloy.
2. Tool wear rate (TWR) of aforesaid tool materials has been explored with t**itanium** as work material.
3. Relationships between different machining parameters (grain size of the abrasive slurry, slurry type, tool material, work material, and power rating of the machine) and machining characteristics (material removal rate, tool wear rate, and surface roughness) have been established in this regard.
4. Material characteristics like microstructure and hardness have also been determined for the given work samples.
5. The results obtained have been modeled for their application in the concerned manufacturing industry.

In light of the objective, the levels for each factor have been decided keeping in view the commercial availability, experimental limitations and machine tool capacity. The information regarding this could be taken from the pilot experimentation performed. Because the use of different tool materials resulted in different trends of MRR and TWR; as observed in the preliminary study, five different levels for tool material factor were selected. Each tool material was designated a level. Similarly, three levels of slurry grit size, power rating and abrasive material were finalized. These levels were selected in

light of the trends of MRR and TWR obtained under different process conditions during the pilot experimentation. Table 3.1 details the different control variables and their levels.

Table 3.1 Control variables and their levels

S. No.	Factor	Levels	Level I	Level II	Level III	Level IV	Level V
A	Tool Material	5	H.C.S.	H.S.S.	Titanium	Titanium alloy	Cemented Carbide
B	Abrasive Type	3	Alumina	Silicon carbide	Boron carbide	___	___
C	Slurry grit size	3	220	320	500	___	___
D	Power Rating	3	100 W	250 W	400 W	___	___

Taguchi's robust design of experiments (DOE) methodology was used to plan the experiments statistically. Before finalizing a particular orthogonal array for the purpose of designing the experiments, the following two things must be established [19, 129]:

1. The number of parameters and interactions of interest
2. The number of levels for the parameters of interest

In the present investigation, four different process parameters have been selected as already discussed. The tool material factor has five levels whereas all other parameters such as abrasive type, grit size and power rating of the machine have three levels each. As per the requirements of the study, L18 orthogonal array has come out as one of the possible solutions for designing the experiments. Hence, L18 array (in modified form) was selected for the present investigation. L18 array has a special property that the two way interactions between the various parameters are partially confounded with various columns and hence their effect on the assessment of the main effects of the various parameters is minimized [3, 13]. It is not possible to assess the possible two factor interactions in L18 array but the main effects of different process parameters can be assessed with reasonable accuracy [32]. The modified L18 OA has been shown in table 3.2.

Table 3.2 Modified L18 Orthogonal Array

Experiment Number	Column 1	2	3	4
1	1	1	1	1
2	1	2	2	2
3	1	3	3	3
4	2	1	1	2
5	2	2	2	3
6	2	3	3	1
7	3	1	2	1
8	3	2	3	2
9	3	3	1	3
10	4	1	3	3
11	4	2	1	1
12	4	3	2	2
13	5	1	2	3
14	5	2	3	1
15	5	3	1	2
16	6	1	3	2
17	6	2	1	3
18	6	3	2	1

Based on the L18 OA, the control log for experimentation has been designed (table 3.3). As the tool material factor involves five levels, any one of these five levels needs to be replicated to take place of the sixth level, which is absent in this study. Level 1 was selected for this replication. Hence, tool made of high carbon steel (HCS) was used to perform experiment number 16, 17 and 18 in place of the sixth level for tool material factor. The standard array (table 3.2) was modified accordingly. The eighteen rows of L18 orthogonal array represent the eighteen experiments to be conducted during the experimentation. Thus, experiment number 1 has to be conducted at level 1 for each of the four control factors. The remaining experiments are conducted in the similar manner.

The levels for each factor during each trial are more conveniently expressed by means of experimenter's log sheet (refer table 3.3). In the present investigation, three response variables have been selected-material removal rate (MRR), tool wear rate

(TWR) and surface roughness (SR). The details of these response variables are given in table 3.4. As it can be observed, all the three response variables are continuous type variables.

Table 3.3 Control Log for Experimentation

Exp. No.	A: Col. 1 Tool Material	B: Col. 2 Abrasive Type	C: Col. 3 Grit Size	D: Col. 4 Power Rating (W)
1	HCS	Alumina	220	100
2	HCS	Silicon carbide	320	250
3	HCS	Boron Carbide	500	400
4	HSS	Alumina	220	250
5	HSS	Silicon carbide	320	400
6	HSS	Boron carbide	500	100
7	Titanium	Alumina	320	100
8	Titanium	Silicon carbide	500	250
9	Titanium	Boron carbide	220	400
10	Titanium alloy	Alumina	500	400
11	Titanium alloy	Silicon Carbide	220	100
12	Titanium alloy	Boron Carbide	320	250
13	Cemented Carbide	Alumina	320	400
14	Cemented Carbide	Silicon Carbide	500	100
15	Cemented Carbide	Boron Carbide	220	250
16	HCS	Alumina	500	250
17	HCS	Silicon carbide	220	400
18	HCS	Boron carbide	320	100

Table 3.4 Response Variables

Response	Response 1	Response 2	Response 3
Response Name	MRR	TWR	SR
Response Units	mm^3/min	mm^3/min	microns
Response Type	Continuous	Continuous	Continuous

For conducting final run of experiments, all the four factors have been denoted by specific letter with a suffix representing specific parameter and its level as shown in table 3.5. The notations used are having following full meanings.

Table 3.5 Representation of a factor's level

Factor Name	Level I	Level II	Level III	Level IV	Level V
Tool Material	A1	A2	A3	A4	A5
Abrasive Type	B1	B2	B3		
Slurry grit size	C1	C2	C3		
Power Rating	D1	D2	D3		

A for Tool Material

A1 (Tool-1) ---------- High carbon steel

A2 (Tool-2) ---------- High speed steel

A3 (Tool-3) ----------Titanium

A4 (Tool-4) ----------Titanium alloy

A5 (Tool-5) ----------Cemented carbide

B for Abrasive Type

B1 (Type-1) Alumina

B2 (Type-2) Silicon carbide

B3 (Type-3) Boron carbide

C for Slurry Grit Size

C1= 220 grit size

C2= 320 grit size

C3= 500 grit size

D for Power Rating (ultrasonic power)

D1 (Low) : 100 W

D2 (Medium) : 250 W

D3 (High) : 400 W

All the experiments were replicated twice; hence three trials were conducted at each experimental run. The output variables were recorded for each trial and then the results for each experimental run were averaged out to obtain the mean value of response variables (MRR, TWR and S.R.) for that particular experiment. The test data pertaining to the input parameter setting for each experimental run has been detailed in Table 3.6.

Table 3.6 Input parameters and process settings for Experimentation

Test data Experiment No. 1	**Test data Experiment No. 2**
A1- Tool B1- Abrasive type C1- Grit size D1- Power Rating	A1- Tool B2- Abrasive type C2- Grit Size D2- Power Rating
Test data Experiment No. 3	**Test data Experiment No. 4**
Input parameters settings A1- Tool B3- Abrasive type C3- Grit size D3- Power Rating	Input parameters settings A2- Tool B1- Abrasive type C1- Grit size D2- Power Rating
Test data Experiment No. 5	**Test data Experiment No. 6**
Input parameters settings A2- Tool B2- Abrasive type C2- Grit size D3- Power Rating	Input parameters settings A2- Tool B3- Abrasive type C3- Grit size D1- Power Rating
Test data Experiment No. 7	**Test data Experiment No. 8**
Input parameters settings A3- Tool B1- Abrasive type C2- Grit size D1- Power Rating	Input parameters settings A3- Tool B2- Abrasive type C3- Grit size D2- Power Rating
Test data Experiment No. 9	**Test data Experiment No. 10**
Input parameters settings A3- Tool B3- Abrasive type C1- Grit size D3- Power Rating	Input parameters settings A4- Tool B1- Abrasive type C3- Grit size D3- Power Rating

Test data Experiment No. 11 Input parameters settings A4- Tool B2- Abrasive type C1- Grit size D1- Power Rating	**Test data Experiment No. 12** Input parameters settings A4- Tool B3- Abrasive type C2- Grit size D2- Power Rating
Test data Experiment No. 13 Input parameters settings A5- Tool B1- Abrasive type C2- Grit size D3- Power Rating	**Test data Experiment No. 14** Input parameters settings A5- Tool B2- Abrasive type C3- Grit size D1- Power Rating
Test data Experiment No. 15 Input parameters settings A5- Tool B3- Abrasive type C1- Grit size D2- Power Rating	**Test data Experiment No. 16** Input parameters settings A6- Tool B1- Abrasive type C3- Grit size D2- Power Rating
Test data Experiment No. 17 Input parameters settings A6- Tool B2- Abrasive type C1- Grit size D3- Power Rating	**Test data Experiment No. 18** Input parameters settings A6- Tool B3- Abrasive type C2- Grit size D1- Power Rating

3.3.3 Tool Design for Experimentation

In ultrasonic machining, the mass and dimensions of the tool constitute a very important design problem to economize the machining operation [9, 16, 56, 102]. As the tool materials selected for the experimentation possess different densities, the designing of the tools is needed to be carried out with a consideration that the mass of each tool should be same to the maximum possible extent and moreover, it should be within the critical limit of 55 gm.

For the experimental study undertaken, it was decided to fix the mass of each tool as 50 gm. All the tools except cemented carbide were made as single piece unit by machining on a centre lathe. Tools for cemented carbide material were made by silver

brazing the tip with the part to be connected to horn. This part contains unified threads and is tightened to the horn manually. The horn is of 25.4 mm size and it contains internal threads. The length of the tool tip in USM needs to be restricted and maintained within the limits of 15-20 mm for optimum results. The use of a length more than 20 mm may result in over stressing of the tool and shortened tool life [151].

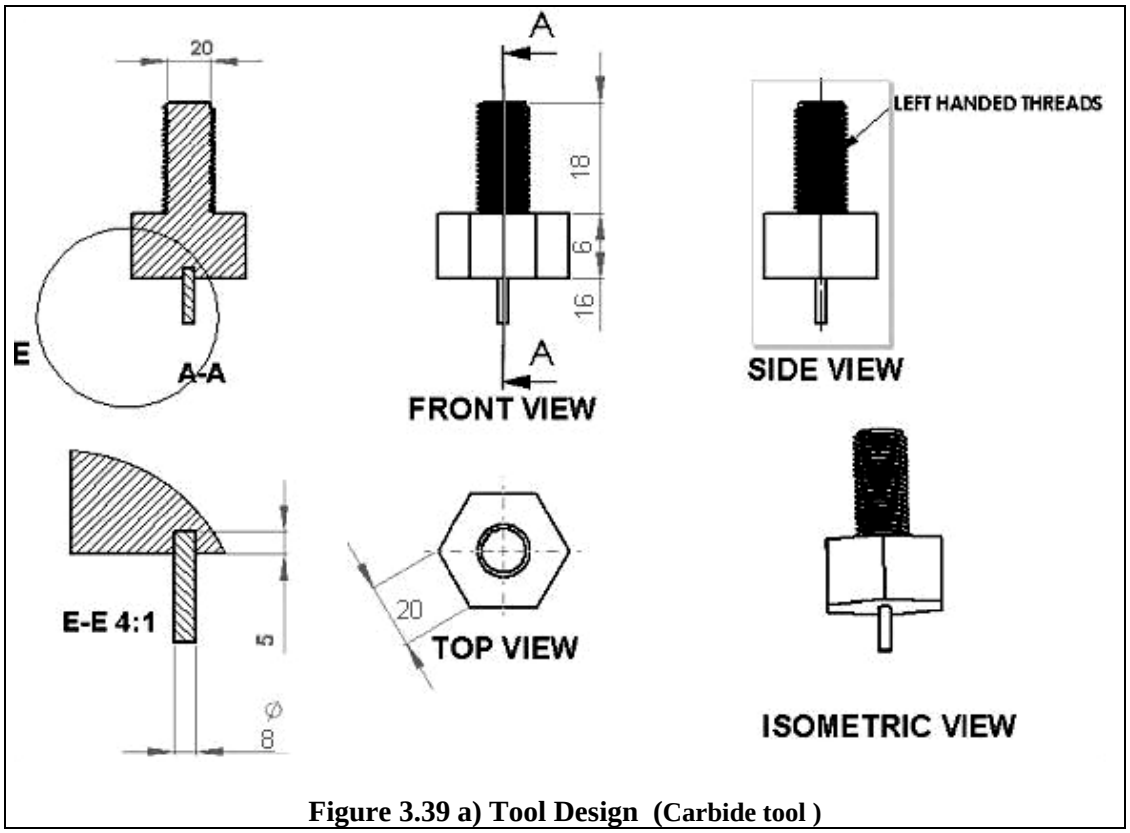

Figure 3.39 a) Tool Design (Carbide tool)

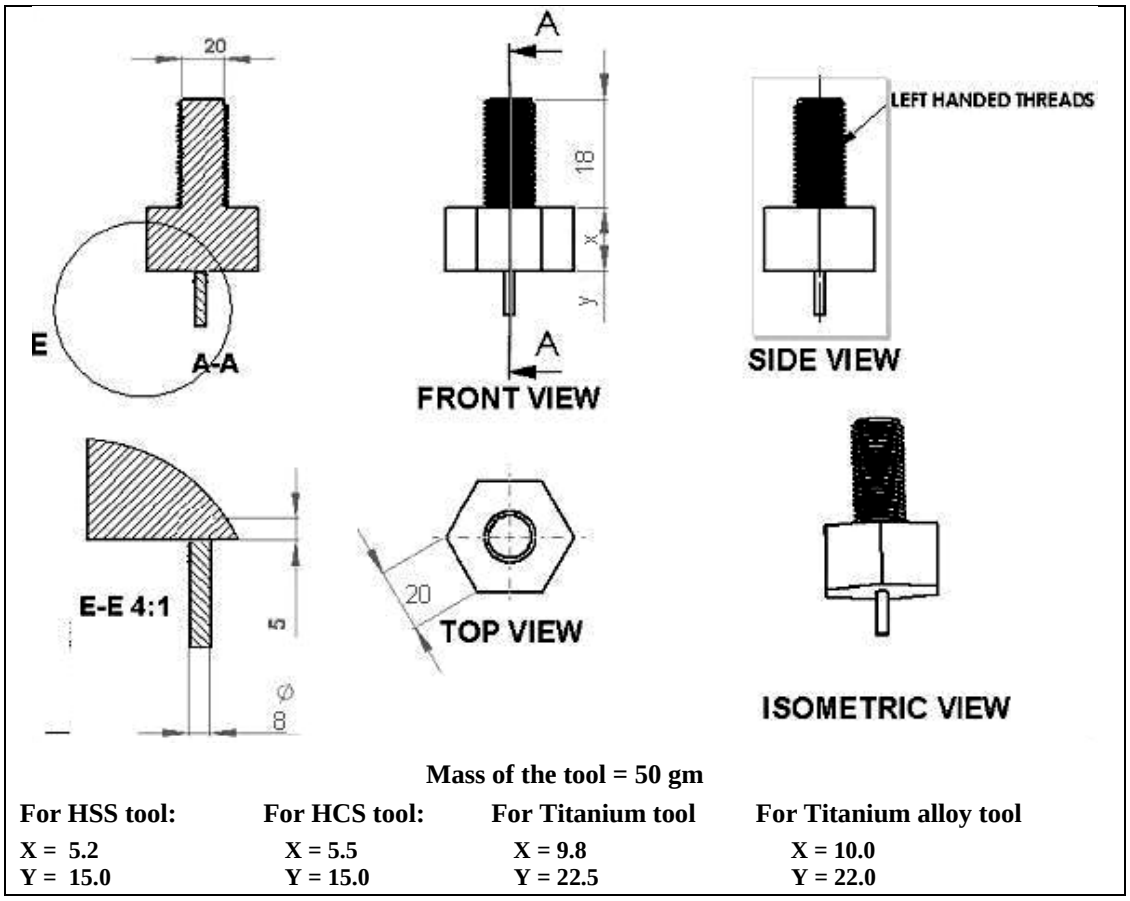

Mass of the tool = 50 gm

For HSS tool:	For HCS tool:	For Titanium tool	For Titanium alloy tool
X = 5.2	X = 5.5	X = 9.8	X = 10.0
Y = 15.0	Y = 15.0	Y = 22.5	Y = 22.0

Figure 3.39 b) Tool Design (HSS, HCS, Ti, Ti alloy tools)

While designing the tools, the dimensions for each tool were decided to ensure that the mass of each tool is same and is equal to 50 g with a permissible variation of 1 g. The detailed tool geometries have been shown in figure 3.39. The tool finish is another important factor that is found to affect the surface finish of the machined surface. Hence, the surface finish of tool face was maintained at a level of 3.0 microns before starting a new experiment. The tool face also tends to gain a convex shape as a result of uneven distribution of the abrasive particles under the tool face while machining takes place [1, 3, 5, 6]. This alters the contour of the machined surface as well as the machining characteristics such as MRR and TWR. To rectify this problem, facing operation was performed on each tool on center lathe after a particular experimental run was executed. This helped to ensure a perfectly flat surface of the tool which is responsible for

machining and thus the undesirable effect on the shape and size of the cavity produced is also controlled. Further, in order to deal with the problems of fatigue failure of the tools while machining and other problems pertaining to the overheating and stress loading of the tools [89], a number of tools were prepared for each tool material. This also helped to maintain the continuity of the experimentation.

3.3.4 Selection of S/N Ratio for Taguchi Design

The signal to noise ratio (S/N ratio) is obtained using Taguchi's methodology. Here, the term 'signal' represents the desirable value (mean) and the 'noise' represents the undesirable value (standard deviation). Thus, the S/N ratio represents the amount of variation present in the performance characteristic. In the Taguchi method, a loss function has been defined to measure the deviation between the experimental and desired value of a performance characteristic [15, 55]. This loss function is further transformed into a signal to noise ratio. By maximizing the S/N ratio, the loss function can be minimized and hence, the objective function can be optimized.

Depending upon the objective of the performance characteristic, there can be various types of S/N ratios. In a particular DOE problem, there can be three different types of performance characteristics- lower-the better, higher-the-better and nominal-the-best. The selection of an appropriate S/N ratio is very important for optimization of the performance characteristics [121]. The three possible types of performance characteristics can be described as follows:

- **Lower-the-Better type problem:**

For lower-the-better type problem, the quality characteristic is always continuous and non-negative. Its most desirable value is zero. As there is no adjustment factor in such type of problems, the thrust is simply on minimizing the quality loss without adjustment-that is, we should minimize

$$Q = k \text{ (mean square of the quality characteristic)}$$

$$= k\left\{\frac{1}{n}.\sum_{1}^{n} y_i^2\right\}$$

Minimizing 'Q' is equivalent to maximizing 'η' defined by the following equation:

$$\eta = -10\log_{10}\left\{\frac{1}{n}.\sum_{1}^{n} y_i^2\right\} \qquad (3.1)$$

In this case the signal remains unchanged, to make the quality characteristic equal to zero. Therefore, the S/N ratio measures only the effect of noise.

- **Higher-the-better type problem:**

In this type of problem, the quality characteristic is again continuous and non-negative and it is to be made as large as possible. There is no adjustment factor to be used in this case as well and one is interested in maximizing the objective function expressed as:

$$\eta = -10\log_{10}\left\{\frac{1}{n}.\sum_{1}^{n}\frac{1}{y_i^2}\right\} \qquad (3.2)$$

- **Nominal-the-best type problem:**

In the nominal-the-best type problem, the quality characteristic is continuous and non-negative, but its target value is non zero and assumes some finite value. For these types of problems, if the mean becomes zero the variance also tends to become zero. A scaling factor can be used as an adjustment factor to shift the mean closer to the target for such type of problems.

The objective function that is to be maximized can be expressed as:

$$\eta = 10\ log_{10}\{\mu^2/\sigma^2\} \qquad (3.3)$$

Where,

$$\mu = \frac{1}{n}.\sum_{1}^{n} y_i^2$$

$$\sigma = \frac{1}{(n-1).\sum_{1}^{n}(y_i - \mu)^2}$$

The identification and selection of a suitable scaling factor can be done either by means of engineering expertise or through experimentation, depending upon the complexity of the situation. The optimization of nominal-the-best type of problems can be achieved in two steps [122, 132]:

1. Maximize 'η' or minimize sensitivity to noise. This is done by selecting those levels for the control factors that maximize η but the mean is ignored.
2. Adjusting the mean on target. During this step, the adjustment factor is used to bring the mean on target without altering the value of η.

In the present investigation, Higher-the-best type situation has been selected as objective function for MRR, as larger values of MRR are desirable. For TWR and SR, Lower-the-Better type situation has been preferred, as both the characteristics are needed to be minimized. Hence, single response optimization has been performed for optimizing MRR, TWR and SR individually. Moreover, these three response variables are interrelated, as observed during the pilot experimentation. Hence, there is a critical need for optimizing these responses collectively and this has been done using utility concept in conjunction with Taguchi method.

3.4 EXPERIMENTATION

The experimentation for the study undertaken consisted of eighteen trial runs, with each trial having three replications. Ultrasonic machining has been designated as a 'very random process' [47] and it is very difficult to keep the signal factors such as frequency of vibration, slurry flow rate and slurry concentration absolutely constant. As far as the slurry flow rate and slurry concentration are concerned, the problem of variation in these process parameters was tackled by preparing a large volume of the slurry for all the three abrasive materials used in this experimentation. The process parameters that were kept constant during the experimentation have been summarized in table 3.7.

Table 3.7 Constant parameters

Process Parameter	Description
Frequency of vibration	21 kHz
Static load	1.63 kg
Amplitude of vibration	25.3-25.8 μm
Depth of cut	02 mm
Thickness of workpiece	10 mm
Tool Geometry	Straight cylindrical 8 mm Ø
Mass of the Tool	50 gm
Slurry Concentration (by volume)	25%
Slurry Temperature (ambient temp.)	28° C
Slurry Flow rate	$36.4x10^3$ mm^3/min
Slurry Media	Water

Figure 3.40 shows the schematic diagram of the USM set up used for the experimentation. To start with the first trial run, the initial weight of titanium work-piece and H.C.S. tool was measured with the help of electronic balance (Least count: 1 mg). Then the machine was allowed to drill the hole until a depth of 02 mm was reached. Meanwhile, the slurry flow rate and temperature were maintained at the predefined values (table 3.7). The depth of cut was closely monitored with the help of dial gauge provided in the machine set up. The time taken for machining 02 mm depth of cut was recorded using a stop watch. The weight of the tool as well as work-piece was measured again after the machining. The weight difference prior to machining and after the machining was then divided by the density of the corresponding tool material or the work material to obtain the value of TWR and MRR respectively.

After this, the surface roughness of the machined surface was measured with the help of Perthometer (Mahr, M_4Pi) for all the machined samples at a tracing length of 1.5 mm and cut-off value of 0.25 mm. For each hole, three readings of surface roughness were taken and then averaged to obtain the value of mean surface roughness. The microstructure of the titanium (prior to machining) was observed using an optical microscope at magnification levels of 100 X and 400 X (Figure 3.41).

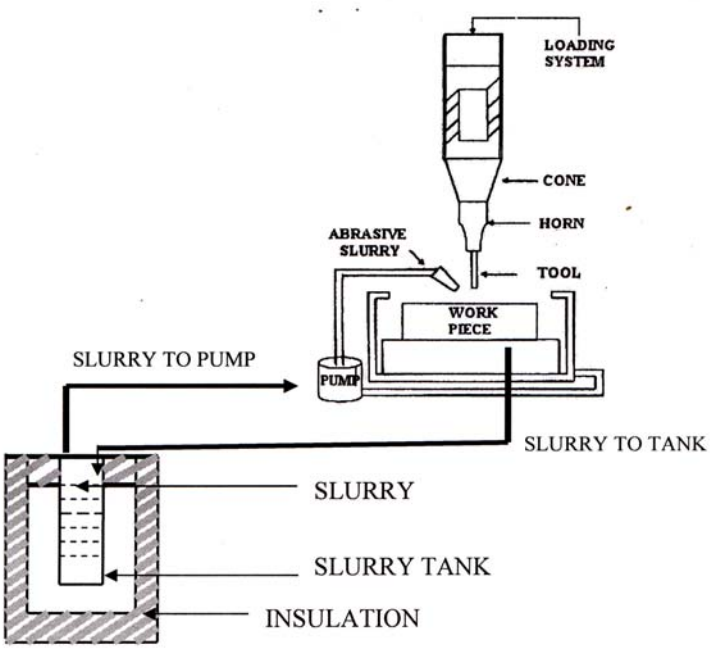

Figure 3.40 Schematic representation of USM process

The microstructure of the machined surface of titanium work-piece was obtained for each machined sample by using scanning electron microscope (figure 3.42) at a magnification level 1500 X. The microstructure of each machined sample at other magnifications was also obtained in order to perform a detailed study of the machined surface. These magnification levels were different for different machined samples.

The hardness of the machined surface was then measured by using micro-hardness tester at a static load of 500 gm. Three readings of micro-hardness were taken at the different possible regions of each cavity and obtain the value of mean hardness (after machining) for each cavity. Hence, the effect of ultrasonic machining on the hardness of titanium work-piece was established. The experiments were conducted in completely randomized order. Table 3.8 shows the values of MRR, TWR, SR and hardness of the machined surface against the input parameter settings for experiment no. 1. Similarly, the values of these machining characteristics for other experimental runs have been tabulated (refer table 3.9-3.25). The microstructures of the machined surface corresponding to various experimental runs have been shown in figures 3.43-3.60.

Table 3.8 Observations table for Experiment no. 1

Control factor settings
A1) Tool = H.C.S.
B1) Abrasive Type = Alumina
C1) Grit size = 220
D1) Power Rating = 100 W (20%)

Trial No.	MRR (mm^3/min)	TWR (mm^3/min)	SR (microns)	Hardness (HV)
1	0.31	0.45	0.92	134
2	0.27	0.40	0.85	140
3	0.36	0.48	0.98	130

Table 3.9 Observations table for Experiment no. 2

Control factor settings
A1) Tool = H.C.S.
B2) Abrasive Type = Silicon carbide
C2) Grit size = 320
D2) Power Rating = 250 W (50%)

Trial No.	MRR (mm^3/min)	TWR (mm^3/min)	SR (microns)	Hardness (HV)
1	0.64	0.65	1.18	145
2	0.58	0.60	1.05	151
3	0.75	0.70	1.24	144

Table 3.10 Observations table for Experiment no. 3

Control factor settings
A1) Tool = H.C.S.
B3) Abrasive Type = Boron Carbide
C3) Grit size = 500
D3) Power Rating = 400 W (80%)

Trial No.	MRR (mm^3/min)	TWR (mm^3/min)	SR (microns)	Hardness (HV)
1	1.09	0.88	0.70	166
2	1.21	0.95	0.75	175
3	0.99	0.84	0.52	162

Table 3.11 Observations table for Experiment no. 4

Test data for Experiment no. 4

Control factor settings
A2) Tool = H.S.S.
B1) Abrasive Type = Alumina
C1) Grit size = 220
D2) Power Rating = 250 W (50%)

Trial No.	MRR (mm^3/min)	TWR (mm^3/min)	SR (microns)	Hardness (HV)
1	0.40	0.56	1.17	132
2	0.28	0.45	0.82	139
3	0.30	0.46	1.10	135

Table 3.12 Observations table for Experiment no. 5

Control factor settings
A2) Tool = H.S.S.
B2) Abrasive Type = Silicon Carbide
C2) Grit size = 320
D3) Power Rating = 400 W (80%)

Trial No.	MRR (mm^3/min)	TWR (mm^3/min)	SR (microns)	Hardness (HV)
1	0.74	1.01	1.20	148
2	0.63	0.94	1.18	153
3	0.80	1.09	1.32	155

Table 3.13 Observations table for Experiment no. 6

Control factor settings
A2) Tool = H.S.S.
B3) Abrasive Type = Boron carbide
C3) Grit size = 500
D1) Power Rating = 100 W (20%)

Trial No.	MRR (mm^3/min)	TWR (mm^3/min)	SR (microns)	Hardness (HV)
1	0.21	0.37	0.64	160
2	0.15	0.33	0.60	164
3	0.15	0.30	0.53	160

Table 3.14 Observations table for Experiment no. 7

Control factor settings
A3) Tool = Titanium
B1) Abrasive Type = Alumina
C2) Grit size = 320
D1) Power Rating = 100 W (20%)

Trial No.	MRR (mm^3/min)	TWR (mm^3/min)	SR (microns)	Hardness (HV)
1	0.13	0.24	0.68	142
2	0.12	0.21	0.72	138
3	0.07	0.12	0.50	144

Table 3.15 Observations table for Experiment no. 8

Control factor settings
A3) Tool = Titanium
B2) Abrasive Type = Silicon carbide
C3) Grit size = 500
D2) Power Rating = 250 W (50%)

Trial No.	MRR (mm^3/min)	TWR (mm^3/min)	SR (microns)	Hardness (HV)
1	0.24	0.27	0.73	147
2	0.27	0.32	0.87	150
3	0.35	0.42	0.90	145

Table 3.16 Observations table for experiment no. 9

Control factor settings
A3) Tool = Titanium
B3) Abrasive Type = Boron Carbide
C1) Grit size = 220
D3) Power Rating = 400 W (80%)

Trial No.	MRR (mm^3/min)	TWR (mm^3/min)	SR (microns)	Hardness (HV)
1	1.33	1.24	2.26	135
2	1.09	1.03	1.90	137
3	1.24	1.15	2.14	140

Table 3.17 Observations table for Experiment no. 10

Control factor settings
A4) Tool = Titanium alloy
B1) Abrasive Type = Alumina
C3) Grit size = 500
D3) Power Rating = 400 W (80%)

Trial No.	MRR (mm^3/min)	TWR (mm^3/min)	SR (microns)	Hardness (HV)
1	0.27	0.14	0.56	131
2	0.26	0.20	0.68	130
3	0.38	0.23	0.75	133

Table 3.18 Observations table for Experiment no. 11

Control factor settings
A4) Tool = Titanium alloy
B2) Abrasive Type = Silicon carbide
C1) Grit size = 220
D1) Power Rating = 100 W (20%)

Trial No.	MRR (mm^3/min)	TWR (mm^3/min)	SR (microns)	Hardness (HV)
1	0.18	0.16	0.64	150
2	0.20	0.17	0.78	154
3	0.15	0.12	0.60	155

Table 3.19 Observations table for Experiment no. 12

Control factor settings
A4) Tool = Titanium alloy
B3) Abrasive Type = Boron carbide
C2) Grit size = 320
D2) Power Rating = 250 W (50%)

Trial No.	MRR (mm^3/min)	TWR (mm^3/min)	SR (microns)	Hardness (HV)
1	0.47	0.40	0.85	162
2	0.55	0.45	0.86	158
3	0.36	0.38	0.80	165

Table 3.20 Observations table for Experiment no. 13

Control factor settings
A5) Tool = Cemented carbide
B1) Abrasive Type = Alumina
C2) Grit size = 320
D3) Power Rating = 400 W (80%)

Trial No.	MRR (mm^3/min)	TWR (mm^3/min)	SR (microns)	Hardness (HV)
1	0.59	0.67	1.04	157
2	0.50	0.62	0.97	165
3	0.72	0.77	1.12	160

Table 3.21 Observations table for Experiment no. 14

Control factor settings
A5) Tool = Cemented carbide
B2) Abrasive Type = Silicon carbide
C3) Grit size = 500
D1) Power Rating = 100 W (20%)

Trial No.	MRR (mm^3/min)	TWR (mm^3/min)	SR (microns)	Hardness (HV)
1	0.32	0.57	0.66	142
2	0.27	0.49	0.60	145
3	0.36	0.64	0.75	140

Table 3.22 Observations table for Experiment no. 15

Control factor settings
A5) Tool = Cemented carbide
B3) Abrasive Type = Boron carbide
C1) Grit size = 220
D2) Power Rating = 250 W (50%)

Trial No.	MRR (mm^3/min)	TWR (mm^3/min)	SR (microns)	Hardness (HV)
1	1.25	1.18	1.70	170
2	1.40	1.25	1.84	173
3	1.16	1.10	1.67	178

Table 3.23 Observations table for Experiment no. 16

Control factor settings
A6) Tool = H.C.S.
B1) Abrasive Type = Alumina
C3) Grit size = 500
D2) Power Rating = 250 W (50%)

Trial No.	MRR (mm^3/min)	TWR (mm^3/min)	SR (microns)	Hardness (HV)
1	0.17	0.19	0.66	130
2	0.14	0.17	0.77	137
3	0.18	0.24	0.83	133

Table 3.24 Observations table for Experiment no. 17

Control factor settings
A6) Tool = H.C.S.
B2) Abrasive Type = Silicon carbide
C1) Grit size = 220
D3) Power Rating = 400 W (80%)

Trial No.	MRR (mm^3/min)	TWR (mm^3/min)	SR (microns)	Hardness (HV)
1	1.45	1.60	2.24	174
2	1.30	1.45	2.18	182
3	1.56	1.68	2.29	179

Table 3.25 Observations table for Experiment no. 18

Control factor settings
A6) Tool = H.C.S.
B3) Abrasive Type = Boron carbide
C2) Grit size = 320
D1) Power Rating = 100 W (20%)

Trial No.	MRR (mm^3/min)	TWR (mm^3/min)	SR (microns)	Hardness (HV)
1	0.36	0.34	0.73	170
2	0.30	0.31	0.77	167
3	0.45	0.43	0.92	175

Figure 3.41 shows the microstructure of titanium prior to machining with USM. It can be observed that the grain size is almost uniform with equiaxed grain shape. As the material was in rolled condition, elongated grains were expected. However, because of the heat treatment given to the work material before machining with USM, the grains were recrystallized. Recrystallized grains are stress free and the possibility of irregular cracking or fracture during machining is very low. Moreover, these grains are softer in comparison to the grains in a rolled structure. Hence, the material possessed fair machinability while undergoing ultrasonic drilling operation. From the magnification level 400 X, different orientations of the grains can also be observed. To study the microstructure of titanium after machining with USM, scanning electron microscopy (SEM) was performed on the machined samples.

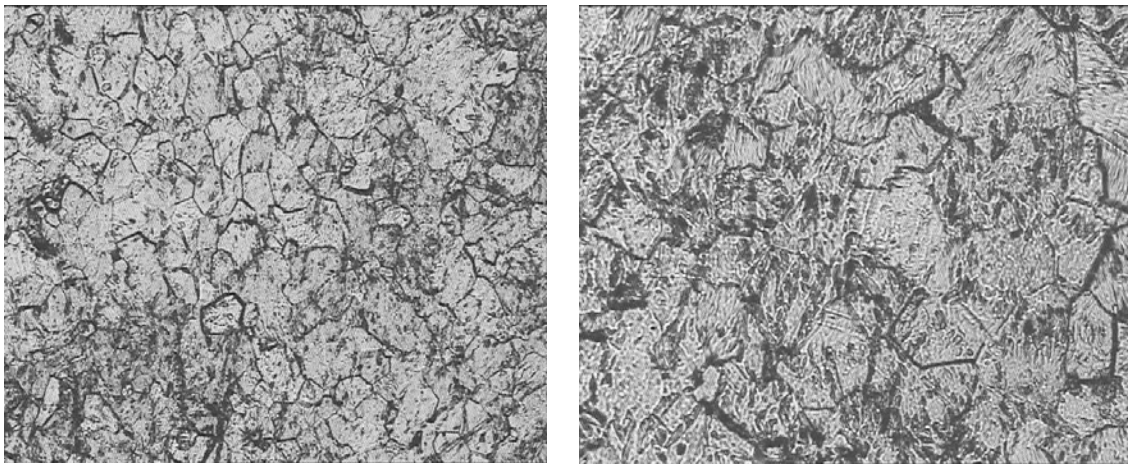

a) 100 X **b) 400 X**

Figure 3.41 Photomicrograph for Titanium (prior to machining)

Material removal in USM process is believed to occur by brittle fracture mode. In mechanical shaping processes for brittle materials such as USM, material has been found to be removed by the propagation and intersection of cracks [42, 50, 66]. While the cutting of brittle materials is performed, in general, by brittle fracture, the chip can be removed plastically at an extremely small depth of cut [95, 116, 124]. In other words, the

mechanism of material removal may change from brittle fracture to plastic deformation at extremely small material removal rates while machining with USM.

Pei et al. [116-117] has established "under all machining conditions, the material removal modes involve the combination of brittle fracture and plastic flow". It has also been suggested that any increase in the variables affecting input energy to the abrasive/tool such as amplitude, grain size of the abrasive, vibration frequency promotes the brittle fracture of the work surface. By manipulating the values of the key parameters affecting energy input to the process, different ratios of the two modes of material removal can be obtained [117, 124].

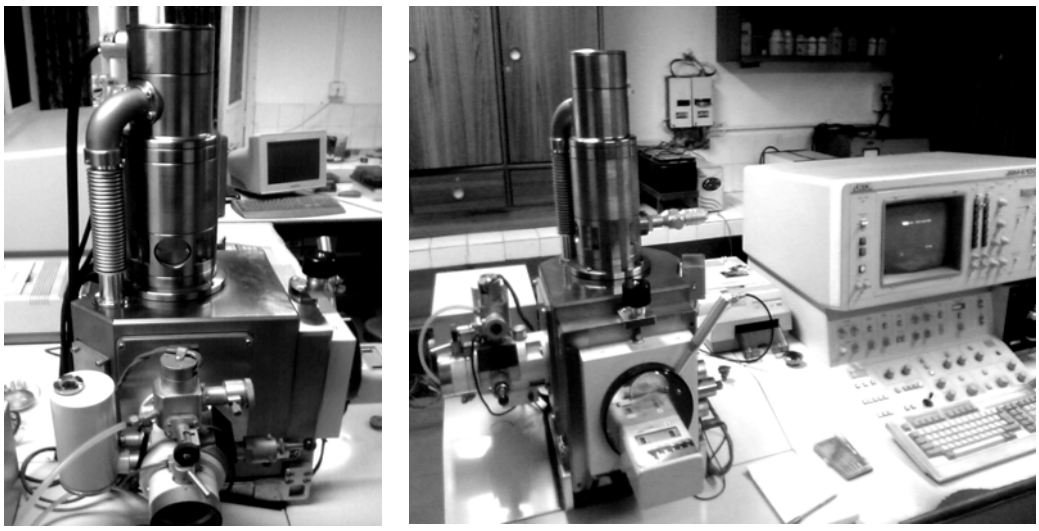

a) Side view **b) Front view**

Figure 3.42 Scanning Electron Microscope

The mode of material removal in USM is also decided by the work material properties such as fracture toughness and hardness. Fracture toughness has been found to be the most important parameter affecting the mode of material removal. While machining a material with high fracture toughness value, the brittle fracture of the surface is preceded by plastic deformation and strain hardening of the work surface [103, 116], as the abrasive grains have a tendency to embed in the work surface during machining.

Figure 3.43 depicts the microstructure of titanium after machining with USM under the experimental conditions corresponding to experiment no. 1. It could be observed that the material faced significant amount of plastic deformation before failure and there is no evidence of brittle fracture. Hence, the material was machined by ductile failure of the work material. This could be attributed to the extremely low energy input into the abrasive as the experimental conditions involved use of a softer abrasive (alumina) with very low power rating (20%). Also, the high fracture toughness associated with the work material (titanium) has contributed towards the increment in the hardness of the work surface (table 3.8) due to work hardening.

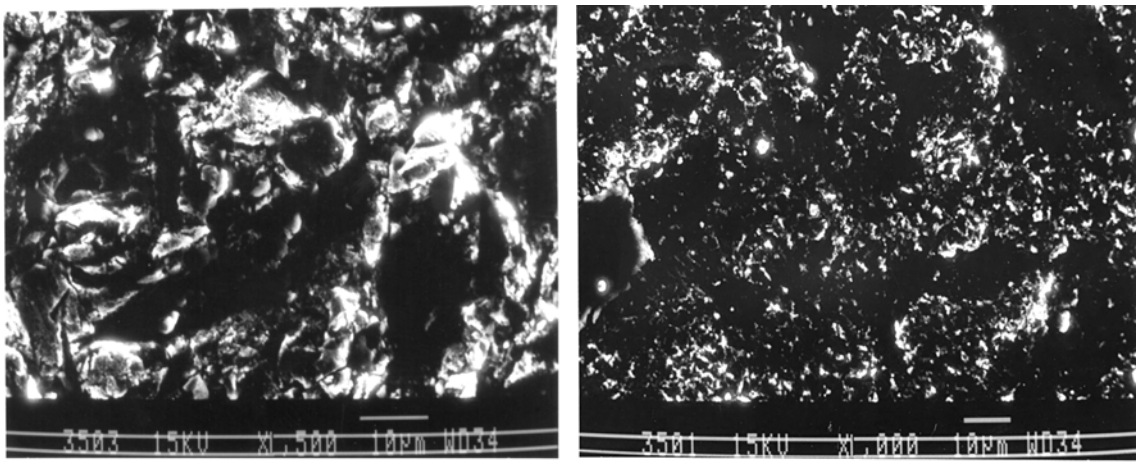

a) 1500 X **b) 1000 X**

Figure 3.43 SEM Photograph for Titanium [Exp No. 1]

Figure 3.44 depicts the microstructure of titanium after machining with USM under the experimental conditions corresponding to experiment no. 2 at magnification levels of 1500 X and 1000 X. It could be observed (figure 3.44 a) that the majority of failure was of brittle fracture type, but very fine dimples were also recognized which suggest some localized plastic deformation before machining took place. The propagation and formation of cracks could also be observed (figure 3.44 b) which lead to the abrasion of work surface finally. The experimental conditions in this case were corresponding to a moderate rate of energy input to the tool/abrasive; hence the proportion of brittle fracture

was expected to be larger than the previous case. The increment in hardness of the work surface (table 3.9) was also found to be larger because of higher rate of machining.

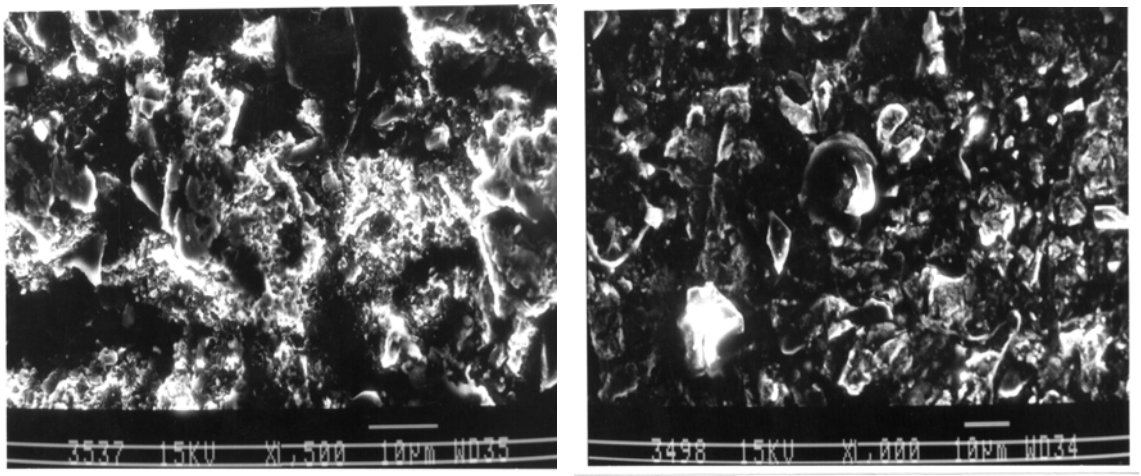

a) 1500 X **b) 1000 X**

Figure 3.44 SEM Photograph for Titanium [Exp No. 2]

Figure 3.45 depicts the microstructure of titanium after machining with USM under the experimental conditions corresponding to experiment no. 3 at magnification levels of 1500 X and 1000 X. It could be observed (figure 3.45 a) that ductile failure dominated the fracture of work surface, but some signs of brittle fracture were also observed in the form of sharp edges. Use of a fine grit size (500) has possibly resulted in considerable plastic deformation of the work surface in this case. Figure 3.45 (b) also suggests a mixed mode of material removal with greater contribution from ductile failure. The hardness gain for the work surface has been even more as compared to the previous cases (table 3.10), which could be due to the faster rate of energy input to the work surface, resulting in higher strain rates and more work hardening.

Figure 3.46 shows the microstructure of titanium after machining with USM under the experimental conditions corresponding to experiment no. 4 at magnification levels of 1500 X and 1000 X. It could be observed (figure 3.46 a) that the material removal took place by a mixed mode, which is evident from the presence of dimples as well as sharp edges (cleavages). Figure 3.46 (b) suggests occurrence of ductile shear

failure which could be due to bigger particle size. The parameter settings corresponding to this case involve the use of alumina as slurry (softer abrasive) with a moderate level of power rating (50%), contributing to the ductile failure of the work surface. However, as a coarse grit size (220) was used for machining purpose, the cleavage of work surface was also evidenced. The increment in work surface hardness in this case is small, which is possibly due to low value of rate of machining (table 3.11).

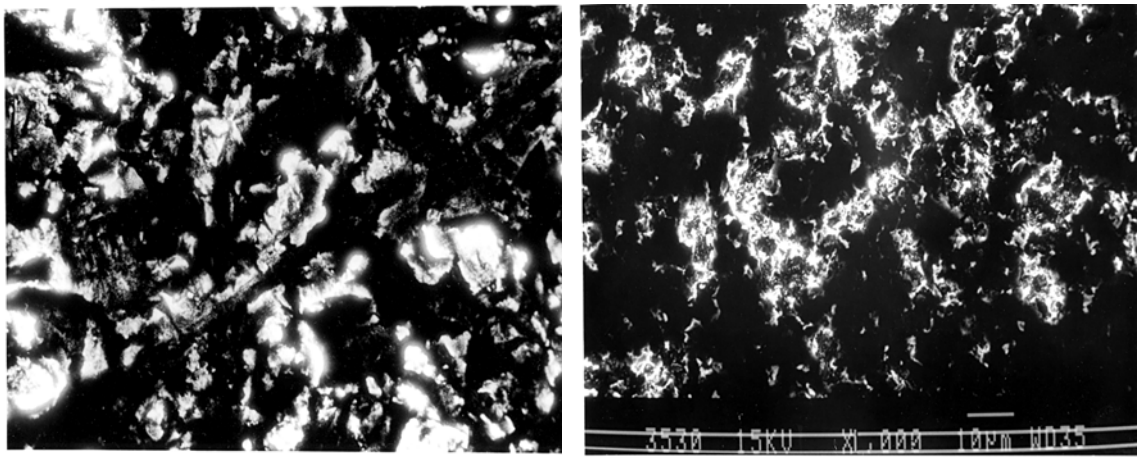

a) 1500 X **b) 1000 X**

Figure 3.45 SEM Photograph for Titanium [Exp No. 3]

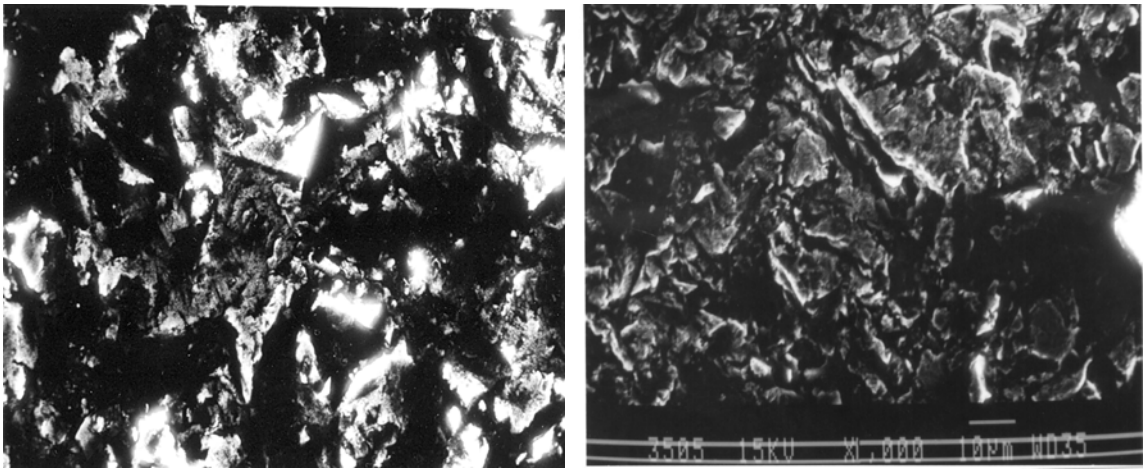

a) 1500 X **b) 1000 X**

Figure 3.46 SEM Photograph for Titanium [Exp No. 4]

Figure 3.47 shows the microstructure of titanium after machining with USM under the experimental conditions corresponding to experiment no. 5 at magnification levels of 1500 X and 1000 X. Elongated projected regions were observed which suggest cleavage type of fracture. Figure 3.47 (b) shows some signs of ductile failure along with predominant cleavage patterns. The parameter settings corresponding to this experimental condition include silicon carbide as slurry which is comparatively harder and high level of power rating (80%); hence the cleavage type of fracture could be expected. The rate of machining is moderately high which leads to a moderate gain in the surface hardness for the work material (table 3.12).

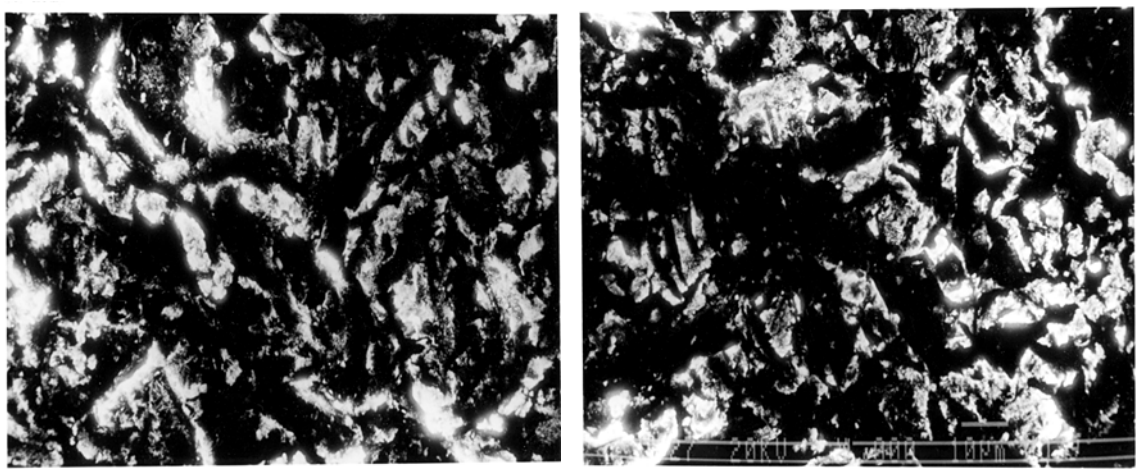

a) 1500 X **b) 1000 X**

Figure 3.47 SEM Photograph for Titanium [Exp No. 5]

Figure 3.48 shows the microstructure of titanium after machining with USM under the experimental conditions corresponding to experiment no. 6 at magnification levels of 1500 X and 2500 X. It can be concluded that the work surface experienced purely ductile failure as lots of dimples with uniform shape and distribution could be observed. The process settings for this experimental condition involve the use of a very fine grit size (500) and lowest level of power rating (20%) which results in very low rate of machining and hence the ductile failure could be expected. The surface hardness after machining was observed to be higher (160 HV) as almost all the machining took place

through continuous plastic deformation which sustained during the entire machining time and as the rate of machining was very low, it took a comparatively larger time period to machine the work surface to the desired depth and hence more work hardening took place (table 3.13).

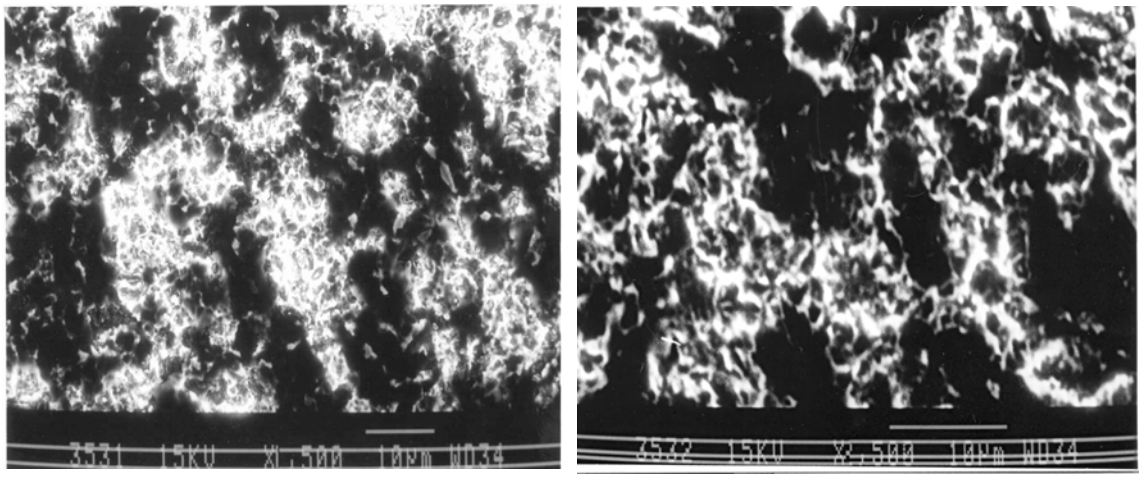

a) 1500 X **b) 2500 X**

Figure 3.48 SEM Photograph for Titanium [Exp No. 6]

Figure 3.49 shows the microstructure of titanium after machining with USM under the experimental conditions corresponding to experiment no. 7 at magnification levels of 1500 X and 1000 X. The input parameter settings involve use of a softer abrasive (alumina) and lowest level of power rating (20%) while the grit size is moderate (320). Hence, the rate of energy input to the tool and abrasive is quite low. The fractured surface shows white and dark contrast in which the brighter contrast is the projected portion of the fractured surface which is comparatively larger than that observed in case of high energy input conditions. This indicates ductile type of failure and slightly longer duration was required to fracture the surface.

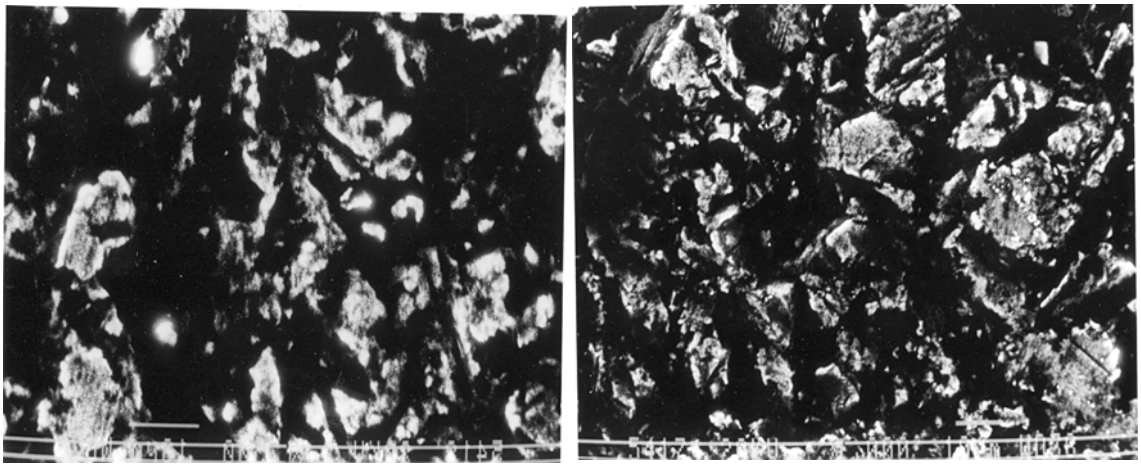

a) 1500 X **b) 1000 X**

Figure 3.49 SEM Photograph for Titanium [Exp No. 7]

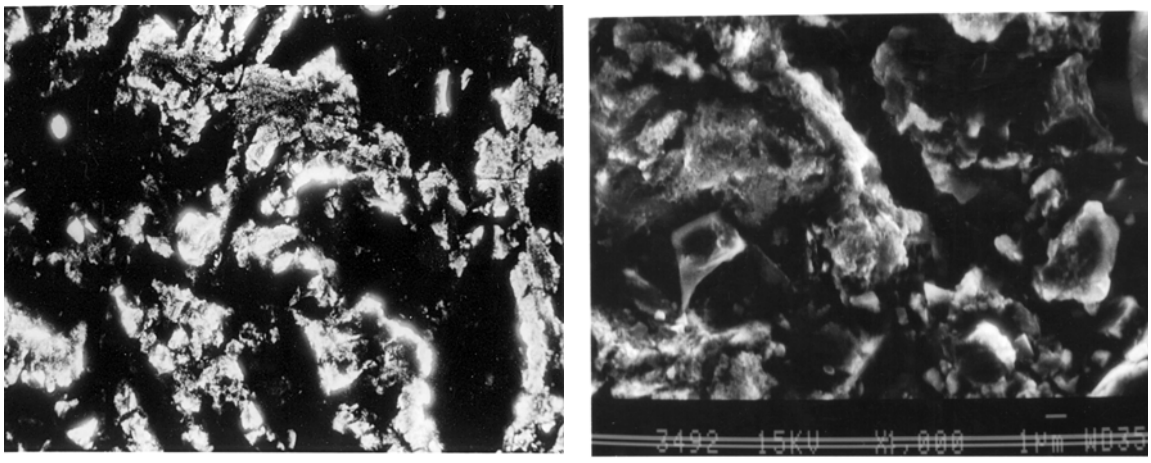

a) 1500 X **b) 2000 X**

Figure 3.50 SEM Photograph for Titanium [Exp No. 8]

Figure 3.50 shows the microstructure of titanium after machining with USM under the experimental conditions corresponding to experiment no. 8 at magnification levels of 1500 X and 1000 X. The process settings include silicon carbide slurry with a fine grit size and moderate power input (250 W). Hence, the rate of energy input to the tool or abrasive is moderately high. It can be observed from figure 3.50 that the cleavage type of fracture took place. The increase in the surface hardness is moderately high

because of a longer machining time required as the machining rate observed was quite low (table 3.15).

Figure 3.51 shows the microstructure of titanium after machining with USM under the experimental conditions corresponding to experiment no. 9 at magnification levels of 1500 X and 2500 X. The process settings include boron carbide slurry with a coarse grit size of 220 and high power input (400 W). Hence, the rate of energy input to the tool or abrasive is extremely high. It can be observed from figure 3.51 (a) that purely ductile type of fracture took place, as a large number of dimples could be seen. Figure 3.51 (b) depicts presence of some cleavage planes in addition to a large number of dimples distributed in the entire surface. Also, there is an evidence of inter-granular fracture and absence of cavitation. The contradiction regarding to the evidence of ductile failure at high energy input conditions was found to be due to the plastic deformation at the center of the tool face while machining because of lesser wear of the tool surface at that location in comparison to the periphery. The area of workpiece which is directly under the center of the tool face also experiences significant amount of plastic deformation and in the present case, the scanning was performed at the same location.

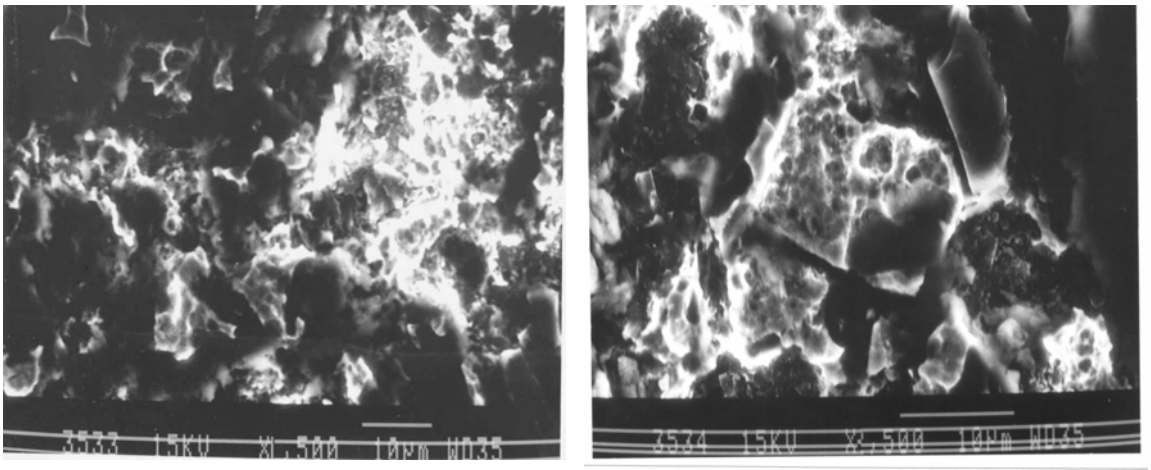

a) 1500 X **b) 2500 X**

Figure 3.51 SEM Photograph for Titanium [Exp No. 9]

The increase in the surface hardness is quite small which could be contributed to extremely high rate of machining obtained in this case (table 3.16), which results in very quick removal of work material by brittle fracture (except from the center) without undergoing significant amount of work hardening.

Figure 3.52 shows the microstructure of titanium after machining with USM under the experimental conditions corresponding to experiment no. 10 at magnification levels of 1500 X and 1000 X. The parameter settings for this trial include alumina slurry with a fine grit size of 500 and highest level of power input (80%). Hence, a low to moderate level of energy input can be assigned to this experimental condition. Figure 3.52 (a) gives evidence of a mixed mode of material removal, with predominant ductile failure of the work material. In figure 3.52 (b), a large number of round dimples could be observed which indicates ductile failure of the work surface. The increment in work surface hardness is quite low as compared to the other similar cases where a low rate of machining was observed (table 3.17).

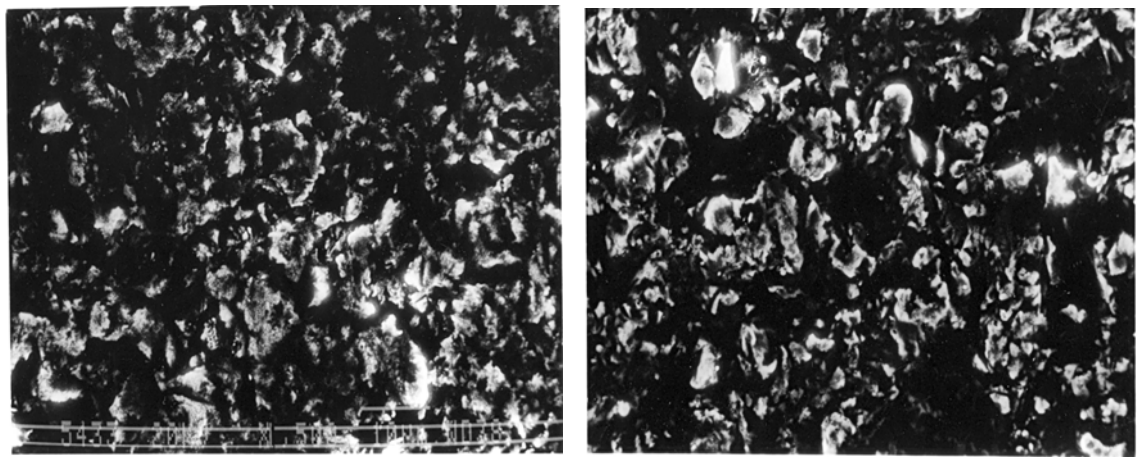

a) 1500 X **b) 1000 X**

Figure 3.52 SEM Photograph for Titanium [Exp No. 10]

Figure 3.53 shows the microstructure of titanium after machining with USM under the conditions corresponding to experiment no. 11 at magnification levels of 1500 X and 1000 X. The parameter settings for this trial include silicon carbide slurry with a coarse grit size of 220 and lowest level of power input (20%). Hence, a moderate level of

energy input can be assigned to this case. Figure 3.53 (a) gives evidence of a mixed mode of material removal with predominant brittle fracture of the work material, which could be due to the use of coarse grit size. In figure 3.53 (b), a large number of cracks can be observed along the grain boundaries indicating inter-granular fracture. The increment in work surface hardness is quite high as expected because a very low rate of machining was observed (table 3.18).

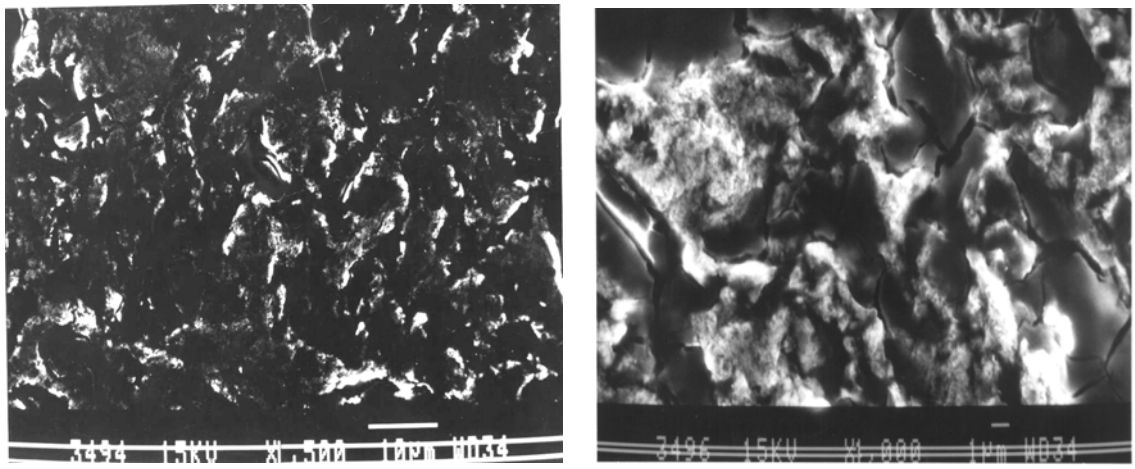

a) 1500 X **b) 1000 X**

Figure 3.53 SEM Photograph for Titanium [Exp No. 11]

Figure 3.54 shows the microstructure of titanium after machining with USM under the conditions corresponding to experiment no. 12 at magnification levels of 1500 X and 1000 X. The input parameters settings for this trail include boron carbide slurry with a medium grit size (320) and moderate level of power rating (50%). Hence, the energy input for the tool and subsequently work surface can be termed as moderate. The figure 3.54 (a) suggests predominant brittle fracture (90-95%) with a very few localized ductile failure regions. Whereas figure 3.54 (b) indicates uniform abrasion of the work surface. The gain in work surface hardness due to strain hardening is very high although the rate of machining observed is quite moderate (table 3.19).

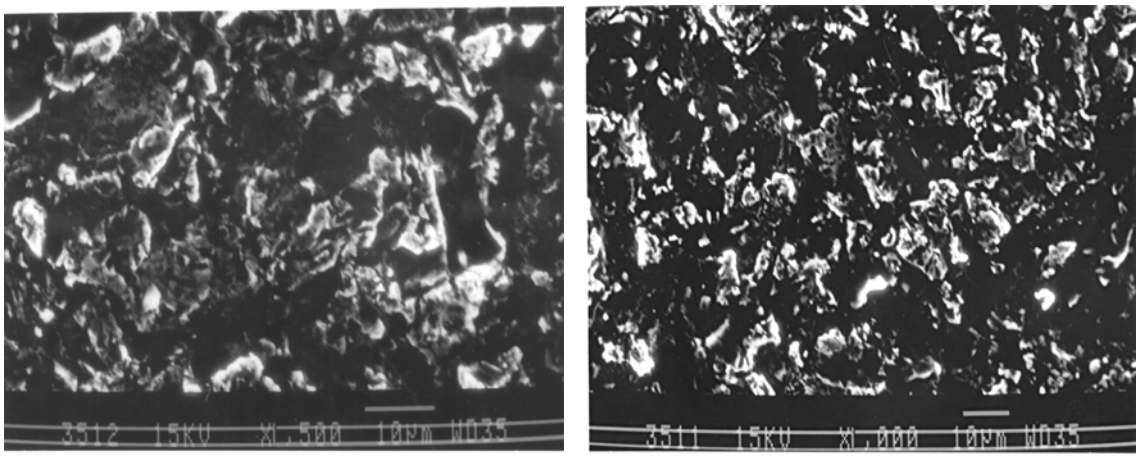

a) 1500 X **b) 1000 X**

Figure 3.54 SEM Photograph for Titanium [Exp No. 12]

Figure 3.55 shows the microstructure of titanium after machining with USM under the conditions corresponding to experiment no. 13 at magnification levels of 1500 X and 1300 X. Purely brittle fracture is observed as the parameter settings indicate a moderate to high level of energy input into the work (table 3.20). The increment in hardness of the work surface is very high because of the reasonably high value of MRR obtained in this case. Also, the momentum with which the abrasive particles strike with the work surface is extremely high due to highest level of power rating used. Hence, the strain hardening of the work surface proceeds at a faster rate.

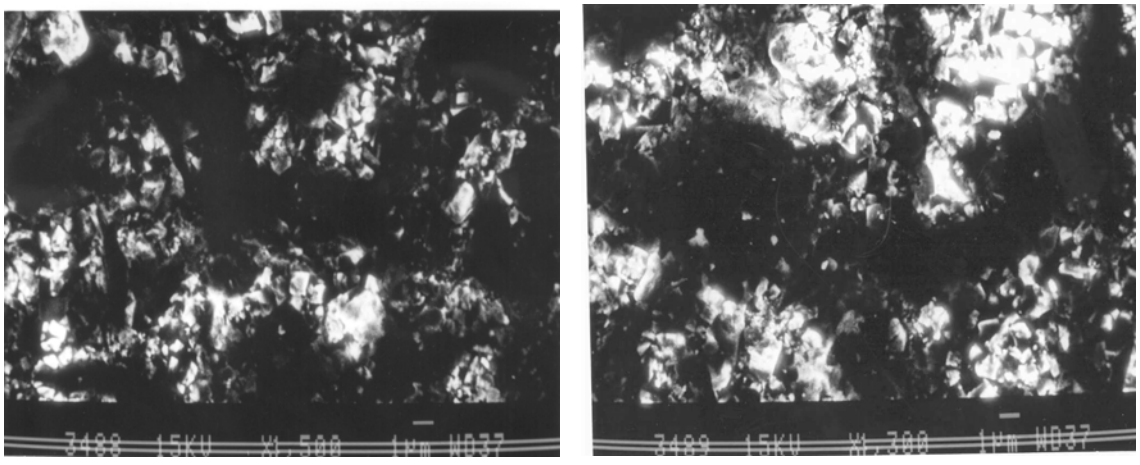

a) 1500 X **b) 1300 X**

Figure 3.55 SEM Photograph for Titanium [Exp No. 13]

Figure 3.56 shows the microstructure of titanium after machining with USM under the conditions corresponding to experiment no. 14 at magnification levels of 1500 X and 1200 X. It could be observed that the material removal has taken place by cleavage of the grains preceded by significant amount of plastic deformation. The energy input for this trail condition can be termed as very low (table 3.21). The increment in work surface hardness is reasonably high because of sustained plastic deformation and work hardening.

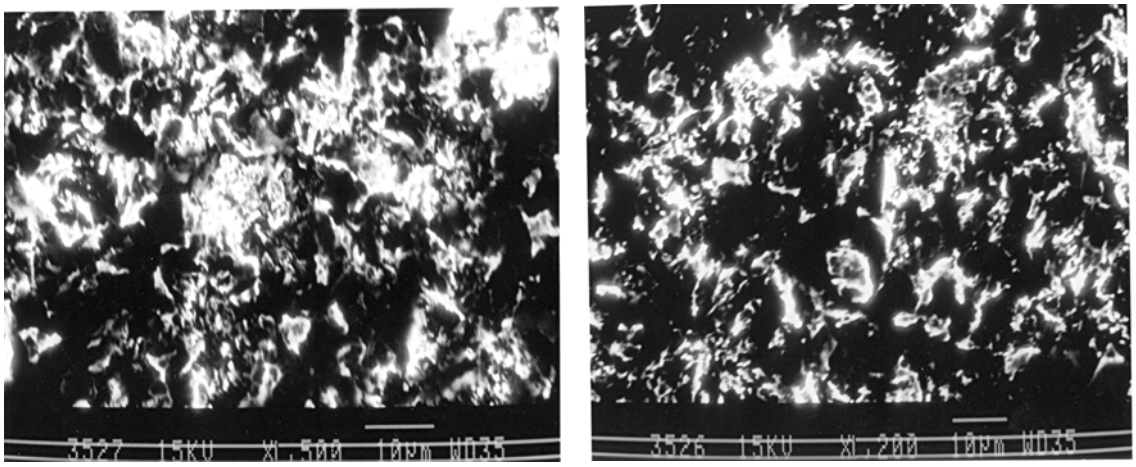

a) 1500 X **b) 1200 X**

Figure 3.56 SEM Photograph for Titanium [Exp No. 14]

Figure 3.57 shows the microstructure of titanium after machining with USM under the conditions corresponding to experiment no. 15 at magnification levels of 1500 X and 3000 X. The process settings corresponding to this trial condition provide a high level of energy input to the tool/abrasive (table 3.22). It can be observed from figure 3.57 (a) that the material fracture took place purely due to ductile failure of the surface, as large number of dimples of uniform size could be visualized. This is due to the fact that the region under consideration in the former case belongs to the center of the work surface where rate of machining is comparatively lower and plastic deformation takes place as already explained. However, figure 3.57 (b) where the area from the periphery of work surface has been considered; indicates presence of cleavage planes and dominant

brittle fracture can be observed. The pulling out of some grains due to propagation of cracks can also be observed from figure 3.57 (b). The gain in hardness for work surface is extremely high which is in consistent with the high rates of machining for the given situation.

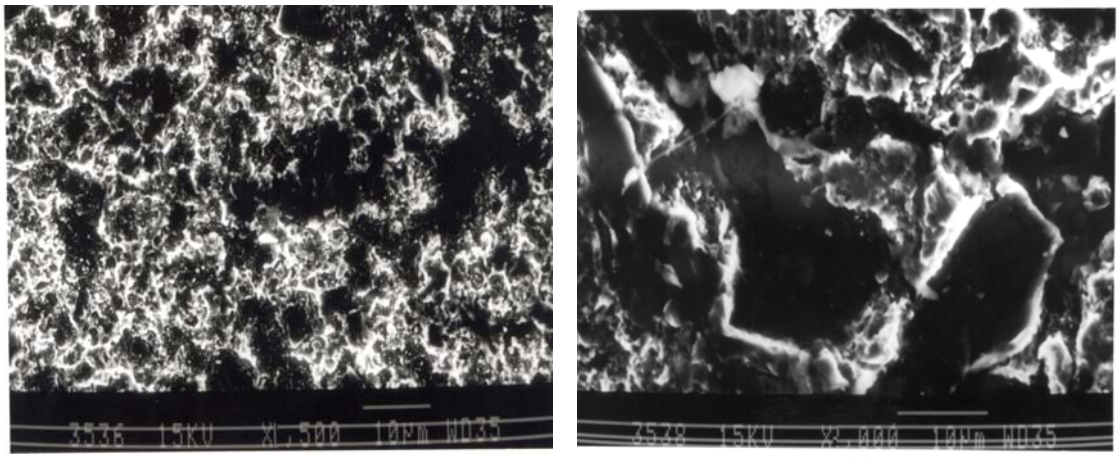

a) 1500 X **b) 3000 X**

Figure 3.57 SEM Photograph for Titanium [Exp No. 15]

Figure 3.58 shows the microstructure of titanium after machining with USM under the conditions corresponding to experiment no. 16 at magnification levels of 1500 X and 2000 X. From the point of view of input parameter settings, it could be said that the rate of energy input into the tool and abrasive is low (table 3.23). Hence, a very low machining rate was observed. The microstructure of the machined surface indicates material failure by brittle fracture. The gain in work surface hardness is also very less which is in contradiction with the low machining rate observed. This might be due to the absence of plastic deformation in this case, which leads to lesser strain hardening.

Figure 3.59 shows the microstructure of titanium after machining with USM under the conditions corresponding to experiment no. 17 at magnification levels of 1500 X and 2500 X. Cleavage type of fracture can be observed in figure 3.59 (a). In figure 3.59 (b) localized plastic deformation can also be seen in the form of a few round dimples. This is expected in this case as the rate of energy input into the tool or abrasive is

extremely high (table 3.24). The increment in surface hardness is also extremely high because of the excessive rate of machining which is related with stronger impacts of abrasive particles over the work surface, imparting more work hardening to it.

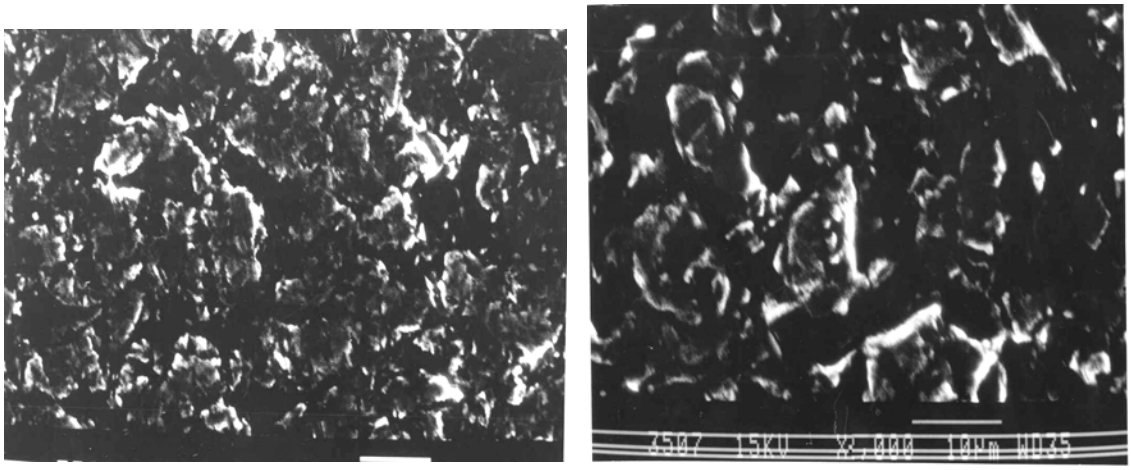

a) 1500 X **b) 2000 X**

Figure 3.58 SEM Photograph for Titanium [Exp No. 16]

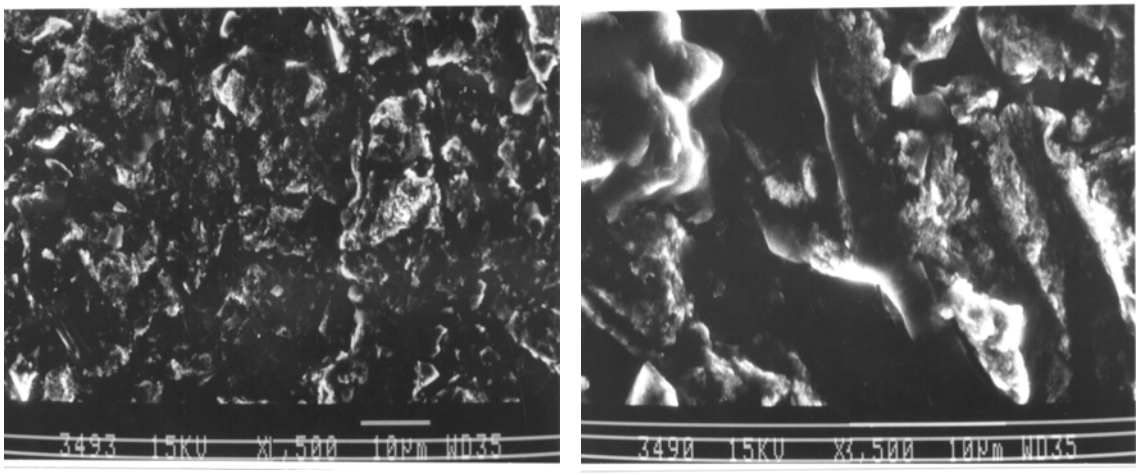

a) 1500 X **b) 2500 X**

Figure 3.59 SEM Photograph for Titanium [Exp No. 17]

Figure 3.60 shows the microstructure of titanium after machining with USM under the conditions corresponding to experiment no. 18 at magnification levels of 1500 X and 2000 X. The process settings in this case render a low rate of energy input to the tool/abrasive, so purely ductile type of failure has been observed which is in consistent

with the low machining rates achieved in this case (table 3.25). There is no evidence of any brittle fracture of the work surface as sharp edges have not been observed. The increment in work surface hardness is extremely high which can be attributed to shear plastic deformation occurring in this case that lead to more strain hardening of the work surface.

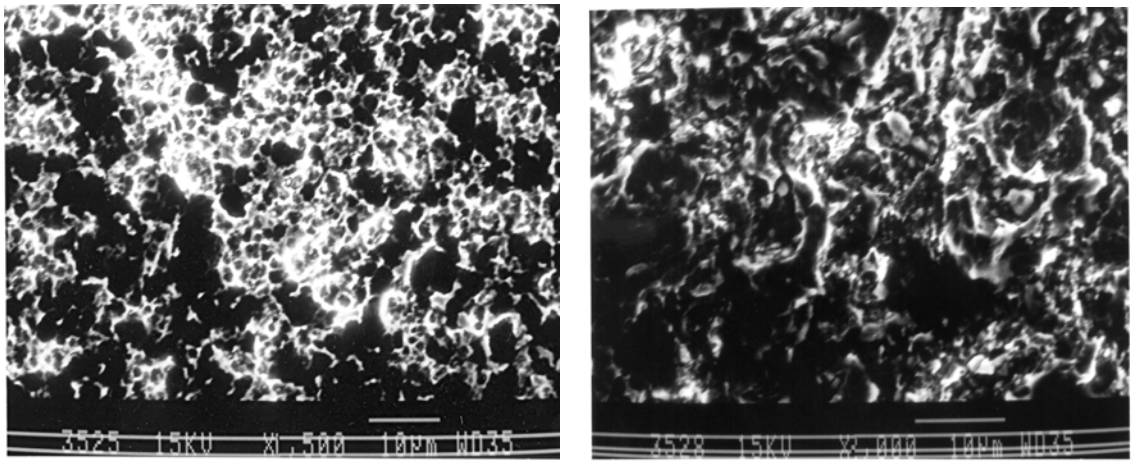

a) 1500 X **b) 2000 X**

Figure 3.60 SEM Photograph for Titanium [Exp No. 18]

Figure 3.61 shows the three dimensional pictorial presentation of the USM apparatus used for conducting this experimentation. Various components of the set-up have been indicated for a clear understanding of the system of USM process.

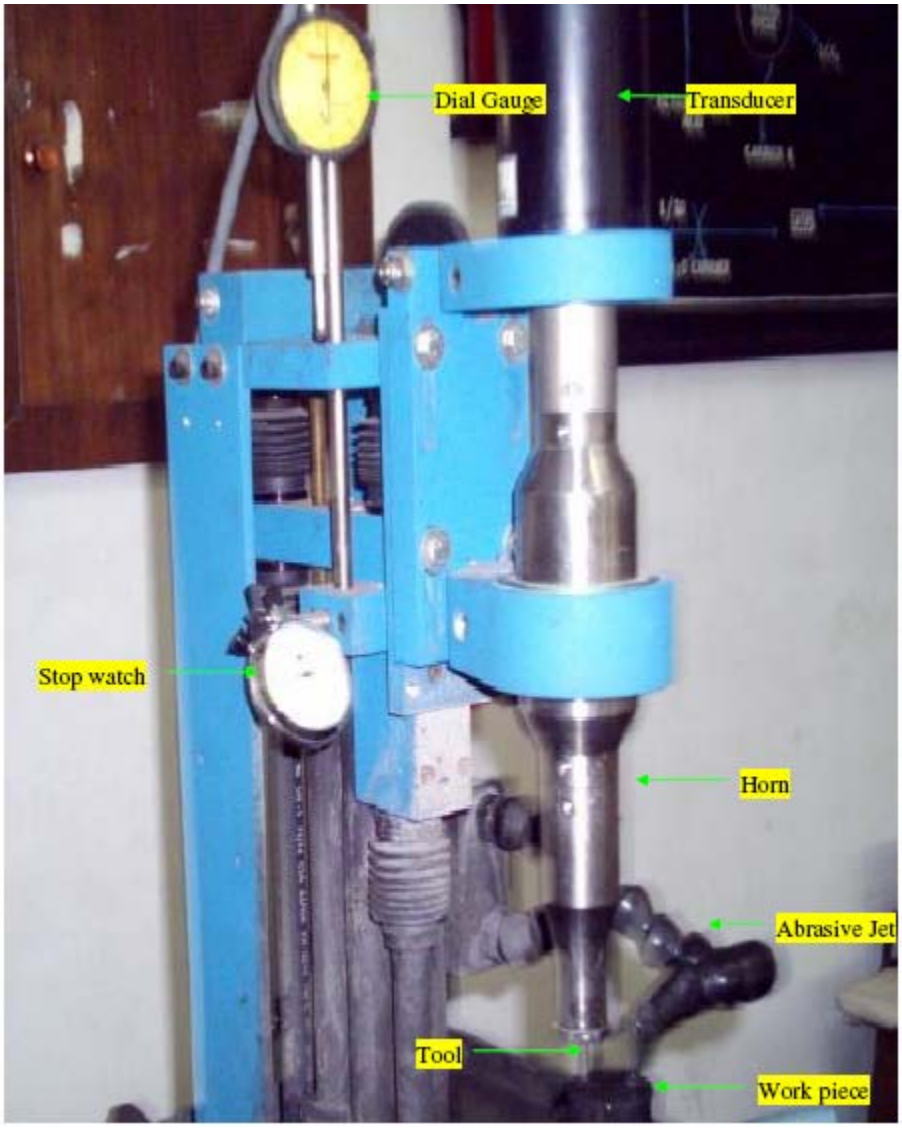

Figure 3.61 Three Dimensional pictorial representation of USM apparatus

CHAPTER 4
RESULTS AND DISCUSSIONS

4.1 INTRODUCTION

After conducting the experiments with different tool materials, different types of abrasive, slurry grit-size and various power ratings, the values of output variables (MRR, TWR and SR) were recorded and plotted as per Taguchi's design of experiments methodology. The analysis of the results obtained has been performed according to the standard procedure recommended by Taguchi. The detailed description of the analysis is given as under.

4.2 ANALYSIS

4.2.1 Evaluation of S/N ratio

The S/N ratio is obtained using Taguchi's methodology. Here, the term 'signal' represents the desirable value (mean) and the 'noise' represents the undesirable value (standard deviation). Thus, the S/N ratio represents the amount of variation present in the performance characteristic. Depending upon the objective of the performance characteristic, there can be various types of S/N ratios [121, 122]. Here, the desirable objective is to optimize the response variables (MRR, TWR and SR). Hence, larger-the-better type S/N ratio was applied for transforming the raw data for MRR as larger values of MRR as desirable. The values of S/N ratio corresponding to different experimental runs have been tabulated (table 4.1) along with the mean values of MRR.

For TWR and SR, as the objective is to minimize the response, lower-the-better type S/N ratio was selected to transform the raw data. The values of S/N ratio for TWR and SR as response have been tabulated (tables 4.2, 4.3).

4.2.2 Main effects due to parameters

The main effects can be studied by the level average response analysis of raw data or of S/N data. The analysis is done by averaging the raw and/or S/N data at each level of each

parameter and plotting the values in graphical form. The level average responses from the raw data help in analyzing the trend of the performance characteristic with respect to the variation of the factor under study. The level average response plots based on the S/N data help in optimizing the objective function under consideration. The peak points of these plots correspond to the optimum condition [15, 24, 132]. The main effects of raw data and those of the S/N ratio for the various response variables have been shown in figures 4.1-4.3. The factor effects of different input parameters with their corresponding levels on S/N ratio and average response have also been tabulated (tables 4.4-4.5).

4.2.3 Analysis of Variance (ANOVA)

The percentage contribution of various process parameters on the selected performance characteristic can be estimated by performing analysis of variance test (ANOVA). Thus, information about how significant the effect of each controlled parameter is on the quality characteristic of interest can be obtained. The total variation in the result is the sum of variation due to various controlled factors and their interactions and variation due to experimental error [24, 55].

The ANOVA (general linear model) for raw data and S/N data have been performed to identify the significant parameters and to quantify their effect on the performance characteristic. The ANOVA based on the raw data signifies the factors, which affect the average response rather than reducing variation. But ANOVA based on S/N ratio takes into account both these aspects and hence it is also used here [19, 129]. The pooled ANOVA S/N data are given in tables 4.6-4.11. The percentage contributions of significant process parameters on material removal rate for raw and S/N data are shown by means of pie charts (figures 4.4-4.6). The most favorable conditions or optimal levels of process parameters have been established by analyzing response curves of S/N ratio associated with the raw data.

Table 4.1 Test Data Summary for MRR

Exp. No.	MRR (mm^3/min) R1	R2	R3	MRR (mm^3/min)	MRR S/N
1	0.31	0.27	0.36	0.31	-10.26
2	0.64	0.58	0.75	0.66	-3.80
3	1.09	1.21	0.99	1.10	0.71
4	0.40	0.28	0.30	0.33	-10.02
5	0.74	0.63	0.80	0.72	-2.94
6	0.21	0.15	0.15	0.17	-15.70
7	0.13	0.12	0.07	0.11	-20.45
8	0.24	0.27	0.35	0.29	-11.17
9	1.33	1.09	1.24	1.22	1.64
10	0.27	0.26	0.38	0.30	-10.72
11	0.18	0.20	0.15	0.18	-15.24
12	0.47	0.55	0.36	0.46	-7.15
13	0.59	0.50	0.72	0.60	-4.67
14	0.32	0.27	0.36	0.32	-10.17
15	1.25	1.40	1.16	1.27	2.00
16	0.14	0.17	0.18	0.16	-15.89
17	1.30	1.45	1.56	1.44	3.07
18	0.30	0.45	0.36	0.37	-8.99
Average				0.56	-7.76
Maximum	1.33	1.45	1.56	1.44	3.07
Minimum	0.13	0.12	0.07	0.11	-20.45

Table 4.2 Test Data Summary for TWR

Exp. No.	TWR (mm^3/min) R1	R2	R3	TWR (mm^3/min)	TWR S/N
1	0.40	0.45	0.47	0.44	7.11
2	0.65	0.70	0.60	0.65	3.72
3	0.87	0.84	0.93	0.89	1.00
4	0.55	0.46	0.47	0.49	6.15
5	1.02	0.94	1.09	1.01	-0.13
6	0.34	0.37	0.30	0.33	9.51
7	0.13	0.24	0.14	0.19	14.12
8	0.31	0.42	0.27	0.34	9.31
9	1.03	1.15	1.20	1.14	-1.16
10	0.22	0.20	0.14	0.19	14.26
11	0.17	0.13	0.16	0.15	16.39
12	0.41	0.45	0.43	0.41	7.72
13	0.65	0.74	0.65	0.69	3.23
14	0.64	0.57	0.49	0.57	4.88
15	1.12	1.25	1.18	1.18	-1.42
16	0.19	0.17	0.25	0.20	13.89
17	1.66	1.45	1.60	1.58	-3.97
18	0.34	0.43	0.30	0.36	8.79
Average				0.60	6.30
Maximum	1.66	1.45	1.60	1.58	16.39
Minimum	0.13	0.13	0.14	0.15	-3.97

Table 4.3 Test Data Summary for SR

Exp. No.	SR (microns) R1	R2	R3	SR (microns)	Surface Roughness S/N
1	0.98	0.85	0.92	0.92	0.74
2	1.18	1.05	1.24	1.16	-1.28
3	0.70	0.75	0.52	0.66	3.56
4	1.17	0.82	1.10	1.03	-0.35
5	1.20	1.18	1.32	1.23	-1.83
6	0.64	0.60	0.53	0.59	4.56
7	0.68	0.72	0.50	0.63	3.83
8	0.73	0.87	0.90	0.83	1.56
9	2.26	1.90	2.14	2.10	-6.47
10	0.56	0.68	0.75	0.66	3.51
11	0.64	0.78	0.60	0.67	3.38
12	0.86	0.85	0.80	0.84	1.54
13	0.97	1.04	1.12	1.04	-0.38
14	0.66	0.60	0.75	0.67	3.44
15	1.70	1.84	1.67	1.74	-4.80
16	0.66	0.77	0.83	0.75	2.42
17	2.24	2.18	2.29	2.24	-6.99
18	0.73	0.77	0.92	0.81	1.82
Average				0.46	1.03
Maximum	2.26	2.18	2.29	2.24	4.56
Minimum	0.64	0.60	0.50	0.59	-6.99

Table 4.4 Factor Effects on S/N

Factor	Level	Material removal rate S/N	Tool wear rate S/N	Surface Roughness S/N
A) Tool Material				
	A1) H.C.S.	**-5.86**	**5.09**	**0.04**
	A2) H.S.S.	**-9.55**	**5.18**	**0.79**
	A3) Titanium	**-9.99**	**7.42**	**-0.35**
	A4) Titanium alloy	**-11.04**	**12.79**	**2.81**
	A5) Cemented carbide	**-4.28**	**2.23**	**-0.58**
B) Abrasive Type				
	B1) Alumina	**-12.00**	**9.79**	**1.63**
	B2) Silicon carbide	**-6.71**	**5.03**	**-0.29**
	B3) Boron Carbide	**-4.58**	**4.07**	**0.04**
C) Slurry Grit Size				
	C1) 220	**-4.80**	**3.85**	**-2.42**
	C2) 320	**-8.00**	**6.24**	**0.62**
	C3) 500	**-10.49**	**8.81**	**3.17**
D) Power Rating				
	D1) 20% (100 W)	**-13.47**	**10.13**	**2.97**
	D2) 50% (250 W)	**-7.67**	**6.56**	**-0.15**
	D3) 80% (400 W)	**-2.15**	**2.20**	**-1.44**

Table 4.5 Factor Effects on Average Response

Factor	Level	Material removal rate (mm^3/min)	Tool wear rate (mm^3/min)	Surface Roughness (microns)
A) Tool Material				
	A1) H.C.S.	**0.67**	**0.69**	**1.09**
	A2) H.S.S.	**0.41**	**0.61**	**0.95**
	A3) Titanium	**0.54**	**0.56**	**1.19**
	A4) Titanium alloy	**0.31**	**0.25**	**0.72**
	A5) Cemented carbide	**0.73**	**0.81**	**1.15**
B) Abrasive Type				
	B1) Alumina	**0.30**	**0.37**	**0.84**
	B2) Silicon carbide	**0.60**	**0.72**	**1.13**
	B3) Boron Carbide	**0.76**	**0.72**	**1.12**
C) Slurry Grit Size				
	C1) 220	**0.79**	**0.83**	**1.45**
	C2) 320	**0.49**	**0.55**	**0.95**
	C3) 500	**0.39**	**0.42**	**0.69**
D) Power Rating				
	D1) 20% (100 W)	**0.24**	**0.34**	**0.72**
	D2) 50% (250 W)	**0.53**	**0.54**	**1.06**
	D3) 80% (400 W)	**0.90**	**0.92**	**1.32**

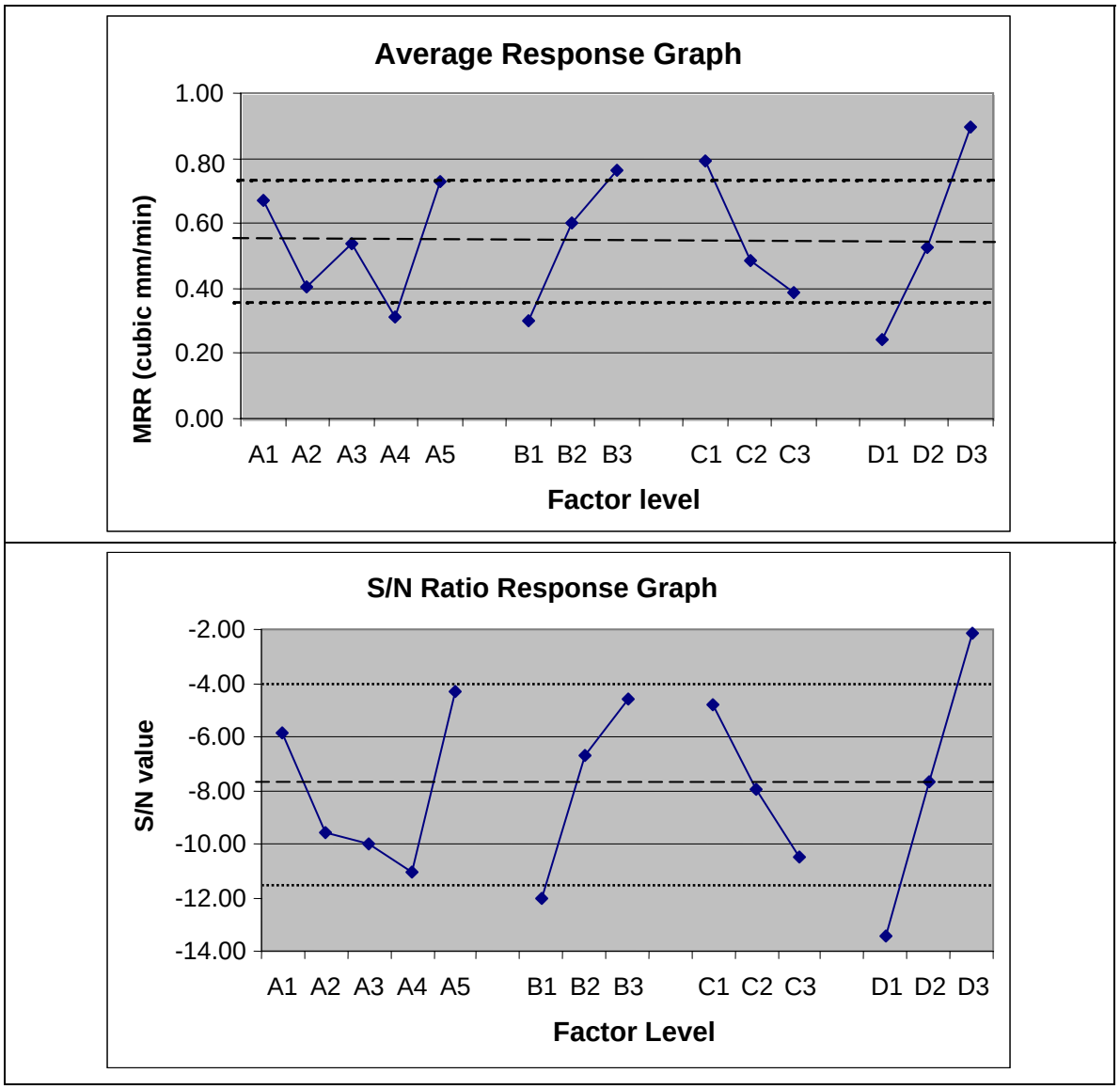

Figure 4.1 Effects of process parameters on MRR-raw data and S/N ratio

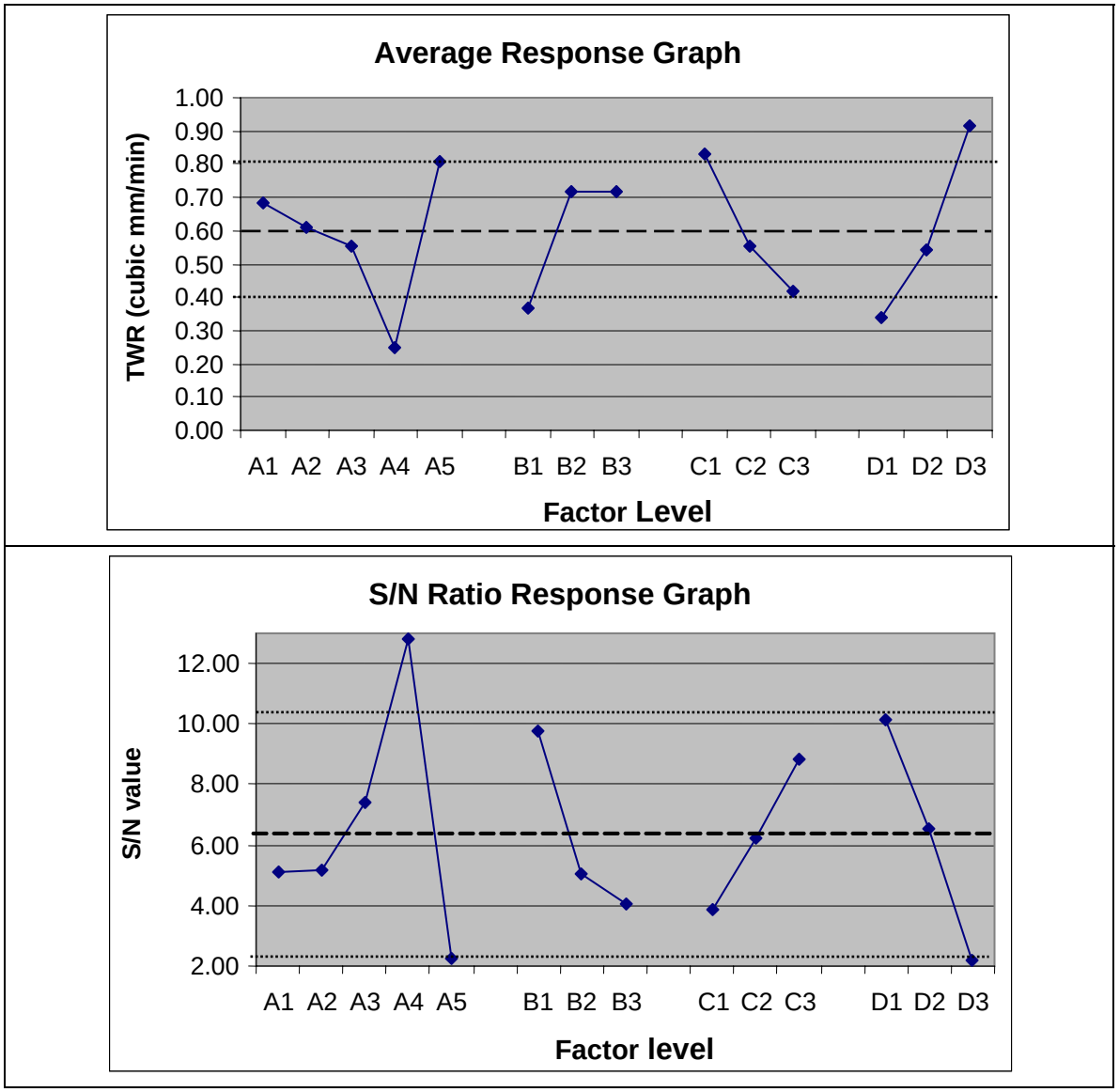

Figure 4.2 Effects of process parameters on TWR- raw data and S/N ratio

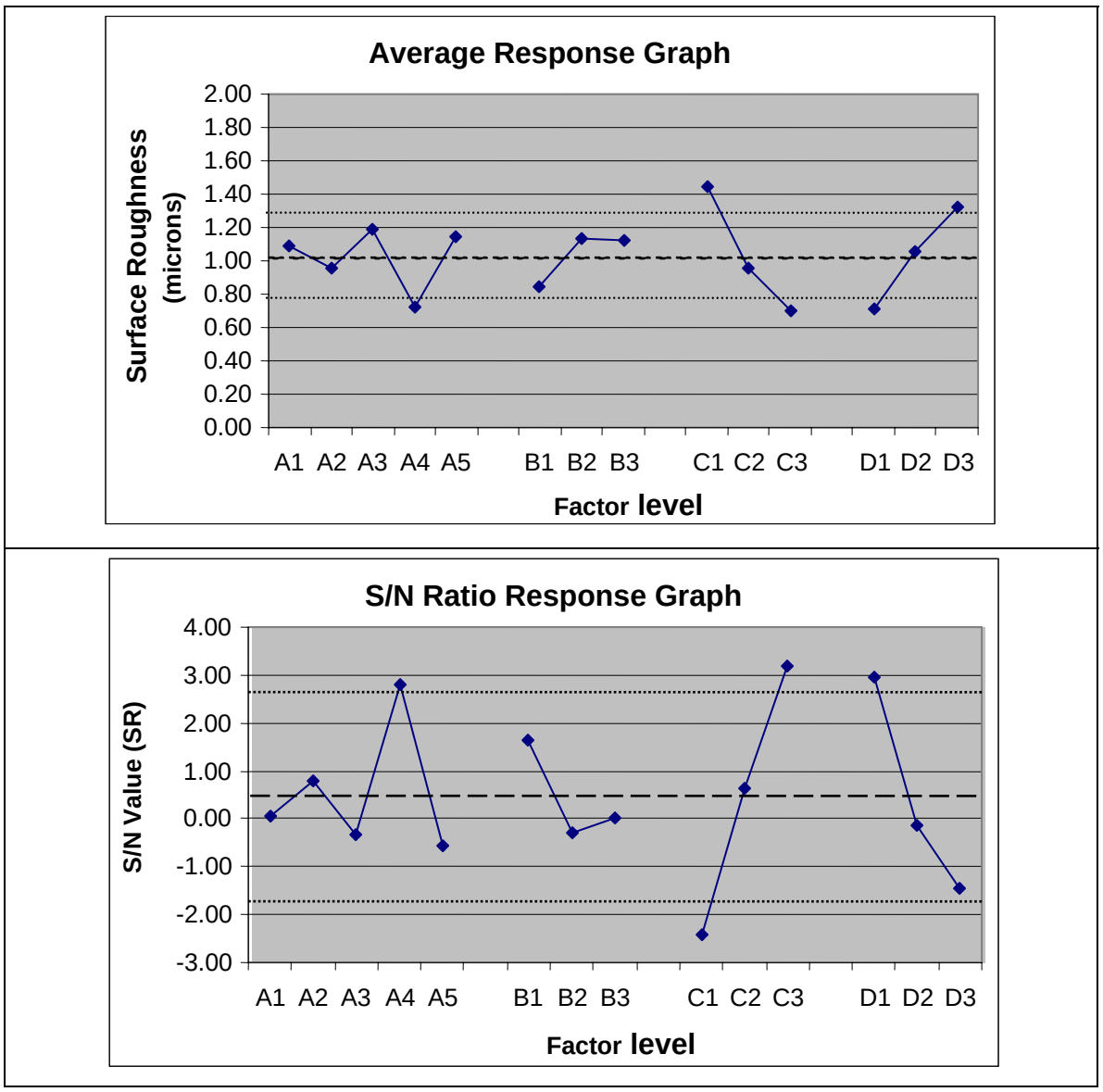

Figure 4.3 Effects of process parameters on SR-raw data and S/N ratio

Table 4.6 ANOVA results for MRR (S/N Data)

Source	DF	Seq. SS	Adj. SS	Adj. MS	F	(%P)
Tool	4	114.812	114.812	28.703	5.77*	**14.2**
Abrasive	2	175.197	175.197	87.598	17.61*	**21.7**
Grit Size	2	97.573	97.573	48.787	9.81*	**12.1**
Power Rating	2	384.277	384.277	192.139	38.63*	**47.6**
Error	7	34.817	34.817	4.974		**4.4**
Total	17	806.677				

F_{tab} = F(4,43)= 2.60; F(2,43)= 3.21

Order of significance:
1. Power rating 2. Abrasive Type 3. Grit Size 4. Tool

Table 4.7 ANOVA results for MRR (raw data)

Source	DF	Seq. SS	Adj. SS	Adj. MS	F	(%P)
Tool	4	1.25	1.25	0.31	18.5*	**13.7**
Abrasive	2	1.97	1.97	0.98	58.1*	**21.3**
Grit Size	2	1.57	1.57	0.79	46.5*	**17.2**
Power Rating	2	3.88	3.88	1.94	114.5*	**42.0**
Error	43	0.72	0.72	0.017		**5.8**
Total	53	9.39				

F_{tab} = F(4,43)= 2.60; F(2,43)= 3.21

Order of significance:
1. Power rating 2. Abrasive Type 3. Grit size 4. Tool

Table 4.8 ANOVA Results for TWR (S/N Data)

Source	DF	Seq. SS	Adj. SS	Adj. MS	F	(%P)
Tool	4	192.581	192.581	48.145	6.38*	**31.0**
Abrasive	2	112.107	112.107	56.053	7.42*	**18.0**
Grit Size	2	74.129	74.129	37.065	4.91*	**12.0**
Power Rating	2	188.656	188.656	94.328	12.49*	**30.5**
Error	7	52.864	52.864	7.552		**8.5**
Total	17	620.336				

F_{tab} = F(4,43)= 2.60; F(2,43)= 3.21

Order of significance:
1. Power rating 2. Abrasive type 3.Tool 4. Grit size

Table 4.9 ANOVA Results for TWR (raw data)

Source	DF	Seq. SS	Adj. SS	Adj. MS	F	(%P)
Tool	4	1.65	1.65	0.41	21.5*	**19.6**
Abrasive	2	1.48	1.48	0.74	38.4*	**17.4**
Grit Size	2	1.57	1.57	0.78	40.8*	**18.7**
Power Rating	2	3.07	3.07	1.53	79.7*	**36.3**
Error	43	0.82	0.82	0.019		**8.0**
Total	53	8.59				

F_{tab} = F(4,43)= 2.60; F(2,43)= 3.21

Order of significance:
1. Power rating 2. Grit size 3. Abrasive type 4. Tool

Table 4.10 ANOVA Results for SR (S/N Data)

Source	DF	Seq. SS	Adj. SS	Adj. MS	F	(%P)
Tool	4	23.147	23.147	5.787	1.81	**10.8**
Abrasive	2	12.728	12.728	6.364	1.99	**6.0**
Grit Size	2	93.927	93.927	46.963	14.68*	**44.0**
Power Rating	2	61.516	61.516	30.758	9.62*	**28.8**
Error	7	22.392	22.392	3.199		**10.4**
Total	17	213.710				

F_{tab} = F(4,43)= 2.60; F(2,43)= 3.21

Order of significance:
1. Grit size 2. Power Rating; other factors are *insignificant*.

Table 4.11 ANOVA Results for SR (raw data)

Source	DF	Seq. SS	Adj. SS	Adj. MS	F	(%P)
Tool	4	1.31	1.31	0.33	6.42**	**10.3**
Abrasive	2	0.99	0.99	0.50	9.72**	**7.8**
Grit Size	2	5.30	5.30	2.65	51.80*	**41.5**
Power Rating	2	3.33	3.33	1.67	32.64*	**26.2**
Error	43	1.40	1.40	0.032		**14.2**
Total	53	12.30				

F_{tab} = F(4,43)= 2.60; F(2,43)= 3.21

Order of significance:
1. Grit size 2. Power Rating 3. Abrasive Type 4. Tool

4.3 DISCUSSION OF THE RESULTS

4.3.1 Effect on Material Removal Rate

It can be observed from figure 4.1 that the tool material affects the material removal rate very significantly. Moreover, the different tool materials used in the experimentation can be ranked in the order of increasing MRR as titanium alloy, high speed steel, titanium, high carbon steel, cemented carbide. The highest MRR has been recorded with cemented carbide as the tool material. This can be attributed to its very higher hardness (92 RC) as compared to the other tool materials used in this investigation. In ultrasonic machining, the indentation of abrasive grains in work and tool is inversely proportional to the hardness ratio of tool and work materials. Hence use of a harder tool results in more indentation in the work piece as compared to tool, increasing the MRR [3, 50, 71, 76, 86]. Use of a tougher and ductile tool such as titanium or titanium alloy tends to lower the material removal rate as it encourages the plastic deformation of the tool as well as work material, which was conformed from the microstructure analysis of the machined samples (refer section 3.4). High carbon steel, being harder than high speed steel and titanium, has also been found to perform better than these tools in terms of material removal rate. In fact, the difference in the performance of high carbon steel and cemented carbide tools has been marginal, the later being on the higher side. It can also be concluded that the material removal rate increases with the increase in relative hardness of the tool work combination, which has also been suggested by many other researchers [50, 76, 86, 134].

The type of abrasive used has been found to produce a significant effect on material removal rate. It has been observed that use of boron carbide as abrasive results in more MRR as compared to that achieved with the use of alumina or silicon carbide. This can be explained on the basis of the relative knoop hardness of the abrasive grains. Boron carbide is having 50-80% more cutting power as compared to other abrasive materials used in this investigation. Hence, the use of boron carbide as abrasive results is faster erosion of work surface thereby improving the MRR [70-71, 79-80].

The MRR obtained has been found to increase with the increase in coarseness of the abrasive grains. This is again in consistent with the findings of most investigators

[50, 87, 136, 140-142, 148]. As it has been previously reported (section 1.1.3), two main wear mechanisms act on the USM process; hammering and free impact of the abrasive particles. The primary mechanism is the hammering action of abrasive particles into the workpiece material. Decreasing the surface density of abrasive particles by increasing the grit size induces a greater augmentation of the effective stress due to each particle acting on the work surface, thus increasing the material removal rate. The secondary mechanism is the impact of free abrasive particles (accelerated by the vibrating tool) over the work surface. In this case, an increase in grit size increases the weight. The impact force against the workpiece surface also increases. Thus, under both mechanisms, the effective load acting on the work surface increases with grit size, which in turn increases the effectiveness of micro-cracking thereby increasing the MRR.

As shown in figure 4.1, MRR drops rapidly while grit size is changed from 220 to 320 and drops further from 320 to 500, but at a diminishing rate. After crossing the grit size of 320, the mean particle size of the abrasive comes closer to the mean gap between the tool and work as well as the vibration amplitude, which promotes more efficient machining of work material. It has also been observed that for a given tool material, MRR obtained is highest at that particular grit size-power level combination which corresponds to the highest value for tool wear rate. In other words, MRR is maximum at the points of maximum TWR. This is an inherent characteristic of the process and has also been found to be applicable in USM of titanium from this research.

As far as the effect of power rating of the ultrasonic machine on MRR is concerned, any increase in power rating is expected to produce a substantial increment in the rate of machining as the momentum with which the abrasive particles strike with the work surface increases manifold with a corresponding increment in power rating [86-87, 145-146]. As titanium is a tough material with good strain hardening capability, the relative tool-work hardening plays a large role in the indifferent behaviour of MRR with change in power rating [86]. The increase in MRR has been found to be sluggish while the power rating is increased from 100 W to 250 W. However, an increase in the power rating from 250 W to 400 W brings a steep rise in the MRR curve. This can be

attributed to the tremendous increment in the momentum with which the abrasive particles strike with the work surface. The particles striking with more momentum cause rapid fracturing of the work surface due to faster propagation of cracks thus promoting MRR.

With regarding to the S/N response, the values of S/N ratio have been found to be highest for those factor levels that correspond to highest average response. Hence, these factor levels can be termed as optimum from the point of view of average response as well as S/N response. As S/N response takes into account both the magnitude as well as the variation in a response, the factor levels that correspond to highest S/N ratio are termed as optimum. Hence, it can be concluded from this discussion that ***"input parameters settings of ultrasonic power rating at 400 W, with Cemented Carbide tool and Boron Carbide slurry with a coarse grit size of 220 have given the optimum results for MRR; when titanium (ASTM Grade-I) was machined***".

In order to estimate the contribution of each factor towards the variation of machining performance in terms of MRR for ultrasonic machining of titanium, Analysis of Variance (ANOVA) test was conducted on the results obtained from the experimentation. The ANOVA test summary for MRR has been recorded for both the average response as well as S/N response (tables 4.6-4.7). The F values for various factors as estimated from the general linear model have been compared with the tabulated F values (F_{tab}) against the particular combination of factor DOF and error DOF. If the estimated F value turns out to be significantly greater than the tabulated F value, the corresponding factor is termed as significant [13, 24, 55]. The factors with larger F values (estimated) are deemed to be having more significance from statistical point of view. The percent contribution of each factor has also been tabulated. With regarding to the average response, power rating factor has emerged as most significant with a percent contribution of 42% (table 4.6) followed by abrasive type (21.3%) and slurry grit size (17.2%). Tool material factor can be termed as the least significant for MRR with a percent contribution of 13.7%. However, for S/N response, power rating has been found to be having highest

percent contribution (47.6%) followed by abrasive type (21.7%). Remaining factors have been found to be almost equally significant.

4.3.2 Effect on Tool Wear Rate

It can be observed from figure 4.2 that the tool material affects the rate of wear of the tool while machining titanium workpiece very significantly. Moreover, the different tool materials used in the experimentation can be ranked in the order of increasing tool wear rate as titanium alloy, titanium, high speed steel, high carbon steel and cemented carbide. The lowest tool wear has been recorded for titanium alloy (ASTM Grade –V). This can be attributed to its excellent combination of higher impact strength and optimum hardness (42 RC) from the point of view of USM process. Also the work hardening ability of this material has been found to be superior as compared to other materials used in this research [12, 36, 133]. Hence, as a result of the repeated impacts of abrasive particles on the tool surface, it goes under significant amount of plastic deformation and subsequent work hardening before fracture, which lowers its abrasion rate. On the other hand, high carbon steel and cemented carbide tools having higher hardeness and brittleness (coupled with poor work hardening capability) are worn out at a faster rate as a result of the rapid brittle fracture of the tool surface under the impact of abrasive grits. Microstructure analysis of the tool surface (figures 4.4-4.5) provides an evidence for the observed behavior of the tools. It could be observed that titanium alloy tool experienced considerable plastic deformation before fracture whereas the carbide tool was worn out by rapid brittle fracture due to propagation and intersection of cracks. Performance of titanium as tool material has been better than H.S.S. and H.C.S. on account of its softness and higher work-hardening capability. It can also be concluded that the tool wear rate increases with the increase in relative brittleness of the tool work combination, which has also been suggested by many other researchers [1, 3, 6, 63, 77, 86].

The type of abrasive used has also been found to put a significant effect on tool wear rate for the different tool materials. It has been observed that use of boron carbide as abrasive results in more tool wear rate as compared to alumina or silicon carbide. This can be explained on the basis of the relative knoop hardness of the abrasive grains. Boron

carbide is having 50-80% more cutting power as compared to alumina and silicon carbide abrasives on account of its higher knoop hardness. This results in rapid erosion of the tool surface as more material is removed per impact of the abrasive particle [79-80, 143].

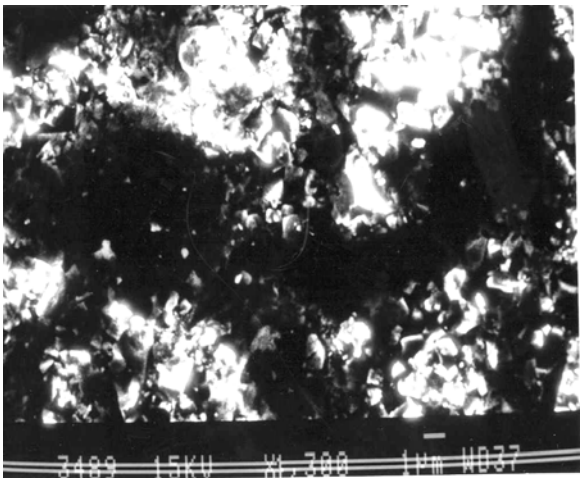

Figure 4.4 Microstructure of carbide tool

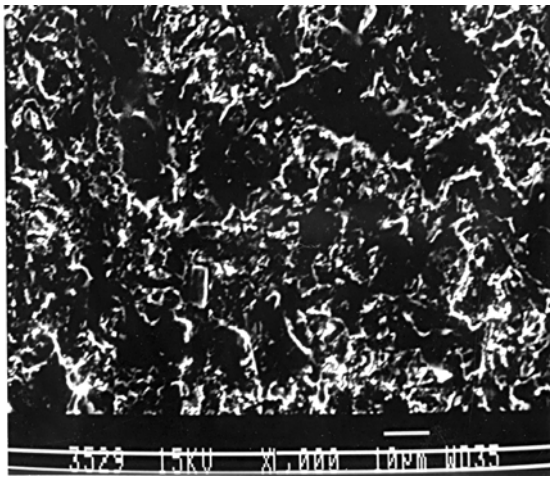

Figure 4.5 Microstructure of Ti alloy tool

The use of a coarser grit size promotes the increase in tool wear rate further (figure 4.2) Use of coarse abrasive grains results in stronger impacts on the tool surface and hence the rate of fracture increases. This can also be explained on the basis of increase in the effective load acting over the tool surface due to hammering and free impact of the abrasive particles. It has also been observed that for a given tool material, TWR is highest at that particular grit size-power level combination which corresponds to the largest value of MRR. In other words, TWR is maximum at the points of maximum MRR. This is in consistent with the findings of other researchers [50, 63, 86, 140].

The tool wear rate (TWR) has been found to be increasing with a corresponding increase in power rating of the ultrasonic machine, the rate of increase being sluggish while the power rating is increased from 100 W to 250 W. But with an increase in the power rating from 250 W to 400 W brings a sharp increment in TWR. This can be attributed to the tremendous increment in the momentum with which the abrasive particles strike with the work surface as well as the tool surface while the power rating is

increased from 250 W to 400 W. The particles striking with more energy cause rapid fracturing of the tool surface thus promoting increase in TWR.

With regarding to the S/N response, the values of S/N ratio for different factor levels have been found to be highest for those factor levels that correspond to highest average response for TWR. Hence, these factor levels can be termed as optimum from the point of view of average response as well as S/N response. Hence, it can be concluded from this discussion that ***"input parameters settings of ultrasonic power rating at 100 W, with Titanium alloy tool and Aluminium oxide slurry with a fine grit size of 500 have given the optimum results for TWR; when titanium (ASTM Grade-I) was machined***".

In order to estimate the contribution of each factor towards the variation of machining performance in terms of TWR for ultrasonic machining of titanium, Analysis of Variance (ANOVA) test was conducted on the results obtained from the experimentation. The ANOVA test summary for TWR has been recorded for both the average response as well as S/N response (tables 4.8-4.9). The percent contribution of each factor has also been tabulated. With regarding to the average response, power rating factor has emerged as most significant with a percent contribution of 36.3% (table 4.8) followed by tool material (19.6%) and slurry grit size (18.7%). Abrasive material factor can be termed as the least significant for MRR with a percent contribution of 17.4%. In other words, for average response, all the factors except power rating are almost equally significant for their contribution to the variation in TWR. For S/N response, tool material has been found to be having highest percent contribution (31.0%) followed by power rating (30.5%) whereas slurry grit size is least significant (12.0%).

4.3.3 Effect on Surface Roughness

It can be observed from figure 4.3 that the tool material affects the surface quality obtained. Moreover, the different tool materials used in the experimentation can be ranked in the order of increasing surface roughness as titanium alloy, high speed steel, high carbon steel, cemented carbide and titanium. The lowest surface roughness has been recorded for titanium alloy (ASTM Grade –V). This can be explained on the basis of very

low material removal rate obtained with use of titanium alloy as a tool material. The rate at which fracture propagates through the work material affects the height of micro-cavities generated in the work surface. Any increase in the MRR of work material corresponds to creation of larger sized micro-cavities in the surface, which is associated with more surface roughness [34, 50, 78, 88]. The higher values of surface roughness for cemented carbide, high carbon steel and titanium tools also indicate the dependence of surface quality on the tool material properties i.e. hardness and rate of machining in USM of titanium.

The type of abrasive used puts a marginally significant effect on surface quality obtained in USM of titanium. It has been observed that use of alumina as abrasive results in best surface quality in terms of least surface roughness as compared to that achieved with the use of boron carbide or silicon carbide. However, the difference between the performance of silicon carbide and boron carbide abrasives is only marginal. The superior performance of alumina can be explained on the basis of its least cutting power among the three abrasives. Because of the low knoop hardness, use of alumina results in formation of smaller sized micro-cavities which contribute to the best surface finish.

The use of a coarser grit size promotes the increase in surface roughness, thus deteriorating the surface quality (figure 4.3). This is in consistent with findings of most researchers [34, 47, 50, 86, 140]. Use of coarse abrasive grains results in stronger impacts on the tool surface and hence the rate of fracture increases, thereby quality of the machined surface is deteriorated. During the ultrasonic abrasion process, abrasive particles continuously move, not only in the working gap but also in the lateral gap between the tool and work piece surface. By increasing the grit size, the frictional forces acting at the lateral interface increase and with the progress of machining, the continuous downward movement of the abrasive particles in the lateral gap gives rise to slurry streamers which draw abrasive grains deep down into the machining zone. The surface damage due to this non-uniform lateral wear is associated with the increase of roughness.

The surface roughness of the machined surface has been found to be increasing with a corresponding increase in power rating of the ultrasonic machine, the rate of

increase being sluggish while the power rating is increased from 100 W to 250 W. But with an increase in the power rating from 250 W to 400 W brings a sharp increment in SR. This can be explained on the similar basis to MRR or TWR. The abrasive particles striking on the work surface with extremely high momentum remove larger chunks of material, thereby increasing the surface roughness [86-87]. It has also been observed that for a given tool material, surface roughness obtained attains the highest value at that particular grit size-power level combination which corresponds to largest value of MRR. In other words, surface roughness is maximum at the points of maximum MRR.

It can be concluded from table 4.10 that only slurry grit size and power rating factors are statistically significant for their effect on surface quality while machining titanium with USM. The percent contribution for slurry grit size has been found to be the highest among all the factors (41.5%) whereas power rating comes next (26.2%). Remaining factors can be termed as relatively insignificant for surface roughness. The S/N results indicate that slurry grit size has highest percent contribution (44.0%) followed by power rating (28.8%) for their effect on surface quality. The other two factors (tool material and abrasive type) have been found to be insignificant as far as S/N response is concerned. Hence, it can be concluded that "***While machining titanium (ASTM Grade-I) with USM, input parameter settings of ultrasonic power rating at 100 W, with titanium alloy tool and aluminium oxide slurry with a fine grit size of 500 have given the optimum results for surface quality***.

A careful visual observation of the tool surface after machining reveals formation of a dish in the centre of the tool face. The hardness of the tool increases by work hardening, thereby, penetration of the abrasive grains into the tool decreases resulting in higher MRR from the periphery of the work zone and consequently a convex surface is formed in the work piece [1-4, 73, 159]. This causes plastic deformation of the centre of the tool face. The tendency of the dish formation has been observed to be most severe with high carbon steel tool. High speed steel and titanium alloy are comparatively tougher materials, hence the dish formation for these tools is lesser pronounced as compared to the other tools.

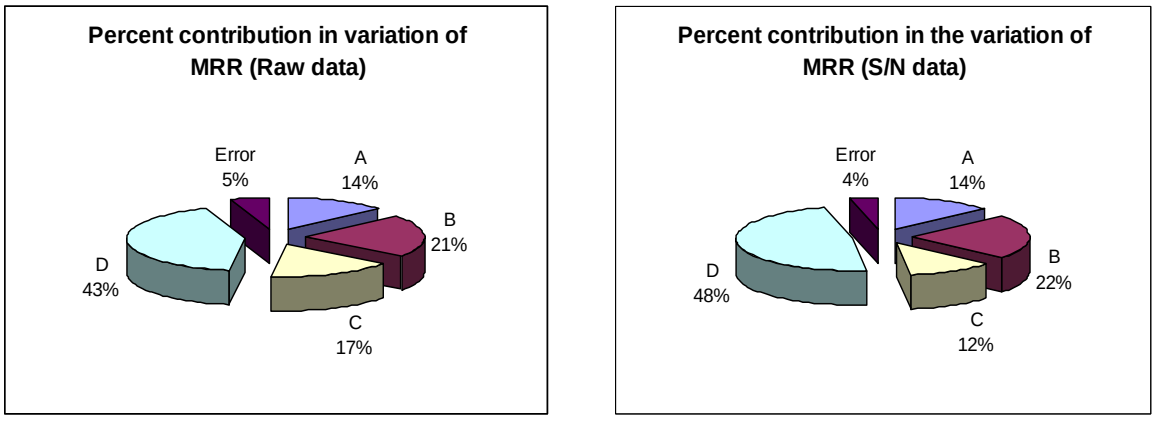

Figure 4.6 Percent Contribution of different factors to variation in MRR

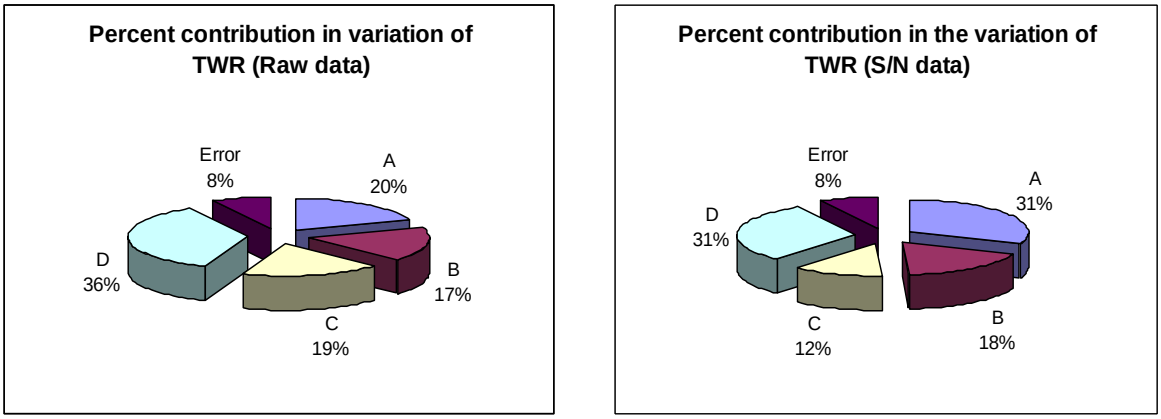

Figure 4.7 Percent Contribution of different factors to variation in TWR

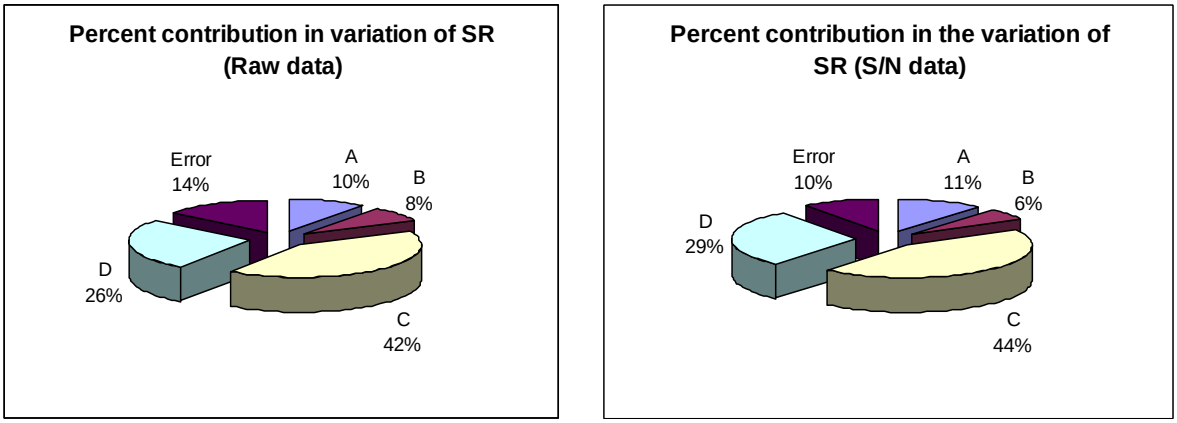

Figure 4.8 Percent Contribution of different factors to variation in SR

Figures 4.6-4.8 show the percent contribution of various factors towards variation in MRR, TWR and surface roughness while machining titanium.

4.3.4 Prediction of the mean and confirmation experiments

The estimate of the mean is only a point estimate based on the average of results obtained from the experiment. Statistically this provides a 50% chance of the true average being greater than μ and a 50% chance of true average being less than μ. It is, therefore, customary to represent the values of a statistical parameter as a range within which it is likely to fall, for a given level of confidence [129]. This range is termed as the Confidence Interval (CI). In other words, the confidence interval is a maximum and minimum value between which the true average should fall at some stated percentage of confidence.

The Taguchi approach for predicting the mean performance characteristics and determination of confidence intervals for the predicted mean has been applied. Three confirmation experiments for each performance characteristics have been performed at optimal settings of the process parameters and the average value has been reported (table 4.12). The average values of the performance characteristics obtained through the confirmation experiments must be within the 95% confidence interval ($\alpha = 0.05$), CI_{CE} (fixed number of confirmation experiments).

For MRR, the overall mean of the population is: $\mu = 0.56$

The predicted optimum value of MRR is calculated as (table 4.5),

$$\mu_{MRR} = (\mu A5+\mu B3+\mu C1+\mu D3) - (3\mu) = 1.52$$

Similarly, for TWR:

$$\mu_{TWR} = (\mu A4+\mu B1+\mu C3+\mu D1) - (3\mu) = 0.06$$

For surface roughness only two factors have been found to be significant (power rating, grit size). Hence other factors have been omitted in estimation of optimum value for SR.

$$\mu_{SR} = (\mu C3+\mu D1) - (\mu) = 0.36\ \mu m$$

For calculation of $CI_{CE,}$ the following equation [129] has been used:

$$CI_{CE} = \sqrt{F_\alpha(1, f_e)\left\{\frac{1}{n_{eff}} + \frac{1}{R}\right\}V_e} \qquad (4.1)$$

$F_\alpha(1, f_e)$ = the F-ratio at a confidence level of (1-α) against DOF 1 and error degrees of freedom f_e (for MRR, f_e = 43, so F_α is 4.05)

V_e = error variance for MRR

V_e = 0.017 (table 4.7)

$$n_{eff} = \frac{N}{1 + Total\ DF\ involved\ in\ estimation\ of\ mean}$$

N = total number of experiments

n_{eff} = 54/ (1+10) = 4.90

R = sample size for confirmatory experiments = 3

Hence, putting all the values in equation (4.1)

$CI_{CE(MRR)} = \pm 0.18$

The 95% confidence interval for μ_{MRR} is,

$CI_{CE(MRR)} = 1.34 < \mu_{MRR} < 1.70$

Similarly, for TWR:

V_e = 0.019 (table 4.9)

n_{eff} = 54/ (1+10) = 4.90

R = 3

$F_\alpha(1, 7)$ = 4.05

Putting all the values in equation (4.1) yields;

$CI_{CE(TWR)} = \pm 0.19$

The 95% confidence interval for μ_{TWR} is,

$$CI_{CE(TWR)} = 0.00<\mu_{TWR}<0.25$$

For surface roughness,

$V_e = 0.032$ (table 4.11)

$n_{eff} = 54/ (1+10) = 4.9$

$R = 3$

$F_\alpha(1, 43) = 4.05$

Putting all the values in equation (4.1) yields;

$$CI_{CE(SR)} = \pm 0.24$$

The 95% confidence interval for μ_{TWR} is,

$$CI_{CE(SR)} = 0.12<\mu_{SR}<0.60$$

The optimum values and the confidence intervals have been tabulated (table 4.12). Three experiments were conducted at the optimum settings of the process parameters for all the responses. The mean values of the responses from these experiments have been found to be well contained by the confidence intervals.

4.3.5 Range of applicability

In the present study, the input parameter settings in ultrasonic machining of titanium (ASTM Grade–I) such as tool material, abrasive type, slurry grit size and power rating have been optimized for three machining characteristics-MRR, TWR and surface roughness.

Table 4.12 Comparison of Predictions and Experimental Results

Response		Predicted value	Experimental Value	CI_{CE}
MRR	mm^3/min	1.52	1.67	$1.34<\mu_{MRR}<1.70$
TWR	mm^3/min	0.06	0.04	$0.00<\mu_{TWR}<0.25$
SR	microns	0.36	0.31	$0.12<\mu_{SR}<0.60$

The results obtained under the optimized process settings have been found to be valid for 90-95% confidence interval. As per the concepts of Taguchi's robust design methodology, the process or product developed for one particular application should possess the design transferability to accommodate changes from time to time and also to be applicable to other applications. In the present study, the process has been developed for ultrasonic machining of titanium (ASTM Grade-I). The process can also be applied to the machining of the other grades of titanium by making minor alterations in the optimized conditions, taking into account the changes in the values of response variables when the original process settings are applied to the machining. Thus, a significant amount of effort and time can be saved in developing a new process for machining of the other grades of titanium.

4.3 MULTIPLE RESPONSE OPTIMIZATION

4.4.1 Determination of Utility Value

To determine the utility value for a number of quality characteristics, a preference scale for each quality characteristic is constructed. Later these scales are allotted weights to obtain a composite number (overall utility). The preference scale chosen [49] is given as,

$$P_i = A \log [X_j/X'] \qquad (4.1)$$

Where X_j is the value of quality characteristic *j, X'* is the non-acceptable value of characteristic *j* and *A* is a constant whose value can be determined as given under:

$$A = 9/ [\log X^*/X'] \qquad (4.2)$$

A is chosen such that $P_i = 9$ at $X_j = X^*$, where X^* is the most desirable (optimum) value of X_j assuming that such a number exists.

For MRR,

X^* = optimum value of MRR 1.52 mm^3/min (table 4.12)

X' = minimum acceptable value of MRR 0.07 mm^3/min (assumed, as all the observed values of MRR are in between 0.07 and 1.56)

Using these values and equations (4.1) and (4.2), the preference scale for MRR is,

$$P_{MRR} = 1.34 \log X_{MRR}/0.07 \quad (4.3)$$

For construction of preference scale for TWR and SR, the largest value obtained from the experiments (tables 3.8-3.25) was considered as the minimum acceptable value as both of these characteristics are "Lower-the-better" type.

For TWR,

X^* = optimum value of TWR 0.06 mm^3/min (table 4.12)

X' = minimum acceptable value of TWR 1.68 mm^3/min (assumed, as all the observed values of TWR are in between 0.12 and 1.68)

Using these values and equations (4.1) and (4.2), the preference scale for TWR is,

$$P_{TWR} = -1.45 \log X_{TWR}/1.68 \quad (4.4)$$

For SR,

X^* = optimum value of SR 0.36 μm (table 4.12)

X' = minimum acceptable value of SR 2.29 μm (assumed, as all the observed values of SR are in between 0.50 and 2.29)

Using these values and equations (4.1) and (4.2), the preference scale for SR is,

$$P_{SR} = -0.80 \log X_{SR}/2.30 \quad (4.5)$$

The weights to the selected quality characteristics have been assigned as;

W_{MRR} = weight assigned to MRR 0.333

W_{TWR} = weight assigned to MRR 0.333

W_{SR} = weight assigned to MRR 0.333

It has been assumed that all the quality characteristics are equally important, hence equal weights have been assigned to them. However, there is no constraint on

allocation to weights to the quality characteristics and they can be assigned any value between 0 and 1 depending upon the customer priorities and subjected to the condition that the sum of individual weights should not exceed 1.

The value of the composite measure has been calculated using the following equation (overall utility function);

$$U(n, R) = P_{MRR}(n, R) \, X \, W_{MRR} + P_{TWR}(n, R) \, X \, W_{TWR} + P_{SR}(n, R) \, X \, W_{SR} \qquad (4.6)$$

Where, n = trial number, n = 1, 2 …..18; R = replication number, R = 1, 2, 3.

The utility values thus calculated are reported in table 4.13.

4.4.2 Estimation of optimal settings using utility data

The data (utility values) were analyzed both for mean response and S/N ratio. Since utility is "larger-the-better" type of characteristic, $(S/N)_{LB}$ is used. The mean responses and main effects in terms of utility values are calculated and reported in table 4.14. The values of main effects for raw data and S/N response have been plotted (figure 4.7).

It can be concluded (figure 4.7) that the fourth level of tool material (A4), third level of abrasive material (B3), third level of grit size (C3) and the third level of power rating (D3) would yield optimal performance in terms of utility value and S/N ratio within the selected range of parameters. Hence, it can be concluded that "***While machining titanium (ASTM Grade-I) with USM, input parameter settings of ultrasonic power rating at 400 W, with titanium alloy tool and Boron Carbide slurry with a fine grit size of 500 have given the best results for simultaneous optimization of MRR, TWR and Surface Roughness.***

The predicted optimal values corresponding to all the machining characteristics for this optimal setting have been reported in table 4.15. The confidence intervals for all the three characteristics have also been indicated. It could be observed that the confirmatory experiments results satisfy the confidence interval limits. It can also be observed that the composite optimal process setting based on utility function is remarkably different from the optimal settings obtained for individual machining characteristics using single response optimization (table 4.16). The composite optimal

setting ensures collective optimization of the three different machining characteristics – MRR, TWR and SR; hence it leads to establishment of a cost effective method while machining titanium with USM.

Table 4.13 Utility Data for Multiple Responses (MRR, TWR and SR)

Exp. No.	Composite index			Avg. Value	S/N ratio (dB)
	R1	R2	R3		
1	0.67	0.68	0.68	0.68	-3.39
2	0.86	0.72	0.71	0.76	-2.44
3	0.87	0.90	0.92	0.90	-0.95
4	0.64	0.66	0.64	0.65	-3.79
5	0.64	0.60	0.61	0.62	-4.21
6	0.68	0.64	0.63	0.65	-3.76
7	0.67	0.67	0.73	0.69	-3.24
8	0.75	0.72	0.71	0.73	-2.78
9	0.70	0.74	0.72	0.72	-2.86
10	0.92	0.94	0.95	0.94	-0.57
11	0.82	0.80	0.86	0.83	-1.67
12	0.78	0.79	0.75	0.77	-2.24
13	0.75	0.72	0.73	0.73	-2.70
14	0.66	0.68	0.65	0.66	-3.57
15	0.67	0.65	0.66	0.66	-3.61
16	0.77	0.75	0.74	0.75	-2.46
17	0.64	0.64	0.60	0.63	-4.07
18	0.79	0.77	0.75	0.77	-2.28

Table 4.14 Main Effects due to Parameters (utility data)

Factor	Level	Effect on mean	Effect on S/N
A) Tool	1) HCS	0.75	-2.60
	2) HSS	0.64	-3.92
	3) Titanium	0.71	-2.96
	4) Titanium alloy	0.85	-1.49
	5) Cemented carbide	0.69	-3.29
B) Abrasive	1) Alumina	0.73	-2.69
	2) Silicon carbide	0.70	-3.12
	3) Boron carbide	0.75	-2.62
C) Grit Size	1) 220	0.69	-3.23
	2) 320	0.72	-2.85
	3) 500	0.77	-2.35
D) Power Level	1) 100 W	0.71	-2.98
	2) 250 W	0.72	-2.89
	3) 400 W	0.76	-2.56

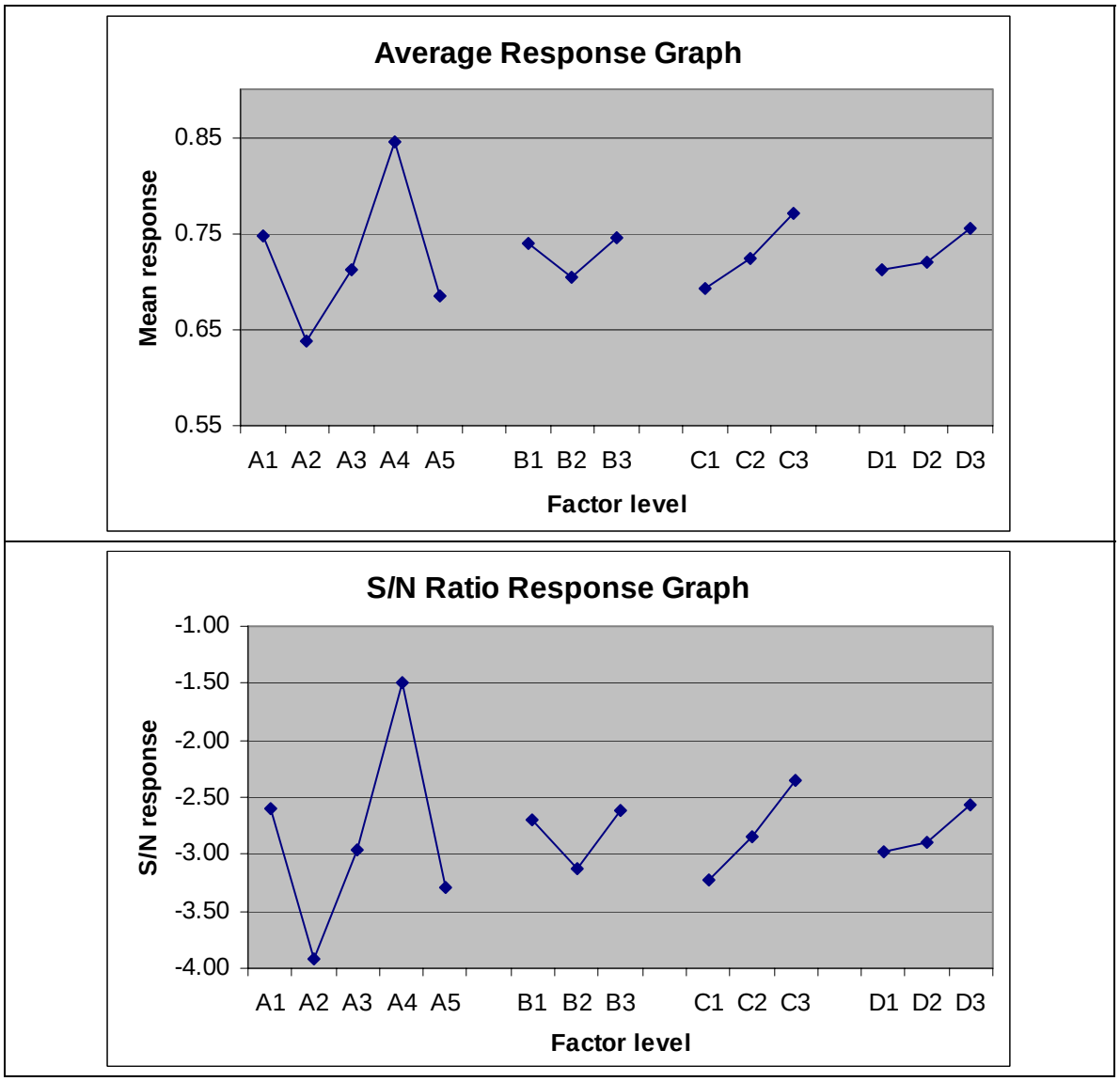

Figure 4.9 Main Effects plots for utility data (mean response and S/N)

(A=Tool, B=Abrasive, C=Grit size, D=Power rating)

Table 4.15 Confirmation Experiments Results

Response		Predicted value	Experimental Value	CI_{CE}
MRR	mm^3/min	0.70	0.64	$0.52<\mu_{MRR}<0.88$
TWR	mm^3/min	0.50	0.55	$0.31<\mu_{TWR}<0.69$
SR	microns	0.77	0.80	$0.53<\mu_{SR}<1.01$

Table 4.16 Comparison of single response and multi-response optimization results

Method	Characteristic	Optimal condition	Optimal value
Single response optimization	MRR TWR SR	A5B3C1D3 A4B1C3D1 A4B1C3D1	1.52 mm^3/min 0.06 mm^3/min 0.36 µm
Multi-Response optimization	MRR, TWR, SR	A4B3C3D3	MRR = 0.70 mm^3/min TWR = 0.50 mm^3/min SR = 0.77 µm

CHAPTER 5
MODELING OF THE RESULTS

5.1 INTRODUCTION

There are two broad approaches for optimization of a complex machining system such as machining characteristics of titanium in USM. The detailed discussion of both approaches is given as following:

1. **Micro-modeling:** This approach is based on an in-depth study of the system. It starts by development of a mathematical model of the system i.e. MRR or TWR in the ultrasonic machining of titanium. To simplify the operation, some assumptions are made to deal with the complexity of the system. USM of titanium could be regarded as one of the complex systems. Furthermore, the more simplification is done, the less realistic the model would be and hence, the less would be the precision in optimization. However, once an adequate model is constructed, a number of well known optimization techniques can be used to develop the optimum system configuration.

2. **Macro-modeling**: In this approach, there is no need of developing a mathematical model of the system. The emphasis is on obtaining an optimum system configuration only, without achieving a detailed understanding of the system. Hence, as compared to micro-modeling, this approach is more efficient and faster. It provides the specific information needed for optimization of the system with a minimum of resources.

To develop a micro-model for the current investigation, initially a macro-model has been developed based upon the concept of Taguchi's robust design methodology. The output of this macro-model has further been used to obtain a micro-model. The micro-model is based on dimensional analysis as per Buckingham's π-theorem.

5.2 MACRO-MODEL FOR USM OF TITANIUM

The prime objective of the current investigation is to obtain the optimum system configuration in USM of titanium in terms for response variables with minimum of experimental resources. Taguchi's robust design method for offline quality control has been applied in this research for planning, conducting and analyzing the experiments. The best settings of control factors have been determined for different machining characteristics (response variables) as shown in table 5.1 as macro-model.

Table 5.1 Optimized Process Settings (Macro-Model)

FOR MRR	
Tool Material	Cemented carbide
Abrasive Type	Boron Carbide
Slurry Grit Size	220 (coarse)
Power Rating	400 W (80%)
For TWR	
Tool Material	Titanium alloy
Abrasive Type	Alumina
Slurry Grit Size	500 (fine)
Power Rating	100 W (20%)
For SR	
Tool Material	Titanium alloy
Abrasive Type	Alumina
Slurry Grit Size	500 (fine)
Power Rating	100 W (20%)

Large and complex systems, such as machining characteristics of titanium using USM, are often managed using single response optimization approach. This approach misses the interactions between the multiple responses. In the present case, success in improving the MRR, TWR and SR in ultrasonic machining of titanium suggests that the Taguchi's robust design approach could be used successfully to optimize the other machining characteristics. Also, the predicted response under the optimized conditions may have large variance. Standardized S/N ratio can be used to reduce the adverse effect

of changing noise conditions, which is encountered in running robust design experiments on live system.

5.3 MICRO-MODEL FOR PREDICTING MRR AND TWR

The micro-model presented here has been based on the macro-model using robust design technique. The macro-model indicates:

- ❖ MRR in USM of titanium is dependant on ultrasonic power rating, type of abrasive, slurry grit size and tool material used.
- ❖ TWR in USM of titanium is dependant on ultrasonic power rating, slurry grit size followed by type of abrasive and tool material.
- ❖ SR in USM of titanium is dependant on slurry grit size followed by power rating. The other factors have not been found to affect the SR significantly.

Taking these results as an input; an attempt has been made to develop micro-model using dimensionless analysis approach (Buckingham's π-theorem). Following assumptions have been made while developing the mathematical micro model for the given situation:

1. Frequency of vibration is fixed through out the experimentation and it is of the order of 20 kHz ± 200 Hz.
2. Amplitude of vibration is constant through out the experimentation and is of the order of 0.0253-0.0258 mm.
3. Static feed force is also constant and is maintained equal to 1.636 kg.
4. The factors declared as *insignificant* by analysis of variance test have been omitted for developing the mathematical relationship for further micro-model construction.

The Buckingham's pie theorem proves that, in a physical problem including "n" quantities in which there are "m" dimensions, the quantities can be arranged in to "n-m" independent dimensionless parameters. In this approach dimensional analysis is used for developing the relations [23].

5.3.1 Micro-model for predicting MRR

MRR "Z" depends upon four input parameters namely ultrasonic power rating, tool hardness factor, slurry hardness factor and grit size of the slurry.

By selecting,

M (mass)

L (length);

T (time);

As basic dimensions, the dimensions of the foregoing quantities would then be:

1. The MRR "*Z*" (mm^3/min) $L^3 T^{-1}$
2. Power rating "*P*" (Watt) $M L^2 T^{-3}$
3. Tool hardness factor *"H*" (GPa) $M L^{-1} T^{-2}$
4. Abrasive hardness factor "μ_s" (GPa) $M L^{-1} T^{-2}$
5. Slurry grit size "ρ" (mm) L

The foregoing quantities or factors have been selected keeping in view the input parameters being investigated in the study. As two of the factors being investigated (tool material, abrasive type) are qualitative factors, the quantification is possible only when some quality characteristic related with each of these factors is identified and used for further dimensional analysis. Hence, tool hardness factor and abrasive hardness factor were the quality characteristics adopted for these two parameters and used in the dimensional analysis.

Now,

$$Z = f(P, H, \mu_s, \rho) \qquad (5.1)$$

In this case, n=5 and m=3, hence we can have (n-m=2) π_1, π_2 two dimensionless groups. Taking *Z* and *H* as the quantities which will go in π_1, π_2 respectively, we obtain:

$$\pi_1 = Z (\mu_s)^{\alpha 1} (P)^{\beta 1} (\rho)^{\gamma 1} \qquad (5.2)$$

$$\pi_2 = H(\mu_s)^{\alpha 2} (P)^{\beta 2} (\rho)^{\gamma 2} \qquad (5.3)$$

Substituting the dimensions of each quantity and equating to zero, the ultimate exponent of each basic dimension is achieved, since the "π_{is}" are dimensionless groups.

Solving for π_1 we get,

$$\pi_1 = L^3 T^{-1} (M L^{-1} T^{-2})^{\alpha 1} (ML^2T^{-3})^{\beta 1} (L)^{\gamma 1} \quad (5.4)$$

Here,

$$3-\alpha_1+2\beta_1+\gamma_1=0$$

$$-1-2\alpha_1-3\beta_1=0$$

$$\alpha_1+\beta_1=0$$

On solving,

$$\alpha_1=1,\ \beta_1=-1,\ \gamma_1=0$$

Putting the values obtained in equation (5.2) we get,

$$\pi_1 = Z\ (\mu_s)(P)^{-1}(\rho)^0$$

$$\boldsymbol{\pi_1 = Z\ \mu_s / P} \quad (5.5)$$

Similarly, we get

$$\pi_2 = M L^{-1} T^{-2} (M L^{-1} T^{-2})^{\alpha 2} (ML^2T^{-3})^{\beta 2} (L)^{\gamma 2} \quad (5.6)$$

$$1+\alpha_2+\beta_2=0$$

$$-1-\alpha_2+2\beta_2+\gamma_2=0$$

$$-2-2\ \alpha_2-3\beta_2=0$$

Solving we get,

$$\alpha_2=-1,\ \beta_2=0,\ \gamma_2=0$$

Thus,

$$\pi_2 = H(\mu_s)^{-1}(P)^0(\rho)^0$$

$$\boldsymbol{\pi_2 = H/\mu_s} \quad (5.7)$$

The functional relationship is of the form,

$$\pi_1 = f(\pi_2) \quad (5.8)$$

Hence,

$$Z\ \mu_s/P = f(H/\mu_s) \quad (5.9)$$

It has been found experimentally that Z directly goes with H [1, 77].

Hence,

$$Z.\mu_s/P = H f (1/\mu_s)$$

$$\boldsymbol{Z = C \{P.H/ \mu_s^2\}} \quad \textbf{(5.10)}$$

Where *C* is a constant of proportionality.

To calculate "*C*", experiments were performed by:

1. Keeping P/μ_s^2 unchanged, varying *H* (different tool materials) to estimate *Z,* for assessment of the impact of tool hardness factor on MRR.
2. Keeping H/ μ_s^2unchanged*,* varying *P* (different power ratings) to estimate Z, for assessment of the impact of power rating on MRR.

Impact of Tool Hardness Factor on MRR

Case I (400 W Power rating, Alumina slurry, 220 Grit size)

To know the impact of *H* on material removal rate, experiments were performed by "changing one factor at a time" approach thus with changing only the tool material and keeping all other factors constant. The experimental data has been given in table 5.2.

Table 5.2 Effect of Tool Hardness Factor on MRR

Abrasive Type	Tool Material	Tool Hardness (GPa)	Mean MRR (mm^3/min.)
Alumina	High carbon steel	1.9	0.85
	High speed steel	1.68	0.70
	Titanium	1.15	0.57
	Titanium alloy	1.36	0.38
	Cemented carbide	18.5	1.02
Boron Carbide	High carbon steel	1.9	1.55
	High speed steel	1.68	1.33
	Titanium	1.15	1.20
	Titanium alloy	1.36	0.86
	Cemented carbide	18.5	1.67
Silicon Carbide	High carbon steel	1.9	1.42
	High speed steel	1.68	1.20
	Titanium	1.15	0.92
	Titanium alloy	1.36	0.60
	Cemented carbide	18.5	1.54

The data collected has been further used for finding the best fitting curve as shown in figure 5.1. Thus the equation of MRR for this case is given as:-

$$Z = (2.807 - 3.681\ H + 1.496\ H^2 - 0.07040\ H^3).P/\mu_s^2$$

μ_s=*18*.0 GPa for alumina slurry

P= 400 W

Similarly, the experimentation was performed with silicon carbide slurry and boron carbide slurry using all the tool materials used in this investigation, keeping power rating (400 W) and grit size (220) unchanged. The best fitted curves for these two cases are given next.

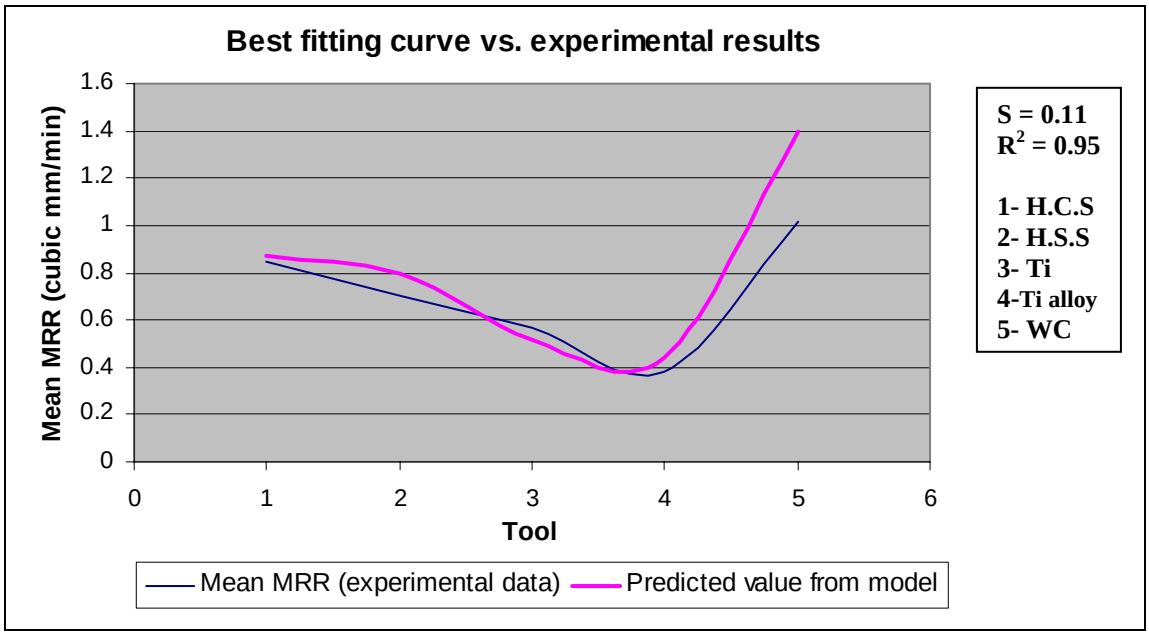

Figure 5.1 Best fitting curve for MRR (alumina slurry/220 grit size)

Case II (400 W Power Rating, Silicon Carbide slurry, 220 Grit size)

The regression equation is,

$$Z = (8.215 - 10.91\ H + 4.503\ H^2 - 0.2125\ H^3).\ P/\mu_s^2$$

μ_s=24.2 GPa for silicon carbide slurry , P= 400 W

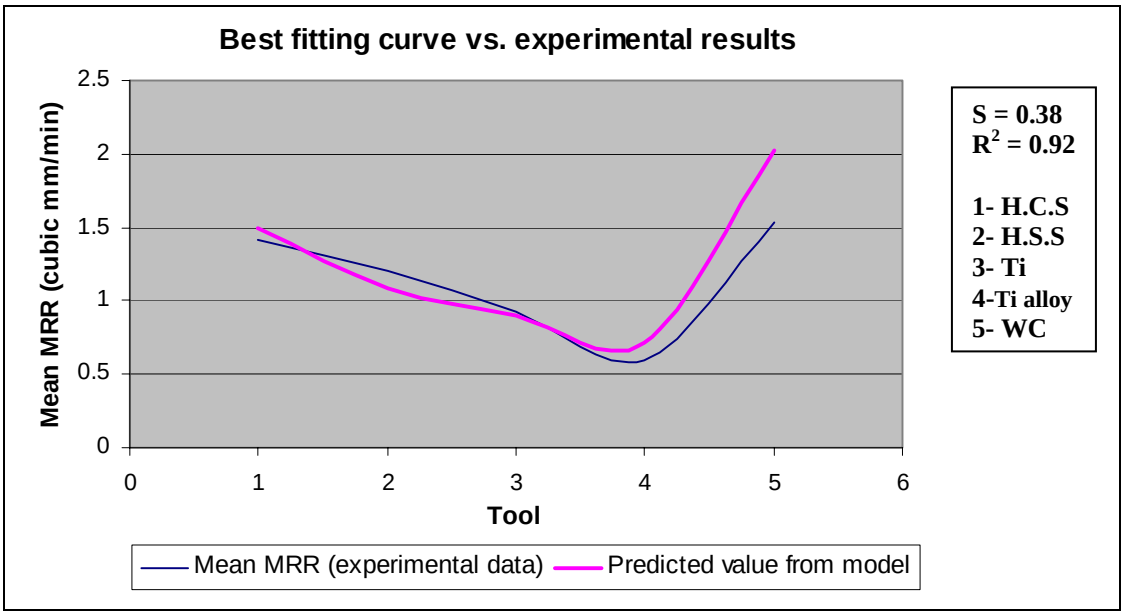

Figure 5.2 Best fitting curve for MRR (slurry: SiC/220)

Case III (400 W Power Rating, Boron Carbide slurry, 220 Grit size)

The regression equation is,

$$Z = (11.30 - 14.10\,H + 5.614\,H^2 - 0.2636\,H^3).\ P/\mu_s^2$$

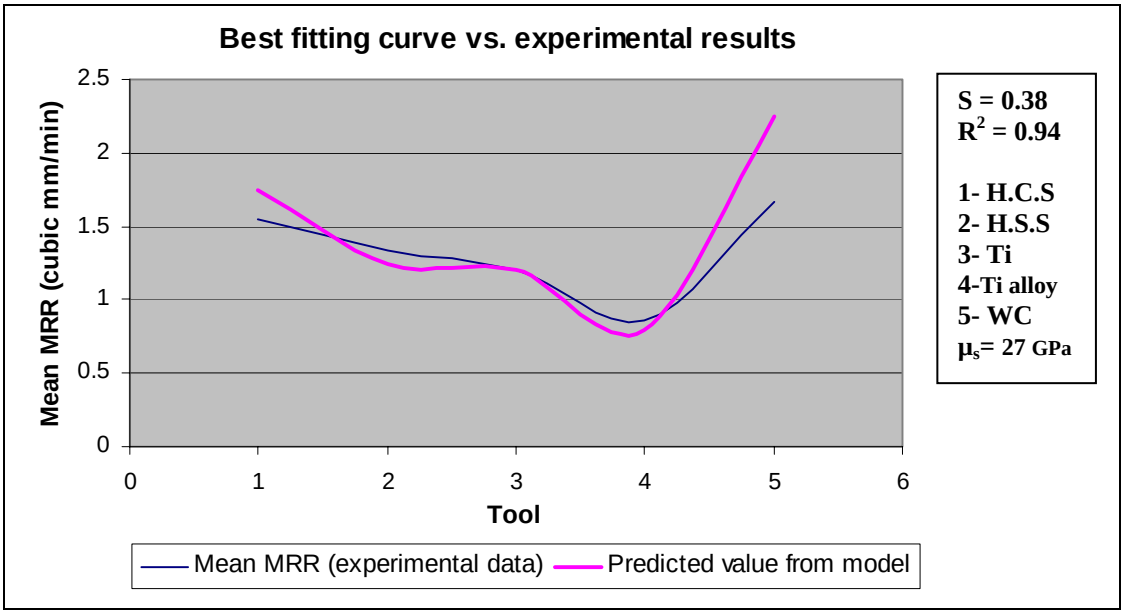

Figure 5.3 Best fitting curve for MRR (slurry: B_4C/220)

Impact of Power Rating on MRR

Case I (H.C.S. tool, Alumina slurry, 220 Grit size)

To know the impact of P on material removal rate, experiments were performed by "changing one factor at a time" approach thus with changing only the power rating and keeping all other factors constant. In the first case, experiments have been performed using high carbon steel tool with alumina as abrasive with a coarse grit size of 220 while the power rating was varied from 100 W to 400 W in four equal increments. The experimental data has been plotted along with the best fitting curve for MRR (figure 5.4). The regression equation is,

$$Z = (161.0 - 1.110\,P + 0.002500\,P^2).H/\mu_s^2$$

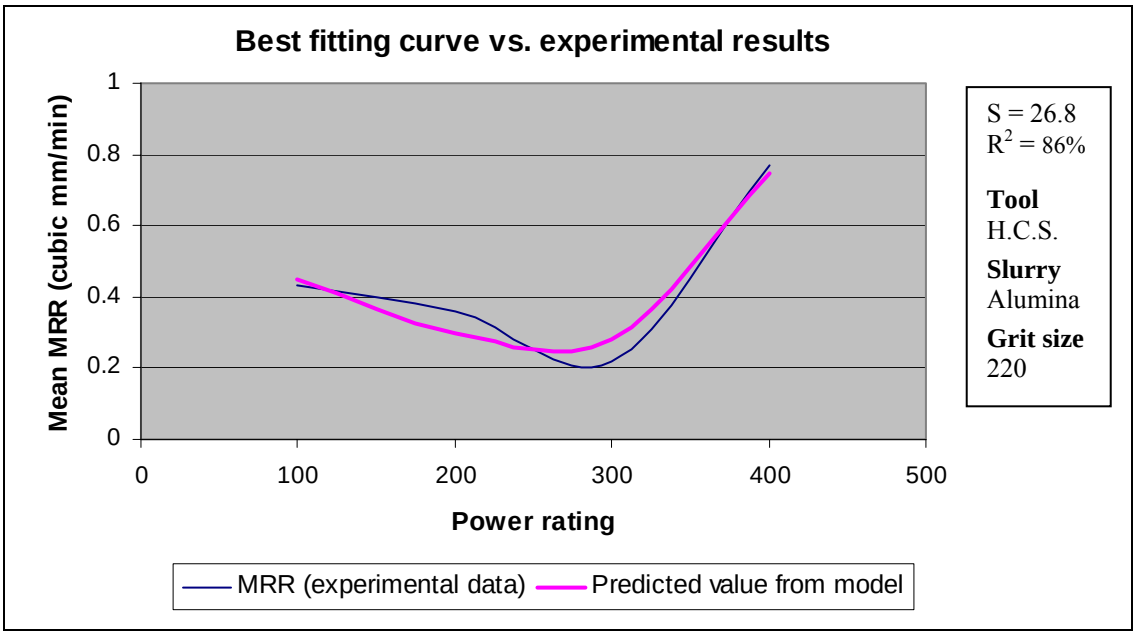

Figure 5.4 Best fitting curve for MRR (H.C.S. tool)

Case II (Titanium alloy tool, Alumina slurry, 220 Grit size)

The equation obtained through regression is:

$$Z = (82.75 - 0.4775\,P + 0.001225\,P^2).\,H/\mu_s^2$$

Where H= 1.15 GPa

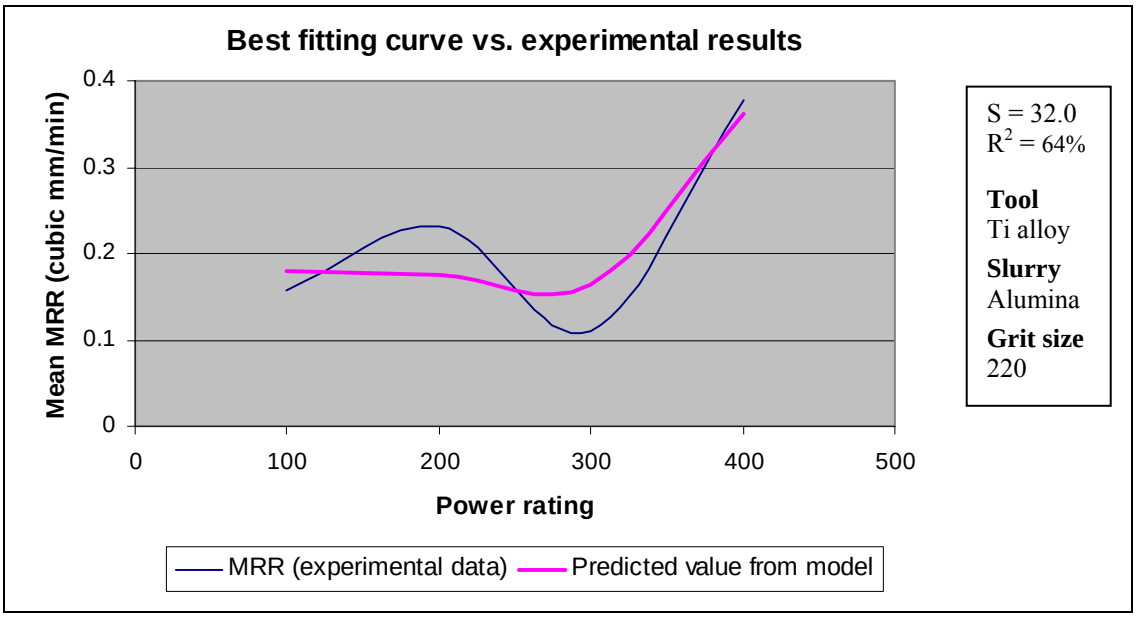

Figure 5.5 Best fitting curve for MRR (Ti alloy tool)

Case III (H.S.S. tool, Silicon carbide slurry, 220 Grit size)

The equation obtained through regression is:

$$Z = (190.0 - 1.094\ P + 0.004255\ P^2).H/\mu_s{}^2$$

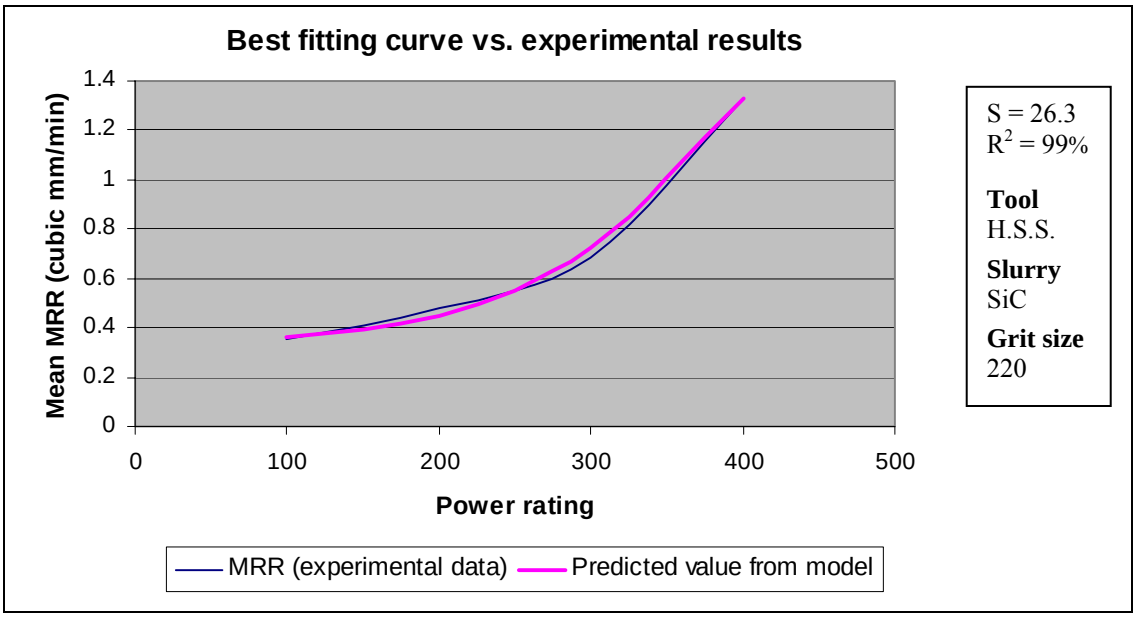

Figure 5.6 Best fitting curve for MRR (H.S.S. tool)

Case IV (Cemented carbide tool, Silicon carbide slurry, 220 Grit size)

The equation obtained through regression is:

$$Z = (30.82 - 0.1708\ P + 0.000517\ P^2).H/\mu_s^2$$

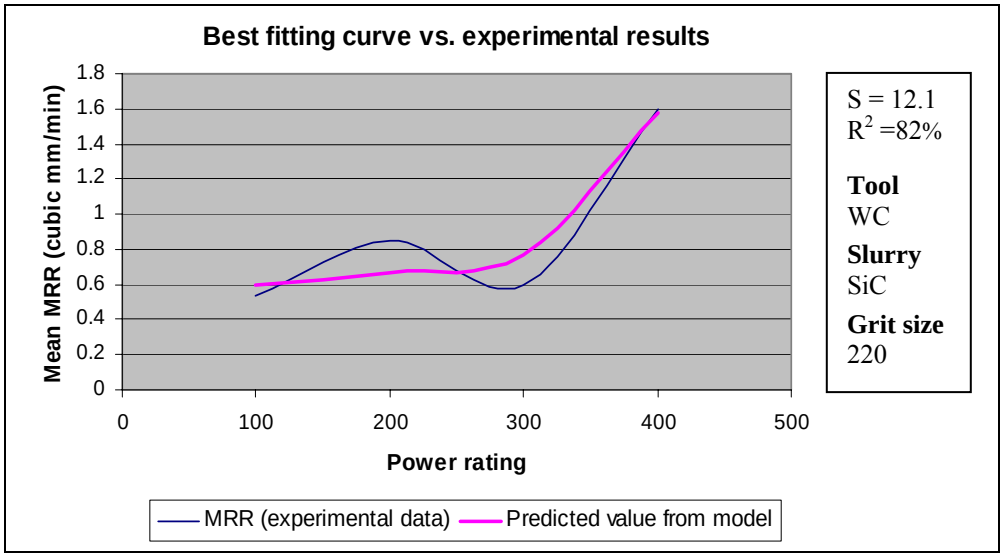

Figure 5.7 Best fitting curve for MRR (Carbide tool)

Case V (Titanium tool, Silicon carbide slurry, 220 Grit size)

The equation obtained through regression is:

$$Z = (46.7 + 0.529\ P + 0.000625\ P^2).H/\mu_s^2$$

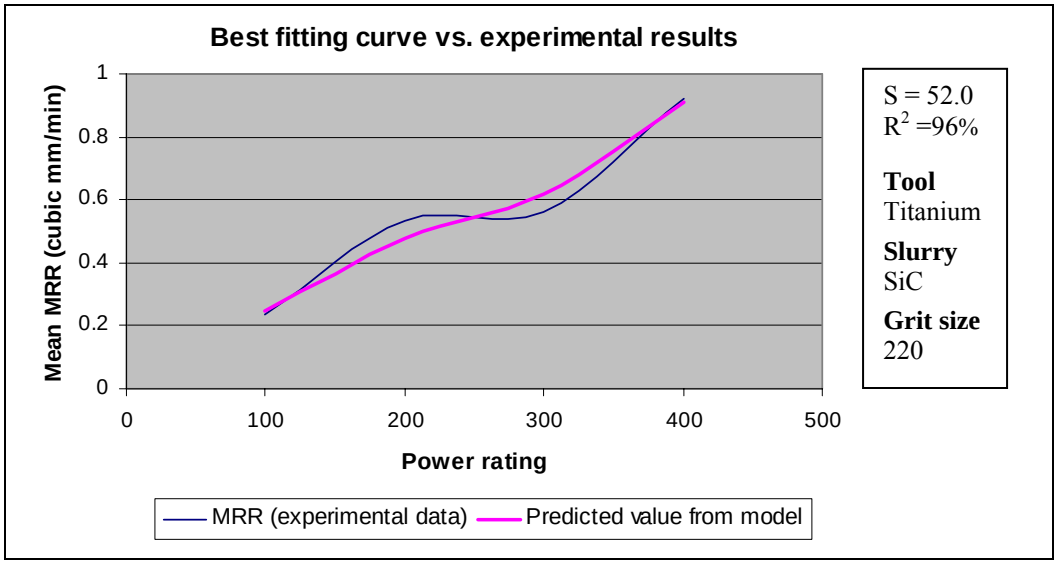

Figure 5.8 Best fitting curve for MRR (Titanium tool)

5.3.2 Micro-model for predicting TWR

TWR "v" depends upon four input parameters; ultrasonic power, elastic modulus of tool, slurry hardness factor and grit size of slurry. The slurry hardness factor indicates the knoop hardness of the slurry used. Again by selecting:

M (mass);

L (length);

T (time);

As basic dimensions, the dimensions of the foregoing quantities would then be:

1. The TWR "v" (mm^3/min) $L^3\ T^{-1}$
2. Power rating "P" (Watt) $M\ L^2\ T^{-3}$
3. Elastic modulus of tool "Y" (G Pa) $M\ L^{-1}\ T^{-2}$
4. Slurry hardness factor "μ_s" (G Pa) $M\ L^{-1}\ T^{-2}$
5. Slurry grit size "ρ" (mm) L

Now,

$$v = f(P,\ Y,\ \mu_s,\ \rho) \qquad (5.11)$$

In this case, n=5 and m=3, hence we can have (n-m=2) π_1, π_2 two dimensionless groups. Taking v and Y as the quantities which will go in π_1, π_2 respectively, we obtain:

$$\pi_1 = v\ (\mu_s)^{\alpha 1} (P)^{\beta 1} (\rho)^{\gamma 1} \qquad (5.12)$$

$$\pi_2 = Y(\mu_s)^{\alpha 2} (P)^{\beta 2} (\rho)^{\gamma 2} \qquad (5.13)$$

Substituting the dimensions of each quantity and equating to zero, the ultimate exponent of each basic dimension is achieved, since the "π_{is}" are dimensionless groups.

Solving for π_1 we get,

$$\pi_1 = L^3\ T^{-1}\ (M\ L^{-1}\ T^{-2})^{\alpha 1} (ML^2T^{-3})^{\beta 1} (L)^{\gamma 1} \qquad (5.14)$$

Here,

$$3-\alpha_1+2\beta_1+\gamma_1=0$$

$$-1-2\alpha_1-3\beta_1=0$$

$$\alpha_1+\beta_1=0$$

On solving,

$$\alpha_1=1,\ \beta_1=-1,\ \gamma_1=0$$

Putting the values obtained in equation (5.2) we get,

$$\pi_1 = v\,(\mu_s)(P)^{-1}(\rho)^0$$

$$\boldsymbol{\pi_1 = v\,\mu_s/P} \qquad (5.15)$$

Similarly, we get

$$\pi_2 = M\,L^{-1}\,T^{-2}\,(M\,L^{-1}\,T^{-2})^{\alpha 2}(ML^2T^{-3})^{\beta 2}(L)^{\gamma 2} \qquad (5.16)$$

$$1+\alpha_2+\beta_2=0$$

$$-1-\alpha_2+2\beta_2+\gamma_2=0$$

$$-2-2\,\alpha_2-3\beta_2=0$$

Solving we get,

$$\alpha_2=-1,\ \beta_2=0,\ \gamma_2=0$$

Thus,

$$\pi_2 = Y(\mu_s)^{-1}(P)^0(\rho)^0$$

$$\boldsymbol{\pi_2 = Y/\mu_s} \qquad (5.17)$$

The functional relationship is of the form,

$$\pi_1 = f(\pi_2) \qquad (5.18)$$

Hence,

$$v\,\mu_s/P = f(Y/\mu_s) \qquad (5.19)$$

It has been found experimentally that v directly goes with Y [71, 131].

Hence,

$$v.\mu_s/P = Y f(1/\mu_s)$$

$$\boldsymbol{v = C\,\{P.Y/\mu_s^2\}} \qquad (5.20)$$

Where *C* is a constant of proportionality.

To calculate "*C*", experiments were performed by:

1. Keeping P/μ_s^2 unchanged, varying *Y* (different tool materials) to estimate *v,* for assessment of the impact of elastic modulus of the tool on TWR.
2. Keeping Y/μ_s^2 unchanged, varying *P* (different power ratings) to estimate *v*, for assessment of the impact of power rating on TWR.

Impact of Tool Elastic Modulus on TWR

Case I (400 W Power rating, Alumina slurry, 220 Grit size)

To know the impact of *Y* on the tool wear rate, experiments were performed by "changing one factor at a time" approach thus with changing only the tool material and keeping all other factors constant. The experimental results have been detailed in Table 5.3. The data collected has been further used for finding the best fitting curve (figure 5.9).

Table 5.3 Effect of Elastic Modulus of the Tool on TWR

Abrasive Type	Tool Material	Elastic Modulus (GPa)	Mean TWR (mm^3/min.)
Alumina	High Carbon steel	195	0.93
	High speed steel	214	0.77
	Titanium	103	0.62
	Titanium alloy	114	0.38
	Cemented Carbide	650	1.16
Boron Carbide	High Carbon steel	195	1.64
	High speed steel	214	1.40
	Titanium	103	1.15
	Titanium alloy	114	0.80
	Cemented Carbide	650	2.05
Silicon Carbide	High Carbon steel	195	1.50
	High speed steel	214	1.30
	Titanium	103	0.95
	Titanium alloy	114	0.66
	Cemented Carbide	650	1.77

Power Rating = 400 W, Grit Size = 220

Thus the equation of TWR for this case is given as:-

$$v = (0.111 + 0.00741\ Y - 0.000016\ Y^2).P/\mu_s^2$$

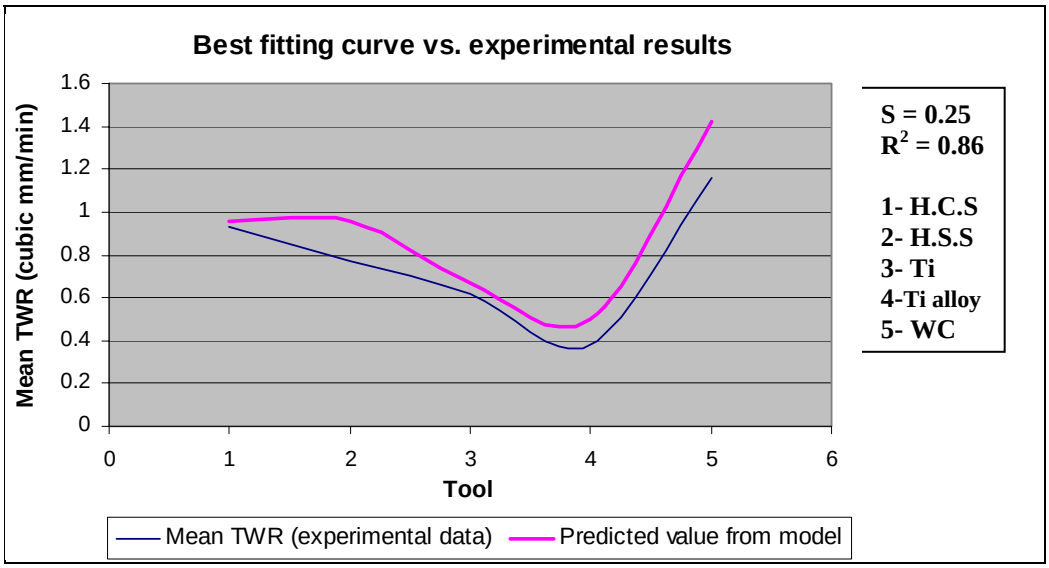

Figure 5.9 Best fitting curve for TWR (slurry: alumina/220)

Case II (400 W Power Rating, Silicon Carbide Slurry, 220 Grit Size)

The regression equation is,

$$v = (-0.408 + 0.0151\ Y - 0.000037\ Y^2).P/\mu_s^2$$

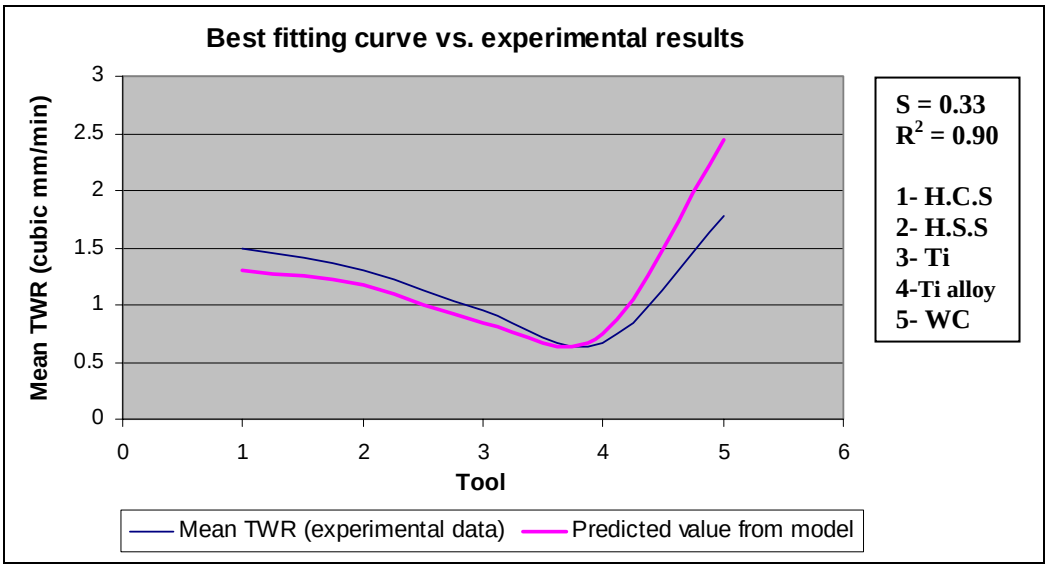

Figure 5.10 Best fitting curve for TWR (slurry: SiC/220)

Case III (400 W Power Rating, Boron Carbide Slurry, 220 Grit Size)

The regression equation is,

$$v = (-0.076 + 0.0131\ Y - 0.000030\ Y^2).P/\mu_s^2$$

The results predicted using the micro-model equations have been plotted in comparison with the experimental results obtained (figures 5.5 and 5.6).

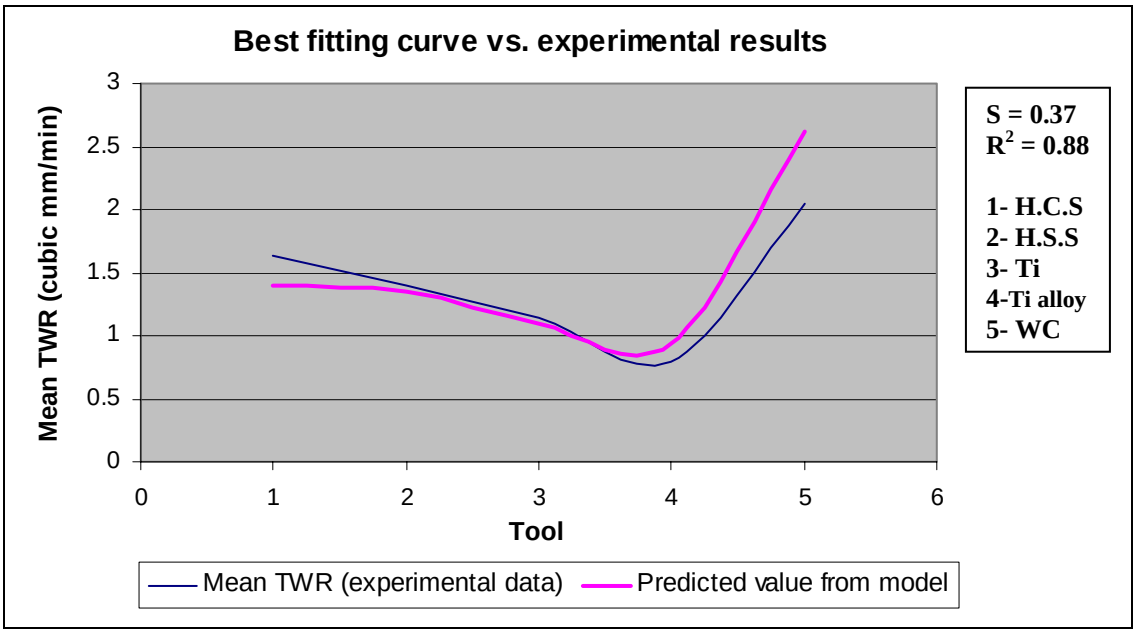

Figure 5.11 Best fitting curve for TWR (slurry: B_4C/220)

Impact of Power Rating on TWR

Case I (H.C.S. tool, Alumina slurry, 220 Grit size)

To know the impact of *P* on TWR, experiments were performed by "changing one factor at a time" approach thus with changing only the power rating and keeping all other factors constant. In the first case, experiments have been performed using high carbon steel tool with alumina as abrasive with a coarse grit size of 220 while the power rating was varied from 100 W to 400 W in four equal increments. The experimental data has been plotted along with the best fitting curve for TWR (figure 5.12). The regression equation is,

$$v = (1.930 - 0.01225\ P + 0.000028\ P^2).Y/\mu_s^2$$

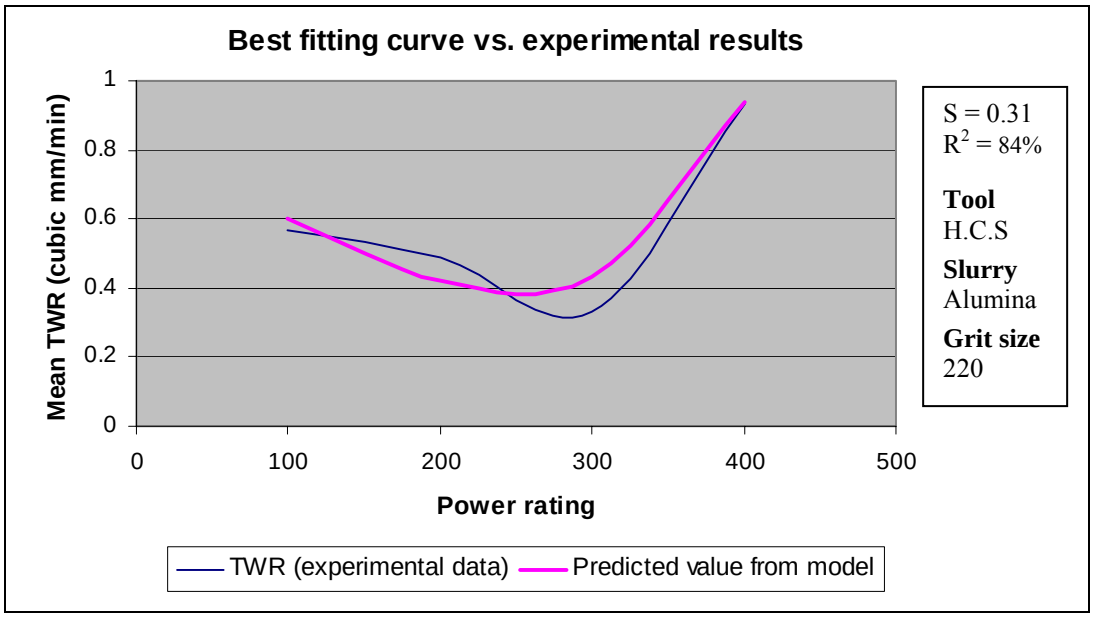

Figure 5.12 Best fitting curve for TWR (H.C.S. tool)

Case II (Titanium alloy tool, Alumina slurry, 220 Grit size)

The regression equation obtained is,

$$v = (0.965 - 0.06360\,P + 0.000016\,P^2).Y/\mu_s^2$$

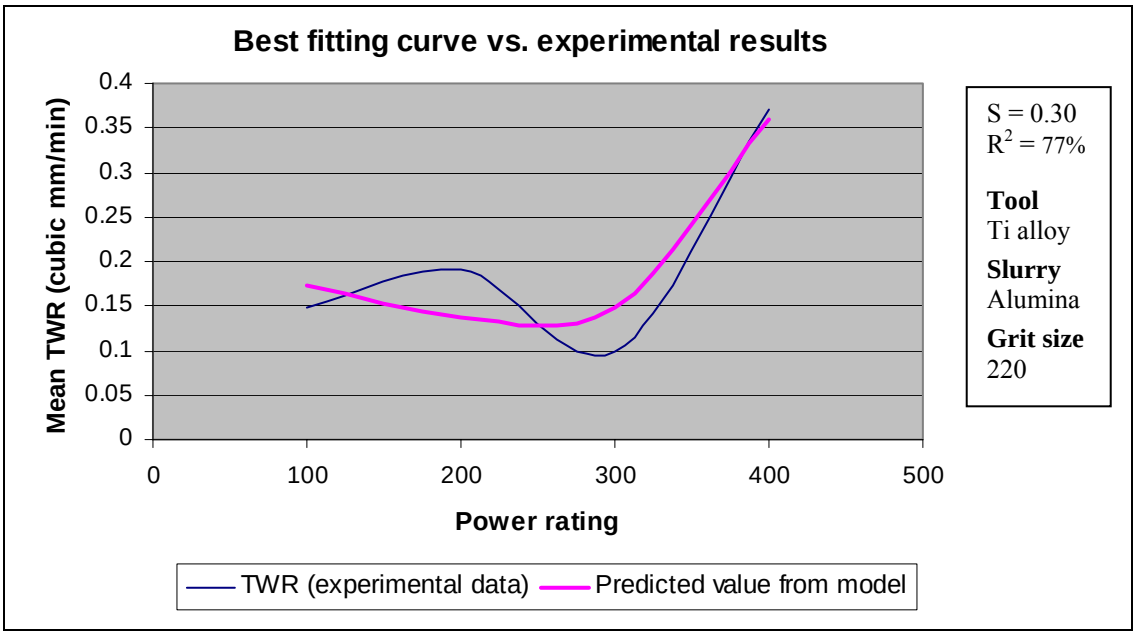

Figure 5.13 Best fitting curve for TWR (Ti alloy tool)

Case III (Titanium tool, Silicon carbide slurry, 220 Grit size)

The regression equation obtained is,

$$v = (0.502 + 0.00832P + 0.000011P^2).Y/\mu_s^2$$

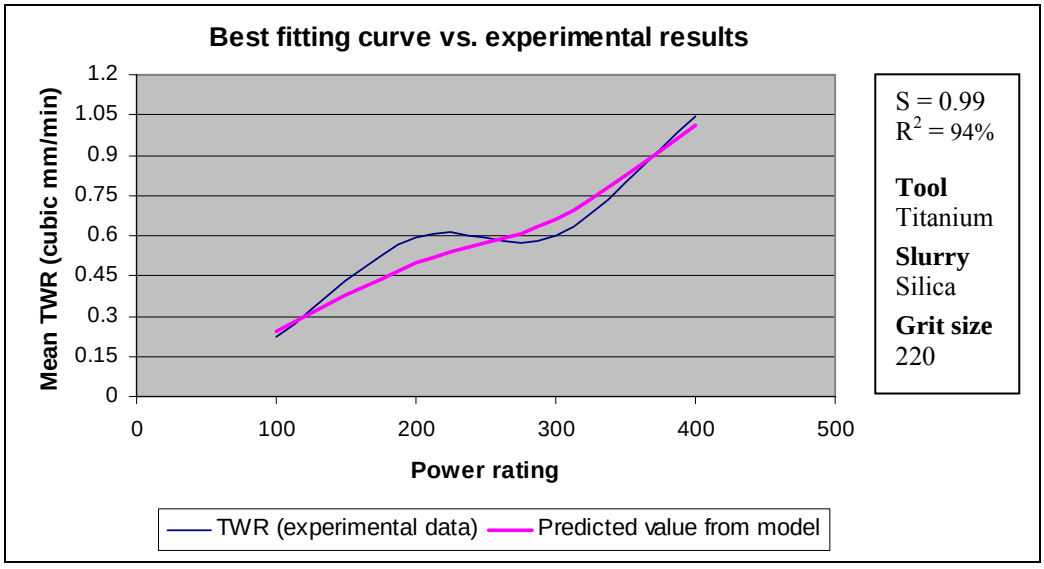

Figure 5.14 Best fitting curve for TWR (Titanium tool)

Case IV (H.S.S. tool, Silicon carbide slurry, 220 Grit size)

The regression equation obtained is,

$$v = (2.702 + 0.01116\ P + 0.000040\ P^2).Y/\mu_s^2$$

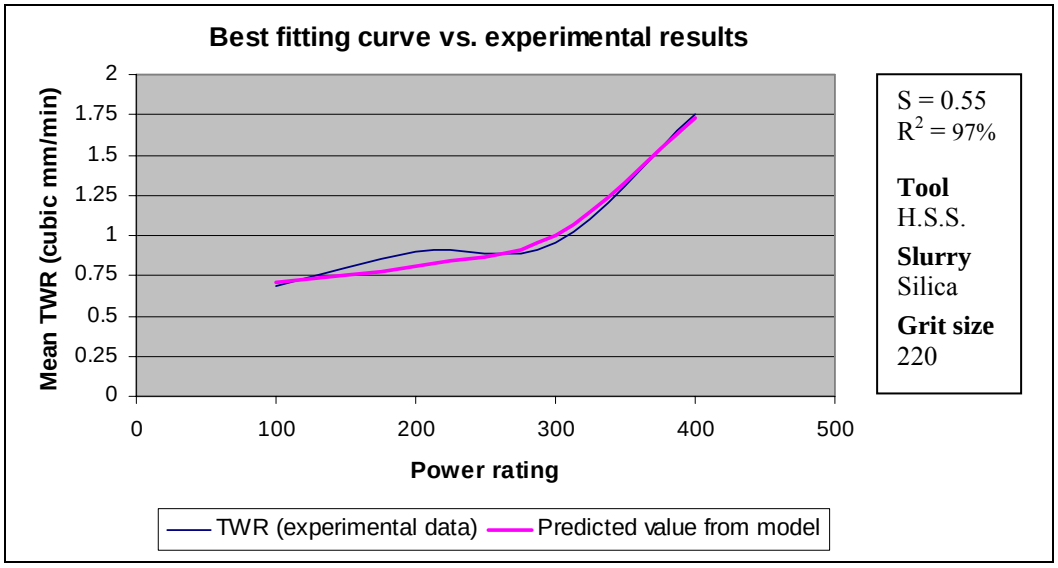

Figure 5.15 Best fitting curve for TWR (H.S.S. tool)

Case IV (Cemented carbide tool, Silicon carbide slurry, 220 Grit size)

The regression equation obtained is,

$$v = (1.212 - 0.00434\,P + 0.000016\,P^2).Y/\mu_s^2$$

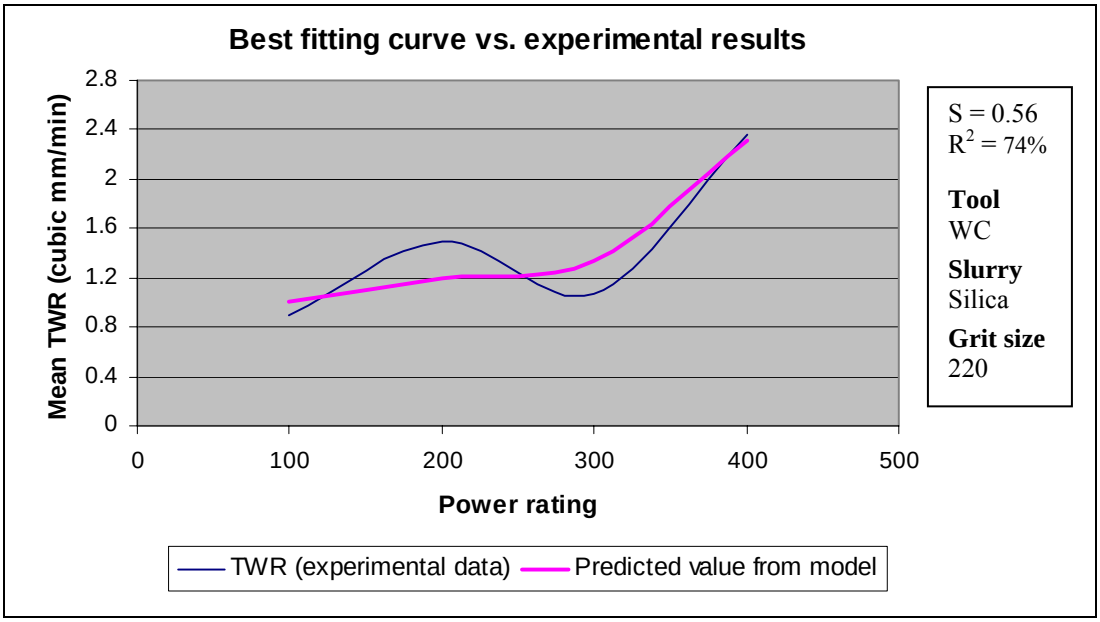

Figure 5.16 Best fitting curve for TWR (Carbide tool)

The results of macro-model based upon the concept of robust design, Taguchi analysis highlight that TWR is affected by power rating; elastic modulus of tool and slurry grit size and optimized results for the said case comes up with use of titanium alloy tool, at 100W of ultrasonic power and 500 grit size. Theses results from macro-model have been used for further development of the micro-model for prediction of TWR under varying conditions. The first three cases described here express TWR in ultrasonic machining of pure titanium at a specific power rating; for particular slurry type by varying elastic modulus of tool, i.e. by selecting different tool materials. The last five cases described here express TWR in ultrasonic machining of pure titanium using a specific tool material and abrasive slurry while varying the power rating of the ultrasonic machine. The same methodology can be further enhanced for developing mathematical model using optimum input parametric settings based upon macro-model.

CHAPTER 6
CONCLUSIONS AND SCOPE FOR FUTURE WORK

6.1 CONCLUSIONS

Based on the experiments conducted in the present investigation, the following conclusions have been drawn:

1. Ultrasonic power rating, type of abrasive used and slurry grit size significantly affect the MRR in ultrasonic machining of titanium. With regarding to the average response, power rating factor has emerged as most significant with a percent contribution of 42.4% (table 2) followed by abrasive type (21.3%) and slurry grit size (17.3%). Tool material factor can be termed as the least significant for MRR with a percent contribution of 13.7%. For S/N response, power rating has been found to be having highest percent contribution (23.8%), followed by abrasive type (21.7%) and tool material (14.2%). It has been concluded from the results that ***"input parameters settings of ultrasonic power rating at 400 W, with cemented carbide tool and boron carbide slurry with a coarse grit size of 220 have given the optimum results for MRR; when titanium (ASTM Grade-I) was machined***". This is in consistent with the conclusions from the study of other investigators.
2. Ultrasonic power rating, slurry grit size and tool material used significantly affect the tool wear rate (TWR) in USM of titanium. With regarding to the average response, power rating factor has emerged as most significant with a percent contribution of 36.3% (table 4.8) followed by tool material (19.6%) and slurry grit size (18.7%). Abrasive material factor can be termed as the least significant for MRR with a percent contribution of 17.4%. In other words, for average response, all the factors except power rating are almost equally significant. For S/N response, tool material has been found to be having highest percent contribution (31.0%). Power rating comes second (30.4%) whereas the other factors contribute almost equally towards the variation in TWR. Hence, it can be concluded from this discussion that ***"input parameters settings of ultrasonic power rating at 100***

W, with titanium alloy tool and alumina slurry with a fine grit size of 500 have given the optimum results for TWR; when titanium (ASTM Grade-I) was machined".

3. Slurry grit size and power rating of the ultrasonic machine have been identified as the significant factors as far as surface quality in USM of titanium is concerned. Other factors such as tool material and type of abrasive slurry used have been found to be relatively insignificant. Slurry grit size has emerged as the most significant factor with a percent contribution of the order of 41.5%, whereas power rating factor has been found to contribute 26.2% to the variation in surface roughness. It has been concluded that "***While machining titanium (ASTM Grade-I) with USM, input parameter settings of ultrasonic power rating at 100 W, with titanium alloy tool and alumina slurry with a fine grit size of 500 have given the optimum results for surface finish".***.
4. Multiple response optimization in USM of titanium has been obtained with the application of utility concept and it has been found that "***While machining titanium with USM, input parameter settings of ultrasonic power rating at 400 W, with titanium alloy tool and boron carbide slurry with a fine grit size of 500 have given the optimum results when MRR, TWR and surface roughness were considered simultaneously".*** Multi response optimization provides a single parametric setting that leads to optimum machining performance in terms of three different machining characteristics collectively.
5. The hardness of the machined surface has been found to be correlated with the MRR and surface quality obtained in USM of titanium. It has been found that the process settings that result in more MRR or better machining performance in terms of MRR also result in more work hardening of the machined surface, thereby promoting a large increment in the hardness of the work material after machining with USM. However, in certain cases, the work hardening has also been found to be more with extremely low MRR. This can be explained on the basis of relative toughness of work and tool and the larger amount of plastic

deformation that the work material undergoes at extremely small rates of machining.

6. The material removal has been found to be correlated with the parameter settings for a particular experimental condition. For process settings that result in a low level of energy input to the tool or abrasive, ductile type of fracture has been found to be predominant with cleavage occurring at a few localized places. The situations where a high level of energy input has been witnessed, the brittle fracture of work material has been found to dominate as the mode of material removal. However, it can be concluded that the work material undergoes a significant amount of plastic deformation before failing finally by propagation and intersection of the cracks. Hence, a mixed mode of material removal can be attributed to ultrasonic machining of titanium under controlled experiment conditions.
7. Pure titanium (ASTM Grade-I) exhibits fair machinability while machined with USM. There is no evidence of any surface damage in form of micro-cracking or heat affected zone. Moreover, the surface roughness of the machined surface has been found to be better than most of the other non-conventional machining processes such as electric discharge machining (EDM), laser beam machining (LBM) etc. The relative toughness of work and tool plays an important role in USM of titanium.
8. USM is a very random process. Even minor fluctuations in the parameters such as slurry concentration can affect the response to considerable extent. Hence, a large volume of the slurry must be used to minimize the effect of variations in the input parameters. Also, the tool may crack if slurry flow rate is inadequate.
9. The selection of tool materials and design of the tools are very critical from point of view of MRR and TWR in ultrasonic machining of titanium. Initial weight of the tool is another important factor. Tool weight should not exceed the maximum limit of 50 g for optimum performance in USM for the present set-up. Improper

design of the tools and excessive length leads to high temperature generation at the tool face and may also lead to fatigue failure.

10. The tool surface undergoes a change in shape with the progress in machining. The tendency of dish formation in the centre of the tool face has been found to be more prevalent in High carbon steel and pure titanium tools as compared to other tougher materials such as high speed steel and titanium alloy. It is necessary to restore the shape of the tool before performing another experiment.

6.2 LIMITATIONS

1. The results are valid within the specified range of the process parameters. In the present investigation, 500 W piezoelectric transducer based USM apparatus was used. The depth of cut was limited as excessive length of tool was adding to the tool weight and tool weight more than 50 gm was resulting in overloading of the machine. Hence the results are limited in present form to machine comparatively small sized workpiece.
2. The use of solid tool leads to the problem of ineffective flushing of slurry particles from the machining zone after a certain depth of cut. Because of this reason, the depth of cut was fixed to a low value of 02 mm in the present work. Also the fabrication of hollow tool was a constraint, especially for cemented carbide tool.
3. Some important process parameters such as amplitude of vibration, frequency of vibration, static load could not be included into the present work because of the machine setup limitations.

6.3 SCOPE FOR FUTURE WORK

1. In the present investigation, only four process parameters viz. tool material, abrasive type, slurry grit size and power rating were included as input factors. Study of other process parameters such as amplitude of vibration, tool geometry, mass flow rate of slurry, temperature of the slurry, static load and type of horn can be included.
2. Further study can be focused on rotary USM or hybrid USM-EDM processes that involve 5-6 times superior efficiency in terms of MRR as compared to static USM used for the present investigation. Also, the flow of slurry can be magnetized while machining with static USM on titanium and its alloys.
3. Although effect of power rating on the machining performance of USM has been investigated in this study, it can be further investigated with different work-tool combinations on high power ultrasonic machines.
4. The study can be extended to other grades of titanium, titanium alloys and other tougher and harder materials such as nickel alloys, polycrystalline diamond compact etc for their commercial application in the manufacturing industry.

REFERENCES

1 Adithan M; (1981), "Tool wear characteristics in ultrasonic drilling", *Tribology International,* **Vol. 14, No. 6**, pp. 351-356.

2 Adithan M. and Krishnamurthy R. (1978), "Structural alterations in the workpiece by ultrasonic drilling", *Wear*, **Vol. 46**, pp. 327-334.

3 Adithan M. and V.C. Venkatesh (1978), "An appraisal of wear mechanisms in ultrasonic drilling", *Annals of the CIRP*, **Vol. 27,** pp. 119-124.

4 Adithan M. and Venkatesh, V.C., (1976), "Production accuracy of holes in ultrasonic drilling", *Wear*, **Vol. 40, No.3**, pp. 309-318.

5 Adithan M. and Venkatesh, V.C., (1975), "Study of performance characteristics of an ultrasonic drilling head", *Wear*, **Vol. 33,** pp. 261-270.

6 Adithan M. and Venkatesh V.C., (1974), "Parametric influence on tool wear in ultrasonic drilling", *Tribology International*, **Vol. 7, No. 6,** pp. 260-264.

7 Almeida I.A., Rossi de W, Lima M.S.F., Berretta J.R., Wetter N.U., Vieira N.D. (2006), "Optimization of titanium cutting by factorial analysis of the pulsed Nd: YAG laser parameters", *Journal of Materials Processing Technology*, **Vol. 179**, pp. 105-110.

8 Amin A.K.M.; Ismail F.A. and Khairushima M.K. (2007), "Effectiveness of uncoated WC-Co and PCD inserts in end milling of titanium alloy-Ti-6Al-4V", *Journal of Materials Processing Technology*, **Vol. 192-193**, pp. 147-158.

9 Amin S.G.; Ahmed M.H. and Youssef H.A. (1993), "Optimum design charts of acoustic horns for ultrasonic machining", *Proc. Int. Conf. on Advances in Materials Processing Technologies*, pp. 139-147

10 Anantha Ramu B.L. and Krishnamurthy R. (1989), "Machining performance of toughened zirconia ceramic and cold compact alumina ceramic in ultrasonic drilling", *Journal of Mechanical Working Technology*, **Vol.20**, pp. 365-375.

11 Aspinwall D.K. and Kasuga V. (2001), "The use of ultrasonic machining for the production of holes in Y-TIAL", *Proceedings of the 13th International Symposium for Electro machining ISEM XIII*, **Vol. 2**, Spain, pp. 925-937.

12 ASM Int. (1988), "Titanium: A Technical Guide", ASM International, Materials Park, OH, pp. 75-85.

13 Astakhov V.P. (2004), "An application of random balance method in conjunction with Plackett-Burman screening tests in metal cutting", *Journal of Testing and Evaluation*, **Vol. 32, No. 1**, pp. 32-39.

14 Babitsky V.I., Mitrofanov A.V., Silverschmidt V.V. (2004), "Ultrasonically assisted turning of aviation materials: simulations and experimental study", *Ultrasonics*, **Vol. 42**, pp.81-86.

15 Bagchi T.P. (1993), "Taguchi methods explained: Practical steps to robust design" Prentice Hall of India Private Ltd., ISBN-0-87692-80804, pp. 11-19.

16 Balamuth L. (1964), "Ultrasonic vibrations assisted cutting tools", *Metalworking Prod*, **Vol. 108, No. 24**, pp. 75-77.

17 Balamuth L.A. (1966), "Ultrasonic assistance to conventional metal removal", *Ultrasonics*, **Vol. 4**, pp. 125-130.

18 Barash M.M. and Watanapongse D. (1970), "On the effect of ambient pressure on the rate of material removal in ultrasonic machining", *International Journal of Mechanical Sciences*, **Vol. 12,** pp.775-779.

19 Barker T.B. (1990), "Engineering Quality by Design: Interpreting the Taguchi approach", New York, Marcel-Dekker, Inc., pp. 78-82.

20 Benedict Gary F. (1987), "Non traditional manufacturing processes", Marcel Dekker, Inc., pp. 67-86.

21 Bhattacharya A. (1973), "New Technology", The institution of Engineers (I), Calcutta, pp. 12-17.

22 Bulat T.J. (1974), "Micro-Sonics in industry, Ultrasonic cleaning", Bendix and Life Supports Division Publication, 120.10.153, U.S.A., pp. 13.

23 Buckingham E. (1915), "Model experiments and the form of empirical equations", *Trans. ASME*, **Vol. 37,** pp. 263-296.

24 Byrne D.M. and Taguchi S. (1987), "The Taguchi approach to parameter design", *Quality Progress*, **Vol. 20**, pp. 19-26.

25 Chang S. and Bone G.M. (2005), "Burr size reduction in drilling by ultrasonic assistance", *Robotics and Computer-Integrated manufacturing*, **Vol**. **21**, pp. 442-450.

26 Che-Haron C.H. and Jawaid A. (2005), "The effect of machining on surface integrity of titanium alloy Ti-6% Al-4% V", *Journal of Materials Processing Technology*, **Vol. 166**, pp. 188-192.

27 Choi J.P. (2007), "Chemical-assisted ultrasonic machining of glass", *Journal of Materials Processing Technology*, **Vol. 191**, pp. 153-156.

28 Cook N.H. (1966), "Manufacturing analysis", Addison-Wesley, New York, pp. 133-148.

29 Dam H. and. Jensen J. (1993), "Surface characterization of ultrasonic machined ceramics with diamond impregnated sonotrode", *Machining of Advanced Materials*, **Vol. 34**, pp. 125-133.

30 Dam H.; Quist P. and Schreiber M. (1995), "Productivity, surface quality and tolerances in ultrasonic machining of ceramics", *Journal of Materials Processing Technology*, V**ol. 51, No. 1-4**, pp. 358-368.

31 Deng Jianxin and Lee Taichu (2000), "Surface integrity in electro-discharge machining, ultrasonic machining and diamond saw cutting of ceramic composites", *Ceramic International*, **Vol. 26, No. 8**, pp. 825-830.

32 Derek W.B. (1982), "Analysis for optimum decisions", Wiley International, New York, pp. 38-45.

33 Dornfeld D.A., Kim J.S., Dechow H., Hewson J., Chen L.J. (1999) "Drilling burr formation in titanium alloy Ti-6Al-4V", *Annals of CIRP*. **Vol. 48**, pp. 73-76.

34 Dvivedi A. and Kumar P. (2007), "Surface quality evaluation in ultrasonic drilling through the Taguchi technique", *International Journal of Advanced Manufacturing Technology*, **Vol. 34, No. 1-2,** pp. 131-140.

35 Elsayed E.A. and Chen A. (1993), "Optimal levels of process parameters for products with multiple characteristics", *International Journal of Production Research*, **Vol. 31**, pp. 1117-1132.

36 Ezugwu E.O. and Wang Z.M. (1997), "Titanium alloys and their machinability – a review", *Journal of Materials Processing Technology,* **Vol. 68, No. 1-4**, pp. 262-274.

37 Farago F.T. (1980), "Abrasives methods engineering", *Industrial Press*, **Vol. 2**, pp. 480-481.

38 Farzin- Nia F. and Sterrett T. (1990), "Effect of machining on fracture toughness of corundum", *Journal of Materials Science*, **Vol. 25, No. 5**, pp 2527-2531.

39 Frederick J.R. (1965), "Ultrasonic engineering", John Wiley and Sons Inc., New York, ISBN 0471277258.

40 Ghabrial S.R. (1986), "Trends towards improving the surfaces produced by modern processes", Proc. 3rd International Conference on Metrology, pp. 113-118.

41 Ghabrial S.R., Saleh S.M., Kohail A., Moison A. (1982), "Problems associated with electro-discharge machined, electro-chemically machined and ultrasonically machined surfaces", *Wea*r, **Vol. 83**, pp. 275-283.

42 Ghahramani B. and Wang Z.Y. (2001), "Precision ultrasonic machining process: A case study of stress analysis of ceramic (Al/2O//3)", *International Journal of Machine Tools and Manufacture*, V**ol. 41, No. 8**, pp 1189-1208.

43 Ghosh Amitabha and Mallik A.K. (1996), "Manufacturing Science", East-West Press Private Ltd., India, pp. 335-353.

44 Gilmore R. (1991), "Ultrasonic machining – a case study", *Journal of Materials Processing Technology,* **Vol. 28, No. 1-2**, pp 139-148.

45 Gilmore R. (1989), "Ultrasonic machining and orbital abrasion techniques", *SME Technical Paper (series) AIR*, **NM89-419**, 1989, pp. 1-20.

46 Ginting A. and Nouari M. (2007), "Optimal cutting conditions when dry end milling the aero engine material Ti-6242S", *Journal of Materials Processing Technology*, **Vol. 184**, pp. 319-324.

47 Goetze D. (1956), "Effect of vibration amplitude, Frequency, and composition of the abrasive slurry on the rate of ultrasonic machining in Ketos Tool Steel", *Journal of Acoustical Society of America*, **Vol. 28**, **No. 6**, pp. 1033-1045.

48 Graff K.F. (1975), "Macrosonics in Industry: ultrasonic machining", *Ultrasonics*, **Vol. 13**, pp. 103-109.

49 Gupta, V. and Murthy, P.N. (1980), "An Introduction to Engineering Design Method", Tata McGraw-Hill, N.D, pp. 76-82.

50 Guzzo P.L. and Shinohara A.H. (2004), "A comparative study on ultrasonic machining of hard and brittle materials", *Journal of Brazilian Society of Mechanical Sciences and Engineering,* **Vol. 26, No. 1**, pp. 56-64.

51 Guzzo P.L., Raslan A.A., Mello De J.D.B. (2003), "Ultrasonic abrasion of Quartz Crystals", *Wear,* **Vol. 255**, pp. 67-77.

52 Halm R. and Schulz P. (1993), "Ultrasonic machining of complex ceramic components", Erosion AC Report, DKG 70, No. 7, pp. 6.

53 Hartung P.D. and Kramer B.M. (1982), "Tool wear in titanium machining", *Annals of CIRP*, **Vol. 31**, p 75.

54 Haun R. and Schulz P. (1994), "New ultrasonic machining route to create complex ceramic components", *Proc. IEEE Ultrasonic Symposium*, NJ, USA, **Vol. 3**, pp. 1389-1392.

55 Hicks R. and Turner V.K. (1999), "Fundamental concepts in the design of experiments", Oxford University Press, Fifth edition, pp. 134-139.

56 Hocheng H. and Kuo K.L. (2002), "On-line tool wear monitoring during ultrasonic machining using tool resonance frequency", *Journal of Materials Processing Technology*, **Vol. 123, No. 1**, pp 80-84.

57 Hocheng H. and Tai N.H. (2000), "Assessment of ultrasonic drilling of C/SiC composite material", *Composites*, Part-A, **Vol. 31**, pp. 133-142.

58 Hocheng H.; Kuo K.L. and Lin J.T. (1999), "Machinability of zirconia ceramics in ultrasonic drilling", *Materials and Manufacturing Processes,* **Vol. 14**, **No. 5**, pp. 713-724.

59 Hocheng H. and Hsu C.C. (1995), "Preliminary study of ultrasonic drilling of Fiber-Reinforced Plastics", *Journal of Materials Processing Technology*, **Vol. 48**, pp.255-266.

60 Hu P., Zhang J.M., Pei Z.J., Treadwell C. (2002), "Modeling of material removal rate in rotary ultrasonic machining: designed experiments", *Journal of Materials Processing Technology*, **Vol. 129**, pp. 339-344.

61 Hong SY; Markus I. and Jeong, W. (2001), "New cooling approach and tool life improvement in cryogenic machining of titanium alloy Ti-6Al-4V", *Int. Journal of Machine Tools Manufacture*, **Vol. 41**, pp. 2245–2260

62 Ishikawa K., Suwabe H., Nishide T., Uneda M. (1998), "A study on combined vibration drilling by ultrasonic and low-frequency vibrations for hard and brittle materials", *Precision Engineering,* **Vol. 22**, pp. 197-206.

63 Jadoun R.S., Kumar Pradeep, Mishra B.K., Mehta R.C.S. (2006), "Manufacturing process optimization for tool wear rate in ultrasonic drilling of engineering ceramics using the Taguchi method", *International Journal of Machining and Machinability of Materials*, **Vol. 1**, **No. 3-4**, pp. 94-114.

64 Jain N.K. and Jain V.K. (2001), "Modeling of material removal in mechanical type of advanced machining processes-a state of the art review", *International Journal of Machine Tools and Manufacture*, **Vol. 41**, pp. 1573-1635.

65 Jain V.K. (2004), "Advanced Machining Processes*"*, Allied Publishers, pp. 21-28.

66 Jianxin Deng and Taichiu Lee (2002), "Ultrasonic machining of alumina based ceramic composites", *Journal of the European Ceramic Society*, **Vol. 22, No. 8**, pp 1235-1241.

67 Kai E. and Takahira M. (1999), "Micro ultrasonic machining by application of work-piece vibration", *CIRP Annals*, **Vol. 48, No. 1**, pp. 131-134.

68 Kainth (1979), "On the mechanisms of material removal in ultrasonic machining", *International Journal of Machine Tool Design*, **Vol. 19**, pp. 33-41.

69 Kaczmarek I. (1976), "Principles of machining by cutting, abrasion and erosion", Peter Peregrinus Ltd., Stevenage, ISBN 0901223662, pp. 448-462.

70 Kazantsev V.F. (1966), "Improving the output and accuracy of ultrasonic machining", *Machines and Tooling*, **Vol. 37, No. 4**, pp. 33-39.

71 Kazantsev V.F. (1963), "The relationship between output and machining conditions

in ultrasonic machining", *Machines and Tooling*, **Vol. 34**, pp. 14-17.

72 Kohals J.B. (1984), "Ultrasonic manufacturing process-ultrasonic machining and ultrasonic impact grinding (USIG)", *The carbide and Tool J*., **Vol. 16, No. 5**, pp. 12-15.

73 Kennedy D.C. and Grieve R.J. (1975), "Ultrasonic machining-A review", *The Production Engineer*, **Vol. 54, No. 9**, pp. 481-486.

74 Kennedy W.J. and Skaar C. (1989), "Improving the machining of ceramics", SME Technical Paper, Orlando, USA, pp. 6-9.

75 Khairy A.B.E. (1990), "Assessment of some dynamic parameters for the ultrasonic machining process", *Wear*, **Vol. 137, No. 2**, pp 187-198.

76 Komaraiah M. and Reddy, P.N. (1993), "A study on the influence of work piece properties in ultrasonic machining", *International Journal of Machine tools and Manufacture*, **Vol. 33**, pp 495-505.

77 Komariah M. and Reddy P.N. (1993), "Relative performance of tool materials in ultrasonic machining", *Wear*, **Vol. 161, No. 1-2**, pp. 1-10.

78 Komaraiah M., Manan M.A., Reddy P.N., Victor S. (1988), "Investigation of surface roughness and accuracy in ultrasonic machining", *Precision Engineering*, **Vol. 10, No. 2**, pp. 59-68.

79 Koops L. (1964), "Investigation into the influence of the wear of abrasive powder on the technological indices of ultrasonic machining", *Annals of the CIRP*, **Vol. 13**, **No. 3**, pp. 151-157.

80 Koval Chenko M.S.; Paustovskii A.V. and Perevyazko V. A. (1986), "Influence of properties of abrasive materials on the effectiveness of ultrasonic machining of ceramics, *Powder Metallurgy and Metal Ceramics,* **Vol. 25**, pp. 560-562.

81 Kremer, D. (1991), "New developments in ultrasonic machining", SME Technical Paper, **MR91-522**, pp. 13.

82 Kremer D. and Mackie J. (1988), "Ultrasonic machining applied to ceramic materials", *Industrial Ceramics*, **Vol. 8**, **No. 3**, pp. 632-637.

83 Kremer D; Bazine G. and Moison A. (1983), "Ultrasonic machining improves

EDM technology, Electro machining", *Proc. 7th Int. Symp*., Birmingham, UK, pp. 67-76.

84 Kremer D. (1981), "The state of the Art of Ultrasonic Machining", *Annals of the CIRP,* **Vol. 30**, pp. 107-115.

85 Kubota M.; Tamura Y. and Shimamura N. (1977), "Ultrasonic machining with a diamond impregnated tool', *Bulletin of Japanese Society of Free. Engineering*, **Vol. 11, No. 3,** pp. 127-132.

86 Kumar J., Khamba J.S. and Mohapatra, S.K. (2008), "An Investigation into the machining characteristics of titanium using ultrasonic machining", *Int. J. Machining and Machinabaility of Materials*, **Vol. 3, No. 1-2**, pp. 143-161.

87 Kumar J., Khamba J.S. and Mohapatra S.K. (2008), "An experimental investigation of the influence of work material properties on performance indices of ultrasonic machining", *Journal of Manufacturing Technology Today*, **Vol. 7, No. 3**, pp.

88 Kumar J.; Khamba J.S. and Mohapatra S.K. (2007) "Investigating tool wear rate and surface quality in ultrasonic machining of titanium", *Proceedings of International Conference on Advanced Manufacturing Technologies*, CMERI, Durgapur, India, 29-30 Nov., 2007, pp. 181-190.

89 Kumehara H. (1984), "Characteristics of threaded joints in ultrasonic vibrating system", *Bulletin of JSME*, **Vol. 27, No. 223**, pp. 117-123.

90 Kuriakose S. and Shunmugam M.S. (2004), "Characteristics of Wire-electro discharge machined Ti-6Al-4V surface", *Materials Letters*, **Vol. 58**, pp. 2231-2237.

91 Laroiya S.C. and Adithan M. (1993), "Tool Wear in machining of advanced ceramics", *Xth National Conference on Industrial Tribology*, March 1993, conducted at Indian institute of Petroleum, pp 164-169.

92 Lau W.S., Yue T.M., Wang M. (1994), "Ultrasonic-aided laser drilling of aluminium based metal matrix composites", *Annals of the CIRP*, **Vol. 43**, pp. 177-182.

93 Legge P. (1966), "Machining without abrasive slurry", *Ultrasonics*, **Vol. 4,** pp 157-162.

94 Lee T.C.; Zhang J.H. and Lau W.S. (1998), "Machining of engineering ceramics by ultrasonic vibration assisted EDM method", *Materials and Manufacturing Processes*, **Vol. 13, No.1**, pp 133-146.

95 Lee T.C. and Chan C.W. (1997), "Mechanism of the ultrasonic machining of ceramic composites", *Journal of Materials Processing Technology*, **Vol. 71**, pp. 195-201.

96 Li Z.C., Jiaoa Y., Deinesa T.W., Pei Z.J. (2005), "Rotary ultrasonic machining of ceramics matrix composites: feasibility study and designed experiments", *International Journal of Machine Tools and Manufacture,* **Vol**. **45, No. 12-13**, pp. 1402-1411.

97 Lin Y.C., Yan B.H., Chang Y.S. (2000), "Machining characteristics of titanium alloy (Ti-6Al-4V) using a combination process of EDM with USM," *Journal of Materials Processing Technology*, **Vol. 104**, pp 171-177.

98 Majeed M.A., Vijayaraghvan L., Malhotra S.K., KrishnaMurthy R. (2008), "Ultrasonic Machining of Al_2O_3/$LaPO_4$ Composites", *International Journal of Machine Tools & Manufacture*, **Vol. 48**, pp. 40-46.

99 Markov A.I. (1977), "Ultrasonic drilling and milling of hard non-metallic materials with diamond tools", *Machines and Tooling*, **Vol. 48, No. 9**, pp. 45-47.

100 Markov A.I. (1959), "Kinematics of the dimensional ultrasonic machining method", *Machines and Tooling*, **Vol. 30, No. 10**, pp. 28-31.

101 McGeough J.A. (1988), "Advanced methods of machining", Chapman and Hall, London, ISBN 0412319705, pp. 170-198.

102 Merkulov L.G. (1957), "Design of ultrasonic concentrations", *Akusticheskiy Zhurnal*, **Vol. 3**, pp. 246-255.

103 Miller G.E. (1957), "Special theory of ultrasonic machining", *Journal of Applied Physics*, **Vol. 28, No. 2**, pp. 149-156.

104 Mishra P.K. (2005), "Non Conventional machining", Narosa Publishing House, N.D., ISBN 81-7319-192-1, pp. 22-44.

105 Moore D. (1985), "Ultrasonic impact grinding", *Proc. Non-Traditional machining*

Conference, Cinicinnati, pp. 137-139.

106 Moreland M.A. (1988), "Ultrasonic advantage revealed in the hole story", *Cer. Applied Manufacturing,* **Vol. 187**, pp. 156-162.

107 Moreland M.A. (1988), "Versatile performance of ultrasonic machining", *Ceramic Bulletin*, **Vol. 67, No.6**, pp. 1045-1047.

108 Moreland M.A. (1984), "Ultrasonic impact grinding: What it is: What it will do", *Proceedings of 22nd Abrasive Engineering Conference: Abrasives and Hi-Technology*, pp.11–117.

109 Murakawa Masao and Jin Masahiko (1998), "Turning of beta-titanium alloys by means of ultrasonic vibration", Proc. 1998 XXXVI NAMRC Conference, Atlanta, U.S.A., pp. 31-40.

110 Nair E.V. and Ghosh A. (1985), "A fundamental approach to the study of mechanics of ultrasonic machining", *Int. Journal of Prod. Research*, **Vol. 23**, pp. 731-753.

111 Neppiars E.A. (1972), "Macrosonics in industry", *Ultrasonics*, **Vol. 10**, pp. 9-13.

112 Neppiars E.A. (1964), "Ultrasonic machining and forming", *Ultrasonics*, **Vol. 2**, pp. 167-173.

113 Neppiars E.A. (1957), "Ultrasonic Machining-II. Operating conditions and performance of ultrasonic drills", *Philips Technology Review*, **Vol. 18, No. 12**, pp. 368-379.

114 Nishimura G. (1954), "Ultrasonic machining-Part I", *Journal of Fracture Engineering,* Tokyo Univ., **Vol. 24, No. 3**, pp. 65-100.

115 Pandey P.C. and Shan H.S. (1980), "Modern Machining Processes", Tata McGraw-Hill, N.D., pp. 7-38.

116 Pei Z.J. and Ferreira P.M. (1998), "Modeling of ductile mode material removal in rotary ultrasonic machining", *International Journal of Machine Tools and Manufacture,* **Vol. 38, No. 10-11**, pp 1399-1418.

117 Pei Z.J., Ferreira P.M., Haselkorn M. (1995), "Plastic flow in ultrasonic machining of ceramics", *J. Materials Processing Technology,* **Vol. 48, No**. **1-4**, pp 771-777.

118 Pei Z.J.; Khanna N. and Ferreira P.M. (1995), "Rotary ultrasonic machining of structural ceramics- a review", *Ceramic Engineering and Science Proceedings*, **Vol. 16, No. 1**, pp 259-278.

119 Pentland E.W. and Ektermanis J.A., (1965), "Improving ultrasonic machining rates-some feasibility studies", *Journal of Engineering For Industry*, Trans. of the ASME, **Vol. 87**, pp. 39-46.

120 Perkins J. (1972), "An outline of power electronics", *Technical report on ultrasonics*, pp. 7

121 Phadke M.S. (1989), "Quality Engineering using robust design", AT & T Bell Laboratories, PTR Prentice-Hall Inc., U.S.A., pp. 231-249.

122 Phadke M.S. (1986), "Design Optimization case study", *AT & T Technical Journal*, **Vol. 65, No. 2**, pp51-68.

123 Prabhakar D. and Haselkorn M. (1992), "An experimental investigation of material removal rates in rotary ultrasonic machining", *Transactions of NAMRI/SME*, **Vol. 20**, pp. 211-218.

124 Rajurkar K.P. and Wang Z.Y (1999)," Micro removal of ceramic material in the precision ultrasonic machining", *Precision Engineering*, **Vol. 23, No.2**, pp 73-78.

125 Ramulu M. (2005), "Ultrasonic machining effects on the surface finish and strength of silicon carbide ceramics", *International Journal of Manufacturing Technology Management*, **Vol. 7, No. 2/3/4,** pp. 107-125.

126 Reddy P.B.S., Nishina K., Subash Babu A. (1985), "Unification of robust design and goal programming for multi-response optimization: a case study", *Quality Reliability Engineering International*, **Vol. 13**, pp. 371-383.

127 Richardson D.W. and Robare M.W. (1978), "Turbine component machining development", Proc. Conference on Ceramic Machining and Surface Finishing, Naval Research Lab, Gaithersburg, Md., pp. 278-289.

128 Riddie V. (1973), "Cavitation erosion- a survey of the literature 1940-1970", *Wea*r, **Vol. 23**, pp. 133-137.

129 Ross P.J. (1988), "Taguchi Technique for Quality Engineering", McGraw-Hill

Book Company, New York, pp. 45-48.

130 Rozenberg L.D. (1973), “Physical principles of ultrasonic technology”, **Vol. 1-2**, Plenum Press, N.Y.

131 Rozenberg L.D.; Kazantsev V.F. and Makarov L.O. (1964), “Ultrasonic Cutting”, *Consultant Bureau*, New York, pp. 97-102.

132 Roy R.K. (1990), “A primer on the Taguchi Method”, Van Nostrand Reinhold, New York, ISBN-0-442-23729-4.

133 RTI International metals (2002), “Titanium alloy guide”, Ohio, U.S.A.

134 Saha J.; Bhattacharya A. and Mishra P.K. (1988), “Estimation of material removal rates in USM process- A theoretical and experimental study”, Proc. 27th Int. Matador Conf, Manchester, England.

135 Satyanaryana A. and Krishan Reddy B.G. (1984), “Design of velocity transformers for ultrasonic machining”, *Electrical India*, **Vol. 24, No. 14**, pp. 11-20.

136 Scab K. H. W. (1990), “Parametric studies of ultrasonic machining”, SME Tech. paper, **MR90-294**, pp. 11.

137 Seah K.H.W., Wong Y.S. and Lee T.C. (1993), “Design of tool holders for ultrasonic machining using FEM”, *Journal of Materials Processing Technology*, **Vol. 37, No. 1-4**, pp. 801-806.

138 Shaw M.C. (1956), "Ultrasonic grinding", *Annals of CIRP*, **Vol. 5**, pp. 25-53.

139 Sharma A., Mishiro S., Suzuki K., Imai T. (2003), “A new longitudinal mode ultrasonic transducer with an eccentric horn for micro machining”, *Key Engineering Materials*, **Vol. 238-239**, pp. 147-152.

140 Singh R. and Khamba J.S. (2008), “Comparison of slurry effect on machining characteristics of titanium in ultrasonic drilling”, *Journal of Materials Processing Technology*, **Vol. 197**, **No. 1-3**, pp. 200-205.

141 Singh R. and Khamba J.S. (2007), “Taguchi technique for modeling material removal rate in ultrasonic machining of titanium”, *Materials Science and Engineering*, **Vol. 460-461**, pp. 365-369.

142 Singh R. and Khamba J.S. (2007), “Macro-model for ultrasonic machining of

titanium and its alloys: designed experiments", *Journal of Engineering Manufacture*, **Vol. 221**, pp. 221-235.

143 Singh R. and Khamba J.S. (2006), "Ultrasonic Machining of titanium and its alloys-a review", *Journal of Materials Processing Technology*, **Vol. 173**, pp. 127-131.

144 Singh R. and Khamba J.S. (2003), "Comparing the machining characteristics of titanium with cylindrical and conical horn in ultrasonic drilling", *Proceedings of the National Conference on Recent Developments in Mechanical Engineering* (NCME 2003), TIET Patiala, India.

145 Singh R. and Khamba J.S. (2003), "Investigating the machining characteristics of titanium alloy (Titan-31) using ultrasonic drilling", *Proceedings of the 13th National Conference of ISME 2003*, IIT, Rorkee, India.

146 Singh R. and Khamba J.S. (2003), "Ultrasonic assisted drilling of titanium (Titan–15) using carbide, H.S.S and stainless steel tool", *Proceedings of the International Conference on Emerging Technology (ICET-2003*), Dec 19-21, 2003, KIIT, Bhuvaneshwar, India.

147 Singh Sehijpal; Shan H.S. and Kumar Pradeep (2002), "Parametric optimization of magnetic-field-assisted abrasive flow machining by Taguchi method", *Journal* of *Quality and Reliability Engineering International*, **Vol. 18**, pp. 273-283.

148 Smith T.J. (1973), Parameter influences in ultrasonic machining, *Tribology International*, **Vol. 11**, No. 5, pp. 196-198.

149 Snoyes R. (1986), "Non-conventional machining techniques: the state of art", *Advances in Non-Traditional Machining*, ASME, pp.1-20.

150 Spur G.; Brucker Th. and Holl S.E. (1997), "Ultrasonic machining of ceramics", *Industrial Ceramics*, **Vol. 17, No. 1**, pp 29-34.

151 SONIC-MILL 500 W model (2002), "Instruction manual for stationary ultrasonic machining", Albuquerque, U.S.A.

152 Soundrajan V. and Radhakrishnan V. (1986), An experimental investigation on the basic mechanisms involved in the ultrasonic machining, *International Journal of*

Machine Tool Design and Research, **Vol. 26, No. 3**, pp. 307-321.

153 Sreejith P.S. and Ngoi B.K.A. (2001), "Material removal mechanisms in precision machining of new materials", *Int. J. of Machine Tools and Manufacture*, **Vol. 41**, pp. 1831-1843.

154 Sun Xi (1996), "Micro ultrasonic machining and its applications in MEMS", *Sensors and Actuators*, **Vol. 57, No. 2**, pp. 159-164.

155 Takeyama H. and Murata R. (1962), "Study on machinability of pure titanium", *Journal of JSPE*, **Vol. 28, No. 6**, pp. 331.

156 Taraman K. (1974), "Multi machining output-multi independent variable turning research by response surface methodology", *International Journal of Production Research*, **Vol.12**, pp. 232-245.

157 Tarang Y.S., Yang W.H., Juang S.C. (2000), "The use of fuzzy logic in the Taguchi method for the optimization of submerged arc welding process", *International Journal of Advanced Manufacturing Technology*, **Vol. 16, No.9**, pp. 688-694.

158 Thoe T.B. and Aspinwall D.K. (1999), "Combined Ultrasonic and Electric Discharge Machining of Ceramic coated Nickel Alloy", *Journal of Materials Processing Technology*, **Vol. 92-93**, pp.323-328.

159 Thoe T.B.; Aspinwall D.K. and Wise M.L.H. (1998), "Review on Ultrasonic Machining", *International Journal of Machine Tools Manufacture*, **Vol.38, No.4**, pp. 239-255.

160 Thoe T.B., Aspinwall D.K. and Wise M.L.H. (1995), "The effect of operating parameters on ultrasonic contour machining", *Proc. 12th Annual Conference of the Irish Manufacturing Committee*, Cork, Ireland, Sep. 1995, pp. 305-312.

161 Treadwell C.; Hu P. and Zhang, J.M. (2002), "Modeling of material removal rate in rotary ultrasonic machining: Designed Experiments", *Journal of Materials Processing Technology*, **Vol. 129, No.1-3**, pp 339-344.

162 Tsutsumi (1993), "High quality machining of ceramics", *Journal of Materials Processing Technology,* **Vol. 37**, pp. 639-650.

163 Venkatesh V.C. (1983), "Machining of glass by impact processes", *Journal*

Mechanical Working Technology, **Vol. 8**, pp. 247-260.

164 Velasquez J.D., Bolle B., Chevrier P., Tidu A. (2007), "Metallurgical study on chips obtained by high speed machining of Ti-6Al-4V alloy", *Materials Science and Engineering*, **Vol. 452-453**, pp. 469-475.

165 Wang H.; Plebni L.J. and Sathyanaryanan G. (1998), "Modeling considerations for ultrasonic machining", *Abrasives*, Oct- Nov 1998, pp 8.

166 Wang Z.Y. and Rajurkar K.P. (1995), "Dynamic analysis of ultrasonic machining process", *Proceedings of the 1995 ASME International Mechanical Engineering Congress and Exposition*, **Part I,** pp 87-97.

167 Wansheng Z., Wang Z., Shichun Di, Guanxin C. (2002), "Ultrasonic and electric discharge machining to deep and small hole on titanium alloy", *Journal of Materials Processing Technology*, **Vol. 120**, pp101-106.

168 Weller E.J. (1984), "Non-Traditional machining processes", Society of Manufacturing Engineers, pp. 15-71.

169 Wiercigroch M., Neilson R.D., Player M.A. (1999), "Material removal rate prediction for ultrasonic drilling of hard materials using an impact oscillator approach", *Physics Letters*, **Vol. 259**, pp. 91-96.

170 Willard G.W. (1953), "Ultrasonically induced cavitation", *Journal of Acoustic Society of America,* **Vol. 25**, pp. 669.

171 Wood R.A. and Favor R.J. (1972), "Titanium alloys Handbook", Air Force Materials Laboratory, Ohio, 45433, pp. 45-46.

172 Xu W.L. and Han L. (1999), "Piezoelectric actuator based active error compensation of precision machining", *Measurement Science and Technology*, **Vol. 10, No. 2,** pp. 106-111.

173 Ya Gang; Quin H.W. and Yang S.C. (2002), "Analysis of rotary ultrasonic machining mechanism", *Journal of Materials Processing Technology*, **Vol. 129**, No. 1-3, pp 182-185.

174 Yan C. and Biing H. (2001), "Surface modification of Al-Zn-Mg alloy using the combined process of EDM and USM", *Journal of Materials Processing*

Technology, **Vol. 115**, **No.3**, pp 359-366.

175 Zeng W.M., Li Z.C., Pei Z.J., Treadwell C. (2005), "Experimental observation of tool wear in rotary ultrasonic machining of advanced ceramics", *International Journal of Machine Tools and Manufacture*, **Vol. 45,** pp. 1468-1473.

176 Zhang Q.H.; Zhang J.H. and Jia Z.X. (1999), "Material removal rate Analysis in the ultrasonic machining of engineering ceramics", *Journal of Materials Processing Technology*, **Vol. 88, No. 1**, pp 180-184.

177 Zhinxin J.; Zhang J.H. and Xing Ai (1997), "Study of a new kind of combined machining technology of ultrasonic machining and electrical discharge machining", *International Journal of Machine Tools and Manufacture*, **Vol. 37, No. 2**, pp 193-199.

178 Zhinxin J; Zhang J.H. and Xing Ai (1995), "Combined machining of USM and EDM for advanced ceramics", *Journal of advanced materials*, **Vol. 26, No. 3**, pp. 16-20.

179 Singh H. and Kumar P. (2006), "Optimizing multi-machining characteristics through Taguchi's approach and utility concept", *Journal of Manufacturing Technology Management,* **Vol. 17, No. 2**, pp. 255-273.

180 Sharman, R.C., Bowen P., Aspinwall D.K. (2001), "Ultrasonic assisted turning of gamma titanium aluminide", *Proceedings of 13th International Symposium for Electromachining*, Spain, Part-I, pp. 939-951.

APPENDIX I

Introduction to Titanium

1. Titanium and its applications

Titanium was discovered in 1910 and got its name from "Titan", a giant Greek mythology. Titanium is a light metal with excellent strength (maintained at high temperatures) and corrosion resistance. Titanium is bio-compatible because it is non allergic. Titanium could be regarded as a familiar metal as it appears in a wide range of applications detailed here.

Chinese Works: Titanium is highly resistant to heat with a melting temperature as high as 1668 ^{o}C. Although heat conductivity of titanium is almost the same as that of stainless steel, its weight is approx. half of stainless steel. Titanium is non-toxic and easy to clean.

Piercing, watches and eye glasses: Titanium is used in piercing, for brooches, tie pins and cuff links. It is very light and allergic reactions are almost nil.

Golf Clubs: With a titanium driver head, it is possible for the ball to travel longer distances. Changing the design of the golf courses is being considered for this reason. With a light-weight club, one can aim for a higher speed swing. Many golfers agree that because of a larger head and consequently, a wider sweep spot, titanium clubs are unbeatable. Recently, many kinds of new titanium alloy heads have been developed.

Foods and Tableware: Titanium is non-toxic and since it does not dissolve in salt water, it does not change the taste of foods. Titanium is most appropriate for processing food and tableware. Titanium is being used for some types of outdoor equipment and will be used even more in the near future.

Automobiles: Titanium is being tested mainly in connecting rods and is very effective when used for moving parts. Use of titanium can enhance the fuel efficiency significantly

Architecture and Building Materials: Because of its high specific strength and excellent corrosion resistance, titanium is being used for construction purposes. The roof of Naya temple, Fukui, Japan and International Conference building at Tokyo Big Site are some of the buildings made from Titanium.

Chemical Plants: Titanium is used in many types of chemical equipment. About 30% of the titanium used domestically is for chemical plants.

Nuclear Power Stations: Titanium is greatly used in nuclear and fossil power stations. It is used for constructing the big heat exchanger, Condenser, which cools the steam from the turbine with seawater. As titanium does not get corroded, the wall thickness of the tube can be kept as low as 0.5 mm. Condenser tubes consume about 20% of the domestic titanium consumption in India.

Aerospace: In the USA, about 70% of the titanium produced is used for aerospace parts. In Japan, only 2-3% of the titanium is consumed for aerospace sector. Titanium is particularly useful for aerospace applications mainly in aircrafts (wings and engine components) because of its light weight and high strength even at elevated temperatures.

Surgical Implants: Titanium is being used widely for bio-medical and surgical applications. Because of its higher corrosion resistance and non-toxic nature, it is being used for surgical implants. Many of the surgical instruments are also made from titanium.

Titanium in daily life: Recently, titanium has also been used in many goods we use such as in sports equipments, building material, motors and accessories. This amounts to about 25% of the domestic consumption.

2. Types and properties of titanium

From a materials science viewpoint, titanium has three types: α-titanium, α + β-titanium and β-titanium. The typical α-titanium is high purity commercially pure unalloyed

titanium (ASTM Grade-I); α + β-titanium is represented by Ti-6Al-4V alloy (ASTM Grade-V); and β-titanium includes the Ti-15V-3Cr-3Sn-3Al alloy.

α + β-titanium and β-titanium are generally called titanium alloys. As unalloyed titanium is softer than stainless steel, it is particularly useful for applications such as golf club heads. It is also an indispensable material when sophisticated fabrications are required. Titanium alloys exceed stainless steel in strength and are used to manufacture cast of forged club heads. There are various titanium alloys, having specific characteristics. By using right kind of titanium alloy for right application, thus making optimum use of properties of each material, products with better performance can be developed. The physical properties of pure titanium have been shown in the table below.

Physical properties of commercially pure Titanium (ASTM Grade-I)

Melting Point	1668 ^{o}C
Density	4.51 g/cm^{3}
Beta transformation temp.	890 ^{o}C
Thermal expansion, 20-100 C	8.6*10^{-6} K^{-1}
Thermal conductivity, 0-300 C	9.2*10^{-6} K^{-1}
Thermal conductivity, room temp.	20.8 W/mK
Thermal conductivity, 400 C	14 W/mK
Specific heat, room temp.	0.56 J/gK
Electrical resistivity, room temp.	52μWcm
Poisson's ratio	0.34-0.40
Fatigue limit (10^{7} cycles)	193 MPa

Heat Treating for pure Titanium (ASTM Grade-I)			
		Temperature	**Time**
Annealing	Air-cooled	650-760 ^{o}C	6 min-2 Hrs
Stress Relieving	Air-cooled	480-595 ^{o}C	15 min-4 Hrs

APPENDIX II

Conventional Machining of Titanium

The technology supporting the machining of titanium alloys basically is very similar to that for other alloy systems. Efficient metal machining requires access to data relating the machining parameters of a cutting tool to the work material for the given operation. The important parameters include:

- Tool life
- Forces
- Power requirements
- Cutting tools and fluids

Detailed description of these parameters for efficient machining of titanium and its alloys has been given below.

Tool Life: Titanium alloys are very sensitive to changes in feed. Industry generally operates at cutting speeds providing long tool life. When cutting titanium, a high shear angle is produced between the workpiece and chip, resulting in a thin chip flowing at high velocity over the tool face. High temperatures develop, and since titanium has low thermal conductivity, the chips have a tendency to gall and weld themselves to the tool cutting edges. This speeds up tool wear and failure. When dealing with high-fixed-cost machine tools production output may be much more important than a cutting tool's life. It thus may be wise to work a tool at its maximum capacity, and then replace it as soon as its cutting efficiency starts to drop off noticeably, thereby maintaining uptime as much as possible.

When machining titanium in circumstances in which production costs are not of paramount concern, it is still unsound practice to allow tools to run to destruction. The other extreme, premature tool changing, may result in a low number of pieces per tool grind, but the lower the tool wear, the less expensive the regrinding. Ideally, a tool should be permitted to continue cutting as long as possible without risking damage to the tool or the work but with the retention of surface integrity.

Forces and Power Requirements: The cutting force is important since, when multiplied by the cutting velocity, it determines the power requirements in machining. The thrust, or separating force, determines the accuracy produced on a part. For general approximations, the power requirements in turning and milling can be obtained by measuring the power input to the machine tool's drive motor during a cutting operation and by subtracting from it the idle power. A good approximation of the horsepower required in most machining operations can be predicted from unit power requirements. Table below shows the power requirements for titanium in comparison to other alloys.

Avg. unit power requirements for turning, drilling or milling of titanium

		Unit power for sharp tools hp/in.^{3}/min.		
Material	**Hardness (BHN)**	**Turning HSS/Carbide tools**	**Drilling HSS drills**	**Milling HSS/Carbide tools**
Steels	35-40 RC	1.4	1.4	1.5
Titanium alloys	250-375	1.2	1.1	1.1
High temperature Ni/Co based alloys	200-360	2.5	2.0	2.0
Aluminium alloys	30-150	0.25	0.16	0.32

Cutting tools: In the past several years, there have been major advancements in the development of cutting tools including coated carbides, ceramics, cermets, cubic boron nitride, and polycrystalline diamond. These have found useful applications in the machining of cast irons, steels, and high-temperature and aluminum alloys. Unfortunately, none of these or other new materials has improved the removal rate of titanium alloys. In studies conducted as early as 1950, the straight tungsten carbide (WC) cutting tools, typically C-2 grades, performed best in operations such as turning and face milling, while the high-cobalt, high-speed steels were most applicable in drilling, tapping, and end milling.

Today, the situation is much the same. C-2 carbides are used extensively in engine and airframe manufacturing for turning and face milling operations. In recent

years, in the United States as well as in Europe, solid C-2 end mills and end mills with replaceable C-2 carbides are finding applications, particularly in aerospace plants. Today, the M7 and, more frequently, the M42 and M33 high-speed steels are recommended for end milling, drilling, and tapping of titanium alloys.

Cutting Fluids: When specifying cutting fluids for machining titanium, some companies have practically no restrictions except that they do not permit the use of cutting fluids containing chlorine on titanium parts which are subjected to higher temperatures in welding processes or in service. Still other organizations in aerospace manufacturing permit no active chlorine in any cutting fluid used for machining titanium alloys. There are excellent cutting fluids available which do not contain any halogen compounds. In fact, from extensive test data collected by the Air Force Materials Laboratory, it can be concluded that chlorine-containing cutting fluids do not always provide better tool life. For certain alloys and operations, dry machining is preferred. Usually the heavy chlorine-bearing fluids excel in operations such as drilling, tapping, and broaching.

Although the basic machining properties of titanium metal cannot be altered significantly, their effects can be greatly minimized by decreasing temperatures generated at the tool face and cutting edge. Economical production techniques have been developed through application of these basic rules in machining titanium:

- **Use low cutting speeds**. Tool tip temperatures are affected more by cutting speed than by any other single variable. A change from 6 to 46 meters per min. with carbide tools results in a temperature change from 427ºC to 927ºC.
- **Maintain high feed rates**. Temperature is not affected by feed rate so much as by speed, and the highest feed rates consistent with good machining practice should be used. A change from 0.05 to 0.51 mm per revolution results in a temperature increase of only 149ºC.
- **Use generous amounts of cutting fluid**. Coolant carries away heat, washes away chips, and reduces cutting forces.

- **Use sharp tools and replace them at the first sign of wear**, or as determined by production/cost considerations. Tool wear is not linear when cutting titanium. Complete tool failure occurs rather quickly after small initial amount of wear takes place.
- **Never stop feeding while a tool and a workpiece are in moving contact**. Permitting a tool to dwell in moving contact causes work hardening and promotes smearing, galling, seizing, and total tool breakdown.

In recent years, ceramic tools have been used successfully in machining high-temperature alloy jet-engine components at speeds much higher than those conventionally used. At speeds of 183 to 213 m/min, tool life is short (3 to 5 min), but it is possible to finish a cut at these speeds and then index the cutting tip for making the next pass. This same technique has potential in machining of titanium with C-2 carbides.

Surface Integrity while machining Titanium

The surface of titanium alloys is thought to be easily damaged during some traditional machining operations. Damage appears in the form of microcracks; built-up edge; plastic deformation; heat-affected zones; and tensile residual stresses. In service, this damage can lead to degraded fatigue strength and stress corrosion resistance. In various studies on grinding of Ti-6Al-4V alloy, gentle or low-stress grinding parameters have displayed no readily identifiable changes at the surface, while conventional and abusive practices altered the surface layer noticeably. Studies indicate an endurance limit of 372 MPa for the gentle grinding and values of 83 and 97 MPa for conventional and abusive conditions, respectively. In those areas of application where maximum fatigue strength is required, not only are appropriated machining parameters used, but also selected surface areas of components may be glass bead blasted to restore, or to retain, a high level of favorable compressive surface stress.